

# **Process Development for Hepatitis B core Antigen Virus-Like Particles as Gene Delivery Vectors**

Processing and Analytics in the Presence of Nucleic Acids

Zur Erlangung des akademischen Grades einer  
DOKTORIN DER INGENIEURWISSENSCHAFTEN (DR.-ING.)

von der KIT-Fakultät für Chemieingenieurwesen und Verfahrenstechnik des  
Karlsruher Instituts für Technologie (KIT)

genehmigte

DISSERTATION

von

Angela Valentic, M.Sc.

aus Karlsruhe

Tag der mündlichen Prüfung: 26.06.2025

Erstgutachter: Prof. Dr. Jürgen Hubbuch

Zweitgutachter: Prof. Dr.-Ing. Dirk Holtmann



This document is licensed under a Creative Commons Attribution 4.0 International License (CC BY 4.0): <https://creativecommons.org/licenses/by/4.0/deed.en>

## Abstract

Virus-like particles (VLPs) have emerged as a highly adaptable platform with broad applications spanning vaccine development to gene therapy. In recent years, there has been a growing need for efficient and targeted delivery systems for nucleic acid (NA)-based therapeutics, including mRNA, siRNA, and antisense oligonucleotides. These therapies offer promising avenues for the treatment of various genetic and acquired diseases; however, obstacles such as stability, cellular uptake, and precise delivery have restricted their clinical utility. VLPs present a compelling solution due to their demonstrated capacity to package and deliver foreign genetic material, along with their stable, repetitive surface architecture that enables modifications to enhance targeting of specific cells or tissues.

Overcoming the technical challenges in downstream processing of VLPs is critical for advancing their potential from the laboratory to clinical applications. Standard purification processes generally involve cell lysis to release VLPs from the expression system, followed by ultracentrifugation or precipitation, disassembly and reassembly, and subsequent polishing and formulation steps. For VLPs intended for NA delivery, an additional loading step is required to encapsulate therapeutic nucleic acids (NA<sub>ther</sub>). While VLPs have shown strong capabilities for packaging, protecting, and delivering foreign NAs, achieving efficient and scalable processing remains a significant challenge.

Hepatitis B core antigen (HBcAg) is a widely studied VLP due to its strong immunogenicity, self-assembly capabilities, and potential as a gene delivery vehicle. Its unique structure and ability to encapsulate NAs make HBcAg VLPs a promising candidate for targeted genetic material delivery. This thesis explored the process development of HBcAg VLPs as potential gene delivery vehicles, with a particular focus on processing and analytical quantification methods in the presence of NA binding regions and bound NAs.

The NA binding region of the HBcAg VLPs, essential for encapsulating significant amounts of NAs, influences not only VLP formation but also poses challenges for downstream processing, such as solubility and disassembly during purification. The first study focused on the impact of varying lengths of the NA binding region on VLP characteristics and purification process. HBcAg VLP constructs with different binding region lengths were produced and analyzed. The results revealed that while capsid size and zeta potential remained consistent across constructs, the length of the NA binding region significantly impacted host cell-derived nucleic acid (NA<sub>hc</sub>) binding, displaying a distinct two-zone pattern. Constructs with shorter binding regions showed a sharp increase in encapsulated NAs, whereas a plateau effect

emerged as binding regions lengthened beyond Cp164 - a construct with an intermediate length of the NA binding region.

The study further demonstrated that while precipitation and re-dissolution steps showed minimal sensitivity to NA loading variations, the disassembly process was strongly affected by both the construct and its NA load. Disassembly screening across liquid-phase conditions highlighted a complex balance between NA-stabilizing forces and destabilizing forces from positive charges in the binding region, following the two-zone binding behavior. Optimized conditions for disassembly, such as high pH and elevated urea concentrations, were critical for achieving higher dimer yields. These findings underscore the importance of the NA binding region's length and NA binding in modulating VLP stability and purification efficiency, informing strategies to enhance purification and enable successful loading of NA<sub>ther</sub>.

Accurate quantification of HBcAg VLPs and their bound NAs is essential for evaluating NA<sub>hc</sub> depletion, VLP protein loss, and effective loading with NA<sub>ther</sub>. The second study developed two robust analytical methods to address existing limitations: (1) a silica spin column extraction method for NA quantification by dye-based fluorescence, and (2) a reversed-phase high-performance liquid chromatography (RP-HPLC) method that enables simultaneous separation and absolute quantification of HBcAg proteins and bound NAs. These methods provided reliable measures of protein and NA content and HBcAg protein purity, offering significant improvements over conventional techniques and supporting the development of gene delivery processes for HBcAg VLPs.

Efficient depletion of NA<sub>hc</sub> from HBcAg VLPs is crucial for enabling successful NA<sub>ther</sub> loading. This work applied the newly developed analytical methods to evaluate a range of established NA<sub>hc</sub> depletion techniques, including nuclease treatments, LiCl precipitation, alkaline treatment, and a novel heparin chromatography-based method. Results showed that heparin chromatography consistently outperformed these alternatives in terms of NA<sub>hc</sub> removal and VLP protein recovery. Specifically, the Cp157 construct demonstrated optimal performance, highlighting a nuanced relationship between binding region length and depletion efficiency. The heparin chromatography-based method offers a robust and reproducible approach for preparing HBcAg VLPs for therapeutic applications.

Further, the study explored factors influencing the reassembly and loading of HBcAg VLPs, focusing on the roles of the NA binding region, NA presence, and the ionic strength of the reassembly buffer, assessing reassembly yields and loading efficiency with novel quantification methods. Results indicated a complex interplay among these factors in determining reassembly yields, with both ionic strength and DNA bound to NA binding regions promoting reassembly. For Cp157 constructs, efficient depletion of NA<sub>hc</sub> enabled successful mixing of HBcAg dimers with NA<sub>ther</sub> and subsequent reassembly into loaded VLPs. Hereby, the NA binding region significantly influenced



NA encapsulation efficiency, with Cp157 showing superior performance compared to Cp149.

In summary, this dissertation addresses the challenges associated with the purification of HBcAg VLPs, advancing the understanding of the factors influencing the phase behavior, stability, purification, and quantification of HBcAg VLPs. The development of robust analytical methods and optimized purification processes lays the groundwork for the scalable production of HBcAg VLPs. By elucidating the role of the NA binding region and impact of encapsulated NAs, this dissertation advances the field of VLP-based gene delivery systems. The methodologies and processes developed enhance the potential of VLPs as versatile nanocarriers for therapeutic NAs. Future research should focus on refining loading and encapsulation efficiencies, scaling production processes, and exploring the biophysical properties of VLPs *in vivo*. With continued innovation, HBcAg VLPs are poised to contribute meaningfully to the future of precision medicine and gene delivery platforms.



## Zusammenfassung

Virusähnliche Partikel (VLPs) haben sich als äußerst anpassungsfähige Plattform mit einem breiten Anwendungsspektrum von der Impfstoffentwicklung bis zur Gentherapie erwiesen. In den letzten Jahren ist der Bedarf an effizienten und zielgerichteten Liefersystemen für Nukleinsäure-basierte Therapeutika, einschließlich mRNA, siRNA und antisense Oligonukleotiden, gestiegen. Diese Therapien bieten vielversprechende Ansätze für die Behandlung verschiedener genetischer und erworbener Erkrankungen. Hindernisse wie Stabilität, zelluläre Aufnahme und präzise Verabreichung haben jedoch die klinische Anwendbarkeit eingeschränkt. VLPs stellen eine überzeugende Lösung dar, da sie nachweislich in der Lage sind, fremdes genetisches Material zu verpacken und zu verabreichen. Außerdem ermöglicht ihre stabile und sich wiederholenden Oberflächenstruktur Modifikationen, welche die Zielgerichtetheit auf spezifische Zellen oder Gewebe verbessern können.

Die Bewältigung der technischen Herausforderungen bei der Aufreinigung von VLPs ist entscheidend, um ihr Potenzial aus dem Labor in klinische Anwendungen zu überführen. Zu den Standard-Aufreinigungsprozessen gehören in der Regel die Zelllyse, um VLPs aus dem Expressionssystem freizusetzen, gefolgt von Ultrazentrifugation oder Fällung, Dissoziation und Reassemblierung sowie nachfolgenden Reinigungs- und Formulierungsschritten. Für VLPs, die für den Transport von Nukleinsäure-basierten Therapeutika bestimmt sind, ist ein zusätzlicher Schritt zur Verkapselung der therapeutischen Nukleinsäuren erforderlich. VLPs haben zwar gezeigt, dass sie sich hervorragend für die Verpackung, den Schutz und die Verabreichung fremder Nukleinsäuren eignen, aber eine effiziente und skalierbare Verarbeitung bleibt eine große Herausforderung.

Hepatitis B Core Antigen (HBcAg) ist ein VLP, das aufgrund seiner starken Immunogenität, Selbstassemblierungsfähigkeit und seines Potenzials als Gentransporter viel Aufmerksamkeit erhalten hat und umfassend untersucht wurde. Seine einzigartige Struktur und die Fähigkeit, Nukleinsäuren zu verkapseln, machen HBcAg-VLPs zu einem vielversprechenden Kandidaten für den gezielten Transport von genetischem Material. Diese Dissertation untersucht die Prozessentwicklung von HBcAg VLPs als potenzielle Gentransportvehikel, mit besonderem Fokus auf den Aufreinigungs-Prozess und analytische Quantifizierungsmethoden in Gegenwart von Nukleinsäure bindenden Regionen und daran gebundenen Nukleinsäuren.

Die Nukleinsäure bindende Region der HBcAg-VLPs, die für die Verkapselung erheblicher Mengen von Nukleinsäuren unerlässlich ist, beeinflusst nicht nur die VLP-Bildung, sondern stellt auch Herausforderungen, wie etwa Löslichkeit und Dissoziation, für die nachgelagerte Aufreinigung dar. Die erste Studie konzentrierte sich auf die Auswirkungen variierender Längen der Nukleinsäure bindenden Region

auf die VLP-Eigenschaften und den Aufreinigungs-Prozess. Es wurden HBcAg-VLP-Konstrukte mit verschiedenen Längen der bindenden Region produziert und analysiert. Die Ergebnisse zeigten, dass die Kapsidgröße und das Zeta-Potential über alle Konstrukte hinweg konstant blieben, während die Länge der Nukleinsäure bindenden Region einen erheblichen Einfluss auf das Binden von Wirtszell-Nukleinsäuren hatte und ein ausgeprägtes Zwei-Zonen-Verhalten zeigte. Konstrukte mit kürzeren Binderegionen zeigten einen starken Anstieg der eingekapselten Nukleinsäuren, während ein Plateau-Effekt auftrat, wenn die bindenden Regionen über Cp164 hinaus verlängert wurden – einem Konstrukt mit einer intermediären Länge der Nukleinsäure bindenden Region.

Die Studie zeigte ferner, dass, während die Schritte der Fällung und Re-Dissolution wenig Sensibilität gegenüber Variationen der Nukleinsäure-Beladung aufwiesen, der Disassemblierungsprozess stark sowohl vom Konstrukt als auch seiner Nukleinsäuren-Beladung beeinflusst wurde. Die Disassemblierungsuntersuchungen unter verschiedenen Flüssigphasenbedingungen verdeutlichten ein komplexes Gleichgewicht zwischen stabilisierenden Kräften der Nukleinsäuren und destabilisierenden Kräften der positiven Ladungen in der Binderegion, gemäß dem Zwei-Zonen-Verhalten der Beladung der Konstrukte. Optimierte Bedingungen für die Disassemblierung, wie ein hoher pH-Wert und hohe Harnstoffkonzentrationen, waren entscheidend, um höhere Dimer-Ausbeuten zu erreichen. Diese Ergebnisse unterstreichen die Bedeutung der Länge und Nukleinsäure-Bindung der Nukleinsäure bindenden Region zur Modulation der VLP-Stabilität und Aufreinigungseffizienz und liefern Informationen für Strategien zur Verbesserung der Aufreinigung und zur erfolgreichen Beladung mit therapeutischen Nukleinsäuren.

Die genaue Quantifizierung der HBcAg-VLPs und ihrer gebundenen Nukleinsäuren ist entscheidend für die Bewertung der Abreicherung von Wirtszell-Nukleinsäuren, des Verlusts von VLP-Proteinen und der effektiven Beladung mit therapeutischen Nukleinsäuren. In der zweiten Studie wurden zwei robuste analytische Methoden entwickelt, um bestehende analytische Limitationen zu überwinden: (1) eine Silica-basierte Extraktionsmethode zur Quantifizierung von Nukleinsäuren mittels Farbstofffluoreszenz und (2) eine Umkehrphasen-Hochleistungsflüssigkeits-Chromatographie Methode, die die gleichzeitige Trennung und absolute Quantifizierung von HBcAg-Proteinen und gebundenen Nukleinsäuren ermöglicht. Diese Methoden lieferten zuverlässige Bestimmungen des Protein- und Nukleinsäuregehalts sowie der Reinheit des HBcAg-Proteins. Somit stellen sie erhebliche Verbesserungen gegenüber konventionellen Techniken dar, wodurch sie die Entwicklung von Gentherapieprozessen für HBcAg-VLPs unterstützen.

Eine effiziente Abreicherung von Wirtszell-Nukleinsäuren aus HBcAg-VLPs ist entscheidend, um eine erfolgreiche Beladung mit therapeutischen Nukleinsäuren zu ermöglichen. In dieser Arbeit wurden die neu entwickelten Analysemethoden angewandt, um eine Reihe etablierter Abreicherungs-Techniken zu evaluieren, darunter Nukleasebehandlungen, LiCl-Fällung, Alkalibehandlung und eine neuartige

Heparin-Chromatographie-basierte Methode. Die Ergebnisse zeigten, dass Heparin-Chromatographie diese Alternativen in Bezug auf Abreicherung von Wirtszell-Nukleinsäuren und VLP-Protein-Rückgewinnung durchweg übertraf. Hierbei zeigte das Cp157-Konstrukt die besten Ergebnisse und verdeutlichte eine nuancierte Beziehung zwischen der Länge der bindenden Region und der Abreicherungseffizienz. Die Heparin-Chromatographie-basierte Methode bietet einen robusten und reproduzierbaren Ansatz zur Aufreinigung von HBcAg-VLPs für therapeutische Anwendungen.

Die Studie untersuchte auch die Faktoren, die die Reassemblierung und Beladung von HBcAg-VLPs beeinflussen, wobei der Schwerpunkt auf der Rolle der Nukleinsäurebindenden Region, der Anwesenheit von Nukleinsäuren und der Ionenstärke des Reassemblierungs-Puffers lag. Dabei wurden Reassemblierungs-Ausbeuten und Beladungseffizienzen mit den neu entwickelten Quantifizierungsmethoden bestimmt. Die Ergebnisse deuteten auf ein komplexes Zusammenspiel dieser Faktoren und ihrer Auswirkung auf Reassemblierungs-Ausbeuten hin, wobei sowohl die Ionenstärke als auch die DNA, die an die Bindestellen gebunden war, die Reassemblierung förderten. Für Cp157-Konstrukte ermöglichte die effiziente Abreicherung von Wirtszell-Nukleinsäuren die Mischung von HBcAg-Dimeren mit therapeutischen Nukleinsäuren und anschließende erfolgreiche Reassemblierung in beladene VLPs. Hierbei beeinflusste die Nukleinsäure-Bindestelle die Beladungseffizienz erheblich und Konstrukt Cp157 erzielte bessere Beladungsergebnisse als Cp149.

Zusammenfassend befasst sich diese Dissertation mit den Herausforderungen bei der Aufreinigung von HBcAg-VLPs und vertieft das Verständnis der Faktoren, die das Phasenverhalten, die Stabilität, die Aufreinigung und die Quantifizierung von HBcAg-VLPs beeinflussen. Die Entwicklung robuster Analysemethoden und optimierter Aufreinigungsprozesse bildet die Grundlage für die skalierbare Produktion von HBcAg-VLPs. Durch die Erläuterung der Rolle der Nukleinsäure-Binderegion und des Einflusses der eingeschlossenen Nukleinsäuren leistet diese Dissertation einen wichtigen Beitrag im Bereich der VLP-basierten Gen-Transfersysteme. Die entwickelten Methoden und Prozesse erhöhen das Potenzial von VLPs als vielseitiges Gentransportsystem für therapeutische Nukleinsäuren. Zukünftige Forschung sollte sich auf die Verfeinerung von Beladungs- und Verkapselungseffizienzen, die Skalierung der Produktionsprozesse und die Untersuchung der biophysikalischen Eigenschaften von VLPs in vivo konzentrieren. Mit fortschreitender Innovation sind HBcAg-VLPs in der Lage, einen bedeutenden Beitrag zur Zukunft der Präzisionsmedizin und Gen-Transfer-Plattformen zu leisten.

# Table of Contents

Abstract.....	iii
Zusammenfassung .....	vii
Table of Contents .....	x
1 Introduction .....	15
1.1 Virus-like particles (VLPs): Structure, Function, and Applications .....	16
1.1.1 Overview of VLPs.....	16
1.1.2 VLP Applications .....	16
1.1.3 Hepatitis B Core Antigen (HBcAg) VLPs.....	17
1.2 Nucleic Acid (NA)-Based Therapeutics.....	18
1.2.1 Types of Nucleic Acid Therapeutics .....	18
1.2.2 Challenges in Delivery .....	19
1.2.3 VLPs as Delivery Vehicles.....	19
1.3 Phase Behaviour and Stability of VLPs .....	20
1.3.1 Phase Behaviour and Capsid Stability in Different Conditions.....	20
1.3.2 Impact of NA Binding on VLP Stability .....	21
1.4 Downstream Processing of VLPs.....	22
1.4.1 Purification Challenges.....	22
1.4.2 Purification Techniques.....	23
1.4.3 Purification Process of VLPs.....	24
1.5 Analytical Techniques for VLP Characterization .....	26
1.5.1 Electrophoretic Techniques .....	26
1.5.2 UV/Vis Spectroscopy .....	27
1.5.3 Fluorescence Assays.....	27
1.5.4 Quantitative PCR.....	27
1.5.5 Chromatographic Separation .....	27
1.5.6 Dynamic Light Scattering Techniques .....	29
1.5.7 Transmission Electron Microscopy .....	30
1.5.8 Challenges in Quantification of VLPs and Bound Nucleic Acids (NAs)....	30
2 Thesis Outline.....	33
2.1 Research Proposal .....	33
2.2 Comprehensive Overview .....	36
3 Effects of Different Lengths of a Nucleic Acid Binding Region and Bound Nucleic Acids on the Phase Behavior and Purification Process of HBcAg Virus-Like Particles.....	41
3.1 Introduction.....	43
3.2 Materials and Methods .....	46
3.2.1 Materials and Buffers .....	46
3.2.2 Cloning of Cp154, Cp157, Cp164, Cp167 and Cp183 .....	46
3.2.3 Intra-cellular Formation and Purification of VLPs.....	47
3.2.4 Characterization of VLP Constructs.....	48
3.2.5 Purification Process Characterization.....	49

3.3	Results.....	49
3.3.1	Characterization of HBcAg VLP Constructs .....	49
3.3.2	Effects of VLP Constructs on the Purification Process.....	51
3.4	Discussion .....	55
3.4.1	Intra-cellular Formation and Characterization of HBcAg VLP Constructs .....	55
3.4.2	Capture by Precipitation and Re-dissolution.....	57
3.4.3	Effects of Liquid Phase Conditions on Disassembly Yield.....	58
3.4.4	Effects of HBcAg VLP Constructs and Loading on Disassembly Yield ....	58
3.5	Conclusions.....	59
4	Absolute Quantification of Hepatitis B Core Antigen (HBcAg) Virus-like Particles and Bound Nucleic Acids .....	63
4.1	Introduction.....	65
4.2	Materials and Methods.....	69
4.2.1	Buffers, VLPs, and DNA .....	69
4.2.2	Silica Spin Column Based Extraction .....	70
4.2.3	RP Based Nucleic Acid and Protein Extraction .....	70
4.2.4	Analytics for Silica-SC Based Extraction, RP Based Extraction and Quantification of Proteins and Nucleic Acids .....	71
4.3	Results.....	72
4.3.1	Silica-SC Based Extraction .....	72
4.3.2	Lysis of VLPs by Proteinase K .....	73
4.3.3	Adsorption of Nucleic Acids.....	73
4.3.4	Elution of Nucleic Acids .....	75
4.3.5	Characterization of the Silica-SC Based Extraction.....	75
4.3.6	Quantification of Proteins and Nucleic Acids using RP-HPLC .....	78
4.4	Discussion .....	81
4.4.1	Absolute Quantification of HBcAg Protein and Bound Nucleic Acids .....	81
4.4.2	Analytical Toolbox for HBcAg VLPs.....	86
4.5	Conclusions.....	87
5	Effective Removal of Host Cell-Derived Nucleic Acids Bound to Hepatitis B Core Antigen Virus-Like Particles by Heparin Chromatography.....	91
5.1	Introduction.....	92
5.2	Materials and methods .....	96
5.2.1	Buffer and VLPs.....	96
5.2.2	Removal of host cell-derived nucleic acids bound to HBcAg VLPs .....	96
5.2.3	Analytics.....	97
5.3	Results.....	99
5.3.1	Heparin chromatography for different HBcAg VLP constructs.....	99
5.3.2	Heparin and sulfate chromatography with and without prior nuclease treatment.....	102
5.3.3	LiCl precipitation .....	104
5.3.4	Alkaline treatment .....	106
5.4	Discussion .....	108
5.4.1	Heparin chromatography with different HBcAg VLP constructs .....	108
5.4.2	Comparison of Cp157 and Cp183 .....	110
5.4.3	Comparison of heparin and sulfate chromatography.....	110
5.4.4	LiCl precipitation and alkaline treatment .....	111

5.5	Conclusions .....	113
6	Loading and Reassembly of Hepatitis B Core Antigen Virus-Like Particles as a Function of a Nucleic Acid Binding Region, Nucleic Acid Type and Ionic Strength in the Liquid Phase .....	117
6.1	Introduction .....	118
6.2	Materials and methods .....	121
6.2.1	Buffers and nucleic acids.....	121
6.2.2	VLP production, purification, disassembly and NA <sub>hc</sub> removal.....	121
6.2.3	Mixing of VLPs with nucleic acids and VLP reassembly.....	122
6.2.4	Analytics.....	122
6.3	Results .....	123
6.3.1	Variation of the presence of a NA binding region, NAs and ionic strength in the liquid phase.....	123
6.3.2	Variation of dimer/ON_DNA ratio and presence of a NA binding region	127
6.4	Discussion .....	129
6.4.1	Influence of the presence of a NA binding region, NAs and the ionic strength in the liquid phase on reassembly yields .....	130
6.4.2	Reassembly kinetics and processing.....	134
6.4.3	Encapsulation efficiency dependent on the presence of a NA binding region and different VLP to NA ratios .....	134
6.5	Conclusions .....	136
7	General discussion and conclusion.....	139
	Bibliography .....	144
	Abbreviations .....	157
	Appendix A: Supplementary Material for Chapter 3 .....	159
	Appendix B: Supplementary Material for Chapter 4 .....	165
	Appendix C: Supplementary Material for Chapter 5 .....	169
	Appendix D: Supplementary Material for Chapter 6 .....	177







# 1

## Introduction

The advancement of biomedical sciences has been marked by the development of innovative tools and techniques that enable precise manipulation and understanding of biological systems. Among these, virus-like particles (VLPs) have emerged as a versatile and powerful platform with applications ranging from vaccine development to gene therapy (Yan et al., 2015; Jeevanandam et al., 2019; Roldao et al., 2020; Nooraei et al., 2021). VLPs are non-infectious mimics of viruses, structurally similar to their viral counterparts but devoid of viral genetic material, making them safe for therapeutic use (Shirbaghaee and Bolhassani, 2016). The Hepatitis B core Antigen (HBcAg) is a prominent example of a VLP that has garnered significant attention due to its ability to self-assemble into highly immunogenic particles and its potential as a gene delivery vehicle (Porterfield et al., 2010; Strods et al., 2015; Moradi Vahdat et al., 2021; Petrovskis et al., 2021). The unique structural properties of HBcAg VLPs, coupled with their capacity to incorporate nucleic acids (NAs), make them an attractive candidate for delivering genetic material to target cells (Choi et al., 2013; Rohovie et al., 2017). The exploration of HBcAg VLPs as gene delivery vehicles sits at the intersection of virology, nanotechnology, and molecular medicine. Understanding the foundational principles behind VLP assembly, NA encapsulation, and targeted delivery is crucial for advancing their application in gene therapy. Moreover, addressing the technical challenges associated with the production, purification, and quantification of these particles is essential for translating their potential from the laboratory to clinical settings.

This dissertation focuses on the production, purification, and quantification of HBcAg VLPs, with the goal of optimizing their use as gene delivery systems. The following sections provide a comprehensive theoretical background on key topics relevant to this research, including the fundamental concepts of VLPs, and NA delivery, the principles and challenges in processing and analysis of VLPs. By grounding the research in these topics, the dissertation aims to contribute to the growing body of knowledge on VLPs and their applications in modern medicine.

### 1.1 Virus-like particles (VLPs): Structure, Function, and Applications

#### 1.1.1 Overview of VLPs

VLPs are nanostructures that mimic the organization and conformation of native viruses but lack the viral genetic material. These particles are composed of viral capsid proteins that self-assemble into structures resembling the actual viruses from which they are derived (Nooraei et al., 2021). However, since VLPs do not contain any NAs, they are non-infectious, making them safe for use in various biomedical applications (Shirbaghaee and Bolhassani, 2016). The structure of VLPs is typically based on the viral capsid, a protein shell that encases the genetic material of a virus. In VLPs, the assembly of these capsid proteins is preserved, but without the accompanying viral genome (Shirbaghaee and Bolhassani, 2016). This structure enables VLPs to present antigens in a highly repetitive manner (Mohsen et al., 2017). The size of VLPs generally ranges from 20 to 200 nanometers, depending on the source virus, which also influences their immunogenicity and biodistribution (Rohovie et al., 2017).

VLPs have been studied extensively for their potential in vaccine development, gene therapy, and drug delivery (Effio and Hubbuch, 2015; Fietze et al., 2016; Hill et al., 2017; Mohsen et al., 2017; He et al., 2022). Their ability to mimic viruses without posing the risk of infection makes them ideal candidates for vaccines, as they can stimulate robust immune responses similar to those induced by live viruses (Roldao et al., 2020; Nooraei et al., 2021). Additionally, VLPs can be engineered to carry specific antigens or therapeutic agents (Mohsen et al., 2017; Rohovie et al., 2017), making them versatile tools in targeted therapy.

#### 1.1.2 VLP Applications

VLPs are used in various biomedical applications, with their utility spanning from preventive vaccines to therapeutic platforms (Le and Müller, 2021). Unlike traditional vaccines that may use inactivated or attenuated viruses, VLP-based vaccines offer a safer alternative because they cannot replicate or revert to a virulent form (Mohsen et al., 2017; Tariq et al., 2022). Examples of successful VLP vaccines include those against human papillomavirus (HPV) and hepatitis B virus (HBV), which have demonstrated high efficacy and safety in clinical use (Schiller and Lowy, 2012; Gerlich, 2015; Shouval et al., 2015). Beyond vaccines, VLPs are also explored for their potential in targeted drug delivery systems (Zdanowicz and Chroboczek, 2016; Rohovie et al., 2017). Their structure allows for the encapsulation or surface attachment of various therapeutic agents, including small molecules, NAs, and proteins. By modifying the surface of VLPs with ligands or antibodies that target specific cells or

tissues, these particles can be directed to deliver their payloads precisely where needed, minimizing systemic side effects and enhancing treatment efficacy (Rohovie et al., 2017). The ability to customize the surface of VLPs further enhances their potential in personalized medicine, where treatments are tailored to individual patient profiles. The versatility of VLPs is further demonstrated in gene therapy, where they can be used as vehicles to deliver therapeutic genes into cells. Their capacity to package NAs and transduce them into target cells, combined with their non-infectious nature, makes VLPs attractive for gene therapy applications, particularly in treating genetic disorders and certain cancers (Rohovie et al., 2017; Nooraei et al., 2021; Banskota et al., 2022; Lyu and Lu, 2022).

### **1.1.3 Hepatitis B Core Antigen (HBcAg) VLPs**

HBcAg VLPs are composed of the core protein of the hepatitis B virus, which naturally self-assembles into icosahedral particles about 34 nm in diameter (Wynne et al., 1999). These particles are highly immunogenic and have been extensively studied as platforms for vaccine development and other biomedical applications (Roldao et al., 2020; Le and Müller, 2021). The structure of HBcAg VLPs is characterized by their ability to form dimers that assemble into capsid-like structures, capable of encapsulating NAs or other molecules (Porterfield et al., 2010; Selzer and Zlotnick, 2015). This makes them suitable for gene delivery applications, as they can package and protect therapeutic genetic material during delivery to target cells. Moreover, HBcAg VLPs have a high degree of flexibility in terms of surface modification, allowing for the display of various antigens or the attachment of targeting molecules, which enhances their potential in targeted therapies (Porterfield et al., 2010; Rohovie et al., 2017). One of the significant advantages of using HBcAg VLPs is their versatility as a platform for multiple biomedical applications. Their strong immunogenicity in preclinical and early clinical studies, coupled with their ability to induce both humoral and cellular immune responses, makes them attractive candidates for developing vaccines against various diseases, including emerging infectious diseases and cancers (Nooraei et al., 2021). Moreover, HBcAg VLPs have demonstrated the capacity to efficiently encapsulate and deliver NAs and other therapeutic cargo, positioning them as promising vehicles for gene therapy and targeted drug delivery (Tariq et al., 2022). Their adaptability for surface modifications further enhances their potential in targeted therapies and personalized medicine approaches. This combination of immunogenic properties and carrier capabilities makes HBcAg VLPs a multifaceted tool in the development of advanced therapeutic strategies.

## 1.2 Nucleic Acid (NA)-Based Therapeutics

### 1.2.1 Types of Nucleic Acid Therapeutics

NA-based therapeutics represent a rapidly expanding class of treatments that target the genetic basis of diseases. These therapies are designed to modulate gene expression or function through various mechanisms, providing opportunities to treat conditions that were previously considered untreatable (Rittiner et al., 2022; Khorkova et al., 2023). The major types of NA therapeutics include messenger RNA (mRNA), antisense oligonucleotides (ASOs), small interfering RNA (siRNA), and other emerging modalities like aptamers and gene editing tools.

mRNA Therapeutics are designed to introduce synthetic mRNA into cells, where it is translated into a therapeutic protein. This approach has gained significant attention, particularly with the development of mRNA vaccines for COVID-19 (Fortner and Schumacher, 2021; Teo, 2022). mRNA therapeutics offer the advantage of rapid development and scalability, and they can be tailored to produce a wide range of proteins, from antigens in vaccines to therapeutic proteins for treating genetic disorders (Qin et al., 2022; Wang et al., 2023). Antisense Oligonucleotides (ASOs) are short, single-stranded DNA or RNA molecules that bind to complementary sequences of RNA. By binding to their target RNA, ASOs can modulate gene expression in several ways, including degradation of the RNA through RNase H activation, blocking translation, or altering splicing patterns. ASOs have shown promise in treating genetic diseases, such as spinal muscular atrophy (SMA) and Duchenne muscular dystrophy (DMD), by targeting specific mRNA sequences associated with these conditions (Matsuo, 2021; Khorkova et al., 2023; Aartsma-Rus, 2024). Small Interfering RNA (siRNA) is a class of double-stranded RNA molecules that induce gene silencing through RNA interference (RNAi). When introduced into cells, siRNA molecules are incorporated into the RNA-induced silencing complex (RISC), which then binds to and degrades target mRNA, effectively silencing the expression of specific genes. siRNA has been successfully used to reduce the expression of disease-related genes, and several siRNA-based therapies have gained clinical approval, including treatments for hereditary transthyretin-mediated amyloidosis and hypercholesterolemia (Hu et al., 2020; Friedrich and Aigner, 2022). Other NA-based modalities, such as aptamers (which bind to specific targets with high affinity) and gene editing tools like CRISPR-Cas9, are also being explored for their therapeutic potential (Zhou and Rossi, 2017; Li et al., 2023). These tools offer precise targeting capabilities, allowing for the correction of genetic mutations or the modulation of gene function at the DNA level.

### 1.2.2 Challenges in Delivery

Despite the promising potential of NA-based therapeutics, their clinical application faces significant challenges, particularly in the efficient and targeted delivery of these molecules to specific cells or tissues. One of the primary obstacles is the degradation by nucleases. NAs are susceptible to degradation by enzymes found in biological fluids, which can significantly reduce their therapeutic efficacy (Hueso et al., 2021). To overcome this, modifications to the NA structure, such as backbone modifications or the use of protective carriers, are often employed (Kulkarni et al., 2021). Inefficient cellular uptake is another major challenge. NAs, due to their size and negative charge, struggle to cross the cellular membrane. This is further complicated by the need for the therapeutic NAs to reach the intracellular target, such as the cytoplasm or nucleus, to exert their effect (Xu and Anchordoquy, 2011; Hueso et al., 2021). Strategies to enhance uptake include the use of delivery vehicles like lipid nanoparticles, viral vectors, and, more recently, VLPs (Kulkarni et al., 2021). Off-target effects pose additional concerns. When NAs bind to unintended targets, they can cause unintended gene silencing or activation, leading to adverse effects (Winkle et al., 2021). This challenge necessitates the need for highly specific delivery systems that can target the right cells and tissues while avoiding others. Moreover, the immune response elicited by exogenous NAs can lead to inflammation and other side effects, which complicates their therapeutic use (Hueso et al., 2021). Researchers are continually working to develop delivery systems that can shield NAs from immune detection while ensuring they reach their target cells (Xu and Anchordoquy, 2011).

### 1.2.3 VLPs as Delivery Vehicles

VLPs have emerged as a promising solution to the challenges associated with the delivery of NA therapeutics. Among the various VLPs, those based on the HBcAg have garnered particular interest due to their ability to efficiently package and deliver NAs. VLPs can encapsulate NAs within their capsid, protecting them from degradation by nucleases in the extracellular environment (An et al., 2024). This encapsulation also helps to shield the NAs from immune recognition, thereby reducing the risk of an adverse immune response (Gutkin et al., 2021). Additionally, the surface of VLPs can be modified to enhance their targeting ability, enabling the delivery of NAs to specific cell types or tissues (Nooraei et al., 2021). HBcAg VLPs are particularly advantageous due to their unique structural properties. These VLPs can self-assemble into particles that can efficiently encapsulate NAs, including mRNA, siRNA, and antisense oligonucleotides (Banskota et al., 2022). The ability of HBcAg VLPs to deliver these therapeutics to target cells has been demonstrated in several studies, showcasing their potential to improve the efficacy of NA-based therapies (Banskota et al., 2022; An et al., 2024). Furthermore, HBcAg VLPs can be engineered to display specific ligands or antibodies on their surface, enhancing

their ability to target specific cells or tissues (Nooraei et al., 2021). This targeting capability is crucial in reducing off-target effects and increasing the therapeutic index of NA-based treatments. By directing the therapeutic payload to the desired site of action, HBcAg VLPs minimize exposure to non-target tissues, thereby reducing potential side effects (Banskota et al., 2022; An et al., 2024). The use of VLPs, especially HBcAg VLPs, in NA delivery also opens up possibilities for co-delivery strategies, where multiple therapeutic agents can be delivered simultaneously to achieve synergistic effects (Nooraei et al., 2021; An et al., 2024). This approach can be particularly beneficial in complex diseases, such as cancer, where combination therapies are often required for effective treatment. In summary, VLPs, and particularly HBcAg VLPs, offer a versatile and effective platform for the delivery of NA therapeutics. Their ability to protect NAs from degradation, enhance cellular uptake, and provide targeted delivery makes them an attractive option for overcoming the current challenges in the field of NA-based therapy (Gutkin et al., 2021; Nooraei et al., 2021; Banskota et al., 2022; An et al., 2024).

## 1.3 Phase Behaviour and Stability of VLPs

### 1.3.1 Phase Behaviour and Capsid Stability in Different Conditions

The stability of VLP capsids is a critical factor influencing their utility in various applications, particularly in the fields of vaccine development, gene therapy, and drug delivery. VLP capsids, which are composed of self-assembling viral proteins, must maintain structural integrity under different conditions to ensure their effectiveness as therapeutic vehicles. Further, it is crucial for understanding how these particles can be manipulated during production and purification processes. Several factors influence the stability of VLP capsids, with pH being one of the most significant. VLPs are typically stable within a specific pH range, beyond which their capsid structure can either disassemble or aggregate (Newman et al., 2003). For example, a lower pH can lead to protonation of amino acid residues, causing repulsion between capsid subunits and potentially leading to disassembly. Conversely, at higher pH levels, deprotonation may reduce inter-subunit interactions, similarly destabilizing the capsid (Ausar et al., 2006). Therefore, maintaining an optimal pH during storage and application is essential to preserve VLP integrity.

Ionic strength also plays a crucial role in capsid stability. The presence of salts in the solution can shield electrostatic interactions between charged residues on the VLP surface, stabilizing the capsid structure. However, if the ionic strength is too high, it can lead to the aggregation of VLPs due to the neutralization of surface charges that otherwise keep particles repelling each other (Hashemi et al., 2021). This balance is particularly important in the formulation of VLPs for



therapeutic use, where maintaining the correct ionic conditions can prevent unwanted aggregation and preserve functionality. Urea, a chaotropic agent, is instrumental in modulating the phase behavior of HBcAg VLPs by disrupting non-covalent interactions like hydrogen bonds and hydrophobic interactions. At low to moderate urea concentrations, HBcAg VLPs may undergo partial destabilization without complete capsid disassembly. Higher urea concentrations can cause full dissociation of VLPs into dimeric subunits, which is useful for purification and removal of contaminants. During downstream processing, urea-induced disassembly followed by gradual removal of urea allows VLPs to reassemble with encapsulated NAs, supporting applications in gene delivery (Rüdt et al., 2019; Zhang et al., 2021a). Managing urea concentration also helps control undesirable aggregation; intermediate levels may lead to VLP aggregation rather than clean dissociation, complicating purification. With precise control, urea enables transitions between capsid, dimer, and aggregated states, offering valuable flexibility in HBcAg VLP purification and loading, ensuring stable, high-purity products optimized for therapeutic use (Rüdt et al., 2019; Hillebrandt et al., 2021; Zhang et al., 2021b). Another important factor is temperature, as VLPs are sensitive to thermal denaturation. Elevated temperatures can cause the capsid proteins to unfold or misalign, leading to a loss of structural integrity (Newman et al., 2003). This thermal sensitivity necessitates careful control of storage conditions to ensure VLP stability over time. Finally, NA binding significantly impacts VLP stability. In many VLPs, including HBcAg VLPs, the encapsidation of NAs contributes to the overall stability of the particle (Newman et al., 2003). The binding of NAs to the inner surface of the capsid can enhance structural integrity by providing additional stabilizing interactions. However, this interaction must be carefully managed, as too much NA can lead to overloading and potential destabilization of the capsid.

### **1.3.2 Impact of NA Binding on VLP Stability**

The binding of NAs to VLPs, particularly to HBcAg VLPs, has a profound impact on their structural stability and behavior during downstream processing (Newman et al., 2003). The encapsulation of NAs within VLPs not only enhances the particle's structural integrity (Zlotnick et al., 1997; Porterfield et al., 2010) but also introduces specific challenges that must be addressed to optimize therapeutic efficacy. NA binding to VLPs can stabilize the capsid by providing additional non-covalent interactions between the NA and the inner surface of the VLP. This interaction often results in a more rigid and stable capsid structure, which can be advantageous for the protection of the NA cargo. In HBcAg VLPs, the interaction between the capsid and encapsulated NAs is critical for maintaining the structural integrity of the particle under various physiological conditions, such as those encountered during *in vivo* delivery. However, this stabilization comes with trade-offs. The binding of NAs can also

affect the VLP's behavior in downstream processes. For instance, during purification, the additional mass and charge contributed by the NAs can alter the VLP's sedimentation rate in ultracentrifugation, its mobility in electrophoretic techniques, and its interaction with chromatographic media (Huhti et al., 2010). These changes can complicate the separation of VLPs from impurities, requiring the optimization of purification protocols to account for the altered physicochemical properties of NA-loaded VLPs. Moreover, the loading capacity of VLPs for NAs is not unlimited. Overloading VLPs with NAs can lead to destabilization of the capsid, resulting in premature disassembly or aggregation (He et al., 2022). This phenomenon is particularly relevant for HBcAg VLPs, where the balance between NA binding and capsid stability must be carefully controlled to prevent aggregation or loss of encapsulated cargo during processing. In summary, while NA binding enhances the stability of HBcAg VLPs, it also introduces complexities that must be carefully managed. The impact of NA binding on VLP stability, phase behavior, and downstream processing underscores the importance of thorough characterization and optimization in the development of VLP-based therapies.

## 1.4 Downstream Processing of VLPs

### 1.4.1 Purification Challenges

The production of VLPs for therapeutic applications, particularly those loaded with NAs, presents several purification challenges. One of the primary issues is the contamination with NA<sub>hc</sub> and proteins. VLPs are typically produced in host cells, such as bacteria, yeast, insect, or mammalian cells, which can lead to the co-purification of unwanted host cell components (Hillebrandt et al., 2020; Nooraei et al., 2021). NA<sub>hc</sub> are a significant concern because they can co-package within the VLPs, especially during the production process. This not only reduces the yield of VLPs loaded with the desired therapeutic NAs but also poses risks of immunogenicity and other adverse reactions when administered to patients. Additionally, these unwanted NAs can complicate the characterization and quantification of the therapeutic VLPs, making it difficult to ensure consistent and reproducible dosing (He et al., 2022). Host cell proteins are another source of contamination that can affect the safety and efficacy of VLP-based therapeutics. These proteins can associate with VLPs during assembly or purification, potentially eliciting an immune response in patients or interfering with the therapeutic action of the VLPs (Nooraei et al., 2021). The presence of host cell proteins can also affect the stability and shelf life of the VLP product, necessitating rigorous purification processes to remove these impurities (Hillebrandt et al., 2020). Another challenge is maintaining the integrity and functionality of VLPs during the purification process. VLPs are complex, self-assembling structures, and their stability can be affected by

changes in pH, ionic strength, and other conditions commonly encountered during purification (Rohovie et al., 2017). Harsh conditions can lead to VLP disassembly or structural alterations, which may compromise their ability to encapsulate and deliver NAs effectively (Hillebrandt et al., 2020). The scale-up of VLP production for clinical and commercial applications further exacerbates these challenges. As production scales increase, the likelihood of contamination and the difficulty of achieving consistent purification also increase (Nooraei et al., 2021). This necessitates the development of robust, scalable purification methods that can efficiently produce high-purity VLPs without compromising their structural integrity or functionality (Rohovie et al., 2017; Hillebrandt et al., 2020).

#### **1.4.2 Purification Techniques**

To address the purification challenges associated with VLP production, a variety of purification techniques have been developed and optimized. These methods aim to selectively isolate VLPs from contaminants while preserving their structural and functional properties. Ultracentrifugation is one of the most traditional and widely used methods for VLP purification. This technique exploits the differences in size and density between VLPs and other cellular components. Through high-speed centrifugation, VLPs can be separated based on their sedimentation coefficients. Gradient ultracentrifugation, using density gradients such as sucrose or cesium chloride, allows for more precise separation, ensuring higher purity of the VLPs (Roldao et al., 2020). However, ultracentrifugation can be time-consuming, labor-intensive, and challenging to scale up, making it less suitable for large-scale production. Chromatography techniques, particularly affinity, ion-exchange, and size-exclusion chromatography, are commonly employed in VLP purification. Affinity chromatography can be highly specific, using ligands that bind to unique epitopes on the VLP surface, thereby achieving high purity. Ion-exchange chromatography separates particles based on their charge, which can be useful for removing host cell proteins and NAs. Size-exclusion chromatography (SEC), on the other hand, separates molecules based on size, effectively isolating VLPs from smaller contaminants (Hillebrandt and Hubbuch, 2023). Recent advancements in chromatography, such as the development of membrane-based chromatography and monolithic columns, offer faster processing times and better scalability for industrial applications. Precipitation methods, such as polyethylene glycol (PEG) precipitation, are also used to concentrate VLPs from crude extracts by exploiting their solubility properties. This method is relatively simple and cost-effective, making it attractive for initial VLP recovery (Hashemi et al., 2021). However, it is often followed by more refined purification steps, such as chromatography, to achieve the necessary purity levels (Hillebrandt et al., 2020). Recent advancements have focused on developing purification strategies tailored to the unique properties

of VLPs. For example, capture and release methods using specific binding interactions between VLPs and ligands immobilized on solid supports are being explored to enhance purification efficiency (Lorenzo et al., 2022). Additionally, flow-through chromatography, where contaminants bind to the column matrix while VLPs flow through, offers a high-throughput alternative for large-scale purification (Hillebrandt et al., 2020). Combining several of these techniques into integrated purification platforms, is also being explored to improve scalability and reduce processing time (Hillebrandt et al., 2020). These methods aim to streamline the purification process while maintaining high yields and purity, which is critical for the commercial viability of VLP-based therapeutics.

### 1.4.3 Purification Process of VLPs

The production of VLPs intended for NA delivery applications involves a complex, multi-step purification process that aims to achieve high purity and precise loading of therapeutic NAs. Following the intra-cellular formation of VLPs in an expression system, such as *E. coli*, yeast or plant cells (Effio and Hubbuch, 2015), a commonly used VLP purification process consists of cell lysis, ultracentrifugation or precipitation, disassembly and reassembly, polishing and formulation (McCarthy et al., 1998; Zhao et al., 2012a; Hillebrandt et al., 2020; Zhang et al., 2021b). The additional requirements for NA<sub>hc</sub> depletion and NA<sub>ther</sub> loading introduce further complexity, necessitating specialized steps that enhance both the purity and functionality of VLPs. A typical production process is shown in Figure 1.1. To improve purity, especially

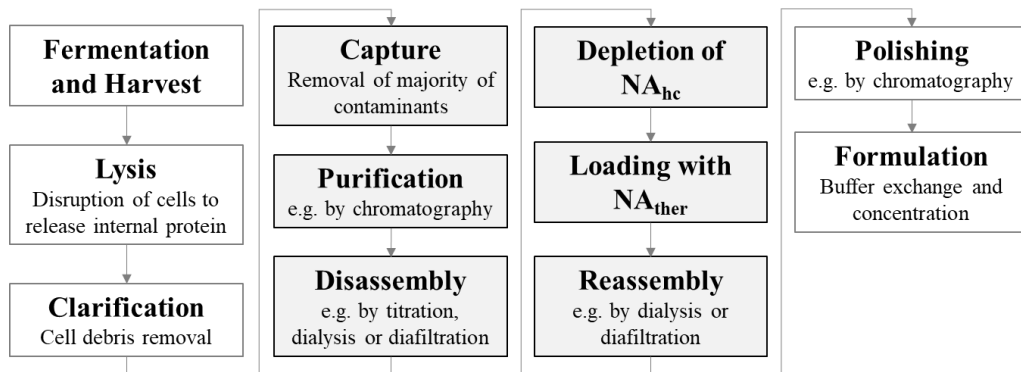


Figure 1.1 A typical VLP production process with central processing steps for VLPs for gene delivery marked in grey. NA<sub>hc</sub>, host cell-derived nucleic acid; NA<sub>ther</sub>, therapeutic nucleic acid; VLP, virus-like particle

for VLPs designed for NA<sub>ther</sub> delivery such as HBcAg VLPs e.g., the disassembly process is employed. Disassembly involves breaking down VLPs into their individual protein subunits (Figure 1.2), exposing the particle interior where unwanted NA<sub>hc</sub> and other impurities may be sequestered (McCarthy et al., 1998; Hillebrandt et al., 2021). This step can be achieved by altering environmental conditions, such as pH and ionic strength, or by adding denaturing agents (McCarthy et al., 1998; Zhao et al., 2012b). Disassembly not

only allows for the removal of non-specifically packaged  $NA_{hc}$  but also enables a controlled environment for subsequent loading of  $NA_{ther}$ , making it a crucial purification step for therapeutic applications (Zhao et al., 2012b).

During expression in host cells, HBcAg VLPs often encapsulate undesired NAs, such as DNA or RNA, which can interfere with therapeutic efficacy and present immunogenic risks. After disassembly, these  $NA_{hc}$  are exposed and can be selectively removed using methods like alkaline treatment or LiCl precipitation (Porterfield et al., 2010; Strods et al., 2015). In parallel, nuclease enzymes degrade residual  $NA_{hc}$ , yielding a purer VLP preparation before reassembly (Zhang et al., 2021a). This depletion process is essential to ensure that the final VLP product is free of unintended NAs that could compromise its therapeutic utility (Zhao et al., 2012a; Hillebrandt et al., 2021). Once unwanted NAs are depleted, VLPs can be loaded with specific  $NA_{ther}$  - such as mRNA, siRNA, or antisense oligonucleotides - during reassembly (Figure 1.2). This loading process is carefully optimized by controlling assembly conditions, such as pH, ionic strength, and the ratio of NAs to protein subunits (Porterfield et al., 2010; Petrovskis et al., 2021).

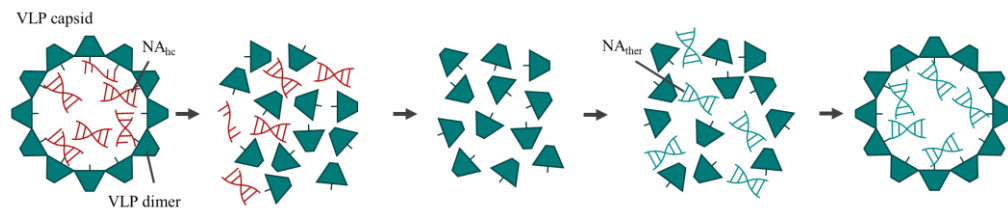


Figure 1.2 Overview on central processing steps for HBcAg VLPs for gene delivery. The VLP capsid with encapsulated  $NA_{hc}$  become disassembled into their individual protein subunits, for HBcAg VLPs protein dimers. Unwanted NAs and other impurities may be depleted. The purified dimers are mixed with  $NA_{ther}$  and reassembled into VLP capsids loaded with  $NA_{ther}$ . HBcAg, Hepatitis B core Antigen; NA, nucleic acid;  $NA_{hc}$ , host cell-derived nucleic acid;  $NA_{ther}$ , therapeutic nucleic acid; VLP, virus-like particle

The reassembly of VLPs is initiated by restoring conditions that favor the self-assembly of protein subunits around the loaded  $NA_{ther}$ . This reassembly step allows for precise control over particle structure, stability, and cargo encapsulation, with variables such as the protein-to-NA ratio and assembly environment playing critical roles (McCarthy et al., 1998). Additionally, stabilizing agents can be introduced to improve VLP stability, and surface modifications can enhance cell targeting, thereby increasing therapeutic potential (Zhao et al., 2012b). Through careful adjustment of reassembly parameters, VLPs are produced with optimal characteristics for NA delivery, ensuring both purity and functional performance in therapeutic applications (Zhao et al., 2012b; Hillebrandt et al., 2021).

The disassembly-reassembly purification cycle in VLP production offers a powerful strategy to generate highly pure and specifically loaded VLPs. By addressing the challenges of removing host cell-derived impurities and precisely loading NA<sub>ther</sub>, this approach allows for the creation of VLPs tailored to various gene delivery applications. The downstream processing steps of VLP purification, including advanced purification and reassembly techniques, shall ensure the production of high-quality VLPs that meet the stringent requirements for clinical and commercial use (McCarthy et al., 1998; Mach et al., 2006; Zhao et al., 2012b; Hillebrandt et al., 2021).

## 1.5 Analytical Techniques for VLP Characterization

The characterization of VLPs, due to their structural complexity and diverse applications, requires a variety of analytical techniques to assess properties such as particle size, purity, stability, and encapsulated NA content. Key analytical methods include electrophoretic techniques, spectroscopic methods, chromatographic separation, light scattering, and imaging techniques, each contributing unique insights into VLP characteristics.

### 1.5.1 Electrophoretic Techniques

Native Agarose Gel Electrophoresis (NAGE) is a versatile technique used to analyze VLP size, integrity, and NA loading under native conditions, preserving VLP structure (Strods et al., 2015; Schumacher et al., 2018). NAGE operates on the principle that macromolecules migrate through a gel matrix of agarose when subjected to an electric field, with migration influenced by size and charge. In the case of VLPs, the technique allows for the distinction between empty and NA-loaded particles based on differences in charge and size, as NAs contribute additional negative charge and mass to the particles (Carvalho et al., 2022). Staining methods, such as ethidium bromide or SYBR Green, enable visualization of NAs within VLPs, facilitating qualitative assessments of loading efficiency.

Sodium dodecyl sulfate–polyacrylamide gel electrophoresis (SDS-PAGE) is an essential technique for assessing VLP protein composition and purity. By denaturing proteins with SDS, which provides a uniform negative charge, SDS-PAGE separates polypeptides based on their molecular weight, regardless of their native structure. For VLP analysis, SDS-PAGE can confirm the presence and purity of the capsid protein, evaluate the success of purification steps, and identify any protein contaminants. Additionally, SDS-PAGE helps ensure the integrity of the capsid protein during VLP production, as degradation or truncation can negatively impact VLP function (Schumacher et al., 2018).

### 1.5.2 UV/Vis Spectroscopy

UV/Vis spectroscopy is widely used to quantify VLP concentration and determine NA content within VLPs (Porterfield et al., 2010; Porterfield and Zlotnick, 2010; Rüdts et al., 2019). The absorbance at 280 nm is typically employed to measure the concentration of capsid proteins based on the presence of aromatic amino acids (e.g., tryptophan and tyrosine), while absorbance at 260 nm indicates NA presence. The A260/A280 ratio provides insights into the relative concentrations of proteins and NAs, assisting in the estimation of encapsulation efficiency. Furthermore, UV/Vis spectroscopy offers a non-destructive method for assessing the stability of VLPs over time by monitoring changes in absorbance profiles, which may indicate degradation or aggregation (Samandoulgou et al., 2015; Rüdts et al., 2019).

### 1.5.3 Fluorescence Assays

Fluorescence assays are widely used to quantify VLP-encapsulated NAs and assess particle stability (Rulli et al., 2007; Ladd Effio et al., 2015; Zhang et al., 2021a). Fluorescent dyes that bind NAs, such as SYBR Green or PicoGreen, emit fluorescence upon binding, providing a direct measure of NA concentration within VLPs. This technique allows researchers to quantify encapsulation efficiency, particularly when comparing loaded versus unloaded VLPs. In addition, fluorescence assays can assess VLP stability by monitoring changes in fluorescence intensity over time, indicative of NA release or degradation. Coupled with a fluorescence spectrophotometer, fluorescence assays offer high sensitivity, making them ideal for low-concentration measurements in VLP studies.

### 1.5.4 Quantitative PCR

Quantitative PCR (qPCR) is a sensitive molecular technique used to quantify the NAs encapsulated within VLPs (Huhti et al., 2010). By amplifying specific sequences of DNA or RNA, qPCR allows for precise quantification of NA load in VLP samples. Fluorescent probes or dyes (e.g., SYBR Green) track the amplification process in real-time, with fluorescence intensity correlating with NA concentration. This technique is particularly useful for validating encapsulation efficiencies and standardizing VLP production. In addition to quantification, qPCR can be used to confirm the integrity of the encapsulated genetic material, as amplification efficiency reflects the intactness of the NAs within the VLPs (Shmidt and Egorova, 2022).

### 1.5.5 Chromatographic Separation

Chromatography is a fundamental technique in VLP research, essential for purifying, analyzing, and quantifying VLPs and their components. Various chromatographic methods - including ion-exchange, size-exclusion, affinity,

and reversed-phase chromatography - each contribute unique capabilities in isolating VLPs, removing impurities, and characterizing structural and compositional attributes.

Ion-Exchange Chromatography (IEX) separates VLPs based on their charge by exploiting interactions between charged groups on the VLP surface and the stationary phase. By adjusting buffer pH and ionic strength, IEX can distinguish loaded from unloaded particles, as the encapsulated NAs alter the overall charge of VLPs. IEX is particularly useful in separating VLPs from host cell contaminants, aiding in the downstream purification process.

Size-Exclusion Chromatography (SEC), also known as gel filtration, separates particles by hydrodynamic size. This technique enables the isolation of VLPs from aggregates, proteins, and other impurities based on their size differences, without disrupting VLP structure (Figure 1.3). SEC is often combined with light scattering for determining molecular weight, aggregation state, and hydrodynamic radius, which are crucial for assessing VLP integrity and homogeneity (Dietrich et al., 2024).

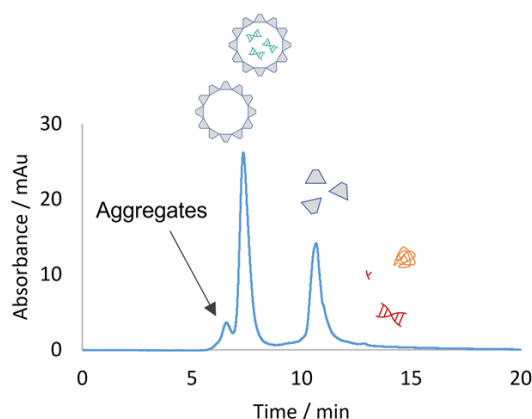


Figure 1.3 SEC chromatogram displaying the separation of VLP capsids, aggregates, VLP subunits and other impurities. SEC, size-exclusion chromatography; VLP, virus-like particle

Affinity chromatography leverages specific interactions between VLPs and immobilized ligands on the stationary phase. VLPs modified with affinity tags (e.g., His-tag) or displaying specific surface proteins can be selectively bound and eluted (Zhang et al., 2021b). This technique provides high specificity, making it ideal for purifying engineered VLPs or isolating VLPs with defined surface properties from complex mixtures.

Reversed-Phase (RP) Chromatography is valuable for quantifying VLPs and analyzing their protein content. In RP chromatography, the stationary phase is nonpolar (hydrophobic), while the mobile phase is relatively polar, typically a gradient of water and organic solvents such as acetonitrile. Hydrophobic interactions between the VLP capsid proteins and the nonpolar stationary phase



enable separation based on protein hydrophobicity (Yuan et al., 1998; Shytuhina et al., 2014; Ladd Effio et al., 2015).

Each chromatography method contributes distinct advantages in the characterization and purification of VLPs. When used in combination, these techniques enable high-resolution separation, precise quantification, and improved scalability, supporting the standardization and large-scale production of VLPs for therapeutic applications.

### **1.5.6 Dynamic Light Scattering Techniques**

Dynamic Light Scattering (DLS) measures the hydrodynamic size and size distribution of particles, including VLPs, by analyzing fluctuations in scattered light intensity due to particle Brownian motion. When a laser beam passes through a solution of VLPs, the particles scatter light in all directions. The intensity of the scattered light fluctuates based on the speed of the particles' random motion, which is influenced by particle size - smaller particles move more quickly than larger ones. DLS uses these fluctuations to calculate the diffusion coefficient of the particles, which is then used to determine the hydrodynamic radius and polydispersity index of the VLPs. The polydispersity index is a measure of the sample's size distribution, with values below 0.1 indicating a monodisperse system and values closer to 0.3 or higher suggesting a broader size distribution, often due to aggregation or polydispersity in VLP preparations. DLS is thus valuable for ensuring batch consistency and optimizing purification steps to obtain homogenous VLP preparations.

Zeta potential is a measure of the surface charge of particles in suspension and is crucial for understanding VLP stability and aggregation behavior. It is typically measured using electrophoretic light scattering, a variant of DLS that applies an electric field to induce particle movement. The zeta potential is calculated from the velocity of this movement, reflecting the balance between attractive and repulsive forces on the particle surface. For VLPs, zeta potential is indicative of surface charge properties influenced by factors such as capsid composition, pH, and ionic strength of the medium. A high absolute zeta potential - positive or negative - suggests good colloidal stability, as repulsive forces prevent particle aggregation. Conversely, a low zeta potential may indicate a tendency toward aggregation, affecting VLP homogeneity, stability, and potential bio-distribution in vivo (Rüdt et al., 2019). Zeta potential measurements are therefore essential for optimizing buffer conditions and predicting long-term stability of VLP formulations.

### 1.5.7 Transmission Electron Microscopy

Transmission Electron Microscopy (TEM) offers high-resolution images of VLP morphology, size, and structural integrity (Porterfield et al., 2010; Strods et al., 2015; Hillebrandt et al., 2020; Zhang et al., 2021b). With electron beams producing nanometer-resolution images, TEM enables direct observation of VLP assembly, while advanced cryo-EM preserves VLP structure under near-native conditions. Negative staining highlights VLP surface features, confirming particle assembly and homogeneity.

### 1.5.8 Challenges in Quantification of VLPs and Bound Nucleic Acids (NAs)

Absolute quantification of VLP proteins and their encapsulated NAs is essential to ensure reliable and reproducible VLP production, which is critical for both research and therapeutic applications. Precise measurement of VLPs and their NA cargo enables consistent dosing, supporting accurate assessments in preclinical and clinical studies and ensuring therapeutic efficacy. Furthermore, absolute quantification is integral to optimizing production and purification processes. By accurately tracking yield and purity at each stage, it becomes possible to identify inefficiencies and enhance manufacturing protocols. This is especially important when scaling up for clinical and commercial use, where achieving high yields and purity is essential to meet regulatory standards and guarantee patient safety.

UV/Vis spectroscopy is a common tool to quantify proteins and NAs, utilizing the absorption maxima of proteins at 280 nm and NAS at 260 nm. In combination with high-performance liquid chromatography (HPLC) methods, UV-spectra allow to quantify different HBcAg VLP protein species (capsids and dimers) and impurities such as host cell proteins and free NAs by size exclusion chromatography (Rüdt et al., 2019; Hillebrandt et al., 2020, 2021; Hillebrandt and Hubbuch, 2023). However, UV/Vis spectroscopy is inherently unable to absolutely quantify HBcAg VLP proteins with bound NAs without prior quantitative separation of proteins and NAs, e.g. by chromatography. In the absence of a successful separation the overlapping signals of the proteins and NAs in the relevant wavelength region of the UV spectra only allow for a relative quantification Figure 1.4.

Relative analysis of the A<sub>260</sub>/A<sub>280</sub> ratio of HBcAg proteins and bound NA<sub>hc</sub> has been used to evaluate the purity of the VLPs after the depletion of NA<sub>hc</sub> (Porterfield et al., 2010; Zhang et al., 2021b, 2021a). For the loading of HBcAg VLPs with NA<sub>ther</sub> of known nucleotide sequence, a method to approximate the absolute amounts of protein and NA was proposed in literature (Porterfield and Zlotnick, 2010) and used to estimate protein and NA composition (Strods et al., 2015; Petrovskis et al., 2021). However, this method is not suited for a precise

quantification of VLP proteins and (i) non-specific  $NA_{hc}$ . Nor can it be applied to (ii) mixtures of residual undesired  $NA_{hc}$  and  $NA_{ther}$  or (iii) mixtures of various types of  $NA_{ther}$ . This information is, however, required for evaluating the successful depletion of  $NA_{hc}$  and possible HBcAg protein loss during the removal, as well as the subsequent effective loading of the VLPs with  $NA_{ther}$ .

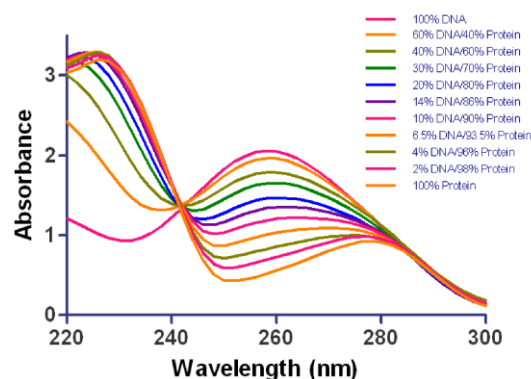


Figure 1.4: Absorbance spectral scans of purified dsDNA, protein, or a mixture. Samples contained purified herring sperm dsDNA, BSA protein, or a DNA/protein mixture at varying ratios (w/w). Figure taken from Brescia, 2021.

While dye-based fluorescence assays are commonly used for NA quantification, they can be sensitive to contaminants that interfere with the binding of the dye to its target (Taylor et al., 2010). In literature, a RiboGreen assay was used for the quantification of RNA in murine leukemia VLPs (Rulli et al., 2007). Before quantification, the RNA was extracted according to a NA extraction protocol including proteinase K lysis and phenol-chloroform extraction. In contrast, no prior extraction of DNA was required in a study by Effio and Hubbuch, 2015, as it was not bound to the VLPs and did not interfere with the binding of the dye to the DNA. Here, a PicoGreen assay was used for the quantification of DNA impurities in HBcAg VLP purification. However, for HBcAg VLPs with NA binding region for gene delivery and thus bound NAs, appropriate NA extraction seems to be necessary to quantify the NAs precisely. This can be concluded from the conflicting results of the relative analysis of the  $A_{260}/A_{280}$  ratio with UV-spectroscopy and a dye-based fluorescence assay without prior extraction of the HBcAg VLPs and bound  $NA_{hc}$  (Zhang et al., 2021a).



# 2

## Thesis Outline

### 2.1 Research Proposal

Virus-like particles (VLPs) have become an important platform in biomedical research, especially in vaccine development and gene delivery. VLPs are composed of viral structural proteins and replicate the architecture of native viruses, but they do not contain infectious material, making them both safe and highly immunogenic. In recent years, the demand for effective and targeted delivery systems for nucleic acid (NA)-based therapeutics, such as mRNA, siRNA, and antisense oligonucleotides, has risen. These therapeutics have the potential to treat various genetic and acquired diseases; however, challenges such as stability, cellular uptake, and targeted delivery limit their clinical use. VLPs show great potential due to their proven ability to incorporate and deliver foreign genetic material, and stable, repetitive surface structure with the potential for modifications to target specific cells or tissues.

However, effective VLP downstream processing is still challenging and needs to be addressed for the transition of VLPs from research to large-scale manufacturing for clinical applications, to fully harness VLPs as gene delivery vehicles. After intracellular formation of VLPs within expression systems such as *E. coli*, yeast, or plant cells, the purification process typically involves cell lysis, ultracentrifugation or precipitation, disassembly and reassembly, followed by polishing and formulation. Traditional purification methods commonly use size-exclusion chromatography and ultracentrifugation. Recent advances have introduced ultrafiltration-based unit operations that leverage size differences between impurities, VLP subunits, and VLP capsids, enabling more efficient and streamlined processing. However, VLPs designed for NA delivery require an even more intricate purification process, as they involve an additional step to load therapeutic nucleic acids (NA<sub>ther</sub>). A typical production process including the additional processing steps required for gene delivery applications is shown in Figure 1.1 in chapter 1.4.3 Figure 1.1.

Hepatitis B core antigen (HBcAg) VLPs are among the candidates being explored as nanocarriers for gene delivery. Typically, HBcAg VLPs are first disassembled, mixed with NA<sub>ther</sub>, and then reassembled to encapsulate the NAs within the VLP capsids. To achieve efficient loading, the full-length NA binding region of the wild-type HBcAg protein, known as Cp183 (comprising amino acids 1 to 183), or variants with minor amino acid substitutions, are often used. Additionally, HBcAg VLP constructs with varying lengths of this naturally occurring arginine-rich NA binding region are being investigated. A significant challenge in the purification process of these VLPs stems from the unintended association and encapsulation of host cell-derived nucleic acids (NA<sub>hc</sub>) during the spontaneous assembly of HBcAg protein subunits, so called dimers, during expression. To address this, various techniques such as lithium chloride precipitation, alkaline treatment, and enzymatic treatment, sometimes combined with affinity chromatography, are employed to separate the NAs derived from *E. coli*. The disassembled and purified VLP dimers are mixed with the NA<sub>ther</sub> and reassembled to load the VLPs. For HBcAg VLPs, reassembly is typically triggered either by increasing the ionic strength of the solution or by the presence of NAs.

This work focuses on the process development of HBcAg VLPs, specifically addressing the processing and analytical methods in the presence of NAs. Hereby, HBcAg VLPs with different lengths of the naturally occurring NA binding region are utilized for the following investigations.

The NA binding region seems to be necessary to encapsulate a considerable amount of NAs, but examining different lengths might be useful to overcome challenges during the purification process such as solubility issues for example. In the first study these HBcAg VLPs with different lengths of the NA binding region will be investigated regarding their size, charge and loading with NA<sub>hc</sub> encapsulated in the VLPs after formation in *E. coli*. Further, NA<sub>hc</sub> encapsulated in the HBcAg VLP after formation, as well as the length of the NA binding region itself, appear to have an influence on the HBcAg VLP purification process and especially on the disassembly reaction. The disassembly reaction is not only crucial for separating bound NAs and enabling effective loading with NA<sub>ther</sub>, but also for subsequent separating encapsulated impurities and improving structural integrity. Therefore, the influence of the NA binding region and bound NAs on early downstream purification steps such as precipitation, re-dissolution and especially the disassembly step will be investigated in the first study to enable successful depletion of NA<sub>hc</sub> and other impurities, and subsequent loading with NA<sub>ther</sub>.

To evaluate a successful depletion of NA<sub>hc</sub> and possible HBcAg protein loss during removal as well as subsequent effective loading of the VLPs with NA<sub>ther</sub> on the basis of e.g. the encapsulation efficiency or payload of the VLPs, a

precise absolute quantification of HBcAg VLPs and VLP-bound NAs is needed. UV/Vis spectroscopy, a common tool to quantify proteins and NAs, utilizing the absorption maxima of proteins at 280 nm and NAs at 260 nm, is inherently unable to absolutely quantify HBcAg VLP proteins with bound NAs without prior quantitative separation of proteins and NAs. In the absence of successful separation, the overlapping signals of proteins and NAs within the relevant UV spectral wavelength range permit only relative quantification. This method is commonly employed to assess VLP purity after NA<sub>hc</sub> depletion. However, this relative analysis is inadequate for precise quantification of VLP proteins and NAs, which is necessary to evaluate the efficiency of NA<sub>hc</sub> depletion, potential HBcAg protein loss during removal, and the subsequent effective loading of the VLPs with NA<sub>ther</sub>. Dye-based fluorescence assays are commonly used for NA quantification, but they can be sensitive to contaminants that interfere with the binding of the dye to its target. A variety of methods are used in for the extraction of NAs in molecular biology and may be applied for separation of NAs bound to proteins before quantification. For their use in molecular biology these methods do not necessarily require a high purity and recovery. The potential loss of NA during the extraction process is often irrelevant for the further processing. However, for accurate quantification of NAs bound to VLP proteins, the NA solution must be of high purity after the extraction and the loss of NAs during these procedures would need to be minimized. In the second study two quantitative analytics based on chromatography followed by UV/Vis, and silica spin column extraction followed by dye-based fluorescence assay quantification will be developed to enable precise absolute quantification of HBcAg VLPs and VLP-bound NAs. This allows for the evaluation of the depletion of NA<sub>hc</sub> and possible HBcAg protein loss during removal, as well as subsequent effective loading of the VLPs with NA<sub>ther</sub>.

The depletion of the NA<sub>hc</sub> bound and encapsulated into HBcAg VLPs is essential to prevent potential side effects and to enable the subsequent loading of the VLPs with NA<sub>ther</sub>. Several techniques have been reported in the literature to remove NA<sub>hc</sub> using various approaches, though these studies typically assess NA<sub>hc</sub> removal qualitatively. In the third study of this work, newly developed analytical methods for the absolute quantification of HBcAg VLPs and VLP-bound NAs will be applied to evaluate a range of NA<sub>hc</sub> depletion techniques from the literature, focusing on both NA<sub>hc</sub> removal efficiency and VLP protein recovery. Additionally, a novel chromatography-based technique for NA depletion will be developed and compared to existing methods.

The successful depletion of NA<sub>hc</sub> allows for mixing the HBcAg VLP dimers with NA<sub>ther</sub> and reassembly to loaded VLPs. The reassembly of HBcAg VLPs, both with and without various types of NAs, has been demonstrated and assessed using native agarose gel electrophoresis (NAGE), dynamic light scattering (DLS), and transmission electron microscopy (TEM). However,

current literature lacks comprehensive data on reassembly yields for loaded HBcAg VLPs and other VLPs being investigated as delivery platforms. Furthermore, an in-depth analysis of the factors influencing the reassembly process - such as the presence of the NA binding region, the incorporation of NAs, and changes in ionic strength in the surrounding medium - has not been thoroughly explored. The fourth story of this work will investigate the loading and reassembly of HBcAg VLPs as a function of a NA binding region, NAs and the ionic strength in the liquid phase. Reassembly yields and the loading efficiency with model NA<sub>ther</sub> will be evaluated with the novel absolute quantification methods and buffer exchange will be conducted by centrifugal concentrators for stepwise buffer exchange to evolve the process towards large scale production solutions, such as tangential flow filtration.

In summary, expected outcomes of this research include an enhanced understanding of the influence of the presence of a NA binding region and NAs onto the purification process. It will possibly lead to a comprehensive purification strategy that effectively removes contaminants while preserving VLP integrity, novel or improved analytical techniques for accurately quantifying VLPs and their encapsulated NAs, and insights into the binding characteristics of NAs within HBcAg VLPs under various conditions. This work will promote the process development for VLPs as gene delivery vectors towards efficient downstream processing, one step further for the transition of the VLPs from research to large-scale manufacturing for clinical applications.

## 2.2 Comprehensive Overview

This section provides an overview of the manuscripts written within the scope of this thesis. Chapters 3 to 6 were published as outlined below. A list of the author contributions signed by the respective authors is attached to the examination copy of this thesis.

### **Chapter 3: Effects of Different Lengths of a Nucleic Acid Binding Region and Bound Nucleic Acids on the Phase Behavior and Purification Process of HBcAg Virus-Like Particles**

Angela Valentic, Jakob Müller, Jürgen Hubbuch

*Frontiers in Biotechnology and Bioengineering (2022), Volume 10*

This study investigates how variations in the length of the NA binding region of HBcAg VLPs and the encapsulation of NA<sub>hc</sub> impact VLP characteristics, including size, zeta potential, phase behavior, and the purification process. HBcAg VLPs with different lengths of the NA binding region were produced in *E. coli* and assessed for their loading with NA<sub>hc</sub>. The study reveals a non-linear



correlation between the length of the binding region and the amount of encapsulated NAs, with a distinct two-zone behavior observed. Despite the differences in encapsulated NAs, the phase behavior during ammonium sulfate precipitation was minimally affected, though disassembly reactions, crucial for structure homogeneity and efficient loading with  $NA_{ther}$ , were significantly influenced. This research underscores the complex interplay between the NA binding region, capsid stability, and disassembly efficiency, suggesting that precise control over these factors is critical for optimizing VLP production processes.

#### **Chapter 4: Absolute Quantification of HBcAg Virus-like Particles and Bound Nucleic Acids**

Angela Valentic, Nicola Böhner, Jürgen Hubbuch

*Journal of Viruses (2024), Volume 16, Issue 1*

The second study addresses the need for accurate and reliable quantification methods for HBcAg VLPs and bound NAs, which are essential for effective process development. Two novel analytical methods were developed: a silica spin column-based extraction procedure for NA quantification followed by dye-based fluorescence assay quantification and a reversed-phase high-performance liquid chromatography (RP-HPLC) method for simultaneous quantification of HBcAg proteins and bound NAs. Both methods overcome the limitations of existing analytical techniques and, in combination with already existing analytical tools, can support gene delivery process development for HBcAg VLPs.

#### **Chapter 5: Effective removal of host cell-derived nucleic acids bound to hepatitis B core antigen virus-like particles by heparin chromatography**

Angela Valentic, Jürgen Hubbuch

*Frontiers in Biotechnology and Bioengineering (2024), Volume 12*

During VLP formation,  $NA_{hc}$  can become encapsulated, necessitating their removal before loading  $NA_{ther}$ . Existing methods for  $NA_{hc}$  removal, such as enzymatic treatments, alkaline treatment, and lithium chloride precipitation, lack quantitative evidence of success and VLP protein recovery. In this study, a heparin chromatography-based process for efficient  $NA_{hc}$  removal from HBcAg VLPs was developed. Six HBcAg VLP constructs with varying NA binding region lengths and  $NA_{hc}$  loadings were evaluated. Our results demonstrated that heparin chromatography outperformed other methods, achieving superior  $NA_{hc}$  removal and VLP protein recovery. A construct with intermediate length of the NA binding region exhibited the best performance, with high  $NA_{hc}$  removal and VLP recovery. Minimal variations were observed in alternative processes for

different constructs, but heparin chromatography consistently proved the most effective approach.

### **Chapter 6: Loading and reassembly of hepatitis B core antigen virus-like particles as a function of a nucleic acid binding region, nucleic acid type and ionic strength in the liquid phase**

Angela Valentic, Jakob Müller, Jürgen Hubbuch

*Submitted to Frontiers in Biotechnology and Bioengineering*

Reassembly of HBcAg VLPs, driven by increasing ionic strength or the presence of NAs, has been demonstrated, but deeper insights into the factors influencing this process are needed. This study examined two HBcAg VLP constructs: Cp149 (lacking the NA binding region) and Cp157 (with an intermediate NA binding region). The effects of varying NaCl concentrations, the presence and type of NAs, and NA concentrations were analyzed. Results showed a complex interplay between these factors, with Cp157 responding to both ionic strength and DNA oligonucleotides to induce reassembly, while Cp149 did not respond to NA presence. Cp157 also demonstrated superior NA encapsulation efficiency, with maximum loading achieved at the highest NA concentration, underscoring the importance of the NA binding region in VLP reassembly and loading.





## Effects of Different Lengths of a Nucleic Acid Binding Region and Bound Nucleic Acids on the Phase Behavior and Purification Process of HBcAg Virus-Like Particles

Angela Valentic<sup>a</sup>, Jakob Müller<sup>a</sup>, Jürgen Hubbuch<sup>a,\*</sup>

<sup>a</sup> Institute of Process Engineering in Life Sciences, Section IV: Biomolecular Separation Engineering, Karlsruhe Institute of Technology, Fritz-Haber-Weg 2, 76131 Karlsruhe, Germany

\* Corresponding author

### Abstract

Virus-like particles (VLPs) are macromolecular structures with great potential as vehicles for the targeted administration of functional molecules. Loaded with nucleic acids (NAs), VLPs are a promising approach for nanocarriers needed for gene therapy. There is broad knowledge for the manufacturing of the truncated wild-type lacking a NA binding region, that is mainly being investigated for vaccine applications. Whereas, for their potential application as nanocarrier for gene therapy Hepatitis B core Antigen (HBcAg) VLPs with a NA binding region for efficient cargo-loading are being investigated. VLP structure, loading and phase behavior is of central importance to their therapeutic efficacy and thereby considerably affecting the production process. Therefore, HBcAg VLPs with different lengths of the NA binding region were produced in *E. coli*. VLP attributes such as size, zeta potential and loading with host cell-derived nucleic acids (NA<sub>hc</sub>) were evaluated. Capsid's size and zeta

potential of the VLP constructs did not differ remarkably, whereas the analysis of the loading with  $\text{NA}_{\text{hc}}$  revealed strong differences in the binding of  $\text{NA}_{\text{hc}}$  dependent on the length of the binding region of the constructs, with a non-linear correlation but a two-zone behavior. Moreover, the phase behavior and purification process of the HBcAg VLPs as a function of the liquid phase conditions and the presence of  $\text{NA}_{\text{hc}}$  were investigated. Selective VLP precipitation using ammonium sulfate was scarcely affected by the encapsulated NAs. However, the disassembly reaction, which is crucial for structure homogeneity, separation of encapsulated impurities and effective loading of the VLPs with therapeutic nucleic acids ( $\text{NA}_{\text{ther}}$ ), was affected both by the studied liquid phase conditions, varying pH and concentration of reducing agents, and the different VLP constructs and amount of bound NAs, respectively. Thereby, capsid-stabilizing effects of the bound NAs and capsid-destabilizing effects of the NA binding region were observed, following the two-zone behavior of the construct's loading, and a resulting correlation between the capsid stability and disassembly yields could be derived.

### 3.1 Introduction

Nucleic acid (NA)-based therapeutics, such as mRNA, antisense oligonucleotides or small interfering RNA, are investigated for selective and efficient therapies used for a broad spectrum of medical fields such as immunotherapy, oncology and infectious diseases (Burnett et al., 2011; Chen and Zhaori, 2011; Sahin et al., 2014; Sharma et al., 2014; Nikam and Gore, 2018; Zhou et al., 2019). Lately, nucleotide-based vaccines have proven their efficacy as vaccines against infectious diseases and their vast potential for fast development up to large-scale manufacturing (Zhong et al., 2018; Fortner and Schumacher, 2021): First vaccines against the coronavirus disease 2019 authorized for emergency use by the FDA and EMA were two mRNA-based vaccines (Fortner and Schumacher, 2021). Lipid nanoparticles were used for packaging and delivery (Hou et al., 2021). Lipid-based nanocarriers have been studied intensively in the last years (Blasi et al., 2007; Xue et al., 2015; Kulkarni et al., 2018; Pardi et al., 2018; Aldosari et al., 2021). However, there are still challenges such as efficient tissue targeting and lipid toxicity (Aldosari et al., 2021). A promising alternative are virus-like particles (VLPs) for targeted delivery of small molecules, proteins and NAs (Rohovie et al., 2017). The main advantages over lipid-based nanocarriers are the possibility of surface modification on genetic level or post-translational modification for effective tissue targeting and precise and uniform structures with large loading capacities, depending on the type of VLP (Rohovie et al., 2017). For several VLPs studies showed the ability to pack RNA (Porterfield et al., 2010; Jinming Li et al., 2013; Petrovskis et al., 2021), protect (Fang et al., 2018) and deliver NAs (Cooper and Shaul, 2005; Choi et al., 2013).

However, effective VLP downstream processing, especially including loading with the therapeutic nucleic acids ( $NA_{ther}$ ), is still a challenge. Following the intra-cellular formation of VLPs in an expression system, such as *E. coli*, yeast or plant cells (Effio and Hubbuch, 2015), a commonly used VLP purification process consists of cell lysis, ultracentrifugation or precipitation, disassembly and reassembly, polishing and formulation (McCarthy et al., 1998; Zhao et al., 2012a; Hillebrandt et al., 2020; Zhang et al., 2021b). Traditional processes utilize size exclusion chromatography (SEC) and ultracentrifugation (Yoon et al., 2013). However, there have been recent advances in the processing using ultrafiltration-based unit operations, exploiting the size differences between impurities, VLP subunits and VLP capsids, investigating VLPs for vaccine applications (Negrete et al., 2014; Carvalho et al., 2019; Rüdts et al., 2019; Hillebrandt et al., 2020, 2021). However, VLPs, being developed for NA delivery, have an even more complex purification process, due to the need of an additional loading step with  $NA_{ther}$ . A typical production process is shown in

Figure 3.1. To be able to make use of these recent developments towards effective and large-scale purification processes for VLPs deeper knowledge of VLP characteristics and influencing factors such as encapsulated NAs, on the purification process needs to be derived.

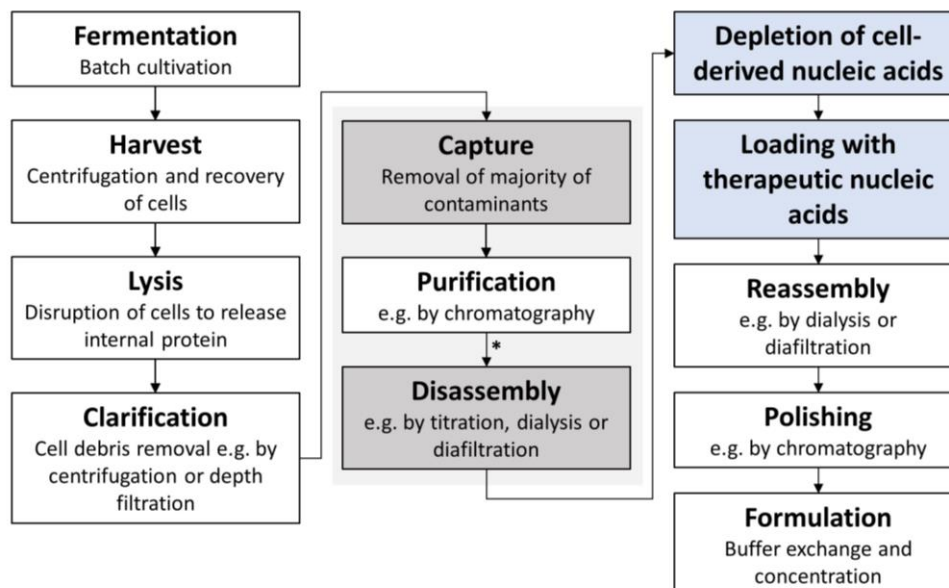


Figure 3.1 Typical HBcAg VLP purification process (Hillebrandt et al., 2021) with additional process steps for application as transport vector for NAs highlighted in blue. The central purification steps capturing by selective precipitation and disassembly, investigated in this study, are highlighted in grey. HBcAg VLP construct characterization was conducted after purification by CaptoCore 400 chromatography and dialysis (marked with an asterisk \*). HBcAg, Hepatitis B core Antigen; NA, nucleic acid; VLP, virus-like particle

Among the candidates investigated for their use as nanocarriers for gene therapy is Hepatitis B core Antigen (HBcAg) VLP. Typically, HBcAg VLPs are mixed with  $NA_{ther}$  in a disassembled state and are then reassembled with the NAs encapsulated in the VLP capsids (Porterfield et al., 2010; Petrovskis et al., 2021; Zhang et al., 2021b). For an effective loading of the VLPs, often the naturally occurring full-length NA binding region of the wild-type HBcAg protein (Nassal, 1992; Zhang et al., 2021b), further referred to as Cp183 (amino acids 1 to 183), and variants with few replaced amino acids (Porterfield et al., 2010; Strods et al., 2015) are employed. Moreover, HBcAg VLP constructs with different lengths of this naturally occurring arginine-rich NA binding region are investigated (Newman et al., 2009; Liu et al., 2010; Sominskaya et al., 2013; Petrovskis et al., 2021). One major challenge for the purification process arising with the NA binding region is the undesired association and encapsulation of host cell-derived nucleic acids ( $NA_{nc}$ ) during spontaneous assembly throughout the expression of HBcAg VLP protein subunits, further referred to as dimers. Various techniques such as lithium chloride precipitation (Porterfield et al., 2010), alkaline treatment (Strods et al., 2015) and enzymatic treatment



(Newman et al., 2009) sometimes coupled with affinity chromatography (Zhang et al., 2021b), are applied during the purification process to separate the *E. coli* derived NAs. Furthermore, the encapsulated NAs appear to have an influence on the purification process and especially on the disassembly reaction. However, the disassembly reaction is not only crucial for separating bound NAs (Porterfield et al., 2010; Strods et al., 2015; Zhang et al., 2021b) and enabling effective loading with NA<sub>ther</sub>, but also for separating encapsulated impurities (Hillebrandt et al., 2021) and improving structural integrity (Zhao et al., 2012a).

Purification processes for the wild-type HBcAg VLP construct with the full-length NA binding region (Cp183) and the arginine-rich C-terminal region truncated HBcAg VLP construct (Cp149) with amino acids 1 to 149 (Zlotnick et al., 1996) were described earlier (Porterfield et al., 2010; Zhang et al., 2021b). Besides varying behaviors of the different constructs during purification, solubility issues for the Cp183 were reported (Porterfield et al., 2010). Moreover, next to Cp183 with the full-length NA binding region, it was shown that constructs with different lengths of the binding region can be successfully expressed in *E. coli*, purified and packed with NA<sub>ther</sub> (Petrovskis et al., 2021), but with a set purification process and main focus on the selection of construct variants. However, a study on HBcAg VLPs without NA binding region demonstrated a distinct dependency of the disassembly reaction on the examined HBcAg VLP constructs (Hillebrandt et al., 2021). Thereby, for the wild-type truncated HBcAg protein (Cp149) and a construct with a chimeric epitope, displayed on the surface of the VLP capsids, different rates and optimal liquid phase conditions for the disassembly reaction were determined. Moreover, for a series of HBcAg VLP constructs with various lengths of the NA binding region its influence on the VLP capsid stability was shown (Newman et al., 2009). This might have major effects on the phase behavior (in which a distinction is made between HBcAg dimers, capsids or aggregated proteins) and the overall purification process.

This points towards a substantial influence of different lengths of the NA bindings regions and encapsulated NAs on the purification process of HBcAg VLPs. A NA binding region appears to be necessary to encapsulate a considerable amount of NAs (Zhang et al., 2021b), but examining different lengths might be useful to overcome challenges during the purification process such as the mentioned solubility issues for the construct Cp183 (Porterfield et al., 2010). Deeper knowledge of the influence of the NA binding region and bound NAs on early downstream purification steps such as precipitation, re-dissolution and especially the disassembly step needs to be derived to enable successful loading with NA<sub>ther</sub>. This is relevant to prospectively enable an effective manufacturing of HBcAg VLPs for NA delivery.

In this study, we investigated six different HBcAg VLP constructs with different lengths of the NA binding region regarding their size, charge and loading with NA<sub>hc</sub> derived from expression in *E. coli*. We further determined the effects of the various constructs and bound NAs on the precipitation, re-dissolution and disassembly step of the purification process. A series of ammonium sulfate concentrations for precipitation and various buffer compositions for re-dissolution were assessed to show possible deviations between the different constructs. For the disassembly reaction several liquid phase conditions varying pH and urea concentrations were systematically examined to compare the disassembly behavior of the various constructs and evaluate the influence of the NA binding region and encapsulated NAs on this phase behavior of the VLPs. Thereby, the results of this study demonstrated (i) the dependency of the phase behavior of the VLPs on the capsid stability, likewise affected by a complex interplay of the NAs binding region and bound NAs within the HBcAg proteins and (ii) its major influence on the disassembly reaction as one crucial purification step for VLP production.

## 3.2 Materials and Methods

### 3.2.1 Materials and Buffers

If not stated otherwise, all chemicals were purchased from Merck (Darmstadt, Germany). Solutions and buffers were prepared with ultrapure water (PURELAB Ultra, ELGA LabWater) and filtered through a 0.2 µm pore-size cellulose acetate filter (Pall Corporation, Port Washington, NY, United States). Buffers were pH-adjusted with 32% HCl. The lysis buffer consisted of 50 mM Tris, 100mM NaCl, 1 mM EDTA (AppliChem, GmbH, Darmstadt, Germany) at pH 8. As wash buffer, lysis buffer adjusted to 1 M (NH<sub>4</sub>)<sub>2</sub>SO<sub>4</sub> (AppliChem, Darmstadt, Germany) and 0.25% (v/v) polysorbate 20 (AppliChem, Darmstadt, Germany) with stock solutions of 4 M (NH<sub>4</sub>)<sub>2</sub>SO<sub>4</sub> and 10% (v/v) polysorbate 20, respectively. The re-dissolution buffer was 50 mM Tris, 150 mM NaCl, pH 7.2 for all experiments. For the disassembly screening a 50 mM Tris, 10 M urea stock solution was used to dilute the protein solution in re-dissolution buffer to the desired urea concentration.

### 3.2.2 Cloning of Cp154, Cp157, Cp164, Cp167 and Cp183

Prof. Adam Zlotnick (Indiana University Bloomington, United States) provided the expression vector for the C-terminally truncated wild-type HBcAg with a sequence of 149 amino acids. Based on this Cp149 expression vector, plasmids coding for VLP constructs with different lengths of the nucleic acid binding region were produced. The amino acid sequences introduced as C-terminal nucleic acid binding regions are listed in Table 3.1. The plasmids coding for Cp154, Cp157, Cp164 and Cp167 were made by modifying the pET11c plasmid

### 3 Effects of Different Lengths of a Nucleic Acid Binding Region and Bound Nucleic Acids on the Phase Behavior and Purification Process of HBcAg Virus-Like Particles

coding Cp149, whereby the bp sequences encoding for the C-terminal amino acids were inserted. The regions encoding for the Cp149 on the pET11-based vector were amplified using overlapping oligonucleotides to introduce site-directed mutagenesis using the polymerase chain reaction (PCR). The wild-type HBcAg Cp183 was obtained by amplifying the Cp167 plasmid in the same manner. The respective forward and reverse primers used for the PCR reaction for the production of the different constructs can be found in Appendix A: S3.1.

Table 3.1 Amino acid sequences in one letter code of arginine rich NA binding region in HBcAg VLP constructs. Residues are located C-terminally at core domain with 149 amino acids (Crowther et al., 1994); HBcAg, Hepatitis B core Antigen; NA, nucleic acid; VLP, virus-like particle

Construct	Amino acid sequence
Cp154	RRRGR
Cp157	RRRGRSPR
Cp164	RRRGRSPRRRTPSPR
Cp167	RRRGRSPRRRTPSPRRRR
Cp183	RRRGRSPRRRTPSPRRRRRSQSPRRRRRSQSRESQC

Amplification was performed with PCRBio HiFi Polymerase (Nippon Genetics Europe GmbH, Düren, Germany). The PCR template and product were digested using DpnI (New England BioLabs, Ipswich, MA, United States), purified by native gel electrophoresis and extracted using a Wizard SV gel and PCR Clean-Up kit (Promega, Madison, WI, United States). Ligation was accomplished with the Gibson Assembly Master Mix (New England BioLabs, Ipswich, MA, United States) and the new vectors were transformed into BL21[DE3] cells (New England Biolabs, Ipswich, MA, United States).

#### 3.2.3 Intra-cellular Formation and Purification of VLPs

VLPs were overexpressed in *E. coli* using a TB-based auto-induction medium and liberated by cell lysis directly as previously described (Hillebrandt et al., 2020). For selective VLP precipitation, the filtered lysate was diluted with  $(\text{NH}_4)_2\text{SO}_4$  and polysorbate 20 stock solutions, adjusted to 1 M  $(\text{NH}_4)_2\text{SO}_4$  and 0.25% (v/v) polysorbate 20, and stirred for 2 h at 4°C. The solution was spun down at 17000 ref for 30 min in a centrifuge 5810 R (Eppendorf, Hamburg, Germany). The supernatant was discarded while the pellet was resuspended with wash buffer and incubated at 10 rpm at room temperature in an overhead shaker LD-79 (Labinco, Breda, Netherlands) for 10 min, centrifuged with the identical settings, and the supernatant was discarded. The pellet was resuspended with re-dissolution buffer and stirred at 150 rpm overnight at 4°C.

The solution was centrifuged at 1700 rcf for 30 min and filtered with 0.2  $\mu$ m cellulose acetate syringe filters. After a dialysis step with 3.5 kDa molecular weight cut-off SnakeSkin Dialysis Tubing (Thermo Fisher Scientific, Waltham, MA, United States) the material was purified with a CaptoCore 400 column (Cytiva, Marlborough, MA, United States), which was equilibrated with re-dissolution buffer. The VLP capsid containing fractions in the flow-through were collected and freshly used or stored in aliquots at -30°C. Prior to the experiments, the material was thawed and filtered again through a 0.2  $\mu$ m syringe filter.

### 3.2.4 Characterization of VLP Constructs

The expression of each HBcAg VLP construct was confirmed by western blot analysis. Re-dissolved VLPs were analysed by SDS-PAGE and transferred onto a nitrocellulose membrane. An anti-HBcAg antibody (abcam, Cambridge, United Kingdom) was used as primary antibody in 1:1000 dilution, followed by an anti-mouse antibody (Merck Millipore, Darmstadt, Germany) at 1:5000 dilution. For SDS-PAGE, NuPage 4-12% BisTris Protein Gels, LDS sample buffer and MES running buffer were used and run on a PowerEase 500 Power Supply (all Invitrogen, Waltham, MA, United States) at reduced mode with 50 mM DTT in the sample solution. Protein staining was performed with a Coomassie blue solution.

SEC coupled with a diode array detector was used to evaluate the phase behavior of the VLPs by quantifying and specifying differently sized species (dimers, capsids, aggregates) and determine the loading of the VLPs with NAs. An Agilent Bio SEC-5, 5  $\mu$ m, 1000 Å, 4.6 x 300 mm column (Agilent, Santa Clara, CA, United States) was used at a Vanquish UHPLC system, controlled by Chromeleon version 7.2 (both Thermo Fisher Scientific, Waltham, MA, United States). To assess loading of VLPs with NAs, the ratio of HBcAg capsid peaks at 260 nm and 280 nm was calculated. Scatter correction was performed as previously described for HBcAg VLPs (Porterfield and Zlotnick, 2010).

Dynamic light scattering (DLS) was used to determine the hydrodynamic radius and size distribution profiles of the particles. Measurements were performed on the DynaPro Plate Reader III (Wyatt Technology, Santa Barbara, CA, United States) using a sample volume of 30  $\mu$ l in a Corning 384 well plate (Corning, NY, United States). Unfiltered samples were measured six times, each measurement consisting of 25 runs of 5 s each at 25°C. The hydrodynamic radius was obtained as calculated by the Dynamics software (Version 7.10.1.21, Wyatt Technology, Santa Barbara, CA, United States). Electrophoretic mobility was measured with disposable folded capillary cells on a Zetasizer Nano ZS instrument (both Malvern Instruments Ltd., Malvern, United Kingdom). Each measurement comprised a 120 s equilibration and five runs with 15 sub runs. The measurements were performed at 40 mV and 25°C. Zeta potential was

calculated by Zetasizer Software (Version 7.12, Malvern Instruments Ltd., Malvern, United Kingdom) with the measured electrophoretic mobility, a material refractive index of 1.45, absorption of 0.001, a viscosity of 0.8872 mPas, a dielectric constant of 78.54, and a Smoluchowski approximation of 1.5 (Smoluchowski, 1921).

### 3.2.5 Purification Process Characterization

For precipitation experiments the filtered lysate was diluted to concentrations of 0.75 M to 1.15 M  $(\text{NH}_4)_2\text{SO}_4$  in increments of 0.05 M and 0.25% (v/v) polysorbate 20, respectively. The solution was incubated for 3 h at 4°C, spun down at 17000 rcf for 30 min in a centrifuge 5810 R (Eppendorf, Hamburg, Germany), and the supernatant was analysed by SDS-PAGE. According to the standard purification procedure, the pellet was resuspended with re-dissolution buffer and stirred at 150 rpm overnight at 4°C. After centrifugation and filtration, the supernatant was analysed by SDS-PAGE. The gels were analysed by VLP band intensity measurements using the open source software ImageJ.

For the disassembly screening, purified VLP constructs in re-dissolution buffer, treated as biological triplicates, were diluted to 3 M, 3.5 M or 4 M Urea with a 50 mM Tris, 10 mM Urea stock solution and titrated to pH 7, 7.5 or 8.0. The material was stirred at 150 rpm for 18 h at 4°C and samples were analysed in triplicates by SEC as described above. The peak areas of aggregates, capsids and dimers were analysed. Control runs at the high-performance liquid chromatography system without a prefilter and column were performed to determine the amount of bigger aggregates and total peak areas at 280 nm were corrected. Dimer yield was calculated by the ratio of HBcAg dimer peak area to total peak area at 280 nm (details on peak identification can be found in Appendix A: S3.2).

## 3.3 Results

### 3.3.1 Characterization of HBcAg VLP Constructs

The expression of the constructs Cp149, Cp154, Cp157, Cp164, Cp167 and Cp183 was verified by western blot analysis (for visualization see Appendix A: S3.3) and different molecular weights of their monomers were displayed with SDS-PAGE (Figure 3.2). Cp149 showed a lane close to the 14.4 kDa marker, Cp183 closer to the 21.5 kDa marker. The intermediate constructs were displayed in between them, in the order of their ascending lengths of amino acid sequences, respectively.

### 3.3.1.1 VLP Size and Zeta Potential Analysis

To determine the hydrodynamic radius of the VLP capsids, the VLP constructs were purified by the CaptoCore 400 step and directly measured by dynamic light scattering. The analysis resulted in average hydrodynamic diameters of  $36.9 \pm 3.2$  nm, not showing distinct differences between the constructs (Figure 3.3). With electrophoretic mobility measurements of the same material, the zeta potential of the different constructs was investigated. For all constructs, similar zeta potentials of  $-11.4 \pm 1.5$  mV were determined (Figure 3.3).

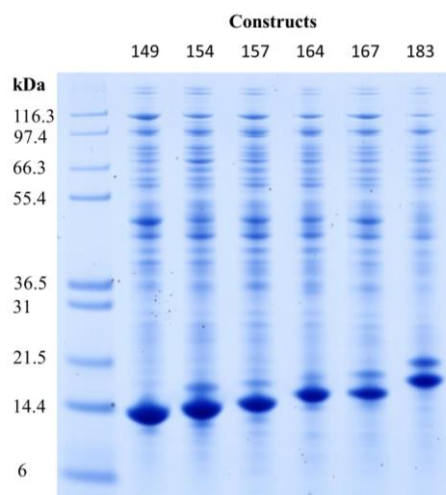


Figure 3.2 Reducing SDS-PAGE scan of HBcAg VLP construct monomers after re-dissolution in lanes 2-7, with Invitrogen Mark 12 Unstained Standard in lane 1. Molecular weights of the proteins in the standard are displayed on the left. Protein staining by Coomassie blue; HBcAg, Hepatitis B core Antigen; VLP, virus-like particle

### 3.3.1.2 Loading with Host Cell-derived Nucleic Acids (NA<sub>hc</sub>)

The SEC chromatography was used to evaluate the loading of purified HBcAg VLP constructs with NA<sub>hc</sub>. The A260/A280 coefficients of the capsid peak areas were determined, respectively (Figure 3.4Figure 3.3). This provides an insight into the ratio of the amount of NAs and proteins without performing an additional separation step of the two species to use protein-specific and NA-specific analytics separately. Cp149 without a NA binding region showed an A260/A280 of 0.60, which is considered to be pure protein (Goldfarb et al., 1951) and only a minimum or no NAs are encapsulated. In general, with an increase in the length of the NA binding region, the A260/A280 coefficient rises, displaying an increased amount of NAs bound inside the capsids, respectively. However, this correlation shows a two-zone behavior. For the constructs Cp149, Cp154 and Cp157, with no or relatively short NA binding region, A260/A280 evinces a steep linear increase with an A260/A280 of 0.95 for Cp154 and 1.31 for Cp157. However, for the constructs with longer binding regions up to full-length wild-type A260/A280 increases from 1.47 for Cp164, to 1.48 for Cp167 and to 1.65 for Cp183. For these constructs, the increased

length of the binding domain shows less effect on the A260/A280, and thus the amount of encapsulated NAs.

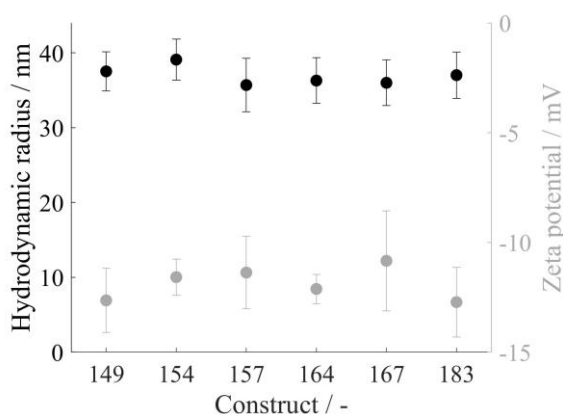


Figure 3.3 Hydrodynamic radius in black and zeta potential in grey of all VLP construct capsids. Measurements were conducted directly after CaptoCore 400 chromatography purification step. DLS measurements were conducted in six replicates and zeta potential measurements in five replicates; VLP, virus-like particle

### 3.3.2 Effects of VLP Constructs on the Purification Process

#### 3.3.2.1 Capture by Precipitation and Re-dissolution

To investigate the precipitation behavior of the VLP constructs, ammonium sulfate concentrations from 0.75 M up to 1.15 M were examined. After the precipitation reaction, the supernatant was analysed for the remaining VLPs as well as the respective re-dissolution material for precipitated and re-dissolved VLPs by SDS-PAGE. The corresponding gel images can be found in the Appendix A: S3.4. Figure 3.5 (A) displays the intensities derived from image analysis of precipitation supernatant samples normalized to the highest determined intensity for the respective construct. For all constructs, an increase in ammonium sulfate concentration in the precipitation step reduced the amount of remaining VLPs, shown by lower intensities for the VLP fraction on the gel images of the supernatant. For Cp149 and Cp154, the intensities decrease with increasing ammonium sulfate concentrations up to 1.05 M and remain fairly constant with even higher concentrations. Cp167 and Cp183 show the same behavior with no further steady decrease in intensity equal and higher than an ammonium sulfate concentration of 0.95 M. Considering the gel images (Appendix A: S3.4) for the high ammonium sulfate concentrations with fairly stable intensities, the VLPs have been precipitated in total and the remaining intensity signal derives from other proteins in the samples. For Cp157 and Cp164, the normalized intensities decrease for all tested ammonium sulfate concentrations which is not in alignment with the gel images where VLPs are not clearly visible for concentrations equal and higher than 1.05 M. Further

decreased intensities might be caused by other proteins co-precipitating with higher tested ammonium sulfate concentrations.

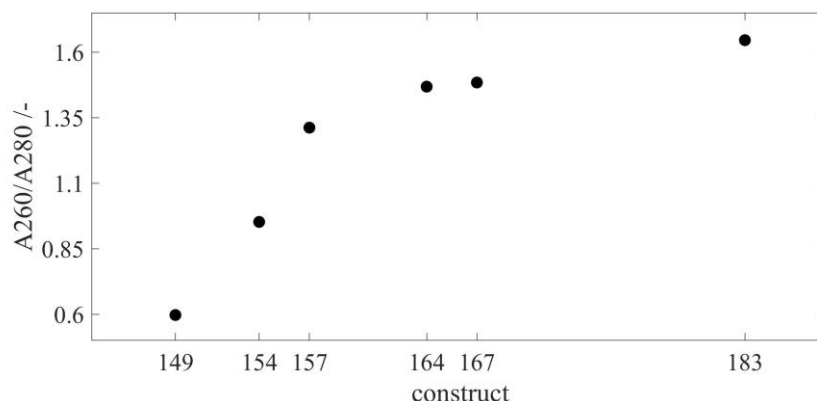


Figure 3.4 Loading of the VLP capsids with host cell-derived nucleic acids for all constructs. SEC chromatography was used to evaluate the loading of the purified VLP capsids by A260/A280 coefficient after scatter correction (Porterfield and Zlotnick, 2010). For every construct samples were analysed by SEC in triplicates, respectively. Error bars are negligible and therefore omitted. Details on capsid peak identification can be found in Appendix A: S3.2; VLP, virus-like particle; SEC, size-exclusion chromatography

For the re-dissolved solutions, displayed in Figure 3.5 (B), high normalized intensities for all constructs were obtained for concentrations equal and higher than 0.95 M ammonium sulfate. The overall highest intensities, considering all constructs, being at 1 M ammonium sulfate. The VLP purity after precipitation and re-dissolution ranged between 10% and 15% for all tested conditions (data not shown). For further processing, an ammonium sulfate concentration of 1 M was chosen.

In preliminary experiments, suitable buffer conditions for VLP re-dissolution were determined by investigating Tris buffer with different sodium chloride molarities. All tested conditions demonstrated the capability to re-dissolve VLPs but 150 mM NaCl showed the highest amount of VLP capsids as opposed to disassembled or aggregated VLP capsid proteins by SEC analysis (for details on analysis, see Appendix A: S3.2), which is the desirable VLP conformation for the following purification steps.

#### 3.3.2.2 Disassembly Screening

After precipitation, re-dissolution and the separation of small contaminants by dialysis and chromatography with CaptoCore 400, the disassembly step is crucial in the purification procedure to separate encapsulated NA<sub>hc</sub> and other impurities. To investigate the phase behavior of the different constructs and the influence of encapsulated NA<sub>hc</sub> on capsid stability, purified VLP constructs were disassembled in reducing conditions varying both the pH and the urea concentration of the liquid phase, respectively.



### 3 Effects of Different Lengths of a Nucleic Acid Binding Region and Bound Nucleic Acids on the Phase Behavior and Purification Process of HBcAg Virus-Like Particles

Dimer yields for all constructs and varying pH values at 4 M urea, the highest urea concentration investigated in this study, are shown in Figure 3.6 (A) + (B). For Cp149, an increased pH of the disassembly solution resulted in an increased dimer yield from 53.4% at pH 7 up to 64.9% at pH 8. All other constructs show the same correlation, however less pronounced, with an increase in dimer yield

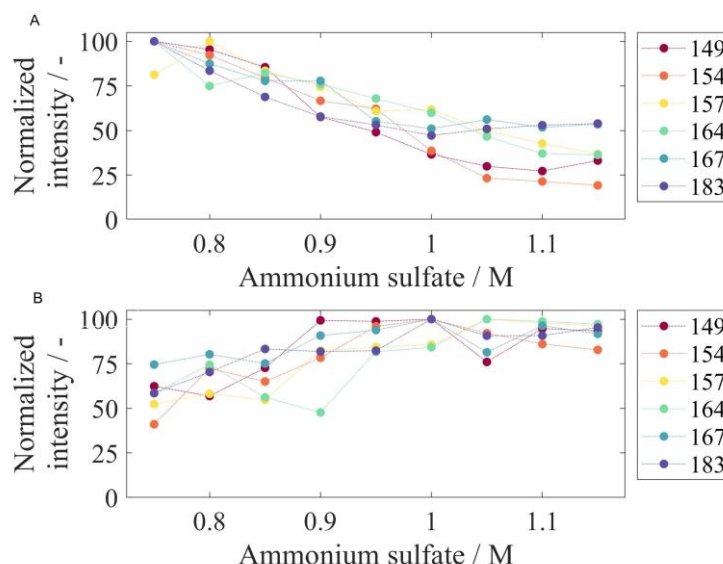


Figure 3.5 Remaining VLP constructs in precipitation supernatant (A) and re-dissolved VLP constructs after precipitation and re-dissolution overnight for different tested ammonium sulfate concentrations. After precipitation with different ammonium sulfate concentrations the supernatant (A) and re-dissolution solution (B) were analyzed by SDS-PAGE and gel scans were evaluated by the intensity of the VLP band on the gel lane with respect to the highest determined intensity for the respective construct. Corresponding gel images can be found in the Appendix A: S3.4; VLP, virus-like particle

between 2.8% for Cp164 and 8.3% for Cp154 from pH 7 to pH 8. Additionally, dimer yields for all constructs and varying molar urea concentrations at pH 8, the highest tested pH value, are shown in Figure 3.6 (C) + (D). For the constructs with no or short NA binding regions Cp149, Cp154 and Cp157 (Figure 3.6 (C)), increasing dimer yields from 4.9% for Cp149 up to 15.5% for Cp154 were determined when increasing the urea concentration from 3 M to 4 M. For the constructs Cp164, Cp167 and Cp183 (Figure 3.6 (D)), the dimer yields remained fairly constant within  $\pm 1\%$ , comparing urea concentrations of 3 M and 4 M.

Results for pH 7 and pH 7.5 and for urea concentrations of 3 M and 3.5 M show equal behavior and can be found in Appendix A: S3.5. Considering all tested conditions and averaging over all constructs and all pH values, the average increase in dimer yield was 4.9% when increasing the molar concentration of urea from 3 M to 4 M. Likewise averaging over all urea concentrations, the average increase of dimer yield was 7.6% when increasing the pH value from 7

to 8. However, the combination of increasing the pH and increasing the urea concentration led to an even higher increase in dimer yield of 13.3%.

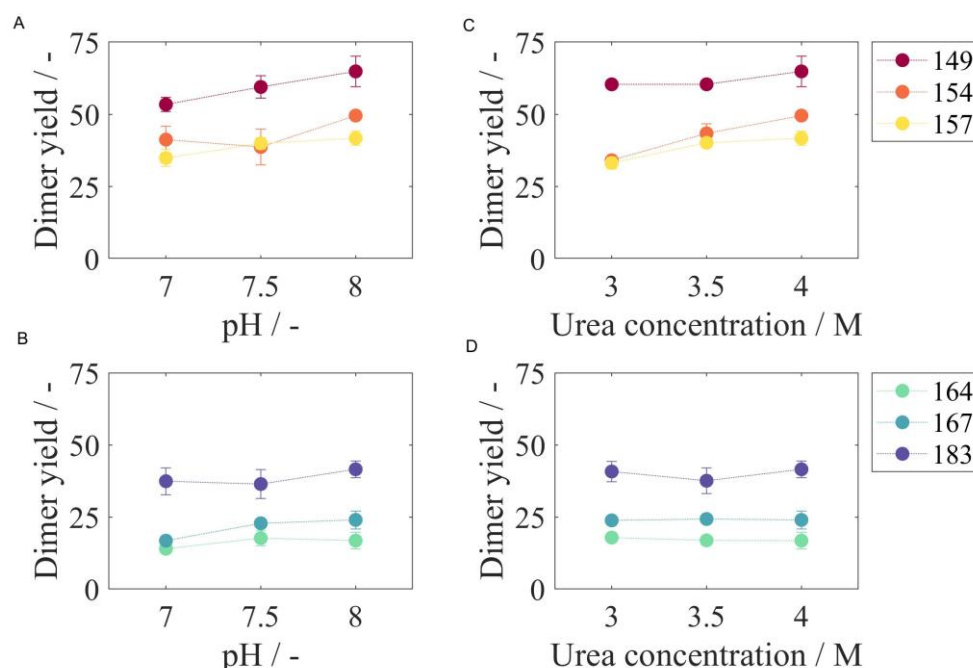


Figure 3.6 Dimer yields after disassembly reaction for different liquid phase conditions and for all constructs. In subfigures (A) and (B) results for a urea concentration of 4 M and varying pH values are displayed. In subfigures (C) and (D) results for a pH of 8 and varying urea concentrations can be found. According to the two-zone behavior subfigures (A) and (C) show results for Cp149, Cp154 and Cp157 and subfigures (B) and (D) for Cp164, Cp167 and Cp183, respectively. Results for 3 M urea, 3.5 M urea, pH 7 and pH 7.5 can be found in Appendix A: S3.5. SEC was used to evaluate the dimer yield after disassembly reaction. Details on capsid peak identification can be found in Appendix A: S3.2; SEC, size-exclusion chromatography

Comparing the disassembly behavior of the different HBcAg VLP constructs, a two-zone behavior can again be distinguished. For all tested conditions, Cp149 without NA binding region showed the highest dimer yields with values between 48.8% (50 mM Tris, 3 M urea, pH 7) and 64.9% (50 mM Tris, 4 M urea, pH 8). As shown for varying pH values in Figure 3.6 (A) and varying urea concentrations in Figure 3.6 (C), for the constructs Cp149, Cp154 and Cp157, an increased length of the NA binding region lead to lower dimer yields for almost every condition. For the constructs with longer binding regions, Cp164, Cp167 and Cp183, this correlation is reversed. As shown for varying pH values in Figure 3.6 (B) and varying urea concentrations in Figure 3.6 (D), Cp164 with an intermediate length of NA binding region results in overall lowest dimer yields. However, further increased lengths of the NA binding regions up to the full-length wild-type Cp183 lead to an increase in dimer yields. This results in similar dimer yields for Cp154, Cp157 and Cp183. These findings for the results

shown in Figure 3.6 also apply to the results for pH 7 and pH 7.5 and to urea concentrations of 3 M and 3.5 M (Appendix A: S3.5).

## 3.4 Discussion

### 3.4.1 Intra-cellular Formation and Characterization of HBcAg VLP Constructs

In this study, HBcAg VLP constructs with various lengths of the naturally occurring NA binding region were produced. To demonstrate the successful intra-cellular formation of all protein variants western blot analysis and SDS-PAGE were performed. The resulting monomer sizes of the constructs under denaturing conditions are consistent with the size values given in literature for Cp183 of 21 kDa (Wynne et al., 1999; Bin Mohamed Suffian et al., 2017) as well as the shorter migration of the truncated constructs (Tan et al., 2003). Despite the different monomer sizes, assembled capsids showed a hydrodynamic radius of  $36.9 \pm 3.2$  nm for all constructs, which is in alignment with the reported 36 nm for Cp183 (Porterfield et al., 2010). In the literature, T=4 and T=3 icosahedral structures of HBcAg VLP capsids with differences in their sizes were reported (Wingfield et al., 1995; Conway et al., 1997, 1998). However, the DLS measurement was unable to resolve these different HBcAg species within this study and in literature (Petrovskis et al., 2021). The independence of the capsid size from HBcAg VLP constructs has already been suggested in the literature by evaluating transmission electron microscope pictures and measuring electrophoretic mobilities and thereby determining a hydrodynamic radius of about 38 nm for all investigated HBcAg protein genotypes (Petrovskis et al., 2021). This underlines the structural homogeneity of HBcAg VLPs with icosahedral structures (Venkatakrishnan and Zlotnick, 2016), which is a big advantage of VLPs over other NA carrier structures investigated in the literature (Rohovie et al., 2017). Furthermore, the zeta potential was also fairly constant for all constructs despite the different lengths of the NA binding region. The positive charges of the arginine-rich binding region do not seem to affect the negative surface charge, likely because of its orientation towards the inside of the capsid (Venkatakrishnan and Zlotnick, 2016) and due to charge compensation by the encapsulated NAs (Le Pogam et al., 2005).

A260/A280 ratios for the capsid peaks in the SEC chromatograms were determined for all constructs to assess the amount of encapsulated NAs. For Cp149 the A260/A280 was 0.60, which is comparable to previously reported values of 0.61 (Hillebrandt et al., 2021) and 0.67 (Zhang et al., 2021b) before further purification. For pure protein, A260/A280 ratios of 0.6 are assumed (Goldfarb et al., 1951) and accordingly for purified HBcAg capsid protein an

A260/A280 ratio of about 0.6 was reported after performing the proposed scatter correction (Porterfield and Zlotnick, 2010). Diverging from this, even lower A260/A280 ratios of 0.55 (Hillebrandt et al., 2021) and 0.57 (Zhang et al., 2021b) were reported after disassembly followed by cross-flow filtration or affinity chromatography, demonstrating that there are still a few NAs encapsulated in Cp149 capsids, which are then depleted by the mentioned subsequent purification steps. Resulting from this, the here scatter-corrected A260/A280 of 0.60 demonstrates that NAs are encapsulated, even without having a NA binding region within the Cp149 capsid. However, assessed on the basis of the absorbance ratios, the amount of encapsulated NAs in Cp149 is low compared to the Cp183 with the full-length wild-type NA binding region (A260/A280 of 1.65), which is in line with previously described results in the literature based on cryogenic electron microscopy analysis of the two constructs (Crowther et al., 1994; Zlotnick et al., 1997). Considering all investigated constructs with varying lengths of the NA binding region, the A260/A280 ratios show that the longer the NA binding region, the more NAs are encapsulated, which was also observed previously by cryogenic electron microscopy (Liu et al., 2010). Interestingly, the analysis of the loading of the NAs did not result in a linear correlation between the encapsulation of NA<sub>hc</sub> after intra-cellular formation and the length of or the amount of positive charges within the NAs binding region. A two-zone behavior was hereby distinguishable. In one zone, including the constructs with no or short binding regions, an increased length of the binding region has a significant impact on the amount of encapsulated NAs. Whereas for the constructs with longer binding regions in the second zone, a longer binding region has little effect on the amount of encapsulated NAs.

This two-zone behavior affects the charge ratios between the positive charges within the NA binding region and the negative charges derived from the NAs within the capsids, which were identified to influence the capsid stability (Le Pogam et al., 2005; Newman et al., 2009). It was hypothesized that a balanced charge density inside the capsid lead to stable capsid structures (Le Pogam et al., 2005). Additionally, NAs bound to the binding region of the HBcAg VLP constructs form an inner shell within the capsid (Zlotnick et al., 1997; Liu et al., 2010) and thus are assumed to stabilize its structure.

Moreover, when considering the loading with NA<sub>hc</sub> as an indicator for the capability of the HBcAg VLP constructs to encapsulate NA<sub>ther</sub> later in the process, the NA binding region seems to be important for an efficient encapsulation. However, the two-zone behavior with the non-linear correlation between the length of the NA binding region and the amount of encapsulated NAs reveals, that an intermediate length of NA binding region might be sufficient for effective encapsulation of the NA<sub>ther</sub>. This is particularly interesting due to stability problems after NA<sub>hc</sub> depletion for Cp183 in the later purification process (Porterfield et al., 2010), as well as for Cp164 and Cp167 (Le Pogam et

al., 2005) were reported, whereas Cp154 showed no such stability problems (Le Pogam et al., 2005).

### 3.4.2 Capture by Precipitation and Re-dissolution

Effects of the different HBcAg VLP constructs and especially their characteristics on production and purification steps such as selective precipitation, re-dissolution and disassembly were investigated in this study.

For all constructs, an ammonium sulfate concentration of 1.05 M was sufficient to fully precipitate the VLPs from the clarified lysate. For Cp167 and Cp183, even a concentration of 0.95 M was enough for precipitation. However, this difference in needed ammonium sulfate concentrations within the here investigated constructs is small compared to the big leap to the reported necessary concentration of only 0.15 M for a chimeric HBcAg without NA binding region, and thus a chimeric version of Cp149 (Hillebrandt et al., 2020). It seems like changes on the surface of the HBcAg VLPs such as the foreign epitopes have a greater influence on the susceptibility to ammonium sulfate as a precipitating agent than the different lengths of the NA binding regions and bound NAs that are both placed within the VLP capsids (Zlotnick et al., 1997; Liu et al., 2010). This could also be the reason for another divergence in the findings for the chimeric HBcAg VLP and the here investigated constructs. Testing ammonium sulfate concentrations in identical increments of 50 mM, the precipitation for the chimeric VLP occurred relatively abrupt within 2 increments at most for every reported experiment (Hillebrandt et al., 2020), whereas for the here tested constructs the precipitation behaved more dynamically with a broader range of at least 4 increments, thus, 200 mM ammonium sulfate, where only a fraction of VLPs was precipitated, and the rest remained in solution.

After investigating the precipitation behavior of the different constructs, an appropriate precipitation condition for further processing was also determined. Due to the relatively small differences in the precipitation behavior of the various constructs, the same precipitation condition with 1 M ammonium sulfate was selected for further processing, showing the highest amounts of VLPs re-dissolved in total. As explained, the re-dissolution buffer was also uniform for all constructs. A detailed investigation of the re-dissolution behavior similarly to the disassembly experiments was not found to be practicable, because a precise analysis of the individual components, especially the determination of the dimer content, was unfeasible due to the presence of impurities with a similar size giving overlapping chromatography peaks with the analytical setup used in this study. The following preparative chromatography step separated the interfering impurities predominantly and

enabled the detailed analysis of the different VLP compositions after the disassembly reaction by analytical size-exclusion chromatography.

#### 3.4.3 Effects of Liquid Phase Conditions on Disassembly Yield

The disassembly reaction is crucial for effectively separating encapsulated impurities (Hillebrandt et al., 2021), improving structural integrity (Zhao et al., 2012a) and separating bound NAs (Porterfield et al., 2010; Strods et al., 2015; Zhang et al., 2021b). Therefore, a comprehensive disassembly screening was conducted for the different constructs in this study. The disassembly experiments showed the expected correlation between liquid phase conditions and dimer yields. In the tested range, higher dimer yields were observed for both higher pH values and higher urea concentrations. Synergistic effects of pH and urea concentration were observed, as already described for Cp149 in an earlier publication of our group (Hillebrandt et al., 2021). High pH, low ionic strength and the addition of reducing agents such as urea or guanidine hydrochloride are widely used in the literature for the disassembly of HBcAg (Porterfield et al., 2010; Strods et al., 2015; Bin Mohamed Suffian et al., 2017; Hillebrandt et al., 2021; Zhang et al., 2021b) and other VLPs (McCarthy et al., 1998; Mach et al., 2006). Commonly, a concentration of 4 M urea is used to disassemble HBcAg Cp149 and Cp183 (Porterfield et al., 2010; Zhang et al., 2021b). For a chimeric version of Cp149, 4 M urea was reported to be the optimal urea concentration for the disassembly reaction (Hillebrandt et al., 2021). Both reported findings of 4 M urea as suggested condition for disassembly are in alignment with the results for the different HBcAg VLP constructs presented in this study. Urea concentrations above 4 M can lead to unfavourable protein denaturation and aggregation (Zhang et al., 2021b). However, the conditions investigated in this study with urea concentrations from 3 M to 4 M and varying pH values all lead to a merely partial disassembly into dimers, and also to aggregation and residual capsids, with a maximal dimer yield of 64.9% for Cp149. This observation has been reported before for Cp149 and a chimeric version of Cp149, with similar dimer yields of 71% and 69%, respectively (Hillebrandt et al., 2021). These slightly better yields compared to the results shown in this study can be explained by differences in tested pH range, the experimental setup with different dilution strategies and observed reaction times, which have an influence on the dimer yields.

#### 3.4.4 Effects of HBcAg VLP Constructs and Loading on Disassembly Yield

In addition to the effects of liquid phase conditions on the disassembly reaction, great differences in the disassembly behavior of the investigated HBcAg VLP constructs were observed. Dimer yields correlate with the two-zone behavior for loading of the different constructs. For the constructs Cp149, Cp154, Cp157 and Cp164 with an increased length of the NA binding region and rising amount

of bound NAs, dimer yields decline steadily. It can be concluded that for these constructs the addition of the NA binding region and the thus elicited binding of NA<sub>hc</sub> as an inner shell within the capsid (Zlotnick et al., 1997; Liu et al., 2010) increase capsid stability, which impedes the disassembly of the VLP capsids into dimers. As the loading results show, the further elongation of the NA binding region has little effect on the loading of the capsids. However, the insertion of more positive charges within the NA binding region appears to impact the capsid stability (Le Pogam et al., 2005) and thus the disassembly reaction in a reversed manner. For the constructs Cp164, Cp167 and Cp183, with an increased length of the NA binding region, dimer yields rise steadily, as opposed to the correlation for the constructs with no or short binding regions. It can be assumed that hereby, the insertion of additional positively charged arginines is not compensated by the small amount of more bound NAs and their negative charges. This has been previously described as part of a charge balance hypothesis (Le Pogam et al., 2005). These surplus positive charges lead to repulsive forces within the VLP capsids and thus destabilize the capsid and enhance disassembly (Newman et al., 2009). This effect is clearly depicted by the rising dimer yields for the constructs Cp164, Cp167 and Cp183 found in this study. The investigation of the disassembly behavior of the various HBcAg VLP constructs with different loads of NA<sub>hc</sub> demonstrated both capsid-stabilizing effects of the bound NAs and capsid-destabilizing effects of the positive charges within the NA binding region. Moreover, it demonstrated the significant influence of these stabilizing and destabilizing effects on the disassembly reaction and dimer yields of the different constructs.

### 3.5 Conclusions

In this study, HBcAg VLP constructs with variable lengths of the natural NA binding, the truncated wild-type Cp149, the wild-type Cp183 and four intermediates, were produced and characterized. The investigated constructs showed no considerable differences in capsid sizes and zeta potential, whereas the length of the NA binding region demonstrated a vast effect on the amount of NA<sub>hc</sub> classified as two-zone behavior. Cp149 showed merely a minimal amount of encapsulated NAs. The insertion of the NA binding region leads to a steep increase in the amount of bound NAs for constructs in the zone with short NA binding regions. In the other zone, from construct Cp164 a further increased length of the NA binding region showed a lower effect on the increase in the amount of encapsulated NAs. Further, effects of the various constructs and their characteristics on purification steps were investigated. The capturing by precipitation and re-dissolution was scarcely affected by the different constructs and the loading with NA<sub>hc</sub>. However, the disassembly reaction appeared to be immensely dependent on the construct and its loading. The comprehensive

screening of the disassembly reaction for all constructs and varying liquid phase conditions revealed a complex interplay of capsid-stabilizing effects of the bound NAs and capsid-destabilizing effects, arising from repulsive forces caused by the positive charges of the NA binding region following the two-zone behavior of the loading of the constructs. The capsid stability significantly influences the disassembly reaction and achievable dimer yields. Thereby, the highest dimer yields were observed for high pH and high urea concentrations in the investigated range.

### **Acknowledgment**

The authors would like to thank Prof. Adam Zlotnick for having provided VLP production plasmids as well as Nicola Böhner and Dr. Jonas Lapp for assistance with cloning the different VLP variants plasmids. The authors also want to thank Thomas Kolleth for assisting with experimental work for the precipitation experiments.

### **Appendix A: Supplementary Material**

The Supplementary Material associated with this chapter contain the following information:

- ❖ S3.1: Oligonucleotides for Plasmid Cloning
- ❖ S3.2: SEC Analysis
- ❖ S3.3: Results of Western Blot Analysis
- ❖ S3.4: SDS-PAGE Scans for Precipitation and Re-dissolution experiments
- ❖ S3.5: Disassembly Screening Results for pH 7, pH 7.5, 3 M urea and 3.5 M urea







## Absolute Quantification of Hepatitis B Core Antigen (HBcAg) Virus-like Particles and Bound Nucleic Acids

Angela Valentic<sup>a</sup>, Nicola Böhner<sup>a</sup>, Jürgen Hubbuch<sup>a,\*</sup>

<sup>a</sup> Institute of Process Engineering in Life Sciences, Section IV: Biomolecular Separation Engineering, Karlsruhe Institute of Technology, Fritz-Haber-Weg 2, 76131 Karlsruhe, Germany

\* Corresponding author

### Abstract

Effective process development towards intensified processing for gene delivery applications using Hepatitis B core Antigen (HBcAg) virus-like particles (VLP) relies on analytical methods for an absolute quantification of HBcAg VLP proteins and bound nucleic acids (NAs). We investigated a silica spin column (SC) based extraction procedure, including proteinase K lysis and silica chromatography, for the absolute quantification of different species of NAs bound to HBcAg VLPs analysed by dye-based fluorescence assays. This revealed load-dependent NA recoveries of the performed silica-SC based extraction. We also developed a reversed-phase high performance liquid chromatography (RP-HPLC) method to separate and quantify the HBcAg proteins and the bound NAs simultaneously without prior sample treatment by dissociation reagents. The method demonstrated sufficient linearity, accuracy, and precision coefficients, and is suited for determining absolute protein and NA concentrations and HBcAg protein purities at various purification stages.

Both the silica-SC based extraction and RP based extraction presented overcome limitations of analytical techniques, which are restricted to relative or qualitative analyses for HBcAg VLPs with bound NAs. In combination with existing analytics, the methods for an absolute quantification of HBcAg VLPs and bound NAs presented here are required to evaluate downstream purification steps, such as the removal of host cell-derived nucleic acids ( $NA_{hc}$ ), concurrent protein loss, and efficient loading with therapeutic nucleic acids ( $NA_{ther}$ ). Hence, the methods are key for an effective process development when using HBcAg VLP as potential gene delivery vehicles.

## 4.1 Introduction

In recent years, virus-like particles (VLPs) gained significant attention due to their importance as potential vaccines and gene delivery vehicles (Jinming Li et al., 2013; Hill et al., 2017; Mohsen et al., 2017; Rohovie et al., 2017; Le and Müller, 2021; Nooraei et al., 2021; He et al., 2022). Among these VLPs, Hepatitis B core antigen (HBcAg) has emerged as a promising candidate for various biomedical applications (Cooper and Shaul, 2005; Porterfield et al., 2010; Choi et al., 2011, 2013; Moradi Vahdat et al., 2021; Petrovskis et al., 2021). For gene delivery purposes, the naturally occurring nucleic acid (NA) binding region of the HBcAg but also biologically engineered binding regions are often utilized to effectively encapsulate therapeutic nucleic acids (NA<sub>ther</sub>) (Porterfield et al., 2010; Petrovskis et al., 2021). During intracellular formation of HBcAg VLPs in *E. coli* (Effio and Hubbuch, 2015), host cell-derived nucleic acids (NA<sub>hc</sub>) are bound to the NA binding region and encapsulated in the VLPs (Porterfield et al., 2010; Sominskaya et al., 2013; Strods et al., 2015; Zhang et al., 2021b). During the subsequent downstream purification process and before reloading the VLPs with NA<sub>ther</sub>, it is crucial to remove entrapped and bound NA<sub>hc</sub>. For this purpose, techniques, such as enzymatic treatment (Newman et al., 2009), affinity chromatography (Zhang et al., 2021b), alkaline treatment (Strods et al., 2015), and lithium chloride precipitation (Porterfield et al., 2010), are investigated in literature. After successful depletion of the NA<sub>hc</sub>, the VLPs are often loaded with the respective NA<sub>ther</sub> by direct mixing (Strods et al., 2015; Petrovskis et al., 2021). To evaluate the successful depletion of NA<sub>hc</sub> and possible HBcAg protein loss during removal as well as subsequent effective loading of the VLPs with NA<sub>ther</sub> on the basis of e.g. the encapsulation efficiency or payload of the VLPs, a precise absolute quantification of HBcAg VLPs and VLP-bound NAs is needed.

However, absolute quantification of HBcAg VLPs and the bound NA<sub>hc</sub> remains challenging. UV/Vis spectroscopy is a common tool to quantify proteins and NAs, utilizing the absorption maxima of proteins at 280 nm and NAs at 260 nm. In combination with high-performance liquid chromatography (HPLC) methods, UV-spectra allow to quantify different HBcAg VLP protein species (capsids and dimers) and impurities such as host cell proteins (HCPs) and free NAs by size exclusion chromatography (Rüdt et al., 2019; Hillebrandt et al., 2020, 2021; Hillebrandt and Hubbuch, 2023). Additionally, reversed-phase (RP) chromatography is commonly used to quantify different VLPs. In this case, the sample is subjected to a preliminary treatment with dissociation buffer containing guanidine-HCl and DTT (Yuan et al., 1998; Ladd Effio et al., 2015) or zwitterionic detergent (Shytuhina et al., 2014). However, a specific RP-

HPLC method for the quantification of HBcAg VLPs with bound NAs has not been published in literature.

UV/Vis spectroscopy is inherently unable to absolutely quantify HBcAg VLP proteins with bound NAs without prior quantitative separation of proteins and NAs, e.g. by chromatography. In the absence of a successful separation the overlapping signals of the proteins and NAs in the relevant wavelength region of the UV spectra only allow for a relative quantification. Relative analysis of the A260/A280 ratio of HBcAg proteins and bound NA<sub>hc</sub> has been used to correlate HBcAg VLP constructs with different lengths of the NA binding region to particle loading with NA<sub>hc</sub> (Valentic et al., 2022). It can also be used to evaluate the purity of the VLPs after the depletion of NA<sub>hc</sub> (Porterfield et al., 2010; Zhang et al., 2021b, 2021a). For the loading of HBcAg VLPs with NA<sub>ther</sub> of known nucleotide sequence, a method to approximate the absolute amounts of protein and NA was proposed in literature (Porterfield and Zlotnick, 2010) and used to estimate protein and NA composition (Strods et al., 2015; Petrovskis et al., 2021). However, this method is not suited for a precise quantification of VLP proteins and (i) non-specific NA<sub>hc</sub>. Nor can it be applied to (ii) mixtures of residual undesired NA<sub>hc</sub> and NA<sub>ther</sub> or (iii) mixtures of various types of NA<sub>ther</sub>. This information is, however, required for evaluating the successful depletion of NA<sub>hc</sub> and possible HBcAg protein loss during the removal, as well as the subsequent effective loading of the VLPs with NA<sub>ther</sub>.

While dye-based fluorescence assays are commonly used for NA quantification, they can be sensitive to contaminants that interfere with the binding of the dye to its target (Taylor et al., 2010). In literature, a RiboGreen assay was used for the quantification of RNA in murine leukemia VLPs (Rulli et al., 2007). Before quantification, the RNA was extracted according to a NA extraction protocol including proteinase K lysis and phenol-chloroform extraction. In contrast, no prior extraction of DNA was required in a study by Effio and Hubbuch (Effio and Hubbuch, 2015), as it was not bound to the VLPs and did not interfere with the binding of the dye to the DNA. Here, a PicoGreen assay was used for the quantification of DNA impurities in HBcAg VLP purification. However, for HBcAg VLPs with NA binding region for gene delivery and thus bound NAs, appropriate NA extraction seems to be necessary to quantify the NAs precisely. This can be concluded from the conflicting results of the relative analysis of the A260/A280 ratio with UV-spectroscopy and a dye-based fluorescence assay without prior extraction of the HBcAg VLPs and bound NA<sub>hc</sub> (Zhang et al., 2021a).

A variety of methods, such as phenol-chloroform extraction, anion exchanger, silica membranes, cesium chloride density gradient centrifugation are polyethylene-glycol (PEG) precipitation are used for the extraction of NAs in molecular biology (Schmitz and Riesner, 2006; Mülhardt and Beese, 2007; Wright et al., 2009; Ali et al., 2017; Toni et al., 2018). Commonly used methods

to specifically separate protein contaminants from NAs are the phenol-chloroform extraction, PEG precipitation or silica column-based purification, coupled with a preceding proteinase K digestion, if proteins are bound to the NAs. However, phenol-chloroform extraction is rarely used today because of the caustic and harmful chemicals involved (Mülhardt and Beese, 2007; Wingfield and Atcharawiriyakul, 2021). PEG precipitation is characterised by a complex interplay of PEG lengths and the type of NAs precipitated (Schmitz and Riesner, 2006; Mülhardt and Beese, 2007), and is also known to precipitate proteins (Hönig and Kula, 1976). While silica column-based purification

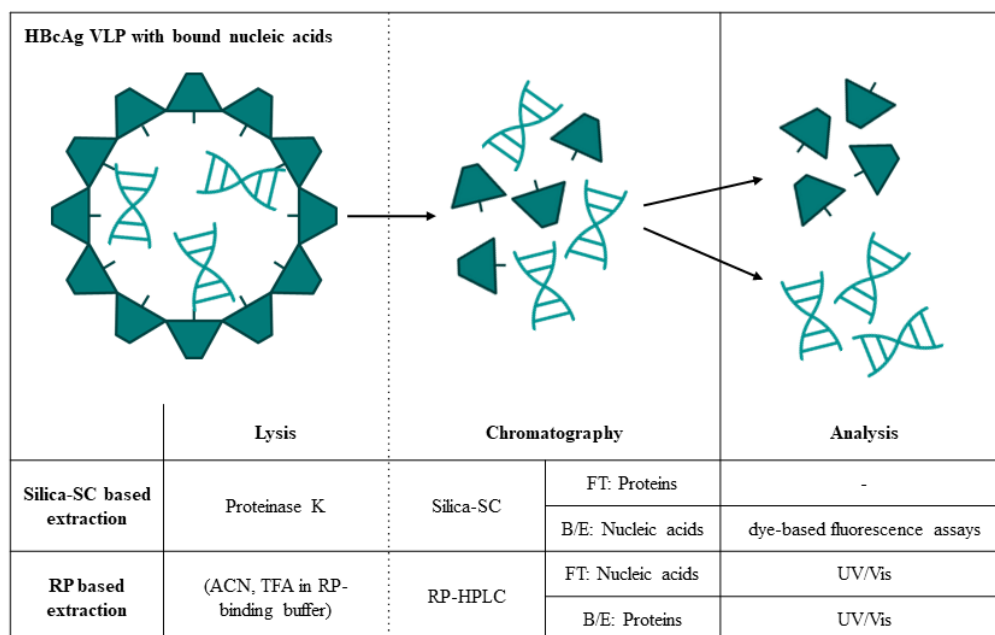


Figure 4.1 Lysis, chromatography and analysis techniques investigated in this work for the absolute quantification of HBcAg VLP proteins and bound nucleic acids. B/E: bind and elute; FT: flow-through; HBcAg: Hepatitis B core Antigen; HPLC: high performance liquid chromatography; RP: reversed phase; SC: spin column; VLP: virus-like particle

provides reproducible results and it appears possible to overcome NA recovery issues, by a yield increase through recirculation of the extracts over anion column membranes (Mülhardt and Beese, 2007). For their use in molecular biology these methods do not necessarily require a high purity and recovery. The potential loss of NA during the extraction process is often irrelevant for the further processing of the NAs or is compensated by reproducing the extracted NAs by polymerase chain reaction prior to analysis (Mülhardt and Beese, 2007).

These methods might be used as NA extraction methods for the absolute quantification of NAs in HBcAg VLP process development. However, for accurate quantification of NAs bound to VLP proteins, the NA solution must be of high purity after the extraction and the loss of NAs during these procedures must be minimized. Indeed, proteinase K treatment followed by phenol-chloroform extraction is used to isolate RNA from HBcAg VLPs in preparation

for native agarose gel electrophoresis (NAGE) (Petrovskis et al., 2021) and to extract RNA from murine leukaemia VLPs prior to the RiboGreen assay (Rulli et al., 2007), but purity and recovery of the extraction procedures are not verified prior to analysis and the analysis thus has to be considered semi-quantitative. Beyond that, for HBcAg VLPs with bound NAs, a NA extraction procedure expressing sufficient purity and specified NA recoveries for accurate quantification of  $NA_{hc}$  or  $NA_{ther}$  by dye-based fluorescence assays to evaluate the successful depletion of  $NA_{hc}$  and possible HBcAg protein loss during the removal, as well as the subsequent effective loading of the VLPs with  $NA_{ther}$ , still remains to be developed.

Table 4.1 Overview of approaches and utilized analytics for the investigated silica-SC based extraction, including Proteinase K lysis and silica spin column chromatography, characterization and analysis. B/E: bind and elute; NAGE: native gel electrophoresis

Silica-SC Based Extraction	Approach	Analytics	Data
Process	protein lysis	SDS-PAGE	Figure 4.2
	B/E: nucleic acid adsorption	NAGE	Figure 4.3
	B/E: nucleic acid elution	NAGE, RiboGreen	Figure 4.4
Characterization	recovery	RiboGreen, qPCR	Figure 4.5
	with / without lysis and extraction	RiboGreen	Table 4.2
Analysis	lambda DNA / 16S RNA	RiboGreen	Figure 4.6
	enzymatic treatment	RiboGreen, PicoGreen	Table 4.3

In this work, we present a comprehensive investigation into a silica spin column (SC) based extraction for the absolute quantification of  $NA_{hc}$  and  $NA_{ther}$  bound to HBcAg VLPs by dye-based fluorescence assays and newly developed an RP-HPLC method for the separation and simultaneous quantification of HBcAg VLP proteins and bound NAs (Figure 4.1). For the silica-SC based extraction,



the lysis and silica-SC chromatography were investigated to achieve an optimal purity and recovery of the NAs to be quantified. The need for NA extraction prior to quantification by dye-based fluorescence assays was demonstrated by comparing samples before and after the silica-SC based extraction. Suitability of the silica-SC based extraction for further processing using RiboGreen assay or quantitative PCR (qPCR) was verified (Table 4.1). Moreover, we developed a novel RP based extraction method for simultaneous quantification of HBcAg VLP proteins and NA<sub>hc</sub> (Figure 4.1). The method separates HBcAg VLP proteins and bound NAs due to lysis of the VLPs by the RP-HPLC loading mobile phase, and with the latter being quantified in the flow-through, and the former in the gradient elution of the RP-HPLC. The method was applied to quantify the absolute amounts of NA<sub>hc</sub> in HBcAg VLP constructs with different lengths of NA binding regions, correlating to relative results described earlier (Valentic et al., 2022). The proposed methods turned out to be suited for absolute quantification of HBcAg VLP proteins and bound NAs. This is required to evaluate the depletion of NA<sub>hc</sub> and possible HBcAg protein loss during the process as well as effective loading of the VLPs with NA<sub>ther</sub> in terms of the encapsulation efficiency or payload of the HBcAg VLPs for its use as gene delivery vehicle.

## 4.2 Materials and Methods

### 4.2.1 Buffers, VLPs, and DNA

If not stated otherwise, all chemicals were purchased from Merck (Darmstadt, Germany). Solutions and buffers were prepared with ultrapure water (PURELAB Ultra, ELGA LabWater) and aqueous buffers were filtered through a 0.2 µm pore-size cellulose acetate filter (Pall Corporation, Port Washington, NY, United States). Buffers were pH-adjusted with 32% HCl or 4 M NaOH. HPLC grade acetonitrile (ACN) was purchased from Avantor (Radnor, PA, United States) and trifluoroacetic acid (TFA) from Thermo Fisher Scientific (Waltham, MA, United States).

HBcAg VLPs were produced and purified as described earlier (Valentic et al., 2022). Constructs Cp149, Cp154, Cp157, Cp164, Cp167, and Cp183, with different lengths of NA binding regions and different amounts of bound NA<sub>hc</sub> (Valentic et al., 2022) after re-dissolution or CaptoCore 400 (CC) purification were used for experiments. Prior to all experiments, HBcAg VLPs were present in purification buffer consisting of 50 mM Tris and 150 mM NaCl at pH 7.2. The dsDNA used with a length of 720 bp, was produced by amplification of a pKR-based vector including an eGFP encoding gene sequence, using 5'-ATGGTGAGCAAGGGCGAG-3' as forward primer and 5'-TTACTTGTACAGCTCGTCCA-3' as reverse primer.

Amplification was performed with PCRBio HiFi polymerase (Nippon Genetics Europe GmbH, Düren, Germany). The PCR product was purified by native gel electrophoresis, and extracted using a Wizard SV gel and a PCR clean-up kit (Promega, Madison, WI, United States).

### 4.2.2 Silica Spin Column Based Extraction

The silica spin column (SC) based extraction consists of (i) enzymatic lysis at 56 °C for 15 min or 60 min using 12 U proteinase K, (ii) addition of ethanol and adsorption of the NAs on a silica SC, centrifugation and disposal of the flow-through, (iii) washing with a wash buffer, and (iv) elution of the NAs from the silica-SC by addition of a total of 100-200 µL of nuclease-free water (New England Biolabs, Ipswich, MA, United States), followed by centrifugation. In the following the terminology ‘silica-SC based extraction’ comprises proteinase K lysis and silica-SC chromatography. The materials used for the silica-SC based extraction were included in the EasyPure Viral DNA/RNA Kit (TransGen Biotech, Beijing, China). To achieve optimal purities and recoveries of the extracts, (i) the lysis, (ii) adsorption, and (iv) elution procedures were investigated. Lysis times of 15 min and 60 min, binding procedures without, and with 5-fold and 20-fold recirculation of the flow-through, and elution with 4-fold and 8-fold 25 µL and 1-fold 200 µL elution volumes were evaluated. To analyse different elution procedures and the recovery of NAs for different loadings, NA<sub>hc</sub>-stocks with a known concentration were produced. For this, CC-purified Cp157 was extracted and the NA concentration was determined by RiboGreen assay. Silica-SC based extraction results were obtained with the materials included in the EasyPure Viral DNA/RNA Kit. Prior to silica-SC based extraction, the NA content of the VLP samples were estimated by UV/Vis absorbance measurements using a NanoDrop™ 2000c UV/Vis spectrophotometer (Thermo Fisher Scientific, Waltham, MA, United States). Samples were diluted to a maximum of 25 ng/µL NAs, if not stated otherwise.

### 4.2.3 RP Based Nucleic Acid and Protein Extraction

Analytical reversed-phase chromatography was performed with a TSKgel Protein C4-300 column (3 µm, 4.6x150 mm) from Tosoh Bioscience (Tokyo, Japan) on a Vanquish UHPLC system, controlled by Chromeleon version 7.2 (both Thermo Fisher Scientific, Waltham, MA, United States). Chromatography was carried out at 50 °C with mobile phase A (mpA) containing 0.5% TFA in water and mobile phase B (mpB) containing 0.4% TFA in ACN. Samples were injected without prior adjustment to the mobile phase composition during injection and adsorption. The chromatographic separation was carried out with a 10 min adsorption step applying 92% mpA and 8% mpB, followed by an 18 min linear AB gradient elution to 100% mpB and a 7 min re-equilibration with 92% mpA and 8% mpB at a flow rate of 0.5 mL/min. Eluting components

were detected with a diode array detector evaluating peak areas at 260 nm and 280 nm.

#### 4.2.4 Analytics for Silica-SC Based Extraction, RP Based Extraction and Quantification of Proteins and Nucleic Acids

For SDS-PAGE, NuPage 4–12% BisTris protein gels, LDS sample buffer, and MES running buffer were used and run on a PowerEase Touch 350W Power Supply (all Invitrogen, Waltham, MA, United States) at reduced mode with 50 mM DTT in the sample solution. Protein staining was performed with a Coomassie blue solution. For NAGE, 0.7% agarose (Carl Roth, Karlsruhe, Germany) in TAE buffer (40 mM Tris, 20 mM acetic acid, 1 mM EDTA) with 1 µg/mL midori green (Nippon Genetics GmbH, Düren, Germany) was used and run on a PowerPac Basic (Bio-Rad, Hercules, CA, United States) followed by protein staining with a Coomassie blue solution of the gels, if necessary.

RiboGreen RNA and PicoGreen dsDNA assays (both Thermo Fisher Scientific, Waltham, MA, United States) were performed according to the manufacturer's manual with minor adaptations. The assays were standardized with NAs included in the respective assay kit and three replicates of six concentrations (0, 10, 30, 100, 300, 1000 ng/mL), if not stated otherwise. Samples were measured in three replicates of three dilutions (10-, 50-, and 100-fold). In one study outlined below enzymatic treatment in 50 µL scale was conducted prior to assay quantification to identify different NA species. 2 U DNase I (New England Biolabs, Ipswich, MA, United States) with reaction buffer provided by the DNase I manufacturer were used to degrade DNA for 10 min at 37°C and heat inactivated for 10 min at 75°C prior to RiboGreen RNA assay. A mix of 2 µg RNase A and 5 U T1 (Thermo Fisher Scientific, Waltham, USA) with reaction buffer (10 mM Tris-HCl, pH 7.5, 300 mM NaCl, 5 mM EDTA) was applied to degrade RNA for 30 min at 37°C. With this RNase A/T1-Mix in corresponding reaction buffer in combination with 100 U S1 Nuclease (both Thermo Fisher Scientific, Waltham, USA) both RNA and ssDNA were degraded prior to PicoGreen DNA assay for 30 min at 37°C. NA concentrations determined by the RiboGreen assay were corrected according to the determined correlation between the observed and loaded NA masses [µg] (Figure 4.5 a)), according to equation (1).

$$Load\ NA_{hc} = \frac{Observed\ NA_{hc}}{0.9467} + 0.2071\ \mu g \quad (1)$$

qPCR was conducted and analysed with a QuantStudio 5 System (Thermo Fisher Scientific, Waltham, MA, United States). The PCR reaction comprised a 96 °C hold step for 7 min, followed by 40 cycles each at 96 °C for 15 sec and 60 °C for 30 sec. The primers used to amplify the dsDNA were 5' TTCTTCAAGTCCGCCATGCCCCG 3' as forward and 5' TCGATGCCCTTCAGCTCGATGC 3' as reverse primer. Reactions were

conducted with a final volume of 20  $\mu\text{L}$  containing 2  $\mu\text{mol}$  of each DNA polymerase primer, SYBR®Green (Bio-Rad Laboratories, Hercules, CA United States) and 5  $\mu\text{L}$  sample in a MicroAmp™ Optical 96-Well Reaction Plate (Thermo Fisher Scientific, Waltham, MA, United States). The analysis was standardized with dsDNA of known concentration, determined by PicoGreen assay and three replicates of six dilutions (1-, 10-, 100-, 1000-, 10.000-, 100.000-fold). Samples were measured in three replicates of three dilutions (100-, 1000-, and 10.000-fold). NA concentrations determined by qPCR, can be corrected according to the determined correlation between observed and loaded dsDNA masses [ $\mu\text{g}$ ] (Figure 4.5 b)), according to equation (2).

$$\text{Load } NA_{ther} = \frac{\text{Observed } NA_{ther}}{0.9592} + 0.3452 \mu\text{g} \quad (2)$$

To determine VLP morphology at RP-HPLC injection, for transmission electron microscopy (TEM) analysis, CC-purified VLPs were diluted with purification buffer filtered through a 0.2  $\mu\text{m}$  syringe filter. The VLPs were mixed 50:50 with either purification buffer for the control sample or solutions containing ACN and TFA to obtain ACN concentrations of 4%, 6% and 8%, where 8% corresponds to the conditions of the adsorption step with 92% mpA and 8% mpB. VLP concentrations were set to 0.75 g/L for every condition. Samples were analysed by TEM on a Fecnei Titan<sup>3</sup> 80-300 microscope (FEI company, Hillsboro, OR, United States). Sample preparation was conducted according to studies with chimeric HBcAg VLPs (Rüdt et al., 2019) with 1% (w/v) alcian blue 8GX (Alfa Aesar, Ward Hill, MA, United States) in 1% acetic acid as hydrophilisation solution and 2% ammonium molybdate (VI) (Acros Organics, Geel, Belgium) solution (at pH 6.25) as staining solution.

Protein and NA concentrations analysed by RP-HPLC and UV/Vis were calculated from the peak area obtained and a conversion factor determined by calibration with Cp149 and dsDNA of known concentrations.

## 4.3 Results

### 4.3.1 Silica-SC Based Extraction

For an accurate quantification of NAs bound to HBcAg VLP proteins by dye-based fluorescence assays, a high recovery of the NAs during silica spin column (SC) based extraction and high purity of the obtained extracts are needed. Consequently, a silica-SC based extraction procedure including a proteinase K lysis followed by silica-SC chromatography was investigated for its use as pre-treatment for the absolute quantification of  $NA_{hc}$  and  $NA_{ther}$  bound to HBcAg VLPs by dye-based fluorescence assays.

### 4.3.2 Lysis of VLPs by Proteinase K

Enzymatic lysis times of 15 min and 60 min were investigated to achieve a high purity of NAs after extraction and, hence, to enable accurate quantification of NAs present. For this, the silica-SC based extraction was carried out with Cp164 after re-dissolution and an approximate total protein concentration of 4 g/L, determined by microvolume UV/Vis absorbance measurements. With a lysis time of 15 min, protein impurities could be detected in the samples after silica-SC based extraction on SDS-PAGE (see lane 3, Figure 4.2). For a lysis time of 60 min, a considerably lower intensity of the impurity bands on the SDS-PAGE gel in the extracts after silica-SC based extraction was observed. No protein contaminants could be determined by SDS-PAGE when VLP samples were diluted to approximately 25 ng/ $\mu$ L NAs prior to the extraction (Figure 4.3 b)). As a result, further silica-SC based extraction experiments in this study were conducted with a proteinase K lysis time of 60 min.

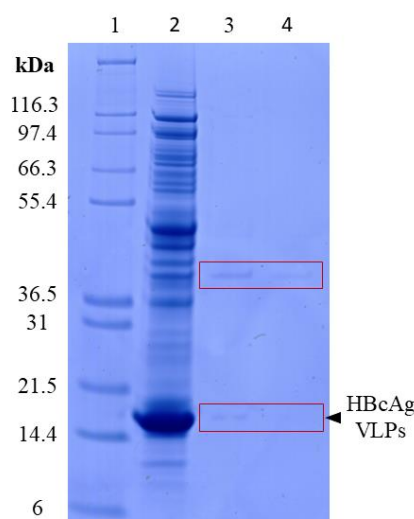


Figure 4.2 Investigation of proteinase K lysis times. Remaining protein impurities after silica-SC based extraction for 15 min (lane 3) and 60 min (lane 4) lysis time on SDS-PAGE for not diluted Cp164. Marker in lane 1 and initial Cp164 VLP sample before extraction in lane 2. The boxes were added to guide the eye. HBcAg: Hepatitis B core Antigen; SC: spin column; VLP: virus-like particle

### 4.3.3 Adsorption of Nucleic Acids

In order to achieve an efficient adsorption of the NAs to the silica-SC matrix varying flow-through recirculation procedures were investigated. The silica-SC based extraction was carried out with Cp164 after re-dissolution and 20-fold diluted to comply with the binding capacity of 5  $\mu$ g for the silica-SC used. Elution of NAs bound to the silica-SC was achieved using 100  $\mu$ L of water. Extraction results by NAGE analysis are depicted in Figure 4.3 a). Samples after silica-SC based extraction without recirculation of the flow-through are shown in lanes 3 and 4 (samples were analysed in duplicates), 5-fold recirculation in

lanes 5 and 6 and 20-fold recirculation in lanes 7 and 8. In summary, an increase in the detected amount of NAs in the extract after silica-SC based extraction is observed when using recirculation procedures. The 5-fold recirculation procedure resulted in the highest fluorescence associated with NAs (and presumably the amount of NAs) on the NAGE. The corresponding final flow-through samples were analysed on NAGE to support mass balance by displaying

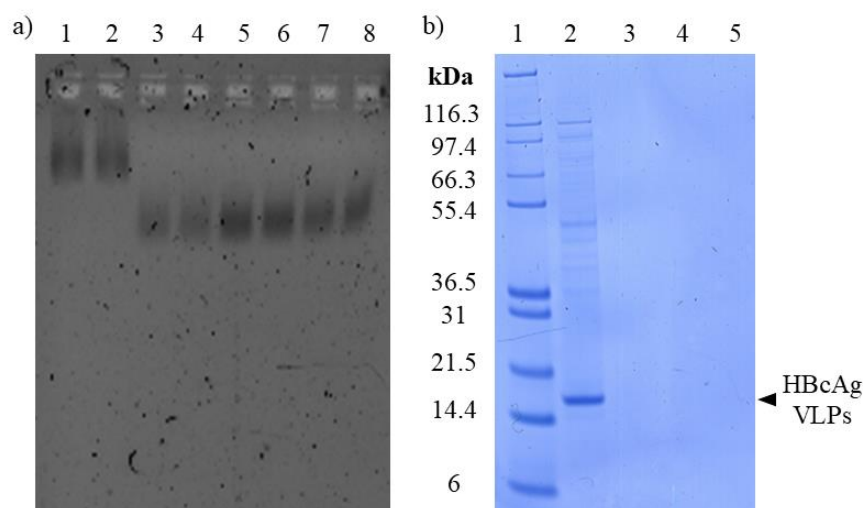


Figure 4.3 Investigation of silica-SC adsorption. a) Nucleic acids on NAGE in the extracts after silica-SC based extraction. Depicted are extracts without recirculation of the flow-through in lanes 3 and 4, extracts with recirculation of the flow-through fivefold (lanes 5 and 6) and 20-fold (lanes 7 and 8), and nucleic acids bound in initial Cp164 VLP sample (diluted 20-fold) prior to extraction in lanes 1 and 2. b) Detection of protein content in the extracts after silica-based extraction without recirculation, 5-fold and 20-fold recirculation in lanes 3, 4 and 5, respectively, on SDS-PAGE. Marker in lane 1 and initial Cp164 VLP sample (diluted 20-fold) before extraction in lane 2. NAGE: native gel electrophoresis; SC: spin column; VLP: virus-like particle

NAs not bound to the silica-SC used in the flow-through fractions (data not shown). NAs were, however, not detected in the flow-through fractions for all adsorption procedures. All investigated flow-through fractions produced high fluorescence signals in the gel pockets. However, NAs that may be trapped in the gel pockets may be untraceable due to interfering fluorescence signals from other components in the flow-through fractions. In particular, analysis of the components present in the flow-through fractions revealed stained areas around the gel pockets for proteinase K and the binding buffer used (see Appendix B: S4.1). Moreover, the extracts after silica-SC based extraction were examined for protein contamination by SDS-PAGE. No protein contaminants were detected in the extracts, see lanes 3, 4 and 5 (Figure 4.3 b), duplicates in Appendix B: S4.2).

#### 4.3.4 Elution of Nucleic Acids

For an absolute quantification of the total amount of NAs, an efficient elution of the NAs bound to the silica-SC matrix is crucial. The silica-SC based extraction was conducted with a load of 0.815  $\mu\text{g}$  NAs (as listed in Appendix B: S4.3, Table S4.1) and the bound NAs were subjected to varying elution conditions comprising 4 x 25  $\mu\text{L}$ , 8 x 25  $\mu\text{L}$  and 1 x 200  $\mu\text{L}$  elution volumes. Even though, the procedure applying 1 x 200  $\mu\text{L}$  elution volume resulted in a lower intensity of the NA band on the NAGE gel (lane 4 in Figure 4.4), compared to the initial load material in lane 1, it showed the highest intensities on NAGE as well as the

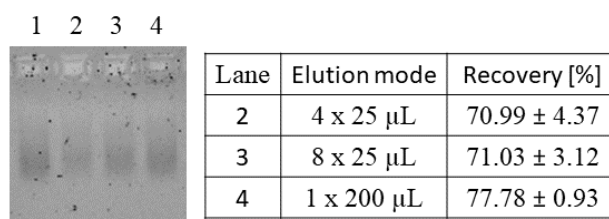


Figure 4.4 Investigation of silica-SC elution procedure. Nucleic acids in the extracts after silica- SC based extraction on NAGE and respective recovery values obtained by RiboGreen analysis for varying elution procedure with 4 times 25  $\mu\text{L}$  (lane 2), 8 times 25  $\mu\text{L}$  (lane 3) and 1 time 200  $\mu\text{L}$  (lane 4). Initial load material of CC purified Cp157 (diluted to comply with silica-SC binding capacity, see chapter 4.2.2) in lane 1. CC: CaptoCore 400; NAGE: native gel electrophoresis; SC: spin column

highest NA recovery of 77.78  $\pm$  0.93%, when comparing the different elution modes. The 4 x 25  $\mu\text{L}$  and 8 x 25  $\mu\text{L}$  elution modes produced lower intensities on the gel, correlating with the lower recoveries measured by RiboGreen (Figure 4.4). PicoGreen analysis was conducted in parallel, but showed the same trends (data not shown). Hence, the best quantitative silica-SC based extraction in terms of purity and recovery was obtained with 60 min lysis time, a 5-fold recirculation of the flow-through and 1 x 200  $\mu\text{L}$  elution.

#### 4.3.5 Characterization of the Silica-SC Based Extraction

##### 4.3.5.1 Nucleic Acid Recovery

To investigate the influence of the amount of NAs loaded onto the silica-SC during silica-SC based extraction, loadings of host cell-derived nucleic acids ( $\text{NA}_{\text{hc}}$ ) and dsDNA were varied. The observed masses in the extracts analysed by RiboGreen for the varying amounts of processed  $\text{NA}_{\text{hc}}$  and the respective final recoveries are depicted in Figure 4.5 a). PicoGreen analysis was conducted in parallel, but showed the same trends (data not shown). With a higher amount of loaded  $\text{NA}_{\text{hc}}$  an increased proportion of NAs is lost during silica-SC based extraction. This is reflected by the gap between the identity line and the observed eluted masses. However, the recoveries rise from 55% for 0.47  $\mu\text{g}$  load

to 81% for 1.4  $\mu\text{g}$  load to 85% for 2.8  $\mu\text{g}$  load, and up to 93% for 4.67  $\mu\text{g}$  load. The results for dsDNA are displayed in Figure 4.5 b). The dsDNA behaviour is similar to that of the  $\text{NA}_{\text{hc}}$ , with loss of NAs increasing with higher amounts of loaded dsDNA, except for a load of 0.95  $\mu\text{g}$  dsDNA. Recovery rates range from 64% for 0.31  $\mu\text{g}$  load up to 86% for 3.12  $\mu\text{g}$  load dsDNA. For a load of 0.95  $\mu\text{g}$  dsDNA, however, a loss of 0.74  $\mu\text{g}$  was observed, resulting in a recovery of 21%, substantiating that this measurement was an outlier. An overview of recovery rates observed in preliminary experiments and data of this work for

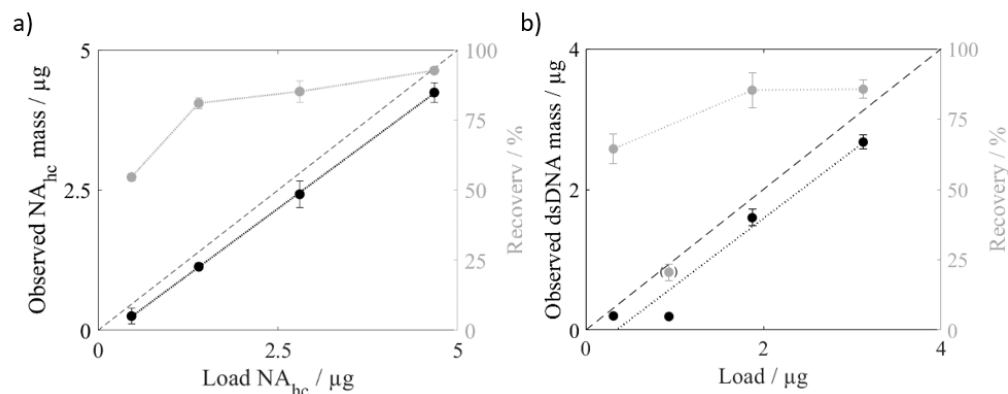


Figure 4.5 Nucleic acid recoveries for silica-SC based extraction. a) Observed  $\text{NA}_{\text{hc}}$  mass and identity line, and respective recoveries for different amounts of loaded  $\text{NA}_{\text{hc}}$  derived from Cp157 HBcAg VLPs, analysed by RiboGreen. b) Observed dsDNA mass and identity line, and respective recoveries for different amounts of loaded dsDNA, analysed by qPCR. Lines were added to guide the eye. HBcAg: Hepatitis B core Antigen;  $\text{NA}_{\text{hc}}$ : host cell-derived nucleic acids;  $\text{NA}_{\text{ther}}$ : therapeutic nucleic acids; VLP: virus-like particle

various loadings of  $\text{NA}_{\text{hc}}$  and dsDNA is provided in the Appendix B: S4.3. Using the recoveries obtained for different loadings of NAs during the silica-SC based extraction, the observed NA concentrations can be corrected as explained in chapter 4.2.4.

#### 4.3.5.2 Quantification with and without prior Silica Spin Column Based Extraction

To demonstrate the need for prior NA extraction, NA quantification of Cp157 was performed by means of the RiboGreen assay both with and without prior silica-SC based extraction. Extraction was performed in biological triplicates for Cp157 and samples were analysed by RiboGreen in four dilutions (undiluted, 10-, 50-, and 100-fold). The NA concentrations and relative standard deviations determined are listed in Table 4.2. The concentration without prior silica-SC based extraction was determined to be  $13.83 \pm 5.97 \text{ ng}/\mu\text{L}$ . In case of prior extraction of NAs, however, RiboGreen analysis yielded significantly higher concentration values of around  $26.64 \text{ ng}/\mu\text{L}$  for Cp157, with small differences between the biological replicates. The relative standard deviation of measurements without prior silica-SC based extraction were high and equalled



43.17%, whereas standard deviations in case of a prior extraction ranged between 3.58% and 6.75%. Similar results for preliminary silica-SC based extraction procedures can be found in the Appendix B: S4.4.

#### 4.3.5.3 Analysis of Extracted Nucleic Acids

To investigate differences in the fluorescent emissions of different NA types lambda DNA (included in the PicoGreen assay) and 16S RNA (included in the

Table 4.2 Results for absolute nucleic acid concentrations of Cp157 HBcAg VLPs samples without and with prior silica-SC based extraction of nucleic acids (in triplicate), analysed by RiboGreen assay. HBcAg: Hepatitis B core Antigen; VLP: virus-like particle

	Concentration in ng/ $\mu$ L	Relative Standard Deviation [-]
Cp157 without extraction	$13.83 \pm 5.97$	43.17
Cp157 with extraction #1	$27.02 \pm 0.97$	3.58
Cp157 with extraction #2	$25.96 \pm 1.75$	6.75
Cp157 with extraction #3	$26.94 \pm 1.41$	5.24

RiboGreen assay) were analysed with RiboGreen without any prior enzymatic treatment. Figure 4.6 presents the fluorescent emissions of lambda DNA and 16s RNA for 1, 10, 100 and 1000 ng/mL. Lambda DNA induces a higher fluorescent emission than 16s RNA with RiboGreen dye. The calculated regression lines show a slope of 0.93 AU\* $\mu$ L/ng for lambda DNA and a smaller slope of 0.24 AU\* $\mu$ L/ng for 16S RNA in this experiment. To evaluate the influence of an enzymatic treatment on measurement accuracy and the composition of NA<sub>nc</sub> in Cp164 VLPs, several enzymatic treatments were conducted after the silica-SC based extraction but prior to PicoGreen and RiboGreen assay analysis. DNase I was used to degrade ssDNA and dsDNA prior to a RiboGreen RNA assay, while a RNase A/T1-Mix was used to degrade RNA and a RNase A/T1-Mix in combination with a S1 Nuclease was used to degrade both RNA and ssDNA prior to a PicoGreen DNA assay. RiboGreen measurement of the extracted NAs without an enzymatic treatment resulted in a total NA concentration of  $220.20 \pm 4.55$  ng/mL, whereas  $121.52 \pm 2.21$  ng/ml was determined by PicoGreen. Enzymatic treatments prior to analysis by dye-

based fluorescence assays resulted in 64.4% RNA, 56.7% ssDNA/dsDNA and 81.4% dsDNA lower NA concentrations compared to the respective analysis without enzymatic treatment (Table 4.3). For the quantification of specific NA species, a suitable quantification assay and enzymatic treatment are required after the silica-SC based extraction.

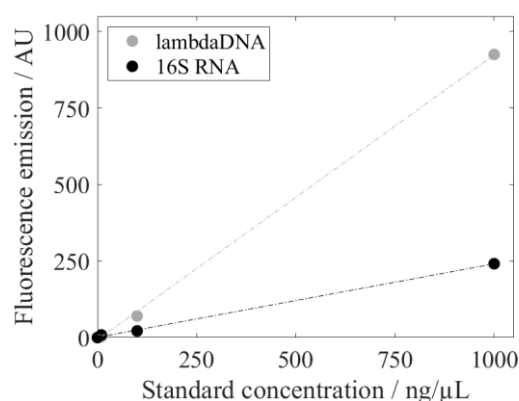


Figure 4.6 Fluorescence emission with RiboGreen dye of lambda DNA (standard solution provided by the PicoGreen assay kit) and 16S RNA (standard solution provided by the RiboGreen assay kit) with standard concentrations of 1, 10, 100 and 1000 ng/μL. Standard deviations are included, but not visible.

#### 4.3.6 Quantification of Proteins and Nucleic Acids using RP-HPLC

##### 4.3.6.1 Lysis of VLPs

In contrast to the silica-SC based extraction described above, the newly established RP based extraction does not require a separate lysis step using proteinase K. Although, samples were injected without prior adjustment to the mobile phase composition, the buffer components necessary for the RP-HPLC, namely ACN and TFA were able to replace the proteinase K step. This was investigated using transmission electron microscopy (TEM). TEM analysis of VLPs treated with ACN and TFA to mimic RP-HPLC injection conditions revealed intact VLPs without ACN and TFA in the solution and decomposed VLPs in the presence of ACN and TFA (Figure 4.7).

##### 4.3.6.2 Development of RP-HPLC for Extraction and Quantification of VLP Proteins and Nucleic Acids

RP-HPLC was investigated as an integrated technique combining the separation of proteins and bound NAs with concomitant quantification. Several HPLC columns with different combinations of mobile phases were screened in preliminary experiments (Appendix B: S3.5) and the most suitable column was evaluated in terms of linearity, precision, and accuracy. The RP-HPLC chromatogram in Figure 4.8 displays the separation of NAs of the sample in the flow-through (average A260/A280 of 1.78) and the gradient elution of the

proteins of the sample (average A260/A280 of 0.59) with increasing the ACN concentration of the mobile phase. Parallel to the RP method, HPLC control runs without prefilter and column were performed with Cp157 at three different dilution levels. Total peak areas at A280 of the control runs and RP method runs were compared and recovery rates between 96.8% and 100.6% were found. No pressure rise was observed in RP-HPLC throughout the injections for all HBcAg constructs and purity levels.

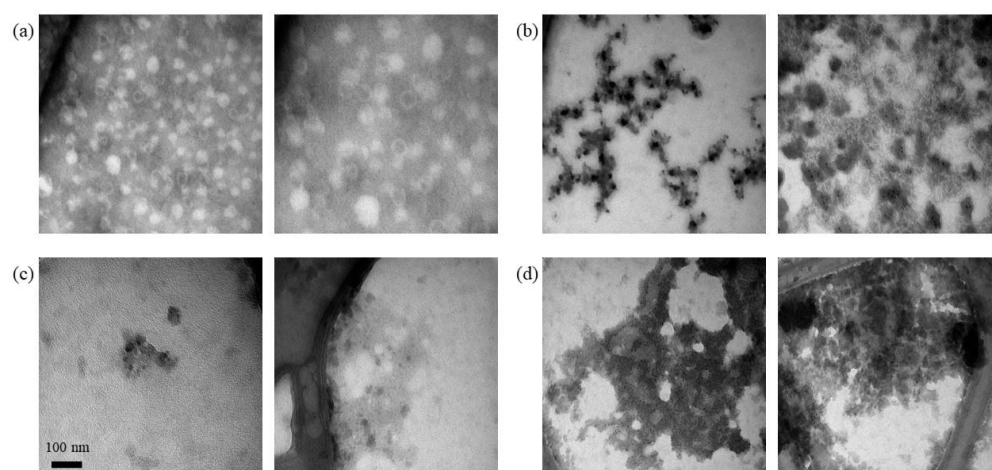
Table 4.3 Quantification of RNA and DNA species in Cp164 HBcAg VLPs after silica-SC based extraction and treatment with different enzymes to identify different nucleic acid species using RiboGreen and PicoGreen. HBcAg: Hepatitis B core Antigen; VLP: virus-like particle

Assay	Treatment	Determined nucleic acid species	Concentration in ng/mL
RiboGreen	-	Total	220.20 ± 4.55
	DNase 1 Treated	RNA	78.34 ± 1.67
PicoGreen	-	Total	121.52 ± 2.21
	RNAse A/T1	DNA	52.63 ± 3.60
	RNAse A/T1 + S1 Nuclease	dsDNA	22.57 ± 1.57

#### 4.3.6.3 Method Performance Assessment

Linearity of the RP protein quantification method was determined with Cp149 standards of known concentrations and resulted in a linear response between 0.29 and 9.27 µg with an R<sup>2</sup> of 0.99. Within that range, Cp157 samples resulted in linear responses of peak areas for both the gradient (protein) and flow-through (NA). Precision of the method was determined by injecting Cp149 and Cp157 samples in triplicate on three different days (Table 4.4). The relative standard deviation (RSD) of the total peak area within each day varied between 1.93% (Cp149, Day 1) and 0.18% (Cp157, Day 2). The RSD of the peak area averaged over three days (intermediate precision) was 3.9% for Cp149 and 1.26% for Cp157. The accuracy of the RP method was determined by analysing the same sample in different dilution stages. For Cp149, four different dilutions in the linear range were analysed. The accuracy, the percentage of measured mass compared to the theoretical mass, ranged between 99% and 106% (Table 4.5).

VLP samples with varying purity levels were analysed with the RP-HPLC method. Retention of HCPs in the RP column differed from VLPs within the elution step, enabling a purity determination of VLP protein to total protein. This analysis resulted in protein purities ranging widely from 17% to 65% for re-dissolved VLPs, while further purified VLP samples after the CaptoCore 400 (CC) purification step showed higher purities from 76% to 96% (data not shown). Six different CC-purified VLP constructs with variable lengths of the



**Figure 4.7** Lysis of VLPs by RP-HPLC injection conditions. TEM analysis of Cp157 HBcAg VLPs, diluted with purification buffer and mixed 50:50 with either purification buffer for the a) untreated control sample or solutions containing ACN and TFA to obtain ACN concentrations of b) 4% c) 6% and d) 8% and VLP concentration of 0.75 g/L, respectively. ACN: acetonitrile; HBcAg: Hepatitis B core Antigen; TEM: transmission electron microscopy; TFA: trifluoroacetic acid; VLP: virus-like particle

NA binding region and with varying amounts of bound NA<sub>hc</sub> were analysed with respect to NA and protein concentration. This resulted in NA to protein mass ratios from 0.0066 for Cp149 and increasing values for constructs with longer NA binding regions and levelling values around 0.2080 for Cp164, Cp167 and Cp183 (Figure 4.9). To compare NA quantification by silica-SC based extraction with subsequent RiboGreen analysis and RP based extraction with subsequent UV/Vis analysis, the six different CC-purified VLP constructs were analysed with both methods. For all constructs, the NA concentration in the samples determined by RP-HPLC and UV/Vis was higher than the value obtained by silica-SC based extraction and RiboGreen (Figure 4.10). When correcting the NA concentrations obtained for the silica-SC based extraction and RiboGreen assay according to equation 1, the resulting NA concentrations for Cp154, Cp157, and Cp167 samples are within the error of the fluorescent assay with maximum deviations of 11.5%. Whereas the results are outside the error of the fluorescent assay for Cp149, Cp164, and Cp183. However, Cp164 seems to be an outlier for both the silica-SC based extraction with subsequent RiboGreen analysis and the RP based extraction with subsequent UV/Vis analysis.

## 4.4 Discussion

### 4.4.1 Absolute Quantification of HBcAg Protein and Bound Nucleic Acids

The naturally occurring nucleic acid (NA) binding region of HBcAg is often used for effective therapeutic nucleic acid (NA<sub>ther</sub>) encapsulation (Porterfield et al., 2010; Petrovskis et al., 2021). During intracellular formation of the VLPs in *E. coli* (Effio and Hubbuch, 2015), host cell-derived nucleic acids (NA<sub>hc</sub>) are encapsulated. To evaluate the removal of the bound NAs and possible HBcAg protein loss during removal as well as effective loading of VLPs with NA<sub>ther</sub> later in the downstream process, precise absolute quantification of HBcAg VLPs and bound NAs is essential.

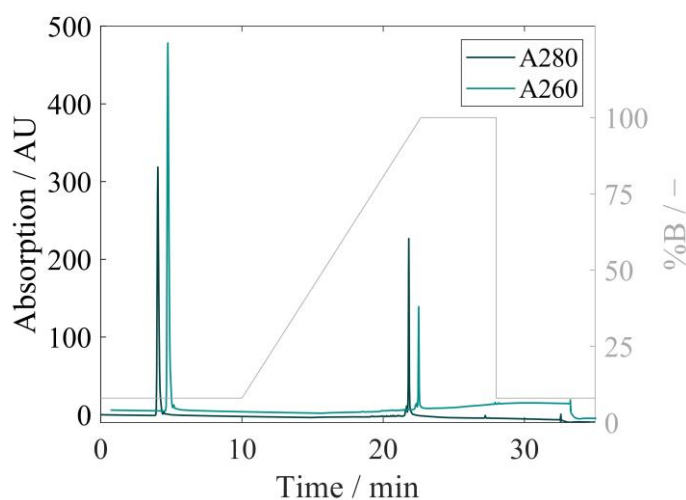


Figure 4.8 RP-HPLC chromatogram of Cp157 HBcAg VLP sample with the A280 and A260 (for clarity shifted +0.7 min in x-direction and +75 AU in y-direction) signals on the primary y-axis and the set percentage of buffer B in the mobile phase to highlight the RP-HPLC method phases on the secondary y-axis over the method run time. HBcAg: Hepatitis B core Antigen; HPLC: high performance liquid chromatography; RP: reversed phase; VLP: virus-like particle

In this work, a silica spin column (SC) based extraction procedure, including an enzymatic lysis and silica-SC chromatography, was investigated to attain a high purity and recovery of the NAs to be quantified, which is required for an accurate quantification. A high purity of the NA extracts after silica-SC based extraction was achieved by an extended proteinase K lysis time. The sufficient lysis of the VLP proteins ensures adequate separation of VLP proteins and bound NAs. The recovery of NAs was increased by recirculating the flow-through during the binding step and by increasing the elution volume, in order to obtain the most accurate quantification of NAs. Whereas in literature, the purity of the extracts after silica-SC based extraction and the recovery of the NAs to be quantified were not evaluated for the extraction procedure reported for RNA in murine leukaemia VLPs (Rulli et al., 2007). The investigation of

varying loadings of NAs in the silica-SC in our work revealed a relative correlation between the load and recovery of the NAs, which was independent of the NA species (unspecific NA<sub>hc</sub> or dsDNA, as model NA<sub>ther</sub>). Despite the higher absolute loss of NAs during the silica-SC based extraction, the relative recoveries increase with higher amounts of loaded NAs. This means that high loads of NAs are advantageous for most precise quantification of bound NAs. However, care needs to be taken not to exceed the binding capacity of the SC used. As this can be challenging due to imprecise approximations of protein and NA concentrations by means of existing techniques, the assessment of the recoveries for a range of NA loads enables a correction of the NA concentrations observed by silica- SC based extraction and dye-based fluorescence measurements to the actual amounts of loaded NAs in the sample, as implemented here.

Table 4.4 RP-HPLC method precision assessed by total peak area at A280 for Cp149 / Cp157. HPLC: high performance liquid chromatography; RP: reversed phase; RSD: relative standard deviation

Injection	Peak areas at A280 Cp149 / Cp157		
	Day 1	Day 2	Day 3
1	14.55 / 9.36	13.74 / 9.11	14.98 / 9.50
2	14.44 / 9.21	13.46 / 9.10	14.53 / 9.22
3	13.92 / 9.06	13.24 / 9.14	14.98 / 9.44
Average	14.31 ± 0.28 / 9.21 ± 0.12	13.48 ± 0.21 / 9.12 ± 0.02	14.82 ± 0.21 / 9.39 ± 0.12
Repeatability / RSD	1.93% / 1.32%	1.53% / 0.18%	1.42% / 1.27%
Intermediate precision	3.9% / 1.26 %		

Analysis of HBcAg VLPs with bound NA<sub>hc</sub> with and without prior NA extraction clearly demonstrated the value of the silica-SC based extraction. NA quantification by RiboGreen provided consistent results with negligible standard deviations between the biological replicates (n=3). Analysis of the same sample without prior silica-SC based extraction yielded in smaller NA

#### 4 Absolute Quantification of Hepatitis B Core Antigen (HBcAg) Virus-like Particles and Bound Nucleic Acids

concentration values compared to the results with prior silica-SC based extraction. Standard deviation of NA concentrations significantly exceeded those determined with a prior extraction. This might also explain the conflicting results in literature between UV-spectroscopy based analysis (A260/A280) and a dye-based fluorescence assay without a prior separation of the HBcAg VLPs and bound NA<sub>hc</sub> (Zhang et al., 2021a). However, the analysis of DNA impurities by the PicoGreen assay in HBcAg VLP purification (Effio and Hubbuch, 2015) does not seem to be affected by a lacking NA extraction, as the DNA presumably was not bound to the VLPs and binding of the dye to the DNA was not sterically impeded. This emphasizes the need for an effective NA extraction to accurately quantify NAs bound to HBcAg VLPs.

Table 4.5 RP-HPLC method accuracy assessed by total peak area at A280 at four concentrations of Cp149 HBcAg VLP. HBcAg: Hepatitis B core Antigen; HPLC: high performance liquid chromatography; RP: reversed phase; VLP: virus-like particle

Concentration level	Measured mass (µg)	Theoretical mass (µg)	Accuracy
1	8.76	8.67	101%
2	4.48	4.54	99%
3	2.70	2.54	106%
4	1.68	1.59	106%

We further analysed the NA<sub>hc</sub> obtained by the silica-SC based extraction procedure to evaluate the need for complex enzymatic treatments prior to analysis and the use of different specific fluorescent dyes to analyse different NA species. As expected, the lambda DNA produced a fluorescence signal other than that of the 16S RNA included in the RiboGreen assay. This clearly demonstrates the need for an enzymatic degradation step prior to the precise quantification of a specific NA species by dye-based fluorescence assays, as outlined by the assay manufacturer. In our study, the lambda DNA fluorescence signal of the RiboGreen dye was much higher than that of the 16S RNA provided in the assay kit, consistent with the stronger fluorescence enhancement of RiboGreen dye binding to dsDNA than for binding to equal mass of RNA described in literature (J. Jones et al., 1998). Further, this correlates with the results for the host cell-derived NA composition, assuming also different fluorescence signals of dsDNA and ssDNA. Results for RiboGreen and PicoGreen assays differ significantly for samples with and without enzymatic

treatment, indicating a complex interplay of fluorescence signals from the different NA species in the untreated samples. To quantify specific NA species, a suitable enzymatic pre-treatment for dye-based fluorescence assay quantification seems inevitable. This might also be useful when evaluating the

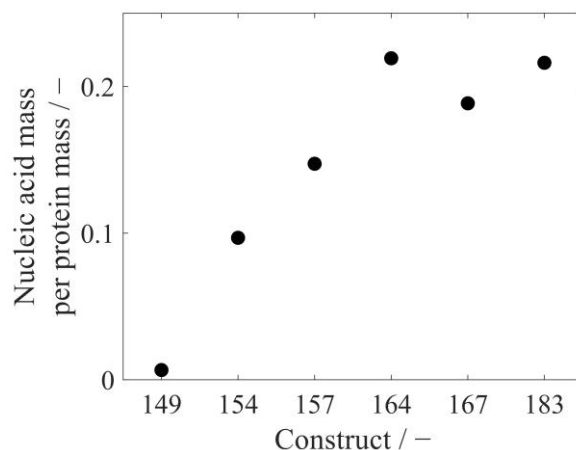


Figure 4.9 Mass ratio of nucleic acids to proteins for six different HBcAg VLP constructs. Absolute quantification was conducted by the developed RP-HPLC method in one replicate. HBcAg: Hepatitis B core Antigen; HPLC: high performance liquid chromatography; RP: reversed phase; VLP: virus-like particle

removal of specific NA<sub>nc</sub> from HBcAg VLPs, as in RNA-specific lithium chloride precipitation (Porterfield et al., 2010) or enzymatic treatments (Newman et al., 2009; Vafina et al., 2018). For the evaluation of general NA depletion (Strods et al., 2015b; Zhang et al., 2021a, 2021b), it may be sufficient and advantageous in terms of time and costs to perform the silica-SC based extraction procedure in combination with a dye-based fluorescence assay such as PicoGreen or RiboGreen, but without an enzymatic treatment. Depending on the objective of the specific experiment and the expected NA species, the complexity of the sample treatment between the silica-SC based extraction proposed here and the absolute quantification of NAs by dye-based fluorescence assays can be varied and adapted to the specific purpose.

The RP based extraction developed separates HBcAg proteins from bound NAs and enables concomitant absolute quantification of both proteins and NAs in the samples by UV/Vis. Unlike other RP-HPLC methods for the quantification of VLP proteins (Yuan et al., 1998; Shytuhina et al., 2014; Effio and Hubbuch, 2015), no dissociating pre-treatment of the samples is required before injection. The often used guanidine-HCl dissociation reagent (Yuan et al., 1998; Effio and Hubbuch, 2015) is visible in the UV-spectra and overlaps with the NA peaks in the flow-through of the chromatograms, which impedes NA quantification. However, injection of the samples into the RP-HPLC buffer containing ACN and TFA, even without prior adjustment of the samples to the mobile phase composition, appears to be sufficient to effectively dissociate the VLPs. This



prevents blockage of the chromatography column and additionally separates the bound NAs from the HBcAg proteins. In contrast to other HPLC-based quantification methods for HBcAg VLPs (Rüdt et al., 2019; Hillebrandt et al., 2020, 2021), the HBcAg proteins and bound NAs are separated and can therefore be accurately quantified by their UV spectra. Having evaluated the critical performance parameters with results being comparable to those presented in literature (Shytuhina et al., 2014), it can be stated that the RP-HPLC method developed can be used to reliably quantify the absolute amounts of HBcAg proteins and bound NA<sub>nc</sub>. The method has not yet been tested with NA<sub>ther</sub>, but it is expected to be applicable to NAs of a certain length. Investigations of different levels of purity of HBcAg VLPs with bound NAs during the downstream purification process, demonstrated the method's potential to determine HBcAg VLP purities. Due to varying retention times for HCPs and HBcAg protein, the method can further be applied to analyse intermediate purification samples and to support purification process development.

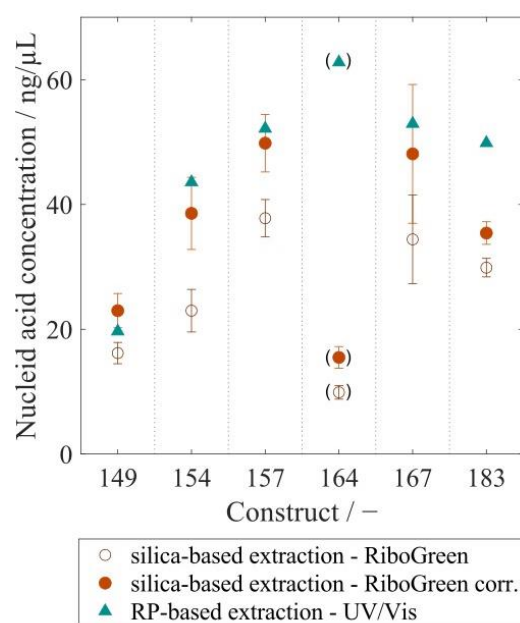


Figure 4.10 Comparison of nucleic acid quantification results obtained by RP based extraction using UV-Vis and silica-SC based extraction using a RiboGreen assay. Results of RiboGreen assay were corrected, following the correction procedure using equation 1 outlined in chapter 4.2.4 and depicted in Figure 5a. RP: reversed phase

The RP based extraction was applied to six different HBcAg constructs with different lengths of the naturally occurring NA binding region. The mass ratios of the measured absolute amounts of NAs and proteins correlate with the loading results of the HBcAg constructs obtained from the relative analysis of the A260/A280 ratio described in an earlier publication of our group (Valentic et al., 2022). Depending on the length of the NA binding region and positive charges present, different amounts of NAs are encapsulated in the HBcAg VLPs

(Le Pogam et al., 2005; Valentic et al., 2022). In Cp183 with around 3600 positive charges in the arginine-rich binding region of one HBcAg VLP capsid, 4970 nucleotides in the form of RNA per capsid were determined earlier by a simplified UV-spectroscopy method (Porterfield and Zlotnick, 2010). This results in a NA to protein mass ratio of around 0.34 when calculating with a molecular weight of 4.8 MDa for a Cp183 HBcAg capsid ( $T=4$ ) and a 326.99 g/mol for a nucleotide. However, the lower mass ratio of 0.22 for Cp183 obtained by RP-HPLC in our study suggests a lower load of HBcAg VLPs with NAs compared to literature (Porterfield and Zlotnick, 2010). A comparison of the results for NA quantification by silica-SC based extraction and subsequent RiboGreen quantification and the RP based extraction and quantification revealed discrepancies in the absolute NA concentration in the samples for the six different HBcAg constructs. After a correction procedure using equation 1, however, the concentrations calculated by the RP-HPLC method are mainly within the error of the corrected NA concentrations obtained by RiboGreen. The residual differences between the concentrations may be explained by operating errors and could be prevented by performing the silica-SC based extractions and RP-HPLC injections in replicates. The dye-based fluorescence NA quantification assays perform highly sensitive with a minimum detectable mass of, for example, 200 pg RNA for the RiboGreen assay, stated by the manufacturer. The sensitivity of the UV/Vis analysis to NAs is dependent on the path length of the sample cell and instrument settings, such as e.g. scan speed. We assume a sensitivity in the low ng range for the analytical setup used in this study. However, the comparison of the two methods presented for NA quantification showed that the sensitivity was not a concern, with values in the nanogram NA range. Both methods are applicable to quantify NAs bound to HBcAg VLPs in the concentration ranges present during process development. For a more specific and sensitive analysis, if needed, the NAs in the flow-through of the RP-HPLC methods could be fractionated and analysed further by the described dye-based fluorescence assay analyses.

### 4.4.2 Analytical Toolbox for HBcAg VLPs

The here investigated silica-SC based extraction, followed by an adaptable quantification with and without prior enzymatic treatments, is a powerful tool to precisely quantify different species of NAs bound to HBcAg VLPs by dye-based fluorescence assays. However, the protein lysis prevents a protein quantification in the flow-through fractions of the silica-SC chromatography procedure by e.g. UV/Vis based methods due to protein degradation. The RP based extraction developed enables simultaneous absolute quantification of both HBcAg proteins and bound NAs by UV/Vis spectroscopy. However, detailed NA species determination is lacking. Both methodologies overcome limitations of existing techniques and effective absolute quantification of HBcAg proteins and bound NAs is added to the analytical toolbox for HBcAg

VLP research. Today, only qualitative analytical techniques such as SDS-PAGE for proteins and NAGE for NAs and proteins, in combination with microvolume UV/Vis spectroscopy measurements for approximations of protein and NA concentrations, are used for HBcAg VLP process development for gene delivery (Porterfield et al., 2010; Strods et al., 2015; Petrovskis et al., 2021; Zhang et al., 2021b, 2021a). Size exclusion HPLC is also used frequently to separate and quantify different HBcAg VLP protein species (capsids and dimers) and impurities such as proteins and free NAs (Rüdt et al., 2019; Hillebrandt et al., 2020, 2021). However, it cannot separate NAs bound to the HBcAg VLPs. The combination of these analytical tools with the two methods presented for absolute quantification of HBcAg VLPs and bound NAs may be used to more accurately evaluate (i) the removal of bound  $NA_{hc}$  (Newman et al., 2009; Porterfield et al., 2010; Strods et al., 2015; Petrovskis et al., 2021; Zhang et al., 2021b, 2021a), (ii) possible HBcAg protein loss during the removal and (iii) the effective loading of the VLPs with  $NA_{ther}$  (Strods et al., 2015; Petrovskis et al., 2021) based on e.g. encapsulation efficiency or payload of the VLPs.

## 4.5 Conclusions

We investigated a NA extraction procedure for the accurate absolute quantification of  $NA_{hc}$  or  $NA_{ther}$  bound to HBcAg VLPs by dye-based fluorescence assays. The silica-SC based extraction revealed load-dependent NA recoveries, which allowed for a back calculation to initial NA concentrations. Moreover, we developed an RP based extraction to separate and simultaneously quantify the HBcAg VLP proteins and bound NAs by RP-HPLC. The method was successfully evaluated using the performance parameters of linearity, precision, and accuracy. It was applied to six different HBcAg VLP constructs with different amounts of encapsulated NAs and found to be suited for determining absolute protein and NA concentrations as well as HBcAg protein purities. Both methods overcome limitations of existing analytical techniques and, in combination with already existing analytical tools, can support gene delivery process development for HBcAg VLPs.

## Acknowledgment

The authors would like to thank Maike Schröder and Annabelle Dietrich for proofreading as well as Nils Hillebrandt for inspiring discussions. The authors express their gratitude to Christopher Berg for performing preliminary experiments for both the silica-SC based extraction and RP based extraction results. The authors would also like to thank Reinhard Schneider for technical and scientific support in performing TEM imaging. We acknowledge support by the KIT-Publication Fund of the Karlsruhe Institute of Technology.

### Appendix B: Supplementary Material

The Supplementary Material associated with this chapter contain the following information:

- ❖ S4.1: Components of flow-through fraction of silica-SC based extraction of the EasyPure Kit on NAGE
- ❖ S4.2: Remaining protein impurities in the extracts after silica-SC based extraction for de novo extractions of CC purified Cp164 VLP
- ❖ S4.3: Recoveries for preliminary experiments with varying silica-SC based extraction procedures
- ❖ S4.4: Nucleic acid concentrations for Cp157 without and with preliminary silica-SC based extraction and respective standard and relative standard deviation
- ❖ S3.5: HPLC columns and mobile phases B screened in preliminary experiments for the RP based extraction and quantification





# 5

## **Effective Removal of Host Cell-Derived Nucleic Acids Bound to Hepatitis B Core Antigen Virus-Like Particles by Heparin Chromatography**

Angela Valentic<sup>a</sup>, Jürgen Hubbuch<sup>a,\*</sup>

<sup>a</sup> Institute of Process Engineering in Life Sciences, Section IV: Biomolecular Separation Engineering, Karlsruhe Institute of Technology, Fritz-Haber-Weg 2, 76131 Karlsruhe, Germany

\* Corresponding author

### **Abstract**

Virus-like particles (VLPs) show considerable potential for a wide array of therapeutic applications, spanning from vaccines targeting infectious diseases to applications in cancer immunotherapy and drug delivery. In the context of hepatitis B core antigen (HBcAg) VLPs, a promising candidate for gene delivery approaches, the naturally occurring nucleic acid (NA) binding region is commonly utilized for effective binding of various types of therapeutic nucleic acids (NA<sub>ther</sub>). During formation of the HBcAg VLPs, host cell-derived nucleic acids (NA<sub>hc</sub>) might be associated to the NA binding region, and are thus encapsulated into the VLPs. Following a VLP harvest, the NA<sub>hc</sub> need to be removed effectively before loading the VLP with NA<sub>ther</sub>. Various techniques reported in literature for this NA<sub>hc</sub> removal, including enzymatic treatments,

alkaline treatment, and lithium chloride precipitation, lack quantitative evidence of sufficient NA<sub>hc</sub> removal accompanied by a subsequent high VLP protein recovery. In this study, we present a novel heparin chromatography-based process for effective NA<sub>hc</sub> removal from HBcAg VLPs. Six HBcAg VLP constructs with varying lengths of the NA binding region and diverse NA<sub>hc</sub> loadings were subjected to evaluation. Process performance was thoroughly examined through NA<sub>hc</sub> removal and VLP protein recovery analyses. Hereby, reversed phase chromatography combined with UV/Vis spectroscopy, as well as silica spin column-based chromatography coupled with dye-based fluorescence assay were employed. Additionally, alternative process variants, comprising sulfate chromatography and additional nuclease treatments, were investigated. Comparative analyses were conducted with LiCl precipitation and alkaline treatment procedures to ascertain the efficacy of the newly developed chromatography-based methods. Results revealed the superior performance of the heparin chromatography procedure in achieving high NA<sub>hc</sub> removal and concurrent VLP protein recovery. Furthermore, nuanced relationships between NA binding region length and NA<sub>hc</sub> removal efficiency were elucidated. Hereby, the construct Cp157 surpassed the other constructs in the heparin process by demonstrating high NA<sub>hc</sub> removal and VLP protein recovery. Among the other process variants minimal performance variations were observed for the selected constructs Cp157 and Cp183. However, the heparin chromatography-based process consistently outperformed other methods, underscoring its superiority in NA<sub>hc</sub> removal and VLP protein recovery.

## 5.1 Introduction

Virus-like particles (VLPs) are extensively exploited for a vast variety of therapeutic applications (Boisg rault et al., 2002; Mohsen et al., 2017; Rohovie et al., 2017; Nooraei et al., 2021). Vaccines using VLP technology against certain types of human papillomavirus (HPV), preventing cervical cancer, other HPV-related diseases, and hepatitis B virus infections are already on the market (Mohsen et al., 2017; Zhao et al., 2020; Illah and Olaitan, 2023). In the context of VLP-based vaccine development, there are ongoing efforts for cancer immunotherapy, engineering VLPs to display tumor-associated antigens, thus triggering an immune response against cancer cells (Klamp et al., 2011; Li et al., 2021). In this context, a hepatitis B core antigen (HBcAg) based vaccine recently demonstrated potency to induce humoral and cell-mediated immune responses against SARS-CoV-2 infection (Hassebroek et al., 2023). By incorporating therapeutic payloads into VLPs, they can potentially be used as drug delivery vehicles, thereby protecting and delivering therapeutic components to target cells (Cooper and Shaul, 2005; Porterfield et al., 2010; Choi et al., 2013; Jinming Li et al., 2013; Rohovie et al., 2017; Fang et al., 2018; Petrovskis et al., 2021). There is for example research on VLP engineering to



display specific targeting ligands on the surface allowing for targeted drug delivery to specific cells or tissues, or combining VLPs with other materials, such as lipids or synthetic polymers, to enhance stability, payload capacity, and drug release characteristics of these hybrid VLPs (Hill et al., 2017; Mohsen et al., 2017; Rohovie et al., 2017).

However, the effective downstream processing of VLPs continues to be a major challenge. The purification process after intracellular formation of VLPs in an expression system, such as *E. coli*, yeast or plant cells (Effio and Hubbuch, 2015), typically involves cell lysis, clarification, precipitation or ultracentrifugation, disassembly and reassembly, followed by polishing and formulation (McCarthy et al., 1998; Zhao et al., 2012b; Hillebrandt et al., 2020; Zhang et al., 2021b). Recent advancements to enhance efficiency and scalability for VLP purification processes, using ultrafiltration-based unit operations, might be applied (Negrete et al., 2014; Carvalho et al., 2019; Hillebrandt et al., 2020, 2021; Hillebrandt and Hubbuch, 2023). However, for gene delivery, VLP purification processes require additional steps (Figure 5.1 a)) such as the loading of VLPs with therapeutic nucleic acids (NA<sub>ther</sub>) (Rohovie et al., 2017; Valentic et al., 2022). In the case of the HBcAg VLP, a promising candidate for gene delivery applications, the naturally occurring nucleic acid (NA) binding region is commonly utilized for effective binding of various types of NA<sub>ther</sub>. The wild-type HBcAg protein with the full-length NA binding region (Nassal, 1992; Zhang et al., 2021b), named Cp183 in the course of this manuscript, and variants with several amino acid modifications (Porterfield et al., 2010; Strods et al., 2015), as well as HBcAg VLP constructs with different lengths of this naturally occurring NA binding region (Newman et al., 2009; Liu et al., 2010; Sominskaya et al., 2013; Petrovskis et al., 2021; Valentic et al., 2022) are employed. To load VLPs with NA<sub>ther</sub>, the disassembled and purified VLP subunits, so called dimers, are mixed with NA<sub>ther</sub> and then reassembled into loaded VLPs (Figure 5.1 c)). However, during initial formation of the HBcAg VLPs in the *E. coli* cells, host cell-derived nucleic acids (NA<sub>hc</sub>) associate also to the NA binding region and are encapsulated into the VLPs (Birnbaum and Nassal, 1990; Newman et al., 2009; Porterfield et al., 2010)(Figure 5.1 b)). These NA<sub>hc</sub> influence the subsequent downstream processing (Valentic et al., 2022) and obstruct the desired binding of NA<sub>ther</sub> during loading. An effective removal of the undesired NA<sub>hc</sub> bound to the HBcAg VLP NA binding region is required both to prevent potential side effects due to the presence of NA<sub>hc</sub> and to subsequently load the VLPs with NA<sub>ther</sub>.

There are several techniques reported in literature that attempt to remove NA<sub>hc</sub> using different approaches. Enzymatic treatments (Newman et al., 2009), sometimes coupled with His-tag affinity chromatography (Zhang et al., 2021b), are applied to degrade and separate undesired NA<sub>hc</sub>. Though, nuclease treatment is expensive and a thorough removal of the nuclease in the subsequent

purification steps is essential prior to loading with  $NA_{ther}$ . In addition, only proteins with His-tag can be purified using His-tag affinity chromatography. Besides, extensive alkaline treatment is used in combination with ammonium sulfate precipitation to separate  $NA_{hc}$  (Strods et al., 2015). However, alkaline treatment may cause pH stress to the proteins, while being time and buffer extensive. Furthermore, Lithium chloride precipitation is used to precipitate encapsulated RNA during disassembly of the VLPs (Porterfield et al., 2010). However, the effects on bound DNA are uncertain and the use of guanidine HCl and LiCl as part of the disassembly and precipitation liquid phase is laborious and expensive.

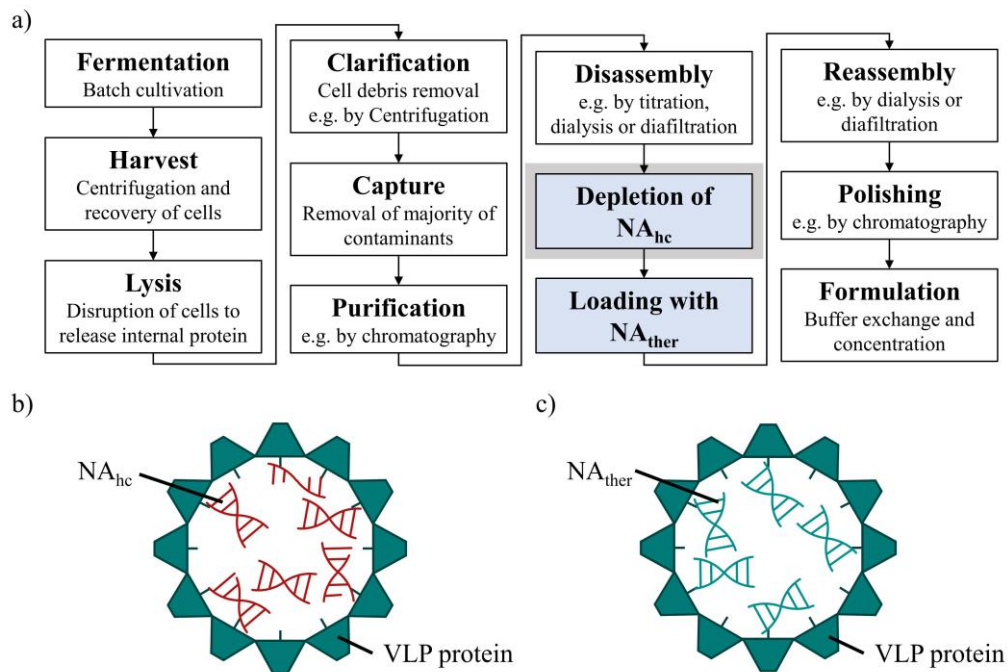


Figure 5.1 a) Common HBcAg VLP purification process (Hillebrandt et al., 2021) with depletion of  $NA_{hc}$  and loading with  $NA_{ther}$ , process steps required for the application as a nucleic acid delivery vector, highlighted in blue. The depletion of  $NA_{hc}$  investigated in this study is highlighted in grey. b) HBcAg VLP with NA binding region and  $NA_{hc}$  encapsulated within the VLP protein capsid. c) HBcAg VLP with NA binding region and  $NA_{ther}$  encapsulated within the VLP protein capsid after depletion of  $NA_{hc}$  and loading with  $NA_{ther}$ . HBcAg: hepatitis B core antigen, NA: nucleic acids,  $NA_{hc}$ : host cell-derived nucleic acids,  $NA_{ther}$ : therapeutic nucleic acids, VLP: virus-like particle

In these studies, the removal of  $NA_{hc}$  is evaluated qualitatively by transmission electron microscopy, native agarose gel electrophoresis (NAGE) and A260/A280 ratios gained by UV/Vis spectroscopy. Quantitative analysis of  $NA_{hc}$  removal with concurrent high VLP protein recovery, which is essential for effective downstream purification processing, is missing. Only recently, novel quantification methods for the absolute quantification of HBcAg VLP proteins and bound NAs were presented by our group (Valentic et al., 2024). This allows

a thorough examination of NA<sub>hc</sub> removal and VLP protein recovery for to evaluate the performance of different NA<sub>hc</sub> removal processes.

Next to the above-mentioned methods used for NA<sub>hc</sub> removal, heparin affinity chromatography appears to be a promising approach for efficient NA<sub>hc</sub> removal. It has already been used for the purification of viruses (Nasimuzzaman et al., 2016; Spannaus et al., 2017) and VLPs (Minkner et al., 2018; Reiter et al., 2019; Zollner et al., 2024). During the purification of HIV-1 gag virus-like particles, both extracellular vesicles and chromatin were separated (Pereira Aguilar et al., 2020). In the case of HBcAg VLPs, studies described the interaction with cell-surface-expressed heparan sulphate by the protamine-like NA binding region (Cooper et al., 2005; Vanladschoot et al., 2005). Moreover, the binding of the NA binding region of HBcAg VLPs to heparin chromatographic media was demonstrated by Broos et al., 2007. This is why heparin chromatography exhibits great potential for effective removal of NA<sub>hc</sub> bound to HBcAg VLPs.

In this work, we present a novel heparin chromatography-based process for an effective removal of NA<sub>hc</sub> bound to HBcAg VLPs. The heparin chromatography step was examined with six different HBcAg VLP constructs with varying lengths of the NA binding region possessing different NA<sub>hc</sub> loadings. Process performance was evaluated by a quantitative determination of NA<sub>hc</sub> removal and VLP protein recovery with reversed phase (RP) chromatography coupled with UV/Vis analysis, and silica spin column (SC) based chromatography followed by dye-based fluorescence assay as described earlier (Valentic et al., 2024). Further, different process variants including sulfate chromatography instead of heparin chromatography and nuclease treatments prior to these chromatographic techniques were investigated. In addition, LiCl precipitation and alkaline treatment procedures were performed according to literature. Process performances were determined enabling a thorough comparison of the various removal techniques. For the comparison of different process variants and procedures, Cp157, a construct with an intermediate length of the NA binding region, and Cp183, one with the full-length NA binding region, were examined. For all processes, efficacy was evaluated by a quantitative determination of NA<sub>hc</sub> removal and VLP protein recovery at different process stages. In addition, A260/A280 ratios were determined by UV/Vis spectroscopy to assess the VLP protein purity. SDS-PAGE and NAGE analyses were carried out to examine the VLP protein and NA content at various stages of the processes to complement the comprehensive comparative study.

## 5.2 Materials and methods

### 5.2.1 Buffer and VLPs

All chemicals were purchased from Merck (Darmstadt, Germany), if not stated otherwise. Solutions and buffers were prepared with ultrapure water (PURELAB Ultra, ELGA LabWater) and aqueous buffers were filtered through a 0.2 µm pore-size cellulose acetate filter (Pall Corporation, Port Washington, NY, United States). Buffers were pH-adjusted with 4 M NaOH or 32% HCl. Trifluoroacetic acid (TFA) was purchased from Thermo Fisher Scientific (Waltham, MA, United States) and HPLC grade acetonitrile (ACN) from Avantor (Radnor, PA, United States). HBcAg VLPs with different lengths of NA binding regions and different amounts of bound host cell-derived nucleic acids (NA<sub>hc</sub>) were produced and purified as described earlier (Valentic et al., 2022). Constructs Cp149, Cp154, Cp157, Cp164, Cp167, and Cp183 (Valentic et al., 2022) after CaptoCore 400 purification and present in purification buffer consisting of 50 mM Tris and 150 mM NaCl at pH 7.2 were used for all experiments.

### 5.2.2 Removal of host cell-derived nucleic acids bound to HBcAg VLPs

All removal techniques were performed in duplicates with Cp157 and Cp183 HBcAg VLP constructs, while the heparin chromatography without prior nuclease treatment was additionally performed for Cp149, Cp154, Cp164, and Cp167. An overview about the investigated removal techniques and VLP constructs can be found in Figure 5.2.

#### 5.2.2.1 Heparin and sulfate chromatography

HBcAg VLP capsids were disassembled overnight at 4°C by dilution with 50 mM Tris, 10 M Urea stock solution to a final concentration of 4 M Urea, 50 mM Tris and titrated to pH 9.0. After filtration by a 0.2 µm cellulose acetate filter, dimers were purified by size-exclusion chromatography (SEC) using a 150 mL Toyopearl HW-65S column equilibrated in disassembly buffer (50 mM Tris, 4 M Urea, pH 9.0). To remove bound NA<sub>hc</sub>, the dimer fractions were purified on a 1 mL HiTrap™ Heparin HP (Cytiva, Marlborough, MA, United States) column or a 5 mL Toyopearl Sulfate-650F (Tosoh Bioscience, Tokyo, Japan) column equilibrated in disassembly buffer, with or without prior nuclease treatment with DENARASE® (c-LEcta GmbH, Leipzig, Germany). Elution was performed with a high-salt buffer (50 mM Tris, 4 M Urea, 1 M NaCl, pH 9.0). Flow-through and elution fractions were analyzed by SDS-PAGE, RP chromatography coupled with UV/Vis analysis, and silica spin column (SC) based chromatography followed dye-based fluorescence assay.

#### **5.2.2.2 LiCl precipitation**

The LiCl precipitation was performed in accordance with the literature, with few adaptations (Porterfield et al., 2010). In brief, the HBcAg VLP capsids were disassembled with 0.5 M LiCl, 1.5 M guanidine HCl 0.05 M Tris, 2 mM DTT, pH 7.5 overnight, followed by centrifugation for 20 min at 12000 rpm at 4 °C and filtration of the supernatant with 0.2 µm cellulose acetate filter. SEC of the filtered supernatant was performed with a 25 mL Superose 6 Increase 10/300 GL (Cytiva, Marlborough, MA, United States) column equilibrated in re-dissolution buffer. Besides initial Cp157 and Cp183 material and final SEC fractions, intermediate process samples after centrifugation were analyzed. Samples were analyzed by SDS-PAGE, NAGE, RP chromatography coupled with UV/Vis analysis, and silica-SC based chromatography followed by dye-based fluorescence assay.

#### **5.2.2.3 Alkaline treatment**

The alkaline treatment was performed in accordance with the literature, with a number of adaptations (Strods et al., 2015). In brief, the HBcAg VLP capsids were dialyzed in 7 M Urea for 16 h at 4 °C, followed by dialysis in 0.1 M Na<sub>2</sub>CO<sub>3</sub>, 2 mM DTT solution. For the alkaline treatment, the VLPs were dialyzed in alkaline buffer (0.1 M sodium phosphate, 0.65 M NaCl, pH 12) for 18 h at 4°C. After dialysis in neutralization buffer (0.1 M sodium phosphate, 0.65 M NaCl, pH 7.8) the VLPs were precipitated with 1 M AMS, centrifugated for 30 min, at 12000 rpm and 4°C, and re-dissolved overnight with purification buffer at 4°C. After centrifugation for 30 min at 6000 rpm and filtration of supernatant with 0.2 µm cellulose acetate filter, SEC was performed with a 25 mL Superose 6 Increase 10/300 GL (Cytiva, Marlborough, MA, United States) column equilibrated in re-dissolution buffer. In parallel, alkaline treatment, precipitation, and SEC were performed without prior dialysis into 7 M Urea and Na<sub>2</sub>CO<sub>3</sub> solutions. Besides initial Cp157 and Cp183 material and final SEC fractions, intermediate process samples after neutralization and after re-dissolution were analyzed. Samples were analyzed by SDS-PAGE, NAGE, RP chromatography coupled with UV/Vis analysis, and silica-SC based chromatography followed by dye-based fluorescence assay.

### **5.2.3 Analytics**

#### **5.2.3.1 SDS-PAGE**

For SDS-PAGE, NuPage 4–12% BisTris protein gels, MES running buffer, and LDS sample buffer were used. Gels were run on a PowerEase Touch 350W Power Supply (all Invitrogen, Waltham, MA, United States) at reduced mode with 50 mM DTT in the sample solution. Coomassie blue solution was used for protein staining.

### 5.2.3.2 NAGE

For NAGE, 0.7% agarose (Carl Roth, Karlsruhe, Germany) in TAE buffer (40 mM Tris, 20 mM acetic acid, 1 mM EDTA) with 1 µg/mL midori green (Nippon Genetics GmbH, Düren, Germany) was used. Gels were run on a PowerPac Basic (Bio-Rad, Hercules, CA, United States). Coomassie blue solution was used for subsequent protein staining, if necessary.

### 5.2.3.3 Protein and nucleic acid quantification

RP chromatography coupled with UV/Vis analysis was used to separate and quantify the bound NA<sub>hc</sub> and VLP proteins in accordance to an earlier publication of our group (Valentic et al., 2024). Hereby, an analytical reversed-phase chromatography was performed with a TSKgel Protein C4-300 column (3 µm, 4.6x150 mm) from Tosoh Bioscience (Tokyo, Japan) on a Vanquish UHPLC system, controlled by Chromeleon version 7.2 (both Thermo Fisher Scientific, Waltham, MA, United States). In parallel, a silica-SC based chromatography followed dye-based fluorescence assay was used to quantify NA<sub>hc</sub>, according to a previous publication of our group (Valentic et al., 2024). Hereby, materials included in the EasyPure Viral DNA/RNA Kit (TransGen Biotech, Beijing, China) were used for NA extraction and RiboGreen assay (Thermo Fisher Scientific, Waltham, MA, United States) was performed for NA<sub>hc</sub> quantification according to the manufacturer's manual with minor adaptations.

To calculate the NA removal and VLP protein recovery, the respective NA or VLP protein mass of the chromatography fraction or intermediate sample was divided by the initial NA or VLP protein mass for all performed quantification techniques. Chromatography fractions were the elution fractions at heparin and sulfate chromatography and the final SEC fractions for the LiCl precipitation and alkaline treatment. NA<sub>hc</sub> removal results deviated for the two utilized analytical methods. Further, NA quantification by RP-UV/Vis of intermediate LiCl precipitation samples after centrifugation was not possible due to the presence of guanidine HCl in the samples, overlapping with the NA peaks in the flow-through of the RP-HPLC method. Therefore, it was decided to show the NA<sub>hc</sub> removals obtained by the two available analytical methods independently. A260/A280 ratio of chromatography fractions were determined by analysis of chromatography peak areas at 260 nm and 280 nm. For initial material and intermediate process samples, the A260/A280 ratio was determined by microvolume UV/Vis absorbance measurements using a NanoDrop<sup>TM</sup> 2000c UV/Vis spectrophotometer (Thermo Fisher Scientific, Waltham, MA, United States).

## 5.3 Results

Effective processing for the removal of host cell-derived nucleic acids (NA<sub>hc</sub>) bound to hepatitis B core antigen (HBcAg) virus-like particles (VLPs) is defined by low final NA<sub>hc</sub> concentrations accompanied with high VLP protein recoveries. NA<sub>hc</sub> removals and VLP protein recoveries were quantitatively assessed by reversed phase (RP) chromatography coupled with UV/Vis analysis, and silica spin column (SC) based chromatography followed by dye-based fluorescence assay (Valentic et al., 2024). Due to discrepancies in the NA<sub>hc</sub> removal results between the two analytical methods, and the interference caused by guanidine HCl in some LiCl precipitation samples during nucleic acid quantification by RP-UV/Vis, it was decided to report the NA<sub>hc</sub> removal data from each method separately throughout the study. VLP protein purities were additionally evaluated by determination of A260/A280 ratios. To qualitatively track the VLP proteins and nucleic acids in the respective samples, SDS-PAGE and native agarose gel electrophoresis (NAGE) analyses were performed for all process samples. An overview of processes to remove NA<sub>hc</sub>, all the initial, intermediate and final process samples analyzed and their labeling is shown in Figure 5.2.

### 5.3.1 Heparin chromatography for different HBcAg VLP constructs

To effectively remove NA<sub>hc</sub> bound to HBcAg VLPs a heparin chromatography-based purification step was developed. Six different constructs with different lengths of a nucleic acid (NA) binding region and varying loads of NA<sub>hc</sub> were investigated. The retention of VLP proteins during the heparin chromatography without previous nuclease treatment was examined by SDS-PAGE. The respective gel scans are depicted in Appendix C: S5.1. Cp149 and Cp154 were mainly present in the flow-through fractions of the heparin chromatography. Cp157 and Cp183 showed clear binding and were thus detected in the elution fractions. SDS-PAGE results for Cp165 and Cp167 were inconclusive due to concentration restrictions or method errors. Further, the purity and recovery of the VLP proteins after the NA<sub>hc</sub> removal step (grey shaded process path in Figure 5.2) were determined for all constructs and are depicted in Figure 5.3.

#### 5.3.1.1 Nucleic acid removal

For Cp149, Cp154, Cp157 and Cp183 the average NA removal was as high as 97%. For Cp164 and Cp167 the NA removal was less successful with NA<sub>hc</sub> removal of around 86% for Cp167 and depending on the NA<sub>hc</sub> quantification method either 58% (silica-SC based chromatography followed by dye-based fluorescence assay) or 72% (RP-UV/Vis) for Cp164.

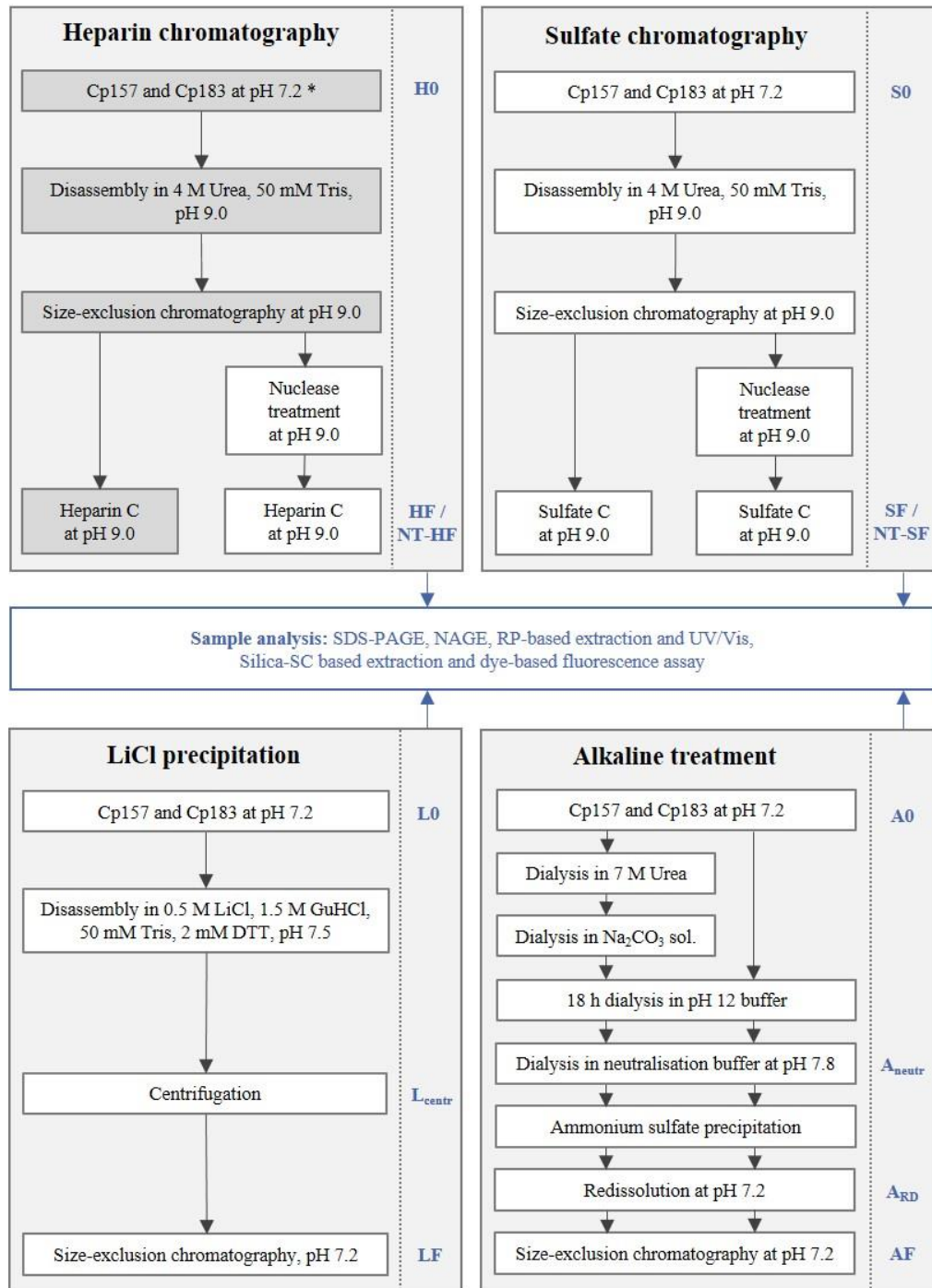


Figure 5.2 Overview of processes investigated in this work to remove host cell-derived nucleic acids bound to HBcAg VLPs. Heparin and sulfate chromatography were performed with and without prior nuclease treatment. LiCl precipitation and alkaline treatment were adapted from reported techniques in literature (Porterfield et al., 2010; Petrovskis et al., 2021). The alkaline treatment procedure was performed with and without the reported preliminary dialysis in 7 M Urea and NaCO<sub>3</sub> solutions. All outlined removal techniques were performed with Cp157 and Cp183 HBcAg VLP constructs (Valentic et al., 2022), while the grey shaded process path was additionally performed for Cp149, Cp154, Cp164, and Cp167 (\*). Initial, intermediate and final samples, which are labelled at the process steps, respectively, were analysed by SDS-PAGE, NAGE, RP chromatography coupled with UV/Vis analysis, and silica-SC based chromatography followed by dye-based fluorescence assay



## 5 Effective Removal of Host Cell-Derived Nucleic Acids Bound to Hepatitis B Core Antigen Virus-Like Particles by Heparin Chromatography

(Valentic et al., 2024). HBcAg: hepatitis B core antigen, NAGE: native agarose gel electrophoresis, NT: nuclease treatment, RP: reversed phase, VLP: virus-like particle

### 5.3.1.2 VLP protein recovery

However, the respective VLP protein recovery has to be considered, as high VLP protein recoveries are required for effective processing. The VLP protein recovery for the heparin chromatography purification step mostly increases with

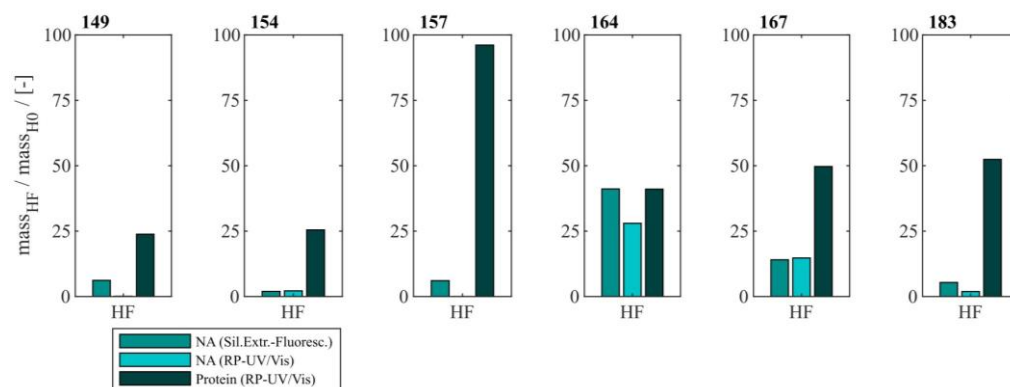


Figure 5.3 Protein and nucleic acid recoveries for six HBcAg VLP constructs after removal of host cell-derived nucleic acids by disassembly and heparin chromatography (highlighted process path in Figure 5.2). Nucleic acid recoveries were analysed by silica-SC based chromatography followed by dye-based fluorescence assay and RP chromatography coupled with UV/Vis analysis. VLP protein recoveries were determined by RP chromatography coupled with UV/Vis analysis. HBcAg: hepatitis B core antigen, NAGE: native agarose gel electrophoresis, RP: reversed phase, SC: spin column, VLP: virus-like particle

the length of the NA binding region. VLP protein recoveries ranged from 24% for Cp149 to 52% for Cp183. Nevertheless, Cp157 showed the highest VLP protein recovery with 96%.

In total, Cp157 demonstrated a high NA removal accompanied with high protein recovery, as desired for an effective removal of NA<sub>hc</sub> bound to HBcAg VLPs. Complementarily, the A260/A280 ratios were assessed as an indicator for VLP protein purity and can be found in Table 5.1. The A260/A280 ratios for the initial samples differed greatly between 0.63 for Cp149 and 2.08 for Cp164. For all six VLP constructs, a decreased A260/A280 ratio was determined after heparin chromatography without nuclease treatment compared to the ratio of the initial sample. Cp157 resulted in the lowest A260/A280 ratio of 0.55. In summary, heparin chromatography demonstrated divergent NA<sub>hc</sub> removal performances depending on the VLP construct, with Cp157 resulting in high NA<sub>hc</sub> removal and high VLP protein recovery.

### 5.3.2 Heparin and sulfate chromatography with and without prior nuclease treatment

Different chromatography-based process variants were investigated regarding their  $NA_{hc}$  removal performance for Cp157 and Cp183. In addition to heparin chromatography, sulfate chromatography was investigated. Moreover, both chromatographic techniques were performed with and without nuclease treatment and the results for  $NA_{hc}$  removal and VLP protein recovery are displayed in Figure 5.4. The presence of VLP proteins in the elution fractions of both chromatography-based techniques were verified by SDS-PAGE. The respective gel scans are depicted in Appendix C: S5.2.

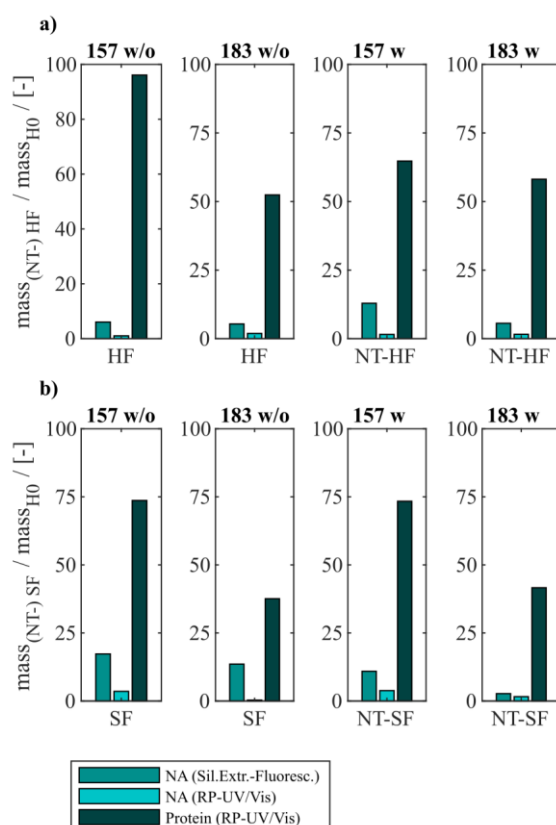


Figure 5.4 VLP protein and nucleic acid recoveries for Cp157 and Cp183 after removal of host cell-derived nucleic acids by disassembly, with (w) or without (w/o) prior nuclease treatment and a) heparin chromatography or b) sulfate chromatography. Nucleic acid recoveries were analysed by silica-SC based chromatography followed by dye-based fluorescence assay and RP chromatography coupled with UV/Vis analysis. VLP protein recoveries were determined by RP chromatography coupled with UV/Vis analysis. RP: reversed phase, SC: spin column

For all investigated process variants averaged NA removals of at least 90% were achieved. This was confirmed by decreased  $A_{260}/A_{280}$  ratios after  $NA_{hc}$  removal compared to the ratio of the initial samples (Table 5.1). However, the VLP protein recoveries ranged from 96% (Cp157, heparin chromatography, without nuclease treatment) to 38% (Cp183, sulfate chromatography, without nuclease treatment).

### 5.3.2.1 Constructs

Cp157 showed higher VLP protein recoveries than Cp183 with each chromatography-based process variant, while NA<sub>hc</sub> removal with Cp157 showed to be comparable to Cp183. In addition, lower A260/A280 ratios were achieved for Cp157 than for Cp183.

### 5.3.2.2 Nuclease treatment

In general, nuclease treatment improved NA<sub>hc</sub> removal performance for the process variants investigated by up to 4.8% (for Cp183 after subsequent sulfate chromatography). However, for Cp157 and subsequent heparin chromatography, the process with nuclease treatment achieved lower NA<sub>hc</sub> removals than the process without nuclease treatment. VLP protein recoveries were not affected by the nuclease treatment, except for the heparin chromatography with Cp157. There, a lower VLP protein recovery was detected for the process with nuclease treatment. Purities evaluated by A260/A280 ratios were improved by nuclease treatment for all process variants investigated (see Table 5.1).

Table 5.1 A260/A280 ratio of investigated HBcAg VLP constructs after removal of host cell-derived nucleic acids bound to HBcAg VLPs by heparin and sulfate chromatography without (w/o) and with (w) prior nuclease treatment and initial material. Ratios were determined by analysis of selected chromatography peak areas at 260 nm and 280 nm, or by microvolume UV/Vis absorbance measurements for initial samples.

	Nuclease treatment	A260/A280 [-]					
		Cp149	Cp154	Cp157	Cp164	Cp167	Cp183
<b>Initial Sample</b>		0.63	1.94	1.24	2.08	1.63	1.74
<b>Heparin chromatography</b>	<b>w/o</b>	0.62	0.74	0.57	0.67	0.66	0.71
	<b>w</b>	-	-	0.55	-	-	0.69
<b>Sulfate chromatography</b>	<b>w/o</b>	-	-	0.62	-	-	0.63
	<b>w</b>	-	-	0.57	-	-	0.59

### 5.3.2.3 Heparin and sulfate chromatography

Heparin chromatography mostly achieved higher NA<sub>hc</sub> removals and VLP protein recoveries than sulfate chromatography. An exception of this was the process investigating Cp157 with nuclease treatment, where a lower VLP protein recovery was detected with heparin chromatography than with sulfate chromatography. Nevertheless, in terms of purity, heparin chromatography achieved lower A260/A280 ratios for Cp157, as for Cp183, throughout all process variants investigated. In summary, the best removal performances with

high NA<sub>hc</sub> removal, high VLP protein recovery and high VLP protein purity were achieved for Cp157 by heparin chromatography with and without prior nuclease treatment.

### 5.3.3 LiCl precipitation

To compare the developed heparin chromatographic procedure with the LiCl precipitation with respect to their NA<sub>hc</sub> removal performance, LiCl precipitation was performed for Cp157 and Cp183. An overview of initial, intermediate and final process samples analyzed and their labeling is shown in Figure 5.2. Samples after disassembly, LiCl precipitation and centrifugation (L1), and samples after size-exclusion chromatography (SEC) (LF) were analyzed. Chromatograms of the final SEC and fraction segmentation for analysis can be found in Appendix C: S5.3. The fraction pools with the highest expected VLP protein purity, estimated from the A260/A280 ratio of the peak areas in the chromatogram, were selected for analysis of NA<sub>hc</sub> removal and VLP protein recovery. The levels of NA<sub>hc</sub> removal and VLP protein recovery for the fraction pool #3 for Cp157 and fraction pool #1 for Cp183 are depicted in Figure 5.5.

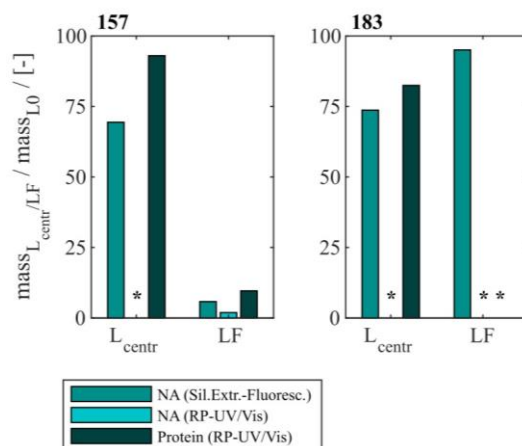


Figure 5.5 VLP protein and nucleic acid recoveries for Cp157 and Cp183 after removal of host cell-derived nucleic acids by disassembly and LiCl precipitation, centrifugation (intermediate sample) and size-exclusion chromatography. Nucleic acid recoveries were analysed by silica-SC based chromatography followed by dye-based fluorescence assay and RP chromatography coupled with UV/Vis analysis. VLP protein recoveries were determined by RP chromatography coupled with UV/Vis analysis. Nucleic acid quantification by RP-UV/Vis was not possible after centrifugation due to the presence of guanidine HCl in the samples, overlapping with the nucleic acid peaks in the flow-through of the RP-HPLC method, and nucleic acid and VLP protein concentrations of Cp183 in SEC fraction were too low for RP-UV/Vis analysis (\*). RP: reversed phase, SC: spin column, SEC: size-exclusion chromatography

For Cp157, a NA<sub>hc</sub> removal of 31% with 93% VLP protein recovery was determined after centrifugation (L1). After SEC the dimer comprising fractions with the lowest A260/A280 values were analyzed. This revealed a high VLP protein loss of 90% with a NA removal of 96% (LF). Similar results were

## 5 Effective Removal of Host Cell-Derived Nucleic Acids Bound to Hepatitis B Core Antigen Virus-Like Particles by Heparin Chromatography

detected for Cp183, achieving 26% NA<sub>hc</sub> removal with 82% VLP protein recovery after centrifugation (L1). Again, the SEC revealed high VLP protein loss, resulting in NA and VLP protein concentrations too low for RP-UV/Vis analysis (LF). On the contrary, the performed silica-SC based chromatography followed by dye-based fluorescence assay resulted in a lower NA<sub>hc</sub> removal of 5% than formerly determined for the centrifugation sample (L1). This might be caused by assay imprecision due to the low concentrations. Guanidine HCl overlaps the NA peaks in the flow-through of the used RP-HPLC method. Therefore, NA quantification by RP-UV/Vis was not possible due to the presence of guanidine HCl in the samples after centrifugation.

The complementary analysis of HBcAg VLP protein purity by A260/A280 ratios listed in Table 5.2 underline these findings. It shows low VLP protein purities in the SEC fractions for both Cp157 and Cp183, with A260/A280 ratios of 0.95 and 1.74, respectively. SDS-PAGE and NAGE analyses were performed for all process samples to qualitatively track the VLP proteins and NAs in the respective samples. Gel scans are depicted in Appendix C: S5.3. Gel-derived results mainly support the findings for NA<sub>hc</sub> removals and VLP protein recoveries described above. However, SDS-PAGE displayed a greatly attenuated Cp157 lane for samples after centrifugation (L1) compared to the initial sample. This indicates VLP protein loss during LiCl precipitation and subsequent centrifugation, unlike 93% VLP protein recovery for this sample described above. In NAGE analysis shifted VLP lanes and an additional strong free NA lane were visible, compared to the initial sample. Similar results were

Table 5.2 A260/A280 ratio of Cp157 and Cp183 samples after removal of host cell-derived nucleic acids bound to HBcAg VLPs by LiCl precipitation and intermediate samples and initial material. Ratios were determined by analysis of selected chromatography peak areas at 260 nm and 280 nm, or by microvolume UV/Vis absorbance measurements for initial and intermediate samples. Ratios of samples after centrifugation might be affected by the presence of guanidine HCl in the samples and are listed in brackets.

	A260/A280 [-]					
	Cp157			Cp183		
LiCl precipitation	initial	centr	SEC frac	initial	centr	SEC frac
	1.33	(1.24)	0.95	1.93	(1.76)	1.74

found for Cp183 in SDS-PAGE and NAGE, but less pronounced due to low concentrations. Overall, LiCl precipitation resulted in high VLP protein losses during processing and low final VLP protein purities. VLP protein recovery of Cp157 was 86% lower than with heparin chromatography.

#### 5.3.4 Alkaline treatment

Finally, an alkaline treatment for Cp157 and Cp183 was performed to assess its NA<sub>hc</sub> removal performance. An overview of the initial, intermediate and final process samples analyzed is shown in Figure 5.2. Samples after alkaline treatment and dialysis in neutralization buffer (A1), precipitation and re-dissolution (A2), and samples after SEC (AF) were analyzed. Moreover, procedures with and without preliminary dialysis in 7 M Urea and NaCO<sub>3</sub> solutions were performed in parallel. Chromatograms of the final SEC and fraction segmentation for analysis can be found in Appendix C: S5.4. For the analysis of NA<sub>hc</sub> removals and VLP protein recoveries the fraction pools were analyzed for Cp157. For Cp183, a quantitative analysis of NA<sub>hc</sub> removals and VLP protein recoveries was not possible, because the VLP protein concentrations were too low for fractionation sampling during SEC. NA<sub>hc</sub> removals and VLP protein recoveries are displayed in Figure 5.6. For the procedures with and without the preliminary dialysis similar performances were obtained, respectively. For Cp157, NA<sub>hc</sub> removal after alkaline treatment and dialysis in neutralization buffer (A1) was found to be 25% without and 7% with preliminary dialysis. Hereby, VLP protein recoveries of 84% and 86% were determined, respectively. The ammonium sulfate precipitation and re-dissolution achieved NA<sub>hc</sub> removals of around 97%, averaged for re-dissolution and SEC fraction samples with and without preliminary dialysis (A2/AF). However, it caused high VLP protein losses resulting in VLP protein recoveries around 13%.

For Cp183, NA and VLP protein concentrations for samples after dialysis in neutralization buffer and precipitation/re-dissolution, both without and with prior preliminary dialysis procedures, were too low for RP-UV/Vis analysis, and concentrations during SEC were too low to collect and analyse fractions. However, the analysis by silica-SC based chromatography followed by dye-based fluorescence assay resulted in NA<sub>hc</sub> removals of 18% without and 10% with preliminary dialysis after alkaline treatment and dialysis in neutralization buffer (A1). NA<sub>hc</sub> removals of 96% both without and with prior preliminary dialysis in SEC fraction samples (A2) were achieved and a similar behaviour of Cp183 and Cp157 was observed. The analysis of VLP protein purity by A260/A280 ratios listed in Table 5.3 supports these findings by showing low VLP protein purities in the SEC fractions for both Cp157 and Cp183 with and without preliminary dialysis respectively. Further, SDS-PAGE and NAGE analyses were performed for all process samples to qualitatively track the VLP proteins and NAs in the respective samples. Gel scans are depicted in Appendix C: S5.4. Gel-derived results support the findings for NA<sub>hc</sub> removals and VLP protein recoveries described above. Interestingly, for Cp157, NAGE analysis showed shifted VLP lanes and proteins in the gel pockets, as well as free NA lanes and NAs in the gel pockets for the samples after alkaline treatment and

## 5 Effective Removal of Host Cell-Derived Nucleic Acids Bound to Hepatitis B Core Antigen Virus-Like Particles by Heparin Chromatography

dialysis in neutralization buffer (A1). On the contrary, in the initial sample Cp157 capsid proteins and NAs were depicted at equal positions in the gel. In

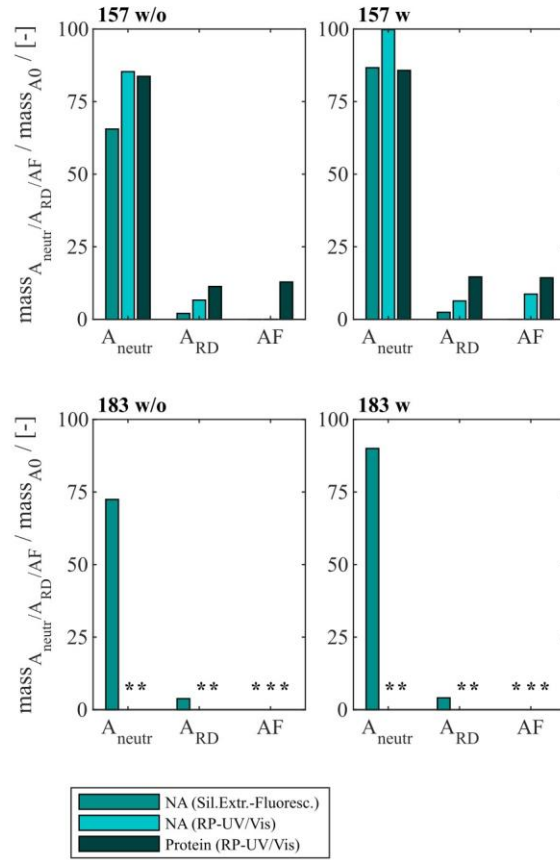


Figure 5.6 VLP protein and nucleic acid recoveries for Cp157 and Cp183 after removal of host cell-derived nucleic acids by alkaline treatment (dialysis in pH 12 buffer) with (w) and without (w/o) preliminary dialysis in 7 M Urea and NaCO<sub>3</sub> solutions, and dialysis in neutralisation buffer (intermediate sample), precipitation and re-dissolution (intermediate sample) and size-exclusion chromatography. Nucleic acid recoveries were analysed by silica-SC based chromatography followed by dye-based fluorescence assay and RP chromatography coupled with UV/Vis analysis. VLP protein recoveries were determined by RP chromatography coupled with UV/Vis analysis. Nucleic acid and VLP protein concentrations of Cp183 for samples after dialysis in restoration buffer and re-dissolution (both without and with prior preliminary dialysis), were too low for RP-UV/Vis analysis, and concentrations during SEC were too low to collect and analyse fractions (\*). RP: reversed phase, SC: spin column

sum, alkaline treatment demonstrated high VLP protein losses during the process, as well as insufficient NA<sub>hc</sub> removals resulting in low purities of A260/A280 ratios between 1.63 and 2.00 compared to ratios between 0.55 and 0.74 for all heparin chromatography-based processes.

## 5.4 Discussion

For gene delivery applications, the naturally occurring nucleic acid (NA) binding region of the hepatitis B core antigen (HBcAg) is commonly utilized for effective binding of various types of therapeutic nucleic acids (NA<sub>ther</sub>). During formation of the HBcAg virus-like particles (VLPs) in the *E. coli* cells host cell-derived nucleic acids (NA<sub>hc</sub>) associate to the NA binding region and obstruct the desired binding of NA<sub>ther</sub> during loading (Birnbaum and Nassal, 1990; Newman et al., 2009; Porterfield et al., 2010). An effective removal of the undesired NA<sub>hc</sub> bound to the HBcAg VLP NA binding region is essential.

### 5.4.1 Heparin chromatography with different HBcAg VLP constructs

In this work, a novel heparin chromatography-based process for an effective removal of NA<sub>hc</sub> bound to HBcAg VLPs is presented. The VLPs were disassembled, purified by size-exclusion chromatography (SEC) and loaded onto the heparin chromatography media with disassembly buffer as running buffer. Bound material was eluted via a salt gradient. Six HBcAg VLP constructs with different lengths of the NA binding region and NA<sub>hc</sub> loadings (Valentic et al., 2022) were investigated in terms of NA<sub>hc</sub> removal performance by heparin chromatography.

Hereby, the different VLP constructs showed binding to the heparin chromatographic media dependent on the presence and length of the NA binding region and we assume the binding of the HBcAg VLP dimers to the heparin chromatographic ligands by the NA binding region, as shown in literature (Broos et al., 2007). For Cp149 and Cp154, the interactions between the affinity

Table 5.3 A260/A280 ratio of Cp157 and Cp183 samples after removal of host cell-derived nucleic acids bound to HBcAg VLPs alkaline treatment (without (w/o) or with (w) preliminary dialysis in 7 M Urea and NaCO<sub>3</sub> solutions), intermediate samples and initial material. Ratios were determined by analysis of selected chromatography peak areas at 260 nm and 280 nm, or by microvolume UV/Vis absorbance measurements for initial and intermediate samples.

	Preliminary dialysis	A260/A280 [-]							
		Cp157				Cp183			
Alkaline treatment		initial	neutr	RD	SEC frac	initial	neutr	RD	SEC frac
	w/o	1.36	1.37	> 2	1.85	1.87	1.77	> 2	1.83
	w	1.36	1.43	> 2	2.00	1.87	1.71	> 2	1.63

chromatography and the VLP proteins are too weak to bind to the column under the conditions investigated, demonstrated by SDS-PAGE analysis of the flow-through and elution fractions. Constructs with intermediate and full length of



the NA binding region bind to the heparin media and are eluted with a NaCl gradient. Thereby, the NA<sub>hc</sub> bound to the protamine-like NA binding region dissociate from the VLP protein and are replaced by the chromatographic ligands during loading. The replaced NA<sub>hc</sub> elute in the flow-through during chromatography. Subsequent elution with the NaCl gradient weakens electrostatic interactions between the bound VLP proteins and chromatography media, leading to elution of these VLP proteins and stabilization of the VLP protein with free NA binding region by the NaCl (Figure 5.7 a)). Depending on the construct, this replacement and thus removal of NA<sub>hc</sub> from the NA binding region was successful to varying degrees in terms of NA<sub>hc</sub> removal and VLP protein recovery.

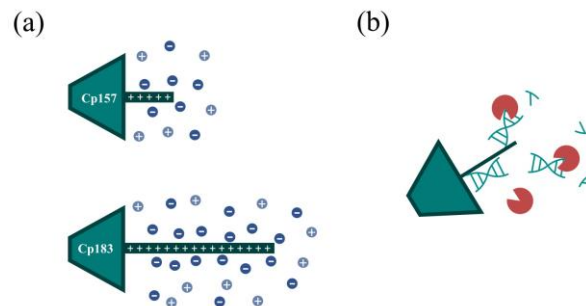


Figure 5.7 (a) Ionic stabilization of the NA binding region of the Cp157 and Cp183 HBcAg VLP constructs after removal of NA<sub>hc</sub> by NaCl. (b) Degradation of NA parts bound to the NA binding region by nucleases impeded by steric hindrance. HBcAg: hepatitis B core antigen, NA: nucleic acids, NA<sub>hc</sub>: host cell-derived nucleic acids, VLP: virus-like particle

For the constructs Cp149 and Cp154 with no or short NA binding regions, low VLP protein recoveries were detected due to the poor binding to the heparin chromatographic media. The length of the NA binding region of Cp154 seems to be too short to effectively bind to the media. The partial binding of Cp149, lacking the NA binding region, could be explained by electrostatic attractions of positively charged amino acid residues of the dimers with the negatively charged stationary phase. This indicates a weak general binding independent from the NA binding region for all constructs. The high NA<sub>hc</sub> removals determined for Cp149 may be caused by removal of free NA<sub>hc</sub> in the samples. However, the already low A260/A280 ratio of the Cp149 initial material was not improved by the heparin chromatography step, confirming the non-specific binding of Cp149 to the stationary phase. Although the A260/A280 ratio for Cp154 decreased as we expected for a construct with a short NA binding region, the extent of reduction was insufficient. For the constructs Cp164, Cp167 and Cp183 we expected strong binding of the NA binding region. However, based on SDS-PAGE results and A260/A280 ratios moderate NA<sub>hc</sub> removals were found. VLP protein recoveries determined by RP chromatography coupled with UV/Vis analysis revealed high VLP protein losses. The reported solubility issues of NA<sub>hc</sub>-free Cp183 (Porterfield et al., 2010) suggest potential post-

elution aggregation or precipitation of the VLP proteins, likely due to the absence of ionic stabilization of the NA binding region (Figure 5.7 a)). However, the recovered Cp183 proteins showed high  $NA_{hc}$  removal, whereas Cp164 and Cp167 showed poor  $NA_{hc}$  removal, which needs to be further investigated in the future. For Cp157, high  $NA_{hc}$  removal accompanied by high VLP protein recovery was detected. The intermediate length of the NA binding region results in effective binding and exchange of  $NA_{hc}$  and, in addition, sufficient ionic strength stabilization of the NA binding region during and after elution. This results in high  $NA_{hc}$  removal and high VLP protein recoveries. The heparin chromatography-based  $NA_{hc}$  removal process enables binding of  $NA_{ther}$  to the NA binding region and effective loading of the HBcAg VLPs with  $NA_{ther}$  for its therapeutic application.

### 5.4.2 Comparison of Cp157 and Cp183

Cp157 consistently resulted in higher VLP protein recoveries than Cp183, when comparing  $NA_{hc}$  removal performances for Cp157 and Cp183 by the different investigated chromatography-based techniques, LiCl precipitation, and alkaline treatment. This substantiates the reported solubility issues of  $NA_{hc}$ -free Cp183 (Porterfield et al., 2010) independent on the conducted removal process. Moreover, this points to a complex interplay between the length of the protamine-like structure and factors such as the presence of bound NAs or required ions to stabilize the VLP proteins (Figure 5.7 a)), already indicated by a charge balance hypothesis for HBcAg VLP capsid stability study by Newman et al., 2009. Cp157 with an intermediate length of the NA binding region seems to be less susceptible to aggregation or precipitation after  $NA_{hc}$  removal. The determined  $NA_{hc}$  removals were on similar levels for Cp157 and Cp183. A260/A280 ratios were however consistently higher for Cp183 than for Cp157 samples for all investigated  $NA_{hc}$  removal techniques. Hence, the  $NA_{hc}$  removal appears to be more difficult with the longer NA binding region due to stronger attraction forces between the positive charges within the NA binding region and the negatively charged NAs. Cp157 outperformed Cp183 in terms of  $NA_{hc}$  removal and VLP protein recovery. Thus, Cp157 is not only the superior construct for effective processing, but also likely to lead to higher  $NA_{ther}$  payloads and therefore higher therapeutic efficacy, accompanied with fewer safety issues and side effects due to  $NA_{hc}$  still present in the VLPs.

### 5.4.3 Comparison of heparin and sulfate chromatography

Heparin is a natural product derived from animal tissues, thus its properties can vary between batches, leading to inconsistencies in purification results and regulatory compliance issues (Liu et al., 2009; Fu et al., 2013; Baytas and Linhardt, 2020). As an alternative, sulfate chromatography (Begic et al., 2021; Steppert et al., 2022) was investigated next to heparin chromatography for an

effective NA<sub>hc</sub> removal for Cp157 and Cp183. Moreover, effects of a prior nuclease treatment on the removal performance of both chromatography-based processes were assessed. Both heparin and sulfate chromatography resulted consistently in high NA<sub>hc</sub> removals. Sulfate chromatography appears to be a suitable heparin alternative for NA<sub>hc</sub> removal. The observed drawbacks of sulfate in terms of VLP protein recovery compared to heparin chromatography are only comparable to a limited extent due to different stationary phase volumes used in the investigations presented. Material in high salt washes during the chromatography uncovered VLP protein loss due to strong binding to the stationary matrix. For a sufficiently meaningful comparison of VLP protein recovery for heparin and sulphate chromatography, experiments would have to be performed using a comparable chromatography column volume.

To evaluate effects of nuclease treatment on removal performance parameters such as NA<sub>hc</sub> removal and VLP protein recovery we aimed to apply quantitative analyses. In our study, nuclease treatment prior to the performed chromatography-based processes improved NA<sub>hc</sub> removal marginally. Our hypothesis here is, that only – to a large extent - NA regions that are not covered by the NA binding region are degraded. Degradation of NA parts bound to the NA binding region may not be effective due to steric hindrance of the enzymatic reaction (Figure 5.7 b)). The degradation of NAs may also have little effect on the proposed replacement of NAs by ligands of the applied chromatography media. Additionally, we observed challenges in the removal of the nucleases in the subsequent downstream process. Nuclease removal is, however, essential to prevent degradation of the NA<sub>ther</sub> after loading. An ultrafiltration step could be successful to separate the nucleases prior to loading (Hillebrandt et al., 2020). However, this additional step would require development and would reduce the VLP protein yield (Hillebrandt and Hubbuch, 2023).

#### 5.4.4 LiCl precipitation and alkaline treatment

LiCl precipitation and alkaline treatment techniques were reported to remove NA<sub>hc</sub> from Cp183 (Porterfield et al., 2010; Petrovskis et al., 2021). This was qualitatively evaluated by transmission electron microscopy and native agarose gel electrophoresis (NAGE) analysis. In order to quantitatively compare the heparin chromatography and process variants presented with LiCl precipitation and alkaline treatment with respect to their NA<sub>hc</sub> removal performance, LiCl precipitation and alkaline treatment were performed with Cp157 and Cp183. NA quantification by RP-UV/Vis of intermediate LiCl precipitation samples after centrifugation was not possible due to the presence of guanidine HCl in the samples, overlapping with the NA peaks in the flow-through of the RP-HPLC method. Therefore, it was decided not to average the NA<sub>hc</sub> removals obtained by the two available analytical methods across the study. The NA<sub>hc</sub> removal by LiCl precipitation from Cp183 has been evaluated by A260/A280

ratio determination at the SEC (Porterfield et al., 2010), resulting in final ratios of 0.6. However, VLP protein recoveries were not reported, which would be required for a final validation of  $\text{NA}_{\text{hc}}$  removal suitable for effective processing. In contrast, our study found a poor A260/A280 ratio of 1.74 for Cp183 in SEC and very low VLP protein recoveries. Cp157 resulted in slightly better  $\text{NA}_{\text{hc}}$  removals and VLP protein recoveries, with a final A260/A280 ratio of 0.95. However, these findings exhibit notably inferior performance of LiCl precipitation when contrasted with all chromatography-based  $\text{NA}_{\text{hc}}$  removal processes presented. Intermediate samples during the LiCl precipitation process were analyzed to identify process steps causing this protein loss. However, this analysis was inconclusive. The RP-UV/Vis determined still high VLP protein recoveries after the centrifugation, whereas SDS-PAGE analysis indicates significant VLP protein losses during the LiCl precipitation and centrifugation step. There may be unknown effects of the components in the disassembly and precipitation buffer used onto the RP-UV/Vis method, that not only interfere with NA quantification, but also affect protein quantification by this method. We suspect an insufficient separation of the VLP proteins and bound  $\text{NA}_{\text{hc}}$ , resulting in co-precipitation of the VLP proteins and low VLP protein recoveries.

So far, the  $\text{NA}_{\text{hc}}$  removal by alkaline treatment from Cp183 has been shown qualitatively by NAGE (Strods et al., 2015). However, quantitative analysis of the VLP protein recovered and  $\text{NA}_{\text{hc}}$  removed required for effective processing was not reported. Evaluation of  $\text{NA}_{\text{hc}}$  removal performance for Cp157 and Cp183 in our study revealed high VLP protein losses during the alkaline treatment process. Due to the already low initial concentration of the Cp183 protein, quantification of NA and VLP protein by RP-UV/Vis was not possible, thus precluding a comprehensive quantitative evaluation of the various steps involved. However, SDS-PAGE and NAGE analyses of Cp183 are in qualitative agreement with the results for Cp157. Cp157 resulted in better performance characteristics after the alkaline treatment procedures than Cp183, as with the other  $\text{NA}_{\text{hc}}$  removing approaches studied. The alkaline treatment resulted in minor VLP protein losses, both with and without the preliminary dialysis in 7 M Urea and  $\text{NaCO}_3$  solutions suggested by Strods et al., 2015. The long dialysis times in high pH buffers impaired VLP protein solubility less than we expected. However, only moderate  $\text{NA}_{\text{hc}}$  removals were achieved after alkaline treatment and dialysis in neutralization buffer. The dialysis in pH 12 buffer may decrease the electrostatic attractions between the NA binding region and bound  $\text{NA}_{\text{hc}}$  by deprotonating guanidinium groups of the arginines within the NA binding region (Hunter and Borsook, 1924; Schmidt et al., 1930). The detached NAs may be separated by dialysis in pH 12 buffer or the subsequent processing steps. Potential reasons for the inefficacious removal of  $\text{NA}_{\text{hc}}$  by dialysis in alkaline buffer include the possibility that pH 12 might not alkalize sufficiently to induce deprotonation of the guanidinium group of arginine (Fitch et al., 2015).

Alternatively, it is plausible that the unbound  $NA_{hc}$  molecules remained entrapped within the VLP capsids and consequently could not be effectively separated via dialysis. However, in contrast to the latter hypothesis, NAGE analysis showed free NAs in the sample, indicating that the NAs are no longer entrapped in the VLPs and need to be separated in further purification steps. Omission of the preliminary dialysis in 7 M Urea and  $NaCO_3$  solutions and direct alkaline treatment by dialysis in pH 12 buffer resulted in more successful removal performances. Given the ambiguous rationale behind the initial dialysis step in the alkaline treatment described by Strods et al., 2015, and the absence of significant disparities in VLP protein and NA attributes using SDS-PAGE and NAGE between samples subjected to preliminary dialysis and those not, discerning potential explanations for these outcomes is challenging. Further separation of free NAs was performed by precipitation, re-dissolution and SEC. The process of precipitation and subsequent re-dissolution led to notable losses of VLP protein and requires refinement for enhanced efficiency in processing. Nevertheless, examination of A260/A280 ratios of target fractions in SEC indicated that the alkaline treatment was insufficient in effectively removing  $NA_{hc}$ .

In summary, the chromatography-based processes presented demonstrated effective removal of  $NA_{hc}$  bound to HBcAg VLPs, required for subsequent binding of  $NA_{ther}$ , likely resulting in high  $NA_{ther}$  payloads and thus therapeutic efficacy. Through a comprehensive comparison of various process variants employing heparin and sulfate chromatography, both with and without prior nuclease treatments, along with novel quantitative assessments of  $NA_{hc}$  removals and VLP protein recoveries reported earlier (Valentic et al., 2024), it has been shown that the performance of LiCl precipitation and alkaline treatment is insufficient when compared to our proposed chromatography-based approaches. Among these approaches, the highest levels of  $NA_{hc}$  removal and VLP protein recovery were achieved for Cp157 using heparin chromatography without prior nuclease treatment.

## 5.5 Conclusions

In conclusion, this study presents a novel heparin chromatography-based process for the effective removal of  $NA_{hc}$  bound to HBcAg VLPs. This is required both to prevent potential side effects due to the presence of  $NA_{hc}$  and to subsequently load the VLPs with  $NA_{ther}$ . The process was evaluated using six different HBcAg VLP constructs with varying lengths of the NA binding region and different  $NA_{hc}$  loadings. Process performance was assessed through  $NA_{hc}$  removal and VLP protein recovery analyses using RP chromatography coupled with UV/Vis spectroscopy, and silica-SC based chromatography combined with a dye-based fluorescence assay. Additionally, alternative process variants such

as nuclease treatments and sulfate chromatography, as well as LiCl precipitation and alkaline treatment procedures were also explored for comparison with the newly developed chromatography-based method. The investigation of the heparin chromatography process using different HBcAg VLP constructs revealed a nuanced relationship between NA binding region length and NA<sub>hc</sub> removal efficiency, with Cp157 exhibiting optimal performances. While slight differences were observed among process variants for the selected constructs Cp157 and Cp183, the heparin chromatography-based process consistently outperformed LiCl precipitation and alkaline treatment methods in terms of NA<sub>hc</sub> removal and VLP protein recovery, highlighting its superiority over these techniques. Finally, the presented method might act as a blueprint for other vector systems where NA<sub>hc</sub> removal is an issue.

### Acknowledgment

The authors would like to thank Annabelle Dietrich for proofreading. The authors express their gratitude to Svea tom Dieck and Marcel Münch for performing preliminary experiments for the presented study. The authors would also like to thank Raphael Nieß for helping to produce HBcAg VLPs used in this study. We acknowledge support from the KIT-Publication Fund of the Karlsruhe Institute of Technology.

### Appendix C: Supplementary Material

The Supplementary Material associated with this chapter contain the following information:

- ❖ S5.1: SDS-PAGE analysis of heparin chromatography for different HBcAg VLP constructs
- ❖ S5.2: SDS-PAGE analysis of heparin and sulfate chromatography with and without prior nuclease treatment
- ❖ S5.3: SEC chromatograms and gel electrophoresis analysis of LiCl precipitation
- ❖ S5.4: SEC and gel electrophoresis analysis of alkaline treatment







# 6

## **Loading and Reassembly of Hepatitis B Core Antigen Virus-Like Particles as a Function of a Nucleic Acid Binding Region, Nucleic Acid Type and Ionic Strength in the Liquid Phase**

Angela Valentic<sup>a</sup>, Jakob Müller<sup>a</sup>, Jürgen Hubbuch<sup>a,\*</sup>

<sup>a</sup> Institute of Process Engineering in Life Sciences, Section IV: Biomolecular Separation Engineering, Karlsruhe Institute of Technology, Fritz-Haber-Weg 2, 76131 Karlsruhe, Germany

\* Corresponding author

### **Abstract**

Hepatitis B core antigen virus-like particles (HBcAg VLPs) are a promising nanocarrier candidate for gene delivery applications. However, VLP processing, in particular nucleic acid (NA) encapsulation and reassembly, remains a challenge. Reassembly of HBcAg VLPs loaded with different types of NAs has been qualitatively demonstrated in the literature, with reassembly being induced by increasing the ionic strength in the liquid phase or by the presence of NAs. For efficient processing, a deeper understanding of VLP loading and reassembly as well as influencing factors such as the presence of a NA binding region, NAs and ionic strength is required. In this study, a HBcAg VLP construct lacking the NA binding region, Cp149, and a construct possessing an intermediate length of the naturally occurring NA binding region, Cp157, were subjected to reassembly with different NaCl molarities in the buffer, varying the presence, concentration and types of NAs. A complex interplay of the effects of ionic

strength in the liquid phase, the presence of NAs and the NA binding region on the reassembly yield was observed. In addition to ionic strength, DNA oligonucleotides (ON) induced reassembly of VLP capsids when bound to the NA binding region of Cp157, whereas they did not affect the reassembly of Cp149 VLP proteins lacking the NA binding region. Furthermore, the NA binding region significantly influenced the efficiency of NA encapsulation, with Cp157 showing superior performance compared to Cp149. Maximum loading of Cp157 was achieved at the highest NA concentration in the reassembly mixture.

## 6.1 Introduction

Virus-like particles (VLPs) have proven successful as vaccines, with VLP-based vaccines against hepatitis B virus, human papillomavirus and hepatitis E virus on the market and quite a number of vaccine candidates in preclinical development and clinical trials (Qian et al., 2020; Le and Müller, 2021; Nooraei et al., 2021; Illah and Olaitan, 2023). In research, new developments contain VLP-based vaccine approaches for cancer immunotherapy with VLPs displaying tumor-associated antigens and thus triggering an immune response against cancer cells (Klamp et al., 2011; Li et al., 2021). VLPs are being explored as platforms for nucleic acid delivery in various therapeutic applications (Nooraei et al., 2021), including the development of vaccines for COVID-19, where they facilitate the delivery of genetic material encoding viral antigens to stimulate immune responses (Mohsen et al., 2017). Despite possible immunogenicity deficits, general benefits such as the possibility of surface modification at the genetic level or post-translational modification for effective tissue targeting, precise and uniform structures with large loading capacities, depending on the type of VLP, and safety advantages over viral vector systems make VLPs a promising alternative to other gene delivery vector systems (Rohovie et al., 2017). However, as many approaches to the use of VLPs for gene delivery applications have been reported in literature, as summarized in Le and Müller (2021), none of them is yet in clinical trials. This lack of progress may also be attributed to VLP processing challenges.

For vaccine solutions, the purification procedure subsequent to the intracellular formation of VLPs within an expression system, such as *E. coli*, yeast, or plant cells (Effio and Hubbuch, 2015), commonly encompasses cell lysis, clarification, precipitation or ultracentrifugation, disassembly and reassembly, followed by polishing and formulation (McCarthy et al., 1998; Zhao et al., 2012b; Hillebrandt et al., 2020; Zhang et al., 2021b). Recent innovations aiming at enhancing efficiency and scalability of VLP purification processes have introduced the application of ultrafiltration-based unit operations (Negrete et al., 2014; Carvalho et al., 2019; Hillebrandt et al., 2020, 2021; Hillebrandt and

## 6 Loading and Reassembly of Hepatitis B Core Antigen Virus-Like Particles as a Function of a Nucleic Acid Binding Region, Nucleic Acid Type and Ionic Strength in the Liquid Phase

Hubburch, 2023). Nevertheless, when considering gene delivery applications, additional purification steps are necessitated for VLPs due to their loading with nucleic acids (NAs), thereby rendering the purification process even more intricate (Rohovie et al., 2017; Valentic et al., 2022). In the case of the Hepatitis B core antigen (HBcAg) VLP, which is being intensively studied for gene

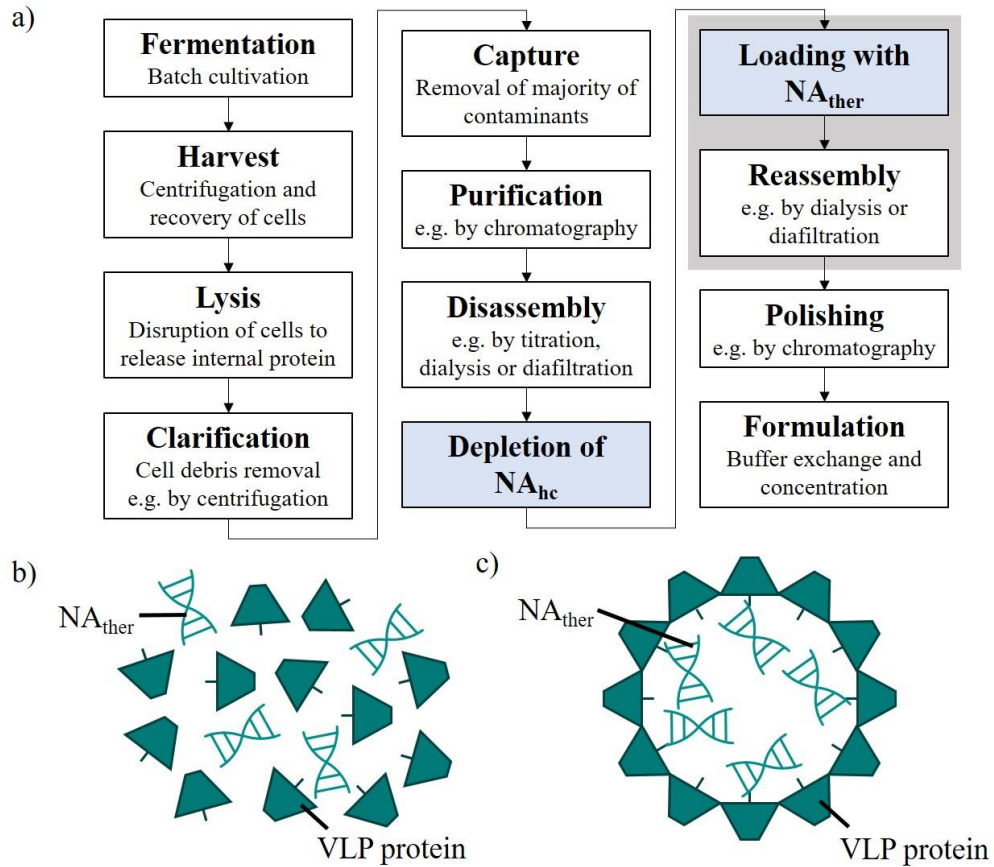


Figure 6.1 a) Common HBcAg VLP purification process (figure adapted from Hillebrandt et al., 2021) with depletion of NA<sub>hc</sub> and loading with NA<sub>ther</sub>, process steps required for the application as a nucleic acid delivery vector, highlighted in blue. The loading with NA<sub>ther</sub> and reassembly of VLP capsids investigated in this study are highlighted in grey. b) Mixture of HBcAg VLP dimers with NA binding region and NA<sub>ther</sub> before VLP reassembly. c) HBcAg VLP with NA binding region and NA<sub>ther</sub> encapsulated within the VLP protein capsid after depletion of NA<sub>hc</sub> and loading with NA<sub>ther</sub>. HBcAg: hepatitis B core antigen, NA<sub>hc</sub>: host cell-derived nucleic acids, NA<sub>ther</sub>: therapeutic nucleic acids, VLP: virus-like particle

delivery applications, efficient loading is achieved by using the naturally occurring NA binding region to bind the therapeutic nucleic acids (NA<sub>ther</sub>). HBcAg VLP constructs with different lengths of the naturally occurring NA binding region (Nassal, 1992; Newman et al., 2009; Liu et al., 2010; Sominskaya et al., 2013; Petrovskis et al., 2021; Zhang et al., 2021b; Valentic et al., 2022) and variants with multiple amino acid modifications (Porterfield et al., 2010; Strods et al., 2015) are investigated. However, host cell-derived nucleic acids (NA<sub>hc</sub>) bind to the NA binding region and are encapsulated within

the VLPs during the formation of HBcAg VLPs in *E. coli* cells (Birnbaum and Nassal, 1990; Newman et al., 2009; Porterfield et al., 2010). These undesired NA<sub>hc</sub> bound to the HBcAg VLP NA binding region need to be removed to facilitate subsequent loading of NA<sub>ther</sub> into the VLPs (Newman et al., 2009; Strods et al., 2015; Zhang et al., 2021b). Our group has recently demonstrated the successful removal of the bound NA<sub>hc</sub> using heparin chromatography (Valentic and Hubbuch, 2024). The disassembled and purified VLP subunits, referred to as dimers, are then mixed with NA<sub>ther</sub> and reassembled to load the VLPs with NA<sub>ther</sub> (Newman et al., 2009; Porterfield et al., 2010; Strods et al., 2015; Petrovskis et al., 2021). A typical production process including the additional processing steps required for gene delivery applications is shown in Figure 6.1. For HBcAg VLPs, reassembly is induced by increasing the ionic strength in the liquid phase (Strods et al., 2015; Schumacher et al., 2018; Rüdte et al., 2019; Zhang et al., 2021b) or by the presence of NAs (Newman et al., 2009). Reassembly for HBcAg VLPs loaded with / without varying types of NAs has been evidenced and monitored by native agarose gel electrophoresis, dynamic light scattering and transmission electron microscopy analyses (Porterfield et al., 2010; Strods et al., 2015; Rüdte et al., 2019; Petrovskis et al., 2021). However, the existing literature lacks information regarding reassembly yields for loaded HBcAg VLPs and other VLPs being explored as delivery platforms (Le and Müller, 2021). Additionally, a thorough investigation into the factors affecting the reassembly process, encompassing variables such as the presence of the NA binding region, the presence of NAs and variations in ionic strength in the liquid phase, remains unexplored in the current body of literature. Notably, the intricate interplay among these factors has been demonstrated to influence disassembly yields in HBcAg VLPs with varying lengths of the NA binding region (Valentic et al., 2022), suggesting a potential impact on the subsequent reassembly reaction.

In this study, we investigated the loading and reassembly of HBcAg VLPs as a function of a NA binding region, NAs and the ionic strength in the liquid phase. Cp149, lacking the NA binding region, and Cp157, which possesses an intermediate length of the naturally occurring NA binding region, were subjected to reassembly through dialysis in buffers with differing NaCl molarities. This process was carried out in two variants, without NAs and in the presence of dsDNA as a model NA<sub>ther</sub>. Additionally, for Cp157, the reassembly was conducted in the presence of NA<sub>hc</sub>. To explore reassembly kinetics and evolve the process towards large scale production solutions, such as tangential flow filtration, centrifugal concentrators were used for stepwise buffer exchange in four diafiltration steps. Hereby, different NaCl molarities in the reassembly buffer, as well as different reassembly process variants with dsDNA and ON\_DNA as model NA<sub>ther</sub> and without NAs present were compared for Cp149 and Cp157. The proportion of dimers, aggregates and capsids, and thus yields of reassembly were subsequently assessed using size-exclusion

chromatography. Furthermore, reassembly yields and the loading efficiency with model NA<sub>ther</sub> were evaluated for Cp149 and Cp157 dependent on the presence of a NA binding region and the VLP dimer to NA ratio.

## 6.2 Materials and methods

### 6.2.1 Buffers and nucleic acids

If not stated otherwise, all chemicals were purchased from Merck (Darmstadt, Germany). Solutions and buffers were prepared with ultrapure water (PURELAB Ultra, ELGA LabWater) and aqueous buffers were filtered through a 0.2 µm pore-size cellulose acetate filter (Pall Corporation, Port Washington, NY, United States). Buffers were pH-adjusted with 4 M NaOH or 32% HCl. Trifluoroacetic acid (TFA) was purchased from Thermo Fisher Scientific (Waltham, MA, United States) and HPLC grade acetonitrile (ACN) from Avantor (Radnor, PA, United States). The dsDNA with a length of 720 bp, was produced by amplification of a pKR-based vector including an eGFP-encoding gene sequence, using 5'- ATGGTGAGCAAGGGCGAG-3' as a forward primer and 5'-TTACTTGTACAGCTCGTCCA- 3' as a reverse primer. Amplification was performed with PCRBio HiFi polymerase (Nippon Genetics Europe GmbH, Dürren, Germany). The PCR product was purified by native gel electrophoresis (NAGE) and extracted using a Wizard SV gel and a PCR clean-up kit (Promega, Madison, WI, United States). The DNA oligonucleotides (ON) with a length of 18 nt, were purchased in HPLC grade from Merck (Darmstadt, Germany).

### 6.2.2 VLP production, purification, disassembly and NA<sub>bc</sub> removal

A typical VLP production process including the additional processing steps required for gene delivery applications is shown in Figure 6.1. Two different hepatitis B core antigen (HBcAg) virus like particle (VLP) constructs, Cp149 with a truncated nucleic acid (NA) binding region and Cp157 with an intermediate length of the naturally occurring NA binding region, were produced and purified as described earlier (Valentic et al., 2022). HBcAg VLP capsids were disassembled overnight at 4°C by dilution with 50 mM Tris, 10 M Urea stock solution to a final concentration of 50 mM Tris, 4 M Urea and titrated to pH 9.0. After filtration by a 0.2 µm cellulose acetate filter, dimers were purified by size-exclusion chromatography (SEC) using a 150 mL Toyopearl HW-65S column equilibrated in disassembly buffer (50 mM Tris, 4 M Urea, pH 9.0) and host cell-derived NAs were depleted on a HiTrap™ Heparin HP (Cytiva, Marlborough, MA, United States) column (Valentic and Hubbuch, 2024), if necessary.

### 6.2.3 Mixing of VLPs with nucleic acids and VLP reassembly

HBcAg VLP dimers were mixed with dsDNA or ON\_DNA in different dimer/NA molar ratios and incubated for 30 min. Reassembly of VLP capsids was performed by dialysis into reassembly buffer using slide-a-lyzer dialysis cassettes (Thermo Fisher Scientific, Waltham, MA, United States) or buffer exchange into reassembly buffer by Vivaspin® centrifugal concentrators (Sartorius, Göttingen, Germany) via batch mode in four diafiltration steps. Reassembly buffers were 50 mM Tris, pH 7.2 with NaCl molarities between 0 M and 1 M. SEC was performed to separate free NAs and VLP capsids using a 25 mL Superose 6 Increase 10/300 GL (Cytiva, Marlborough, MA, United States) column equilibrated in reassembly buffer.

### 6.2.4 Analytics

#### 6.2.4.1 Analytical size-exclusion chromatography

SEC coupled with a diode array detector was used to evaluate the reassembly yields of the VLPs by quantifying differently sized species (dimers, capsids, and aggregates). An Agilent Bio SEC-5, 5  $\mu$ m, 1,000 Å, 4.6  $\times$  300 mm column (Agilent, Santa Clara, CA, United States) was used on a Vanquish UHPLC system, controlled by Chromeleon version 7.2 (both Thermo Fisher Scientific, Waltham, MA, United States). To assess the loading of VLPs with NAs, the ratio of HBcAg capsid peaks at 260 and 280 nm was calculated.

#### 6.2.4.2 NAGE

For NAGE, 0.7% agarose (Carl Roth, Karlsruhe, Germany) in TAE buffer (40 mM Tris, 20 mM acetic acid, 1 mM EDTA) with 1  $\mu$ g/mL midori green (Nippon Genetics GmbH, Düren, Germany) was used. GeneRuler 1-kb DNA ladder (Thermo Fisher Scientific, Waltham, MA, United States) was used as marker. Gels were run on a PowerPac Basic (Bio-Rad, Hercules, CA, United States).

#### 6.2.4.3 Protein and nucleic acid quantification

RP-based extraction and UV/Vis was used to separate and quantify the bound NA<sub>he</sub> and VLP proteins in accordance to an earlier publication of our group (Valentic et al., 2024). Hereby, an analytical reversed-phase chromatography was performed with a TSKgel Protein C4-300 column (3  $\mu$ m, 4.6x150 mm) from Tosoh Bioscience (Tokyo, Japan) on a Vanquish UHPLC system, controlled by Chromeleon version 7.2 (both Thermo Fisher Scientific, Waltham, MA, United States).

## 6.3 Results

To obtain deeper knowledge into the loading and reassembly of hepatitis B core antigen (HBcAg) virus-like particles (VLPs), factors affecting these processes were investigated. Reassembly yields and loading of the VLPs with nucleic acids (NAs) were determined. Hereby, reassembly was examined varying the presence of the HBcAg VLP NA binding region, the presence and type of NAs, and the ionic strength in the liquid phase of the reassembly buffer. The proportions of dimers, aggregates and capsids, and thus yields of reassembly were assessed using size-exclusion chromatography (SEC). Loading of the HBcAg VLPs with NAs was approximated by A260/A280 ratio analysis of the capsid peaks in the analytical SEC, visualized by native gel electrophoresis (NAGE) and assessed by reversed phase (RP)-based extraction and UV/Vis.

### 6.3.1 Variation of the presence of a NA binding region, NAs and ionic strength in the liquid phase

#### 6.3.1.1 Reassembly by dialysis

Cp149, lacking the NA binding region, and Cp157, which possesses an intermediate length of the naturally occurring NA binding region, were reassembled by dialysis in buffers with different NaCl molarities. This process was carried out both without NAs and in the presence of dsDNA as a model therapeutic nucleic acid (NA<sub>ther</sub>) with a dimer/dsDNA ratio of 60. Additionally, for Cp157, the reassembly was conducted in the presence of host cell-derived nucleic acids (NA<sub>hc</sub>). The resulted proportions of dimers, aggregates and capsids for Cp149 and Cp157 after reassembly by dialysis are depicted in Figure 6.2 and Figure 6.3 respectively.

The reassembly of empty Cp149 capsids resulted in reassembly yields between 53% for 300 mM NaCl and 65% for 1 M NaCl in the liquid phase. An increased NaCl molarity in the reassembly buffer lead to a smaller proportion of dimers, but to more aggregation of HBcAg VLPs due to solubility issues. The reassembly of Cp149 in the presence of dsDNA as model NA<sub>ther</sub> displayed the same behavior with decreased proportions of dimers and increased proportions of aggregates with higher NaCl molarities. However, the reassembly yields for 0.5 M and 1 M NaCl in the reassembly buffer were around 38% lower for the reaction with dsDNA present than without NAs present. Further, a low NaCl molarity of 0.05 mM NaCl lead to a VLP reassembly yield of 0.2% in the presence of dsDNA. Here, 82% of the VLP proteins were still present as dimers after the reassembly process.

The reassembly of empty Cp157 capsids resulted in increased reassembly yields with a rise in NaCl molarity in the reassembly buffer. However, the reassembly

yields of 28% and 38% for 0.5 M and 1 M NaCl were only about half of those determined for Cp149. For reassembly of Cp157 in the presence of either dsDNA or NA<sub>hc</sub> the reassembly yields further decreased and VLP proteins aggregated prevalently. Low NaCl molarities of 0.05 M and 0.15 M NaCl and

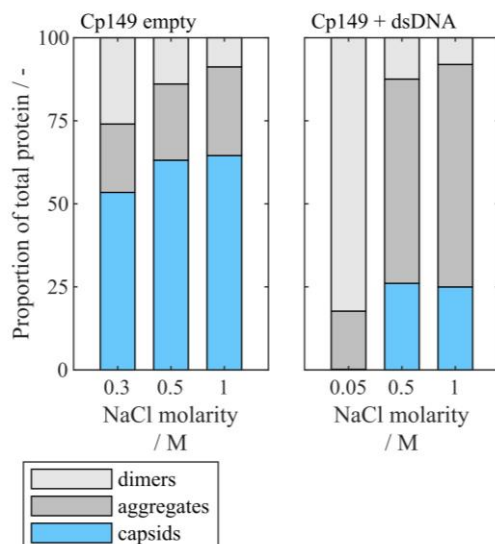


Figure 6.2 Proportion of dimers, capsids and aggregates for the empty HBcAg VLP construct Cp149 and mixed with dsDNA, after reassembly by dialysis into 50 mM Tris, pH 7.2 buffer with different NaCl molarities. Cp149 dimers were mixed with dsDNA in a dimer/dsDNA ratio of 60. HBcAg: hepatitis B core antigen, VLP: virus-like particle

the highest NaCl molarity of 1 M resulted in yields around 18%. Intermediate molarities of 0.3 M and 0.5 M NaCl lead to even lower reassembly yields of around 8%. The reassembly of Cp157 in the presence of NA<sub>hc</sub>, due to the omission of the NA<sub>hc</sub> depletion step during VLP purification, resulted in reassembly yields of approximately 5%. Hereby, the variation of the NaCl molarity in the reassembly buffer showed only minor effects.

### 6.3.1.2 Reassembly by centrifugal concentrators

To explore reassembly kinetics and evolve the process towards large scale production solutions centrifugal concentrators were used for stepwise buffer exchange in four diafiltration steps. Thereby, different NaCl molarities in the reassembly buffer were compared. Further, dsDNA in a dimer/dsDNA ratio of 60 and DNA oligonucleotide (ON) in a dimer/ON\_DNA ratio of 2 as model therapeutics and no NAs were investigated in the reassembly process of Cp149 and Cp157. The proportions of dimers, aggregates and capsids for Cp149 and Cp157 after reassembly are depicted in Figure 6.4 a) and Figure 6.4 b), respectively. Dialysis in the centrifugal concentrators resulted in inconsistent but small effects of different NaCl molarities. However, factors such as the VLP construct, diafiltration volumes and the presence of NAs were predominant. Following the stepwise buffer exchange into reassembly buffer, within the



## 6 Loading and Reassembly of Hepatitis B Core Antigen Virus-Like Particles as a Function of a Nucleic Acid Binding Region, Nucleic Acid Type and Ionic Strength in the Liquid Phase

progression of the diafiltration volumes the proportion of dimers decreased, while the proportions of aggregates and capsids increased for Cp149. However, the final reassembly yields for 0.5 M NaCl of 32% for empty Cp149 and 14%

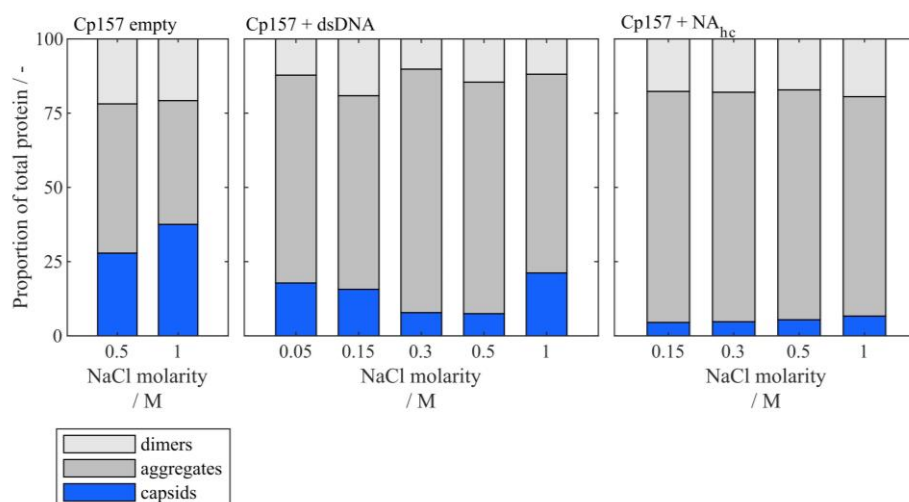


Figure 6.3 Proportion of dimers, capsids and aggregates for HBcAg VLP construct Cp157 after reassembly by dialysis into 50 mM Tris, pH 7.2 buffer with different NaCl molarities. Cp157 dimers were either empty, were mixed with dsDNA in a dimer/dsDNA ratio of 60, or contained NA<sub>hc</sub>, because depletion of NA<sub>hc</sub> by heparin chromatography was not performed prior to reassembly. HBcAg: hepatitis B core antigen, NA<sub>hc</sub>: host cell-derived nucleic acids, VLP: virus-like particle

of Cp149 in the presence of dsDNA were only about half of those gained by reassembly by dialysis, resulting in higher proportions of both dimers and aggregates. For Cp157, the reassembly yields for empty capsids after two diafiltration volumes were highest for all NaCl molarities. The reassembly yield after two diafiltration volumes for 0.5 M NaCl of 32% for empty Cp157 and 6% of Cp157 in the presence of dsDNA were similar to those gained by reassembly by dialysis. As for Cp149, within the stepwise buffer exchange by the centrifugal concentrators the proportion of dimers decreased for all Cp157 approaches investigated. However, for Cp157, within diafiltration volumes three and four, the proportion of capsids decreased while the proportion of aggregates increased mostly. The presence of ON\_DNA led to reassembly yields with a maximum of 14% for Cp149 with 200 mM NaCl after four diafiltration volumes and 7% for Cp157 with 0 M NaCl after two diafiltration volumes. For both constructs, both the presence of dsDNA and the presence of ON\_DNA led to comparable VLP reassembly yields. The yields were however lower than for empty VLP capsids. However, the presence of ON\_DNA resulted in lower proportions of aggregates and thus higher proportions of dimers compared to the presence of dsDNA.

In addition, similar studies were performed with a dimer/ON\_DNA ratio of 60. This showed effects of ON\_DNA on reassembly yields comparable to the

presence of ON\_DNA with a dimer/ON\_DNA ratio of 2 for Cp149 and to empty VLP capsids for Cp157. The respective proportions of dimers, aggregates and capsids are shown in Appendix D: S6.1. Samples of all studies with NAs present were further analyzed by NAGE to visualize the loading of the VLPs with NAs.

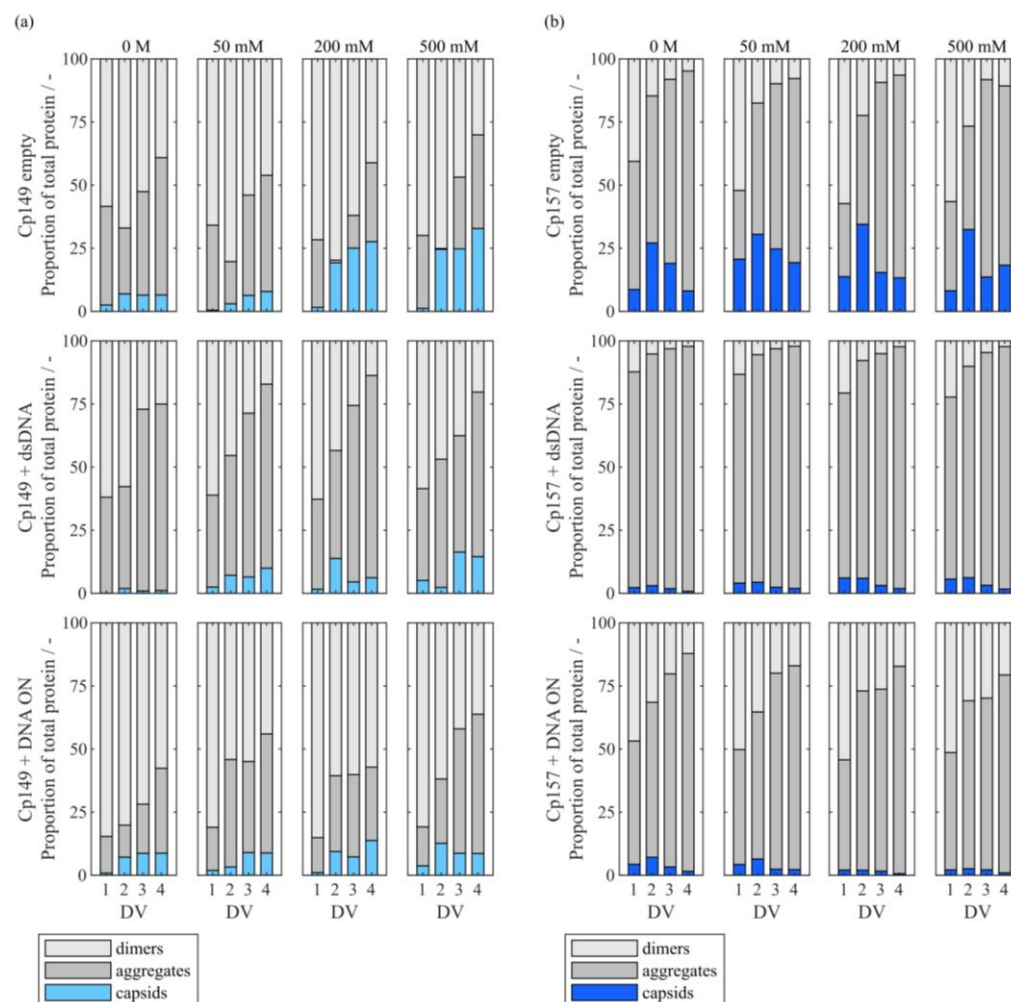


Figure 6.4 Proportion of dimers, capsids and aggregates for HBcAg VLP constructs (a) Cp149 and (b) Cp157 during reassembly by Vivaspin® centrifugal concentrators with 50 mM Tris, pH 7.2 buffer with different NaCl molarities in four diafiltration steps. Constructs were either empty, were mixed with dsDNA in a dimer/dsDNA ratio of 60, or were mixed with ON\_DNA in a dimer/ON\_DNA ratio of 2. DV: diafiltration volume, HBcAg: hepatitis B core antigen, ON: oligonucleotide, VLP: virus-like particle

An overview of samples and the respective gel scans can be found in Appendix D: S6.2 and S6.3. For reassembly in the presence of dsDNA, NA bands were weakly visible at the position of VLPs in addition to free NAs for Cp157 with 0 M NaCl and diafiltration volumes 1 and 2 in Appendix D: S6.3 c). Only free NAs were visible in all other samples. NA amounts in the samples of reassembly in the presence of ON\_DNA with a dimer/ON\_DNA ratio of 60 were under the detection limit of the NAGE method. However, reassembly with a dimer/ON\_DNA ratio of 2 resulted in NA bands at the position of VLPs in

## 6 Loading and Reassembly of Hepatitis B Core Antigen Virus-Like Particles as a Function of a Nucleic Acid Binding Region, Nucleic Acid Type and Ionic Strength in the Liquid Phase

addition to free NAs for all conditions and both constructs. Notably, the intensities of NA bands at the position of Cp157 VLPs were higher compared to the ones at the position of Cp149 VLPs. However, the overall NA band intensity decreased with increasing diafiltration volume, particularly for Cp157.

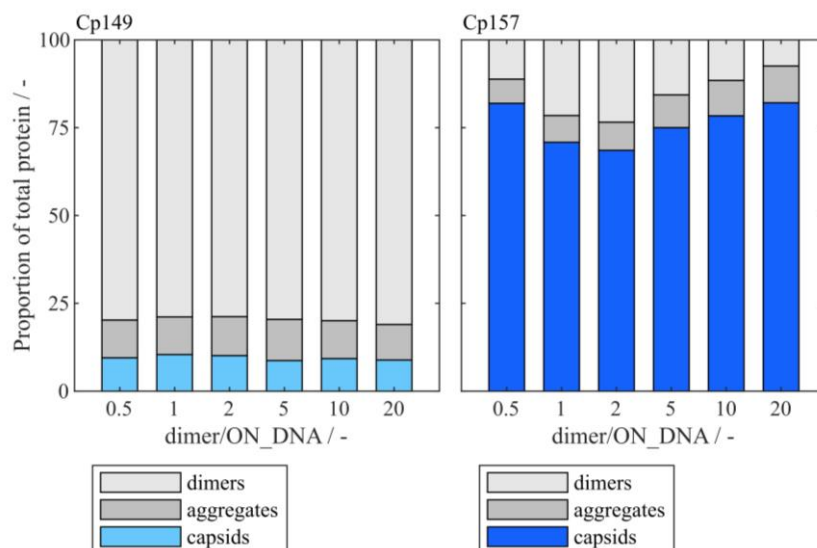


Figure 6.5 Proportion of dimers, capsids and aggregates for HBcAg VLP constructs Cp149 and Cp157 and different dimer/ON\_DNA ratios after reassembly by dialysis in 50 mM Tris, 150 mM NaCl, pH 7.2 buffer. HBcAg: hepatitis B core antigen, ON: oligonucleotide, VLP: virus-like particle

### 6.3.2 Variation of dimer/ON\_DNA ratio and presence of a NA binding region

To evaluate reassembly yields and loading efficiencies dependent on the dimer/ON\_DNA ratio and the presence of a NA binding region, Cp149 and Cp157 were reassembled by dialysis in 50 mM Tris, 150 mM NaCl, pH 7.2 buffer with different dimer/ON\_DNA ratios. Cp149 lacks the NA binding region, whereas Cp157 possesses an intermediate length of the naturally occurring NA binding region. The proportions of dimers, aggregates and capsids, and thus yields of reassembly were determined using SEC. Additionally, loading of the HBcAg VLPs with NAs was approximated by A260/A280 ratio analysis of the capsid peaks in the analytical SEC, visualized by NAGE and determined by RP-based extraction and UV/Vis. In Figure 6.5 the proportions of dimers, aggregates and capsids for both constructs depending on the dimer/ON\_DNA ratio are depicted. Proportions of capsids and thus reassembly yields around 9.5% were achieved with Cp149, similar for all investigated dimer/ON\_DNA ratios. Around 80% of the Cp149 VLP proteins were still present as dimers after reassembly for all conditions. Cp157 resulted in significantly higher reassembly yields of at least 69% for a dimer/ON\_DNA ratio of 2. Both with a decrease and increase of dimer/ON\_DNA ratio, the

reassembly yields increased gradually up to 82% for a ratio of 0.5 and 20. The differences in capsid proportions were compensated by different dimer proportions, whereas the proportion of aggregates remained stable for the different ratios investigated. NAGE analysis was performed to visualize VLP

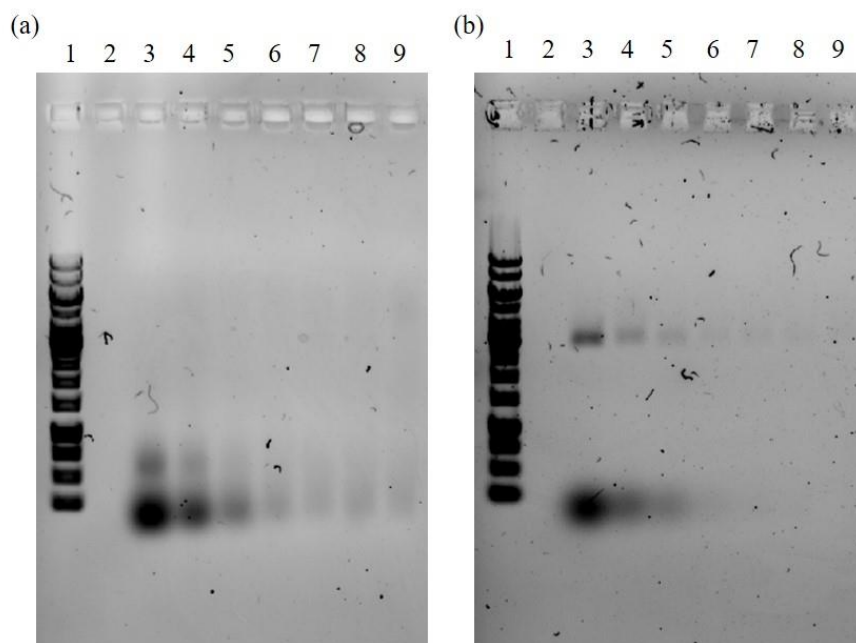


Figure 6.6 NAGE analysis of HBcAg VLP constructs (a) Cp149 and (b) Cp157 and different dimer/ON\_DNA ratios after reassembly by dialysis in 50 mM Tris, 150 mM NaCl, pH 7.2 buffer. Lanes correspond to the following dimer/ON\_DNA ratios: 0.5 (lane 3), 1 (lane 4), 2 (lane 5), 5 (lane 6), 10 (lane 7), and 20 (lane 8). An initial sample of the construct before mixing with ON\_DNA was analysed in lane 9 and a marker in lane 1. HBcAg: hepatitis B core antigen, ON: oligonucleotide, VLP: virus-like particle

loading and the respective gel scans are displayed in Figure 6.6. For both constructs, the more NAs were present in the mixture, the higher intensity of the NA bands for free NAs in the gels. However, no NA bands at the position of VLPs were visible for Cp149, regardless of the dimer/ON\_DNA ratio. On the contrary, the mixing and reassembly of Cp157 with ON\_DNA resulted in NA bands at the position of VLPs with intensities dependent on the ratio of dimer/ON\_DNA. For a ratio of 0.5 the highest intensity of NA bands at the position of VLPs were visible. The intensity gradually decreased with a decrease in ON\_DNA present, conterminous with higher dimer/ON\_DNA ratios. A260/A280 ratio analysis of the capsid peaks in SEC, displayed in Figure 6.7, revealed loading outcomes for Cp149 and Cp157 similar to NAGE analysis. Low A260/A280 ratios between 0.65 for dimer/ON\_DNA ratio of 0.5 and 0.62 for dimer/DNA ratio of 20 were achieved for Cp149. Mixing and loading of Cp157 resulted in A260/A280 ratio of 0.93 for a dimer/ON\_DNA ratio of 0.5, gradually decreasing to 0.63 with decreased ON\_DNA amounts in the reassembly mixture.

## 6 Loading and Reassembly of Hepatitis B Core Antigen Virus-Like Particles as a Function of a Nucleic Acid Binding Region, Nucleic Acid Type and Ionic Strength in the Liquid Phase

An additional preparative SEC was conducted to separate VLP capsids from other VLP species and free NAs subsequent to the reassembly by dialysis. SEC was performed for all Cp157 dimer/ON\_DNA ratios investigated, and for a Cp149 dimer/ON\_DNA ratio of 0.5. This allowed for an absolute quantification of VLP proteins and encapsulated model NA<sub>ther</sub> by RP-based extraction and UV/Vis, outlined in Table 6.1. With the determined absolute concentrations of NAs and VLP protein in the samples, an effective dimer/ON\_DNA ratio of the

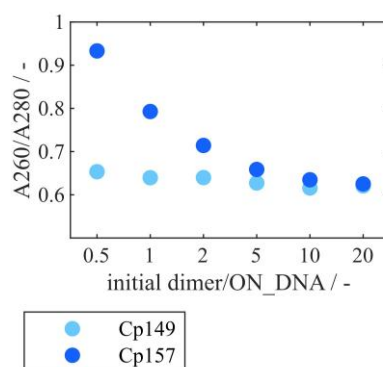


Figure 6.7 A260/A280 ratio of HBcAg VLP constructs Cp149 and Cp157 for different initial dimer to ON\_DNA ratios after reassembly by dialysis in 50 mM Tris, 150 mM NaCl, pH 7.2 buffer. Ratios were determined by analytical SEC. HBcAg: hepatitis B core antigen, ON: oligonucleotide, SEC: size-exclusion chromatography, VLP: virus-like particle

loaded and reassembled capsid was calculated. This effective dimer/ON\_DNA ratio increased stepwise from 2.43 up to 57.68 for initial dimer/ON\_DNA ratios of 0.5 up to 20. Thus, the more ON\_DNA present in the mixture, the greater number of ON\_DNA encapsulated in the Cp157 VLP capsids. Mixing and reassembling of Cp149 with a dimer/ON\_DNA ratio of 0.5 resulted in an effective dimer/ON\_DNA ratio of 25.56 and an encapsulation of 5 ON\_DNA per Cp149 VLP capsid compared to an initial ON\_DNA per VLP capsid of 240. This results in a low ratio of effective dimer/ON\_DNA ratio in the capsid to initial dimer/ON\_DNA ratio in the reassembly mixture of 0.02, as illustrated in Figure 6.8. On the contrary, Cp157 resulted in ratios above 0.20 for every dimer/ON\_DNA ratio investigated. Notably, there is a maximum of the ratio of effective dimer/ON\_DNA ratio in the capsid to initial dimer/ON\_DNA ratio in the reassembly mixture of 0.91 for an intermediate initial dimer/ON\_DNA ratio of 5. For both an increase and decrease of this initial dimer/ON\_DNA ratio of 5 the correlation of effective dimer/ON\_DNA ratio in the capsid and initial dimer/ON\_DNA ratio in the reassembly mixture decreases gradually.

## 6.4 Discussion

For gene delivery applications, the disassembled and purified hepatitis B core antigen (HBcAg) virus-like particle (VLP) dimers with a nucleic acid (NA)

binding region are loaded with therapeutic nucleic acids (NA<sub>ther</sub>) by mixing VLPs with NA<sub>ther</sub> followed by reassembly (Newman et al., 2009; Porterfield et al., 2010; Strods et al., 2015; Petrovskis et al., 2021). The reassembly of HBcAg VLPs loaded with varying types of NAs has been evidenced in literature by native agarose gel electrophoresis (NAGE), dynamic light scattering and transmission electron microscopy analyses (Porterfield et al., 2010; Strods et al., 2015; Petrovskis et al., 2021), however, lacking information regarding reassembly yields and absolute quantification of VLP capsid loadings. In this study, we investigated the loading and reassembly of HBcAg VLPs as a function

Table 6.1 Loading analysis of HBcAg VLP constructs Cp149 and Cp157 for different initial dimer/ON\_DNA ratios after reassembly by dialysis in 50 mM Tris, 150 mM NaCl, pH 7.2 buffer. NA and protein concentrations of the capsids were determined by RP-based extraction and UV/Vis. HBcAg: hepatitis B core antigen, ON: oligonucleotide, RP: reversed phase, VLP: virus-like particle

Construct	Initial dimer to ON_DNA	Initial ON_DNA per VLP capsid	NA in capsid [ng/ $\mu$ L]	Protein in capsid [g/L]	NA/protein in capsid [g/g]	Dimer/ON_DNA	ON_DNA per VLP capsid
Cp157	0.5	240	24.44	0.374	0.0654	2.43	49
	1	120	18.89	0.376	0.0503	3.16	38
	2	60	17.33	0.351	0.0494	3.21	37
	5	24	9.28	0.321	0.0289	5.50	22
	10	12	3.84	0.324	0.0118	13.42	9
	20	6	1.11	0.403	0.0028	57.68	2
Cp149	0.5	240	2.66	0.403	0.0066	25.56	5

of a NA binding region, NAs and ionic strength in the liquid phase to gain deeper knowledge on the intricate interplay among these factors and promote effective processing of HBcAg VLPs for gene delivery applications.

#### 6.4.1 Influence of the presence of a NA binding region, NAs and the ionic strength in the liquid phase on reassembly yields

For HBcAg VLPs the reassembly is commonly induced by increasing the ionic strength in the liquid phase (Strods et al., 2015; Schumacher et al., 2018; Rüdert et al., 2019; Zhang et al., 2021b). In our study, the increase in ionic strength by increasing the NaCl molarity in the reassembly buffer led to higher reassembly yields of empty VLPs. However, Cp157, with an intermediate length of the naturally occurring NA binding region, resulted in lower reassembly yields but higher aggregation than Cp149, lacking the NA binding region. Solubility issues

## 6 Loading and Reassembly of Hepatitis B Core Antigen Virus-Like Particles as a Function of a Nucleic Acid Binding Region, Nucleic Acid Type and Ionic Strength in the Liquid Phase

for HBcAg VLPs with the full length of naturally occurring NA binding region after depletion of host cell-derived nucleic acids (NA<sub>hc</sub>) (Porterfield et al., 2010) and fragile ionic stabilization of NA binding region (Newman et al., 2009), illustrated in Figure 6.9, were reported. This indicates possible stability problems of the Cp157 proteins due to the NA binding region, leading to higher aggregation than with Cp149. The solubility issues would explain the higher reassembly yields for 1 M NaCl than for 0.5 M NaCl at similar proportions of dimers but different levels of aggregation for Cp157. The higher ionic strength in the liquid phase may stabilise the NA binding region more efficiently, thereby preventing aggregation, and thus resulting in higher reassembly yields for the empty Cp157. Furthermore, the NA binding region itself could act as a steric hindrance to reassembly, resulting in

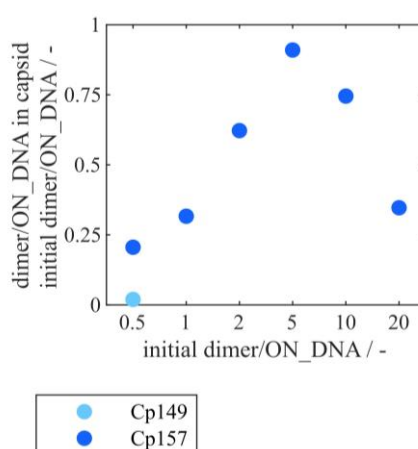


Figure 6.8 Ratio of the determined dimer/ON\_DNA ratio in the capsid to the initial dimer/ON\_DNA ratio for HBcAg VLP constructs Cp149 and Cp157 for different initial dimer/ON\_DNA ratios after reassembly by dialysis in 50 mM Tris, 150 mM NaCl, pH 7.2 buffer. HBcAg: hepatitis B core antigen, ON: oligonucleotide, VLP: virus-like particle

aggregation rather than correct capsid assembly. Steric hindrance might also be the reason for the fact, that the combination of the presence of dsDNA and high NaCl molarities resulted in high levels of aggregates of Cp149, drastically reducing the yield of reassembly compared to empty Cp149. Calculated on the basis of an average of 340 pm per bp (Bruce et al., 2014), the 720 bp dsDNA has a linear length of 245 nm. Thus the size of the dsDNA surpasses the size of the final HBcAg VLP capsids of around 36 nm (Porterfield et al., 2010; Valentic et al., 2022) significantly (Figure 6.10). Lacking the NA binding region, the assembly of Cp149 capsids seems to be disturbed by the presence of dsDNA, resulting in aggregation of the VLP proteins. Reassembly of Cp157 in the presence of dsDNA resulted in even lower reassembly yields. These low reassembly yields could be explained by both the general stability problems of Cp157 discussed above, and the fact that in this case the long dsDNA is bound to the NA binding region. The latter may have an even stronger steric hindrance



effect on the reassembly of VLP particles compared to Cp149. The differences in reassembly yield for Cp157 in the presence of dsDNA depending on the different NaCl molarities might be explained by the intricate interplay of the ionic stabilization of the NA binding region affected by the NaCl molarities (Figure 6.9) and binding of the dsDNA. Interestingly, the low NaCl molarity of

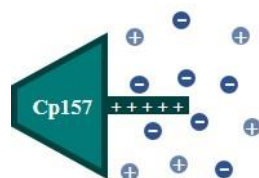


Figure 6.9 Ionic stabilization of the NA binding region of the Cp157 HBcAg VLP construct. HBcAg: hepatitis B core antigen, NA: nucleic acids, NA<sub>hc</sub>: host cell-derived nucleic acids, VLP: virus-like particle

0.05 M resulted in a high proportion of dimers still present after reassembly of Cp149 in the presence of dsDNA, whereas reassembly of Cp157 under these conditions resulted in high levels of aggregation. This contradicting behaviour suggests that the binding of the dsDNA to the Cp157 construct may induce reassembly of the VLP capsid, as already suggested by Newman et al. (2009), even though it is disturbed by the length of NA in this case. The reassembly of Cp157 in the presence of NA<sub>hc</sub> led to even lower reassembly yields, independent

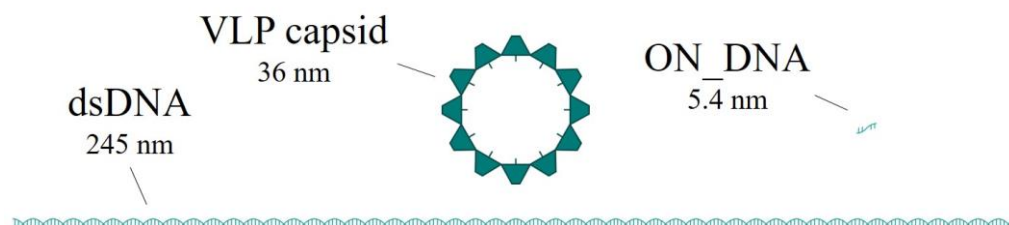


Figure 6.10 Size comparison of the HBcAg VLP capsid and the dsDNA and ON\_DNA investigated for loading in this study. The DNA lengths were calculated on the basis of an average of 340 pm per bp (Bruce et al., 2014). The size of the HBcAg VLP capsids of around 36 nm was taken from literature (Porterfield et al., 2010; Valentic et al., 2022) HBcAg: hepatitis B core antigen, ON: oligonucleotide, VLP: virus-like particle

from the NaCl molarity. We assume, that most of the NA binding regions were occupied by the NA<sub>hc</sub>, resulting in an independence from the NaCl molarity in the surrounding liquid phase. The concentration of bound NA<sub>hc</sub> was higher than in the experiments with model NA<sub>ther</sub>, proven by a higher A260/A280 ratio of 1.31 for capsids loaded with NA<sub>hc</sub> (Valentic et al., 2022) and a higher NA<sub>hc</sub> to protein mass ratio of 0.15 (Valentic et al., 2024). Whereas in our study a maximum A260/A280 ratio of 0.93 and NA<sub>ther</sub> to protein mass ratio of 0.0654, respectively, were achieved by loading with model NA<sub>ther</sub>. The high NA concentration resulted in reassembly induction and aggregation due to the stability problems and steric hindrance discussed.



The mixing and reassembly of Cp149 and Cp157 in the presence of short DNA oligonucleotides (ON) by centrifugal concentrators resulted in similarly low reassembly yields as the reassembly in the presence of dsDNA. Additionally, reassembly conducted via centrifugal concentrators generally resulted in lower reassembly yields compared to the dialysis method. Consequently, this approach is not deemed substantially informative for assessing the impact of factors such as ionic strength and the presence of NAs on the reassembly of the HBcAg VLP constructs. The mixing and reassembly in the presence of ON\_DNA by dialysis resulted in significantly different reassembly yields for Cp149 and Cp157. The constant NaCl molarity of 150 mM NaCl was not sufficient to induce Cp149 reassembly and big proportions of dimers were still present. In literature, significantly higher molar ratios of 500 mM (Zhang et al., 2021b), 650 mM (Strods et al., 2015), and 800 mM (Schumacher et al., 2018) are utilized for the reassembly of HBcAg VLPs, corresponding to our findings for the NaCl molarity-dependent reassembly of Cp149. However, reassembly in the presence of a NA binding region and the presence of NAs are performed with 150 mM NaCl (Porterfield et al., 2010) or even only 5 mM NaCl (Newman et al., 2009). For Cp149, the molarity of 150 mM NaCl in combination with the ON\_DNA, regardless of the dimer/ON\_DNA ratio, did not induce Cp149 capsid reassembly and resulted in a big proportion of remaining dimers. On the contrary, 150 mM NaCl and the presence of ON\_DNA resulted in the highest Cp157 reassembly yields observed in this study. As opposed to the long dsDNA, the short ON\_DNA appear to avoid steric hindrance complications and do not disturb the reassembly of Cp157, even when bound to the NA binding region. In fact, the combination of the NaCl molarity and the presence and binding of ON\_DNA effectively induces reassembly of Cp157, thereby avoiding aggregation. The differences in reassembly yields for varying dimer/ON\_DNA ratios indicate a complex interplay of the effects of ionic strength and NAs on the reassembly, that needs to be investigated further in future studies.

In summary, our observations reveal a complex interplay of ionic strength in the liquid phase, the presence of NAs, and of a NA binding region affecting reassembly yields. Additionally, ON\_DNA induced reassembly when bound to the NA binding region, particularly evident for Cp157, whereas they did not impact the reassembly of Cp149 VLP proteins. Long dsDNA also induced reassembly of Cp157 upon binding to the NA binding region, but led to significant aggregation for both constructs due to steric hindrance during the reassembly reaction. These divergent effects of distinct model NAs on reassembly yields underscore the importance of considering effects of various NA types, with different lengths and structures, loaded into the VLPs in literature (Porterfield et al., 2010; Strods et al., 2015; Petrovskis et al., 2021).

### 6.4.2 Reassembly kinetics and processing

To explore reassembly kinetics and evolve the process towards large scale production solutions, such as tangential flow filtration, as it is utilized for HBcAg VLPs for vaccine applications (Rüdt et al., 2019; Hillebrandt et al., 2021, 2022; Hillebrandt and Hubbuch, 2023), centrifugal concentrators were used for stepwise buffer exchange via batch mode in four diafiltration steps. Different NaCl molarities in the reassembly buffer, reassembly process variants with dsDNA and ON\_DNA as model NA<sub>ther</sub> as well as without NAs present were compared for Cp149 and Cp157. Reassembly conducted via centrifugal concentrators generally yielded lower reassembly yields compared to the dialysis method. Consequently, this approach is not deemed substantially informative for assessing the impact of studied factors. The centrifugal forces against the filtration membranes present in the centrifugal concentrators and the batch diafiltration by dilution with reassembly buffer and concentration to the initial volume seem to cause high aggregation of the HBcAg VLP proteins, compared to reassembly by dialysis. It does, however, provide relevant information for the development of the loading and reassembly process of HBcAg VLPs for large-scale production. The diafiltration volumes represent the stepwise buffer exchange into reassembly buffer, as it is also present during tangential flow filtration. For example, Cp157 exhibited its highest reassembly yields after diafiltration volumes two or three. Further processing within the centrifugal concentrators caused additional aggregation and loss of capsids. In contrast, Cp149 achieved its highest reassembly yields after four diafiltration volumes. These findings highlight the importance of comprehensive process development, especially for larger scale operations such as tangential flow filtration systems, in the context of loaded HBcAg VLPs for future applications.

### 6.4.3 Encapsulation efficiency dependent on the presence of a NA binding region and different VLP to NA ratios

Reassembly for HBcAg VLPs loaded with NAs has been evidenced by NAGE, dynamic light scattering and transmission electron microscopy analyses (Porterfield et al., 2010; Strods et al., 2015; Petrovskis et al., 2021). Further, VLP loading dependent on dimer/NA ratios for constructs with NA binding region has been qualitatively demonstrated by NAGE (Porterfield et al., 2010; Strods et al., 2015). In our study, HBcAg VLP constructs Cp149 and Cp157 were reassembled by dialysis with different dimer/ON\_DNA ratios to evaluate loading efficiencies dependent on the dimer/ON\_DNA ratio and the presence of a NA binding region. NAGE analysis evidenced the loading of Cp157 with ON\_DNA. The more ON\_DNA available in the reassembly mixture, the more ON\_DNA was encapsulated in the Cp157 capsids during reassembly. This was additionally confirmed by the A260/A280 ratio determined by capsid peak analysis of the analytical SEC. Conversely, Cp149 capsids exhibited minimal

encapsulation of NAs across all dimer/ON\_DNA ratios examined, as evidenced by the presence of only free NAs observed in the NAGE scan and low A260/A280 ratios. The NA binding region is indeed required for efficient loading of HBcAg VLPs with NAs. Concentration-dependent stochastic loading by engulfment during assembly, as suggested by Le and Müller (2021) appears to be surpassed by binding of NAs to the NA binding region. This is additionally highlighted by the analysis of capsid loadings. A preparative SEC was conducted to separate VLP capsids from other VLP species and free NAs subsequent to the reassembly to enable the absolute quantification of capsid loadings by RP-based extraction and UV/Vis. Analysis of the Cp149 reassembly approach with a dimer/ON\_DNA ratio 0.5, exhibiting the highest A260/A280 ratio, confirmed poor loading of Cp149 capsids even with high NA concentrations in the reassembly mixture, compared to Cp157. The loading analysis for Cp157 and different dimer/ON\_DNA ratios confirmed the fact that the more ON\_DNA were available in the reassembly mixture, the more ON\_DNA were encapsulated in the Cp157 capsids during reassembly, as found by the qualitative NAGE and A260/A280 ratio analysis. However, the absolute quantification of NAs and VLP proteins uncovered more noteworthy findings. For the highest loading of Cp157 capsids with a dimer/ON\_DNA ratio in the reassembly mixture of 0.5, the determined NA to protein mass ratio was 0.0654. However, the analysis of Cp157 capsids loaded with NA<sub>hc</sub> resulted in a NA to protein mass ratio of 0.15, reported in an earlier study of our group (Valentic et al., 2024). The binding and encapsulation of NA<sub>hc</sub> during the formation of VLPs in the expression system results in significantly higher loadings of the capsids, than achieved by our loading studies. One potential explanation could be the presence of even higher concentrations of NA<sub>hc</sub> in the host cells. Alternatively, it is more plausible that the reduced loadings observed in our study are attributed to the investigations being conducted with short ON\_DNA, which occupy solely the inner surface of the capsid and fail to fill the capsid void. Longer NA<sub>ther</sub> or a mixture of NA lengths may fill the capsid more completely and result in higher capsid loads. Moreover, the relationship between the dimer/ON\_DNA ratio within the capsids and the initial dimer/ON\_DNA ratio in the reassembly mixture presents an intriguing observation. Specifically, for an intermediate dimer/ON\_DNA ratio of 5 in the reassembly mixture, analysis revealed the most effective encapsulation of 22 out of 24 potential NAs within the Cp157 capsid. Both increasing and decreasing the dimer/ON\_DNA ratio in the reassembly mixture led to gradual decrease of the ratio of effective dimer/ON\_DNA ratio in the capsid to initial dimer/ON\_DNA ratio in the reassembly mixture, meaning that the available NAs are encapsulated less effectively. This optimal encapsulation efficiency could be attributed to stochastic constraints resulting from low NA concentrations for high dimer/ON\_DNA ratios, and less frequent encounters between NA and available binding sites for lower dimer/ON\_DNA ratios. Nevertheless, this observation warrants further investigation in future

studies, as there have been no comparable investigations in literature so far. Nonetheless, the maximum loading of Cp157 capsids was attained with the lowest dimer/ON\_DNA ratio, albeit accompanied by a simultaneous maximum loss of NAs used as free NAs after reassembly.

In summary, encapsulation efficiencies of ON\_DNA were dependent on the presence of a NA binding region and the dimer/ON\_DNA ratio. Cp149, lacking the NA binding region encapsulated significantly lower amounts of ON\_DNA than Cp157, independent from the dimer/ON\_DNA ratio. On the contrary, the NA binding region in the Cp157 construct demonstrated its effectiveness in NA binding. The maximum loading of Cp157 was achieved with the highest NA concentration in the reassembly mixture. However, the correlation between dimer/ON\_DNA ratio in the capsid after reassembly and the initial dimer/ON\_DNA ratio revealed a maximum in binding efficiency for an intermediate dimer/ON\_DNA ratio, which needs to further investigated in the future.

## 6.5 Conclusions

This study investigated factors affecting the reassembly and loading of HBcAg VLPs - the presence of a NA binding region, NAs and ionic strength in the liquid phase of the reassembly buffer. It revealed a complex interplay of these factors on reassembly yields. As well as ionic strength, ON\_DNA induced reassembly when bound to the NA binding region, particularly evident for Cp157, whereas they did not impact the reassembly of Cp149 VLP proteins. Further, we found that the NA binding region significantly influenced NA encapsulation efficiency, with Cp157 showing superior performance compared to Cp149. Further research is needed to optimize loading strategies and understand the correlation between dimer/NA ratio and binding efficiency.

## Acknowledgment

The authors would like to thank Annabelle Dietrich for proofreading. The authors express their gratitude to Nicola Böhner for producing the dsDNA used in this study and performing preliminary experiments for the presented study. The authors would also like to thank Raphael Nieß for producing HBcAg VLPs used in this study. We acknowledge support from the KIT-Publication Fund of the Karlsruhe Institute of Technology.

## **Appendix D: Supplementary Material**

The Supplementary Material associated with this chapter contain the following information:

- ❖ S6.1: Proportion of dimers, capsids and aggregates for HBcAg VLP constructs (a) Cp149 and (b) Cp157 during reassembly by centrifugal concentrators
- ❖ S6.2: Overview of samples in lanes of NAGE analysis of HBcAg VLP constructs Cp149 and Cp157 during reassembly by centrifugal concentrators
- ❖ S6.3: Gel scans of NAGE analysis of HBcAg VLP constructs Cp149 and Cp157 during reassembly by centrifugal concentrators



## General discussion and conclusion

Virus-like particles (VLPs) have emerged as a highly adaptable platform with broad applications spanning vaccine development to gene therapy. In recent years, there has been a growing need for efficient and targeted delivery systems for nucleic acid (NA)-based therapeutics, including mRNA, siRNA, and antisense oligonucleotides. These therapies offer promising avenues for the treatment of various genetic and acquired diseases; however, obstacles such as stability, cellular uptake, and precise delivery have restricted their clinical utility. VLPs present a compelling solution due to their demonstrated capacity to package and deliver foreign genetic material, along with their stable, repetitive surface architecture that enables modifications to enhance targeting of specific cells or tissues.

Overcoming the technical challenges in downstream processing of VLPs is critical for advancing their potential from the laboratory to clinical applications. Standard purification processes generally involve cell lysis to release VLPs from the expression system, followed by ultracentrifugation or precipitation, disassembly and reassembly, and subsequent polishing and formulation steps. For VLPs intended for NA delivery, additional steps are required to encapsulate therapeutic nucleic acids (NA<sub>ther</sub>). While VLPs have shown strong capabilities for packaging, protecting, and delivering foreign NAs, achieving efficient and scalable processing remains a significant challenge. Hepatitis B core antigen (HBcAg) is a widely studied VLP due to its strong immunogenicity, self-assembly capabilities, and potential as a gene delivery vehicle. Its unique structure and ability to encapsulate NAs make HBcAg VLPs a promising candidate for targeted genetic material delivery.

This thesis explored the process development of HBcAg VLPs as potential gene delivery vehicles, with a particular focus on the processing and analytical quantification methods in the presence of NA binding regions and bound NAs.

The NA binding region of the HBcAg VLPs, essential for encapsulating significant amounts of NAs, influences not only VLP formation but also poses challenges for downstream processing, such as solubility and disassembly during purification. In the first study, HBcAg VLP constructs with varying lengths of the NA binding region were produced and analyzed. Results revealed that while capsid size and zeta potential remained consistent across constructs, the length of the NA binding region significantly impacted host cell-derived nucleic acid (NA<sub>hc</sub>) binding, displaying a distinct two-zone pattern. Constructs with shorter binding regions showed a sharp increase in encapsulated NAs, whereas a plateau effect emerged as binding regions lengthened beyond Cp164 – a constructs with an intermediate length of the NA binding region.

Further, while precipitation and re-dissolution steps showed minimal sensitivity to NA loading variations, the disassembly process was strongly affected by both the construct and its NA load. Disassembly screening across liquid-phase conditions highlighted a complex balance between NA-stabilizing forces and destabilizing forces from positive charges in the binding region, also following the two-zone binding behavior. Optimized conditions for disassembly, such as high pH and elevated urea concentrations, were critical for achieving higher dimer yields. These findings underscore the importance of the NA binding region's length and composition in modulating VLP stability and purification efficiency, informing strategies to enhance purification and enable successful loading of NA<sub>ther</sub>.

Precise quantification of HBcAg VLPs and their bound NAs is essential to evaluate NA<sub>hc</sub> depletion, potential VLP protein loss, and effective loading with NA<sub>ther</sub>. Conventional UV/Vis spectroscopy, though commonly used for protein and NA analysis, is limited by overlapping absorption peaks at 260 and 280 nm, which complicates absolute quantification of VLP-bound NAs without prior separation. Dye-based fluorescence assays offer sensitivity for NA quantification but are susceptible to interference from contaminants, requiring high-purity NA extracts.

This work developed two robust analytical methods to address these limitations: (1) a silica spin column extraction method for NA quantification by dye-based fluorescence, which exhibited load-dependent recoveries allowing for accurate back-calculation to initial concentrations; and (2) an RP-HPLC method that enables simultaneous separation and absolute quantification of HBcAg proteins and bound NAs. This RP-based approach was validated with performance parameters of linearity, precision, and accuracy and was successfully applied across six HBcAg VLP constructs with varying NA<sub>hc</sub> loads, providing reliable measures of protein and NA content and HBcAg protein purity. These methods offer significant improvements over conventional techniques, facilitating accurate assessment of NA<sub>hc</sub> depletion, HBcAg protein recovery, and NA<sub>ther</sub>



loading, and, in combination with existing analytical tools, support the development of gene delivery processes for HBcAg VLPs.

Effective depletion of  $NA_{hc}$  from HBcAg VLPs is crucial to mitigate potential side effects and to allow efficient loading with  $NA_{ther}$ . While many existing studies have explored  $NA_{hc}$  removal techniques, they typically provide only qualitative assessments. In this work, the newly developed analytical methods were applied for the absolute quantification of HBcAg VLPs and bound NAs to evaluate a range of established  $NA_{hc}$  depletion techniques, assessing both removal efficiency and VLP protein recovery.

A novel heparin chromatography-based method was developed and tested alongside alternative methods, including nuclease treatments, sulfate chromatography, LiCl precipitation, and alkaline treatment. Results showed that the heparin chromatography process consistently outperformed these alternatives in terms of  $NA_{hc}$  removal and VLP protein recovery, especially across six HBcAg VLP constructs with varying NA binding region lengths and  $NA_{hc}$  loads. Notably, the Cp157 construct demonstrated optimal performance, highlighting a nuanced relationship between binding region length and depletion efficiency. The heparin chromatography-based method, with its superior results in  $NA_{hc}$  removal and protein recovery, offers a robust and reproducible approach for preparing HBcAg VLPs for therapeutic applications. This method could serve as a model for NA depletion in other vector systems, advancing their potential for gene delivery applications.

Further, this work examined the factors influencing reassembly and loading of HBcAg VLPs, focusing on the roles of the NA binding region, the presence of NAs, and the ionic strength of the reassembly buffer. Results indicated a complex interplay among these factors in determining reassembly yields, with both ionic strength and DNA oligonucleotides bound to NA binding regions promoting reassembly, particularly for Cp157 constructs. In contrast, these factors did not impact Cp149 VLP proteins, highlighting the significant influence of the NA binding region on NA encapsulation efficiency, with Cp157 demonstrating superior performance.

Efficient depletion of host cell-derived NAs enabled successful mixing of HBcAg dimers with  $NA_{ther}$  and subsequent reassembly into loaded VLPs. Native agarose gel electrophoresis, dynamic light scattering, and transmission electron microscopy confirmed successful reassembly and encapsulation; however, comprehensive data on reassembly yields for loaded VLPs remains limited in existing literature. This work further investigated an optimized reassembly procedure by systematically varying the NA binding region, NA type, and ionic strength, assessing reassembly yields and  $NA_{ther}$  loading efficiency with novel quantification methods.

This investigation into reassembly factors provides critical insights to advance HBcAg VLP loading strategies. Future research should aim to refine dimer/NA ratios and further scale up the process using stepwise buffer exchange methods like tangential flow filtration, enhancing the potential of HBcAg VLPs as delivery platforms for gene therapy applications.

The combined findings of this work provide a comprehensive understanding of the factors influencing the phase behavior, stability, purification, and quantification of HBcAg VLPs. By elucidating the role of the NA binding region and its interaction with bound NAs, this dissertation advances the field of VLP-based gene delivery systems. The development of robust analytical methods and optimized purification processes lays the groundwork for the scalable production of HBcAg VLPs, making them viable candidates for therapeutic applications, including gene therapy and vaccine delivery. Through this body of work, significant progress has been made in addressing the challenges associated with the purification of HBcAg VLPs. The insights gained into VLP stability, structural integrity, and the impact of encapsulated NAs will guide future research and development efforts aimed at harnessing the full potential of VLPs as versatile nanocarriers for NA<sub>ther</sub>. The methodologies and processes developed in this dissertation not only enhance our understanding of VLP behavior but also contribute to the broader goal of advancing precision medicine through innovative delivery platforms.

Building on the advances achieved in this work, several promising avenues for future research and development in the field of HBcAg VLPs as gene delivery platforms can be envisioned. First, further optimization of loading and encapsulation efficiency, particularly through fine-tuning of the dimer-to-NA ratios and adjustments to the NA binding region, will be essential for enhancing therapeutic payloads and targeting efficiency. Additionally, exploring alternative NA types, including mRNA and siRNA, may reveal specific interactions that could improve VLP encapsulation and release profiles, enabling broader applications for HBcAg VLPs in gene therapy and RNA-based therapies. The developed purification and quantification methodologies present opportunities to scale the HBcAg VLP production process towards clinical applications. Implementing these processes within a tangential flow filtration system, for example, may facilitate the transition from lab-scale to industrial-scale production, aligning with Good Manufacturing Practice standards and ensuring high-quality VLP production. Moreover, investigating the biophysical properties of these VLPs in *in vivo* models will be critical for assessing stability, biodistribution, and cellular targeting, advancing our understanding of their therapeutic potential and safety. Finally, the insights from this research into the structural integrity and reassembly behaviors of VLPs could be applied to other VLP systems, broadening the impact of these methodologies beyond HBcAg to other promising nanocarriers. This could foster the design of new, modular

VLP-based delivery platforms, capable of precise targeting and therapeutic payload delivery. With continued innovation, HBcAg VLPs are well-positioned to contribute meaningfully to the future of precision medicine, serving as a versatile and scalable platform for gene therapy and vaccine applications.

## Bibliography

- Aartsma-Rus, A. (2024). Applying Lessons Learned from Developing Exon Skipping for Duchenne to Developing Individualized Exon Skipping Therapy for Patients with Neurodegenerative Diseases. *Synlett* 35, 1247–1252. doi:10.1055/a-2211-6490.
- Aldosari, B. N., Alfagih, I. M., and Almurshedi, A. S. (2021). Lipid nanoparticles as delivery systems for RNA-based vaccines. *Pharmaceutics* 13, 1–29. doi:10.3390/pharmaceutics13020206.
- Ali, N., Rampazzo, R. D. C. P., Costa, A. Di. T., and Krieger, M. A. (2017). Current Nucleic Acid Extraction Methods and Their Implications to Point-of-Care Diagnostics. *Biomed Res. Int.* 2017. doi:10.1155/2017/9306564.
- An, M., Raguram, A., Du, S. W., Banskota, S., Davis, J. R., Newby, G. A., et al. (2024). Engineered virus-like particles for transient delivery of prime editor ribonucleoprotein complexes in vivo. *Nat. Biotechnol.* 42. doi:10.1038/s41587-023-02078-y.
- Ausar, S. F., Foubert, T. R., Hudson, M. H., Vedvick, T. S., and Middaugh, C. R. (2006). conformational stability and disassembly of norwalk virus-like particles: Effect of ph and temperature. *J. Biol. Chem.* 281, 19478–19488. doi:10.1074/jbc.M603313200.
- Banskota, S., Raguram, A., Suh, S., Du, S. W., Davis, J. R., Choi, E. H., et al. (2022). Engineered virus-like particles for efficient in vivo delivery of therapeutic proteins. *Cell* 185, 250-265.e16. doi:10.1016/j.cell.2021.12.021.
- Baytas, S. N., and Linhardt, R. J. (2020). Advances in the preparation and synthesis of heparin and related products. *Drug Discov. Today* 25, 2095–2109. doi:10.1016/j.drudis.2020.09.011.
- Begic, M., Pecenkovic, S., Gajdosik, M. S., Josic, D., and Müller, E. (2021). Salt-tolerant cation exchanger-containing sulfate groups as a viable alternative for mixed-mode type and heparin-based affinity resins. doi:10.1002/biot.202100100.
- Bin Mohamed Suffian, I. F., Garcia-Maya, M., Brown, P., Bui, T., Nishimura, Y., Palermo, A. R. B. M. J., et al. (2017). Yield Optimisation of Hepatitis B Virus Core Particles in E. coli Expression System for Drug Delivery Applications. *Sci. Rep.* 7, 1–9. doi:10.1038/srep43160.
- Birnbaum, F., and Nassal, M. (1990). Hepatitis B virus nucleocapsid assembly: primary structure requirements in the core protein. *J. Virol.* 64, 3319–3330. doi:10.1128/jvi.64.7.3319-3330.1990.
- Blasi, P., Giovagnoli, S., Schoubben, A., Ricci, M., and Rossi, C. (2007). Solid lipid nanoparticles for targeted brain drug delivery. *Adv. Drug Deliv. Rev.*

- 59, 454–477. doi:10.1016/j.addr.2007.04.011.
- Boisgérault, F., Morón, G., and Leclerc, C. (2002). Virus-like particles: A new family of delivery systems. *Expert Rev. Vaccines* 1, 101–109. doi:10.1586/14760584.1.1.101.
- Brescia, P. (2021). Application Note Molecular Biology and Biochemical Microvolume Purity Assessment of Nucleic Acids Using A 260 /A 280 Ratio and Spectral Scanning.
- Broos, K., Vanlandschoot, P., Maras, M., Robbens, J., Leroux-Roels, G., and Guisez, Y. (2007). Expression, purification and characterization of full-length RNA-free hepatitis B core particles. *Protein Expr. Purif.* 54, 30–37. doi:10.1016/j.pep.2007.02.006.
- Bruce, A., Alexander, J., Lewis, J., Morgan, D., and Martin, R. (2014). *Molecular Biology of the Cell*. Garland Publishing Inc.
- Burnett, J. C., Rossi, J. J., and Tiemann, K. (2011). Current progress of siRNA/shRNA therapeutics in clinical trials. *Biotechnol. J.* 6, 1130–1146. doi:10.1002/biot.201100054.
- Carvalho, S. B., Silva, R. J. S., Moleirinho, M. G., Cunha, B., Moreira, A. S., Xenopoulos, A., et al. (2019). Membrane-Based Approach for the Downstream Processing of Influenza Virus-Like Particles. *Biotechnol. J.* doi:10.1002/biot.201800570.
- Carvalho, S. B., Silva, R. J. S., Sousa, M. F. Q., Peixoto, C., Roldão, A., Carrondo, M. J. T., et al. (2022). Bioanalytics for Influenza Virus-Like Particle Characterization and Process Monitoring. *Front. Bioeng. Biotechnol.* 10, 1–15. doi:10.3389/fbioe.2022.805176.
- Chen, S. H., and Zhaori, G. (2011). Potential clinical applications of siRNA technique: Benefits and limitations. *Eur. J. Clin. Invest.* 41, 221–232. doi:10.1111/j.1365-2362.2010.02400.x.
- Choi, K. M., Choi, S. H., Jeon, H., Kim, I. S., and Ahn, H. J. (2011). Chimeric capsid protein as a nanocarrier for siRNA delivery: Stability and cellular uptake of encapsulated siRNA. *ACS Nano* 5, 8690–8699. doi:10.1021/nn202597c.
- Choi, K. M., Kim, K., Kwon, I. C., Kim, I. S., and Ahn, H. J. (2013). Systemic delivery of siRNA by chimeric capsid protein: Tumor targeting and RNAi activity in vivo. *Mol. Pharm.* 10, 18–25. doi:10.1021/mp300211a.
- Conway, J. F., Cheng, N., Zlotnick, A., Stahl, S. J., Wingfield, P. T., Belnap, D. M., et al. (1998). Hepatitis B virus capsid: Localization of the putative immunodominant loop (residues 78 to 83) on the capsid surface, and implications for the distinction between c and e-antigens. *J. Mol. Biol.* 279, 1111–1121. doi:10.1006/jmbi.1998.1845.
- Conway, J. F., Cheng, N., Zlotnick, A., Wingfield, P. T., Stahl, S. J., and Steven, A. C. (1997). Visualization of a 4-helix bundle in the hepatitis B virus

- capsid by cryo-electron microscopy. *Nat.* 386 11, 91–94. doi:<https://doi.org/10.1038/386091a0>.
- Cooper, A., and Shaul, Y. (2005). Recombinant viral capsids as an efficient vehicle of oligonucleotide delivery into cells. *Biochem. Biophys. Res. Commun.* 327, 1094–1099. doi:[10.1016/j.bbrc.2004.12.118](https://doi.org/10.1016/j.bbrc.2004.12.118).
- Cooper, A., Tal, G., Lider, O., and Shaul, Y. (2005). Cytokine Induction by the Hepatitis B Virus Capsid in Macrophages Is Facilitated by Membrane Heparan Sulfate and Involves TLR2. *J. Immunol.* 175, 3165–3176. doi:[10.4049/jimmunol.175.5.3165](https://doi.org/10.4049/jimmunol.175.5.3165).
- Crowther, R. A., Kiselev, N. A., Böttcher, B., Berriman, J. A., Borisova, G. P., Ose, V., et al. (1994). Three-dimensional structure of hepatitis B virus core particles determined by electron cryomicroscopy. *Cell* 77, 943–950. doi:[10.1016/0092-8674\(94\)90142-2](https://doi.org/10.1016/0092-8674(94)90142-2).
- Dietrich, A., Schiemer, R., Kurmann, J., Zhang, S., and Hubbuch, J. (2024). Raman-based PAT for VLP precipitation: systematic data diversification and preprocessing pipeline identification. *Front. Bioeng. Biotechnol.* 12, 1–20. doi:[10.3389/fbioe.2024.1399938](https://doi.org/10.3389/fbioe.2024.1399938).
- Effio, C. L., and Hubbuch, J. (2015). Next generation vaccines and vectors: Designing downstream processes for recombinant protein-based virus-like particles. *Biotechnol. J.* 10, 715–727. doi:[10.1002/biot.201400392](https://doi.org/10.1002/biot.201400392).
- Fang, P. Y., Bowman, J. C., Gómez Ramos, L. M., Hsiao, C., and Williams, L. D. (2018). RNA: Packaged and protected by VLPs. *RSC Adv.* 8, 21399–21406. doi:[10.1039/c8ra02084a](https://doi.org/10.1039/c8ra02084a).
- Fitch, C. A., Platzer, G., Okon, M., Garcia-Moreno, B. E., and McIntosh, L. P. (2015). Arginine: Its pKa value revisited. *Protein Sci.* 24, 752–761. doi:[10.1002/pro.2647](https://doi.org/10.1002/pro.2647).
- Fortner, A., and Schumacher, D. (2021). First COVID-19 Vaccines Receiving the US FDA and EMA Emergency Use Authorization. *Discoveries* 9, e122. doi:[10.15190/d.2021.1](https://doi.org/10.15190/d.2021.1).
- Friedrich, M., and Aigner, A. (2022). Therapeutic siRNA: State-of-the-Art and Future Perspectives. *BioDrugs* 36, 549–571. doi:[10.1007/s40259-022-00549-3](https://doi.org/10.1007/s40259-022-00549-3).
- Frietze, K. M., Peabody, D. S., and Chackerian, B. (2016). Engineering virus-like particles as vaccine platforms. *Curr. Opin. Virol.* 18, 44–49. doi:[10.1016/j.coviro.2016.03.001](https://doi.org/10.1016/j.coviro.2016.03.001).
- Fu, L., Li, G., Yang, B., Onishi, A., Li, L., Sun, P., et al. (2013). Structural characterization of pharmaceutical heparins prepared from different animal tissues. *J. Pharm. Sci.* 102, 1447–1457. doi:[10.1002/jps.23501](https://doi.org/10.1002/jps.23501).
- Gerlich, W. H. (2015). Prophylactic vaccination against hepatitis B: achievements, challenges and perspectives. *Med. Microbiol. Immunol.* 204, 39–55. doi:[10.1007/s00430-014-0373-y](https://doi.org/10.1007/s00430-014-0373-y).

- Goldfarb, R., Saidel, L. J., and Mosovich, E. (1951). The ultraviolet absorption spectra of proteins. *J. Biol. Chem.* 193, 397–404. doi:10.1016/s0021-9258(19)52465-6.
- Gutkin, A., Rosenblum, D., and Peer, D. (2021). RNA delivery with a human virus-like particle. *Nat. Biotechnol.* 39, 1512–1514. doi:10.1038/s41587-021-01149-2.
- Hashemi, K., Ghahramani Seno, M. M., Ahmadian, M. R., Malaekheh-Nikouei, B., Bassami, M. R., Dehghani, H., et al. (2021). Optimizing the synthesis and purification of MS2 virus like particles. *Sci. Rep.* 11, 1–14. doi:10.1038/s41598-021-98706-1.
- Hassebroek, A. M., Sooryanarain, H., Heffron, C. L., Hawks1, S. A., LeRoith, T., and Cecere, T. E. (2023). A hepatitis B virus core antigen-based virus-like particle vaccine expressing SARS-CoV-2 B and T cell epitopes induces epitope-specific humoral and cell-mediated immune responses but confers limited protection against SARS-CoV-2 infection. doi:10.1002/jmv.28503.
- He, J., Yu, L., Lin, X., Liu, X., Zhang, Y., Yang, F., et al. (2022). Virus-like Particles as Nanocarriers for Intracellular Delivery of Biomolecules and Compounds. *Viruses* 14. doi:10.3390/v14091905.
- Hill, B. D., Zak, A., Khera, E., and Wen, F. (2017). Engineering Virus-like Particles for Antigen and Drug Delivery. *Curr. Protein Pept. Sci.* 19, 112–127. doi:10.2174/1389203718666161122113041.
- Hillebrandt, N., and Hubbuch, J. (2023). Size-selective downstream processing of virus particles and non-enveloped virus-like particles. *Front. Bioeng. Biotechnol.* 11, 1–8. doi:10.3389/fbioe.2023.1192050.
- Hillebrandt, N., Vormittag, P., Bluthardt, N., Dietrich, A., and Hubbuch, J. (2020). Integrated Process for Capture and Purification of Virus-Like Particles: Enhancing Process Performance by Cross-Flow Filtration. *Front. Bioeng. Biotechnol.* 8. doi:10.3389/fbioe.2020.00489.
- Hillebrandt, N., Vormittag, P., Dietrich, A., and Hubbuch, J. (2022). Process monitoring framework for cross-flow diafiltration-based virus-like particle disassembly: Tracing product properties and filtration performance. 1522–1538. doi:10.1002/bit.28063.
- Hillebrandt, N., Vormittag, P., Dietrich, A., Wegner, C. H., and Hubbuch, J. (2021). Process development for cross-flow diafiltration-based VLP disassembly: A novel high-throughput screening approach. *Biotechnol. Bioeng.* 118, 3926–3940. doi:10.1002/bit.27868.
- Hönig, W., and Kula, M. R. (1976). Selectivity of protein precipitation with polyethylene glycol fractions of various molecular weights. *Anal. Biochem.* 72, 502–512. doi:10.1016/0003-2697(76)90560-1.
- Hou, X., Zaks, T., Langer, R., and Dong, Y. (2021). Lipid nanoparticles for mRNA delivery. *Nat. Rev. Mater.* 6, 1078–1094. doi:10.1038/s41578-021-

00358-0.

Hu, B., Zhong, L., Weng, Y., Peng, L., Huang, Y., Zhao, Y., et al. (2020). Therapeutic siRNA: state of the art. *Signal Transduct. Target. Ther.* 5. doi:10.1038/s41392-020-0207-x.

Hueso, M., Mallén, A., Suñé-pou, M., Aran, J. M., Suñé-negre, J. M., and Navarro, E. (2021). Nerns in therapeutics: Challenges and limitations in nucleic acid-based drug delivery. *Int. J. Mol. Sci.* 22. doi:10.3390/ijms222111596.

Huhti, L., Blazevic, V., Nurminen, K., Koho, T., Hytönen, V. P., and Vesikari, T. (2010). A comparison of methods for purification and concentration of norovirus GII-4 capsid virus-like particles. *Arch. Virol.* 155, 1855–1858. doi:10.1007/s00705-010-0768-z.

Hunter, A., and Borsook, H. (1924). The Dissociation Constants of Arginine. *Biochem. J.* 18, 883–890. doi:10.1042/bj0180883.

Illah, O., and Olaitan, A. (2023). Updates on HPV Vaccination. *Diagnostics* 13. doi:10.3390/diagnostics13020243.

J. Jones, L., T. Yue, S., Cheung Ching-Ying, and L. Singer, V. (1998). RNA Quantitation by Fluorescence-Based Solution Assay- RiboGreen Reagent Characterization. *Anal. Biochem.* 374, 368–374. Available at: <http://files/191/J. Jones et al. - 1998 - RNA Quantitation by Fluorescence-Based Solution As.pdf>.

Jeevanandam, J., Pal, K., and Danquah, M. K. (2019). Virus-like nanoparticles as a novel delivery tool in gene therapy. *Biochimie* 157, 38–47. doi:10.1016/j.biochi.2018.11.001.

Jinming Li, Sun, Y., Jia, T., Zhang, R., Zhang, K., and Wang, L. (2013). Messenger RNA vaccine based on recombinant MS2 virus-like particles against prostate cancer. *Intl J. Cancer.* doi:10.1002/ijc.28482.

Khorkova, O., Stahl, J., Joji, A., Volmar, C. H., and Wahlestedt, C. (2023). Amplifying gene expression with RNA-targeted therapeutics. *Nat. Rev. Drug Discov.* 22, 539–561. doi:10.1038/s41573-023-00704-7.

Klamp, T., Schumacher, J., Huber, G., Kühne, C., Meissner, U., Selmi, A., et al. (2011). Highly specific auto-antibodies against claudin-18 isoform 2 induced by a chimeric HBcAg virus-like particle vaccine kill tumor cells and inhibit the growth of lung metastases. *Cancer Res.* 71, 516–527. doi:10.1158/0008-5472.CAN-10-2292.

Kulkarni, J. A., Cullis, P. R., and Van Der Meel, R. (2018). Lipid Nanoparticles Enabling Gene Therapies: From Concepts to Clinical Utility. *Nucleic Acid Ther.* 28, 146–157. doi:10.1089/nat.2018.0721.

Kulkarni, J. A., Witzigmann, D., Thomson, S. B., Chen, S., Leavitt, B. R., Cullis, P. R., et al. (2021). The current landscape of nucleic acid therapeutics. *Nat. Nanotechnol.* 16, 630–643. doi:10.1038/s41565-021-



00898-0.

- Ladd Effio, C., Wenger, L., Ötes, O., Oelmeier, S. A., Kneusel, R., and Hubbuch, J. (2015). Downstream processing of virus-like particles: Single-stage and multi-stage aqueous two-phase extraction. *J. Chromatogr. A* 1383, 35–46. doi:10.1016/j.chroma.2015.01.007.
- Le, D. T., and Müller, K. M. (2021). In Vitro Assembly of Virus-Like Particles and Their Applications. *Life* 11, 334. doi:10.3390/life11040334.
- Le Pogam, S., Chua, P. K., Newman, M., and Shih, C. (2005). Exposure of RNA Templates and Encapsidation of Spliced Viral RNA Are Influenced by the Arginine-Rich Domain of Human Hepatitis B Virus Core Antigen (HBcAg 165-173). *J. Virol.* 79, 1871–1887. doi:10.1128/jvi.79.3.1871-1887.2005.
- Li, T., Yang, Y., Qi, H., Cui, W., Zhang, L., Fu, X., et al. (2023). CRISPR/Cas9 therapeutics: progress and prospects. *Signal Transduct. Target. Ther.* 8. doi:10.1038/s41392-023-01309-7.
- Li, W., Jing, Z., Wang, S., Li, Q., Xing, Y., Shi, H., et al. (2021). P22 virus-like particles as an effective antigen delivery nanoplatfrom for cancer immunotherapy. *Biomaterials* 271, 120726. doi:10.1016/j.biomaterials.2021.120726.
- Liu, H., Zhang, Z., and Linhardt, R. J. (2009). Lessons learned from the contamination of heparin. *Nat. Prod. Rep.* 26, 313–321. doi:10.1039/b819896a.
- Liu, S., He, J., Shih, C., Li, K., Dai, A., Hong Zhou, Z., et al. (2010). Structural comparisons of hepatitis B core antigen particles with different C-terminal lengths. *Virus Res.* 149, 241–244. doi:10.1016/j.virusres.2010.01.020.
- Lorenzo, E., Miranda, L., Godia, F., and Cervera, L. (2022). Downstream process design for Gag HIV-1 based virus-like particles.pdf. doi:10.1002/bit.28419.
- Lyu, P., and Lu, B. (2022). New Advances in Using Virus-like Particles and Related Technologies for Eukaryotic Genome Editing Delivery. *Int. J. Mol. Sci.* 23. doi:10.3390/ijms23158750.
- Mach, H., Volkin, D. B., Troutman, R. D., Wang, B. e. ., Luo, Z., Jansen, K. U., et al. (2006). Disassembly and reassembly of yeast-derived recombinant human papillomavirus virus-like particles (HPV VLPs). *J. Pharm. Sci.* 95, 2195–2206. doi:10.1002/jps.20696.
- Matsuo, M. (2021). Antisense Oligonucleotide-Mediated Exon-skipping Therapies: Precision Medicine Spreading from Duchenne Muscular Dystrophy. *JMA J.* 4, 232–240. doi:10.31662/jmaj.2021-0019.
- McCarthy, M. P., White, W. I., Palmer-Hill, F., Koenig, S., and Suzich, J. A. (1998). Quantitative Disassembly and Reassembly of Human Papillomavirus Type 11 Viruslike Particles In Vitro. *J. Virol.* 72, 32–41. doi:10.1128/jvi.72.1.32-41.1998.

- Minkner, R., Baba, R., Kurosawa, Y., Suzuki, S., Kato, T., Kobayashi, S., et al. (2018). Purification of human papillomavirus-like particles expressed in silkworm using a *Bombyx mori* nucleopolyhedrovirus bacmid expression system. *J. Chromatogr. B Anal. Technol. Biomed. Life Sci.* 1096, 39–47. doi:10.1016/j.jchromb.2018.08.007.
- Mohsen, M. O., Zha, L., Cabral-Miranda, G., and Bachmann, M. F. (2017). Major findings and recent advances in virus-like particle (VLP)-based vaccines. *Semin. Immunol.* 34, 123–132. doi:10.1016/j.smim.2017.08.014.
- Moradi Vahdat, M., Hemmati, F., Ghorbani, A., Rutkowska, D., Afsharifar, A., Eskandari, M. H., et al. (2021). Hepatitis B core-based virus-like particles: A platform for vaccine development in plants. *Biotechnol. Reports* 29, e00605. doi:10.1016/j.btre.2021.e00605.
- Mülhardt, C., and Beese, E. W. (2007). *Molecular Biology and Genomics*. doi:https://doi.org/10.1016/B978-0-12-088546-6.X5000-3.
- Nasimuzzaman, M., Lynn, D., van der Loo, J. C., and Malik, P. (2016). Purification of baculovirus vectors using heparin affinity chromatography. *Mol. Ther. Methods Clin. Dev.* 3, 16071. doi:10.1038/mtm.2016.71.
- Nassal, M. (1992). The arginine-rich domain of the hepatitis B virus core protein is required for pregenome encapsidation and productive viral positive-strand DNA synthesis but not for virus assembly. *J. Virol.* 66, 4107–4116. doi:10.1128/jvi.66.7.4107-4116.1992.
- Negrete, A., Pai, A., and Shiloach, J. (2014). Use of hollow fiber tangential flow filtration for the recovery and concentration of HIV virus-like particles produced in insect cells. *J. Virol. Methods* 195, 240–246. doi:10.1016/j.jviromet.2013.10.017.
- Newman, M., Chua, P. K., Tang, F.-M., Su, P.-Y., and Shih, C. (2009). Testing an Electrostatic Interaction Hypothesis of Hepatitis B Virus Capsid Stability by Using an In Vitro Capsid Disassembly/Reassembly System. *J. Virol.* 83, 10616–10626. doi:10.1128/jvi.00749-09.
- Newman, M., Suk, F.-M., Cajimat, M., Chua, P. K., and Shih, C. (2003). Stability and Morphology Comparisons of Self-Assembled Virus-Like Particles from Wild-Type and Mutant Human Hepatitis B Virus Capsid Proteins. *J. Virol.* 77, 12950–12960. doi:10.1128/jvi.77.24.12950-12960.2003.
- Nikam, R. R., and Gore, K. R. (2018). Journey of siRNA: Clinical Developments and Targeted Delivery. *Nucleic Acid Ther.* 28, 209–224. doi:10.1089/nat.2017.0715.
- Nooraei, S., Bahrulolum, H., Hoseini, Z. S., Katalani, C., Hajizade, A., Easton, A. J., et al. (2021). Virus-like particles: preparation, immunogenicity and their roles as nanovaccines and drug nanocarriers. *J. Nanobiotechnology* 19, 1–27. doi:10.1186/s12951-021-00806-7.

- Pardi, N., Parkhouse, K., Kirkpatrick, E., McMahon, M., Zost, S. J., Mui, B. L., et al. (2018). Nucleoside-modified mRNA immunization elicits influenza virus hemagglutinin stalk-specific antibodies. *Nat. Commun.* 9, 1–12. doi:10.1038/s41467-018-05482-0.
- Pereira Aguilar, P., Reiter, K., Wetter, V., Steppert, P., Maresch, D., Ling, W. L., et al. (2020). Capture and purification of Human Immunodeficiency Virus-1 virus-like particles: Convective media vs porous beads. *J. Chromatogr. A* 1627, 1–11. doi:10.1016/j.chroma.2020.461378.
- Petrovskis, I., Lieknina, I., Dislers, A., Jansons, J., Sominskaya, I., Bogans, J., et al. (2021). Production of the hbc protein from different HBV genotypes in e. coli. use of reassociated HBC vlps for packaging of SS-and DSRNA. *Microorganisms* 9, 1–15. doi:10.3390/microorganisms9020283.
- Porterfield, J. Z., Dhason, M. S., Loeb, D. D., Nassal, M., Stray, S. J., and Zlotnick, A. (2010). Full-Length Hepatitis B Virus Core Protein Packages Viral and Heterologous RNA with Similarly High Levels of Cooperativity. *J. Virol.* 84, 7174–7184. doi:10.1128/jvi.00586-10.
- Porterfield, J. Z., and Zlotnick, A. (2010). A simple and general method for determining the protein and nucleic acid content of viruses by UV absorbance. *Virology* 407, 281–288. doi:10.1016/j.virol.2010.08.015.
- Qian, C., Liu, X., Xu, Q., Wang, Z., Chen, J., Li, T., et al. (2020). Recent progress on the versatility of virus-like particles. *Vaccines* 8, 1–14. doi:10.3390/vaccines8010139.
- Qin, S., Tang, X., Chen, Y., Chen, K., Fan, N., Xiao, W., et al. (2022). mRNA-based therapeutics: powerful and versatile tools to combat diseases. *Signal Transduct. Target. Ther.* 7. doi:10.1038/s41392-022-01007-w.
- Reiter, K., Aguilar, P. P., Wetter, V., Steppert, P., Tover, A., and Jungbauer, A. (2019). Separation of virus-like particles and extracellular vesicles by flow-through and heparin affinity chromatography. *J. Chromatogr. A* 1588, 77–84. doi:10.1016/j.chroma.2018.12.035.
- Rittiner, J., Cumaran, M., Malhotra, S., and Kantor, B. (2022). Therapeutic modulation of gene expression in the disease state: Treatment strategies and approaches for the development of next-generation of the epigenetic drugs. *Front. Bioeng. Biotechnol.* 10, 1–22. doi:10.3389/fbioe.2022.1035543.
- Rohovie, M. J., Nagasawa, M., and Swartz, J. R. (2017). Virus-like particles: Next-generation nanoparticles for targeted therapeutic delivery. *Bioeng. Transl. Med.* 2, 43–57. doi:10.1002/btm2.10049.
- Roldao, A., Silva, A., and Mellado, M. (2020). Viruses and Virus-Like Particles in Biotechnology: Fundamentals and Applications.
- Rüdt, M., Vormittag, P., Hillebrandt, N., and Hubbuch, J. (2019). Process monitoring of virus-like particle reassembly by diafiltration with UV/Vis spectroscopy and light scattering. *Biotechnol. Bioeng.* 116, 1366–1379.

- doi:10.1002/bit.26935.
- Rulli, S. J., Hibbert, C. S., Mirro, J., Pederson, T., Biswal, S., and Rein, A. (2007). Selective and Nonselective Packaging of Cellular RNAs in Retrovirus Particles. *J. Virol.* 81, 6623–6631. doi:10.1128/jvi.02833-06.
- Sahin, U., Karikó, K., and Türeci, Ö. (2014). mRNA-based therapeutics-developing a new class of drugs. *Nat. Rev. Drug Discov.* 13, 759–780. doi:10.1038/nrd4278.
- Samandoulgou, I., Hammami, R., Rayas, R. M., Fliss, I., and Jean, J. (2015). Stability of secondary and tertiary structures of virus-like particles representing noroviruses: Effects of pH, ionic strength, and temperature and implications for adhesion to surfaces. *Appl. Environ. Microbiol.* 81, 7680–7686. doi:10.1128/AEM.01278-15.
- Schiller, J. T., and Lowy, D. R. (2012). Understanding and learning from the success of prophylactic human papillomavirus vaccines. *Nat. Rev. Microbiol.* 10, 681–692. doi:10.1038/nrmicro2872.
- Schmidt, C. L. A., Kirk, P. L., and Appleman, W. K. (1930). the Apparent Dissociation Constants of Arginine and of Lysine and the Apparent Heats of Ionization of Certain Amino Acids. *J. Biol. Chem.* 88, 285–293. doi:10.1016/s0021-9258(18)76810-5.
- Schmitz, A., and Riesner, D. (2006). Purification of nucleic acids by selective precipitation with polyethylene glycol 6000. *Anal. Biochem.* 354, 311–313. doi:10.1016/j.ab.2006.03.014.
- Schumacher, J., Bacic, T., Staritzbichler, R., Daneschdar, M., Klamp, T., Arnold, P., et al. (2018). Enhanced stability of a chimeric hepatitis B core antigen virus-like-particle (HBcAg-VLP) by a C-terminal linker-hexahistidine-peptide. *J. Nanobiotechnology* 16, 1–21. doi:10.1186/s12951-018-0363-0.
- Selzer, L., and Zlotnick, A. (2015). Assembly and release of hepatitis B virus. *Cold Spring Harb. Perspect. Med.* 5, 1–18. doi:10.1101/cshperspect.a021394.
- Sharma, V. K., Sharma, R. K., and Singh, S. K. (2014). Antisense oligonucleotides: Modifications and clinical trials. *Medchemcomm* 5, 1454–1471. doi:10.1039/c4md00184b.
- Shirbaghaee, Z., and Bolhassani, A. (2016). Different applications of virus-like particles in biology and medicine: Vaccination and delivery systems. *Biopolymers* 105, 113–132. doi:10.1002/bip.22759.
- Shmidt, A. A., and Egorova, T. V. (2022). PCR-based analytical methods for quantification and quality control of recombinant adeno-associated viral vector preparations. *Pharmaceuticals* 15. doi:10.3390/ph15010023.
- Shouval, D., Roggendorf, H., and Roggendorf, M. (2015). Enhanced immune response to hepatitis B vaccination through immunization with a Pre-

- S1/Pre-S2/S Vaccine. *Med. Microbiol. Immunol.* 204, 57–68. doi:10.1007/s00430-014-0374-x.
- Shytuhina, A., Pristatsky, P., He, J., Casimiro, D. R., Schwartz, R. M., Hoang, V. M., et al. (2014). Development and application of a reversed-phase high-performance liquid chromatographic method for quantitation and characterization of a Chikungunya virus-like particle vaccine. *J. Chromatogr. A* 1364, 192–197. doi:10.1016/j.chroma.2014.05.087.
- Sominskaya, I., Skrastina, D., Petrovskis, I., Dishlers, A., Berza, I., Mihailova, M., et al. (2013). A VLP Library of C-Terminally Truncated Hepatitis B Core Proteins: Correlation of RNA Encapsidation with a Th1/Th2 Switch in the Immune Responses of Mice. *PLoS One* 8, 1–13. doi:10.1371/journal.pone.0075938.
- Spannaus, R., Miller, C., Lindemann, D., and Bodem, J. (2017). Purification of foamy viral particles. *Virology* 506, 28–33. doi:10.1016/j.virol.2017.03.005.
- Steppert, P., Mosor, M., Stanek, L., Burgstaller, D., Palmberger, D., Preinsperger, S., et al. (2022). A scalable, integrated downstream process for production of a recombinant measles virus-vectored vaccine. *Vaccine* 40, 1323–1333. doi:10.1016/j.vaccine.2022.01.004.
- Strods, A., Ose, V., Bogans, J., Cielens, I., Kalnins, G., Radovica, I., et al. (2015). Preparation by alkaline treatment and detailed characterisation of empty hepatitis B virus core particles for vaccine and gene therapy applications. *Sci. Rep.* 5, 1–16. doi:10.1038/srep11639.
- Tan, W. S., Dyson, M. R., and Murray, K. (2003). Hepatitis B virus core antigen: Enhancement of its production in *Escherichia coli*, and interaction of the core particles with the viral surface antigen. *Biol. Chem.* 384, 363–371. doi:10.1515/BC.2003.042.
- Tariq, H., Batool, S., Asif, S., Ali, M., and Abbasi, B. H. (2022). Virus-Like Particles: Revolutionary Platforms for Developing Vaccines Against Emerging Infectious Diseases. *Front. Microbiol.* 12. doi:10.3389/fmicb.2021.790121.
- Taylor, S., Wakem, M., Dijkman, G., Alsarraj, M., and Nguyen, M. (2010). A practical approach to RT-qPCR-Publishing data that conform to the MIQE guidelines. *Methods* 50, S1. doi:10.1016/j.ymeth.2010.01.005.
- Teo, S. P. (2022). Review of COVID-19 mRNA Vaccines: BNT162b2 and mRNA-1273. *J. Pharm. Pract.* 35, 947–951. doi:10.1177/08971900211009650.
- Toni, L. S., Garcia, A. M., Jeffrey, D. A., Jiang, X., Stauffer, B. L., Miyamoto, S. D., et al. (2018). Optimization of phenol-chloroform RNA extraction. *MethodsX* 5, 599–608. doi:10.1016/j.mex.2018.05.011.
- Vafina, G., Zainutdinova, E., Bulatov, E., and Filimonova, M. N. (2018). Endonuclease from gram-negative bacteria *Serratia marcescens* is as

- effective as pulmozyme in the hydrolysis of DNA in sputum. *Front. Pharmacol.* 9, 1–8. doi:10.3389/fphar.2018.00114.
- Valentic, A., Böhner, N., and Hubbuch, J. (2024). Absolute Quantification of Hepatitis B Core Antigen (HBcAg) Virus-like Particles and Bound Nucleic Acids. *Viruses*. doi:10.3390/v16010013.
- Valentic, A., and Hubbuch, J. (2024). Effective removal of host cell-derived nucleic acids bound to hepatitis B core antigen virus-like particles by heparin chromatography. 1–15. doi:10.3389/fbioe.2024.1475918.
- Valentic, A., Müller, J., and Hubbuch, J. (2022). Effects of Different Lengths of a Nucleic Acid Binding Region and Bound Nucleic Acids on the Phase Behavior and Purification Process of HBcAg Virus-Like Particles. *Front. Bioeng. Biotechnol.* 10, 1–11. doi:10.3389/fbioe.2022.929243.
- Vanladschoot, P., Van Houtte, F., Serruys, B., and Leroux-Roels, G. (2005). The arginine-rich carboxy-terminal domain of the hepatitis B virus core protein mediates attachment of nucleocapsids to cell-surface-expressed heparan sulfate. *J. Gen. Virol.* 86, 75–84. doi:10.1099/vir.0.80580-0.
- Venkatakrishnan, B., and Zlotnick, A. (2016). The Structural Biology of Hepatitis B Virus: Form and Function. *Annu. Rev. Virol.* 3, 429–451. doi:10.1146/annurev-virology-110615-042238.
- Wang, Y. S., Kumari, M., Chen, G. H., Hong, M. H., Yuan, J. P. Y., Tsai, J. L., et al. (2023). mRNA-based vaccines and therapeutics: an in-depth survey of current and upcoming clinical applications. *J. Biomed. Sci.* 30, 1–35. doi:10.1186/s12929-023-00977-5.
- Wingfield, L. K., and Atcharawiriyakul, J. (2021). Evaluation of simple and rapid dna extraction methods for molecular identification of fungi using the internal transcribed spacer regions. *Asia-Pacific J. Sci. Technol.* 26, 1–7.
- Wingfield, P. T., Stahl, S. J., Williams, R. W., and Steven, A. C. (1995). Hepatitis Core Antigen Produced in Escherichia Coli: Subunit Composition, Conformation Analysis, and in Vitro Capsid Assembly. *Biochemistry* 34, 4919–4932. doi:10.1021/bi00015a003.
- Winkle, M., El-Daly, S. M., Fabbri, M., and Calin, G. A. (2021). Noncoding RNA therapeutics — challenges and potential solutions. *Nat. Rev. Drug Discov.* 20, 629–651. doi:10.1038/s41573-021-00219-z.
- Wright, J. J., Lee, S., Zaikova, E., Walsh, D. A., and Hallam, S. J. (2009). DNA Extraction from 0.22  $\mu$ M Sterivex Filters and Cesium Chloride Density Gradient Centrifugation. *J. Vis. Exp.* (31), e1352. doi:10.3791/1352.
- Wynne, S. A., Crowther, R. A., and Leslie, A. G. W. (1999). The crystal structure of the human hepatitis B virus capsid. *Mol. Cell* 3, 771–780. doi:10.1016/S1097-2765(01)80009-5.
- Xu, L., and Anchordoquy, T. (2011). Drug delivery trends in clinical trials and

- translational medicine: Challenges and opportunities in the delivery of nucleic acid-based therapeutics. *J. Pharm. Sci.* 100, 38–52. doi:10.1002/jps.22243.
- Xue, H., Guo, P., Wen, W.-C., and Wong, H. (2015). Lipid-Based Nanocarriers for RNA Delivery. *Curr. Pharm. Des.* 21, 3140–3147. doi:10.2174/1381612821666150531164540.
- Yan, D., Wei, Y. Q., Guo, H. C., and Sun, S. Q. (2015). The application of virus-like particles as vaccines and biological vehicles. *Appl. Microbiol. Biotechnol.* 99, 10415–10432. doi:10.1007/s00253-015-7000-8.
- Yoon, K. Y., Tan, W. S., Tey, B. T., Lee, K. W., and Ho, K. L. (2013). Native agarose gel electrophoresis and electroelution: A fast and cost-effective method to separate the small and large hepatitis B capsids. doi:10.1002/elps.201200257.
- Yuan, Y., Shane, E., and Oliver, C. N. (1998). Reversed-phase high-performance liquid chromatography of virus-like particles. 816, 21–28.
- Zdanowicz, M., and Chroboczek, J. (2016). Virus-like particles as drug delivery vectors. *Acta Biochim. Pol.* 63, 469–473. doi:10.18388/abp.2016\_1275.
- Zhang, B., Yin, S., Wang, Y., Su, Z., and Bi, J. (2021a). Cost-effective purification process development for chimeric hepatitis B core (HBc) virus-like particles assisted by molecular dynamic simulation. *Eng. Life Sci.* 21, 438–452. doi:10.1002/elsc.202000104.
- Zhang, Y., Liu, Y., Zhang, B., Yin, S., Li, X., and Zhao, D. (2021b). In vitro preparation of uniform and nucleic acid free hepatitis B core particles through an optimized disassembly- purification-reassembly process. *Protein Expr. Purif. Protein Ex.* doi:10.1016/j.pep.2020.105747.
- Zhao, H., Zhou, X., and Zhou, Y. H. (2020). Hepatitis B vaccine development and implementation. *Hum. Vaccines Immunother.* 16, 1533–1544. doi:10.1080/21645515.2020.1732166.
- Zhao, Q., Allen, M. J., Wang, Y., Wang, B., Wang, N., Shi, L., et al. (2012a). Disassembly and reassembly improves morphology and thermal stability of human papillomavirus type 16 virus-like particles. *Nanomedicine Nanotechnology, Biol. Med.* 8, 1182–1189. doi:10.1016/j.nano.2012.01.007.
- Zhao, Q., Modis, Y., High, K., Towne, V., Meng, Y., Wang, Y., et al. (2012b). Disassembly and reassembly of human papillomavirus virus-like particles produces more virion-like antibody reactivity. *Virol. J.* 9. doi:10.1186/1743-422X-9-52.
- Zhong, Z., Mc Cafferty, S., Combes, F., Huysmans, H., De Temmerman, J., Gitsels, A., et al. (2018). mRNA therapeutics deliver a hopeful message. *Nano Today* 23, 16–39. doi:10.1016/j.nantod.2018.10.005.
- Zhou, J., and Rossi, J. (2017). Aptamers as targeted therapeutics: Current

- potential and challenges. *Nat. Rev. Drug Discov.* 16, 181–202. doi:10.1038/nrd.2016.199.
- Zhou, L.-Y., Qin, Z., Zhu, Y.-H., He, Z.-Y., and Xu, T. (2019). Current RNA-based Therapeutics in Clinical Trials. *Curr. Gene Ther.* 19, 172–196. doi:10.2174/1566523219666190719100526.
- Zlotnick, A., Cheng, N., Conway, J. F., Booy, F. P., Steven, A. C., Stahl, S. J., et al. (1996). Dimorphism of hepatitis B virus capsids is strongly influenced by the C-terminus of the capsid protein. *Biochemistry* 35, 7412–7421. doi:10.1021/bi9604800.
- Zlotnick, A., Cheng, N., Stahl, S. J., Conway, J. F., Steven, A. C., and Wingfield, P. T. (1997). Localization of the C terminus of the assembly domain of hepatitis B virus capsid protein: Implications for morphogenesis and organization of encapsidated RNA. *Proc. Natl. Acad. Sci. U. S. A.* 94, 9556–9561. doi:10.1073/pnas.94.18.9556.
- Zollner, A. M., Ruiz, L. G., Mayer, V., Stohl, S., Jakob, L. A., Lingg, N., et al. (2024). Heparin-affinity chromatography is a generic purification platform for chimeric. *Sep. Purif. Technol.*, 126673. doi:10.1016/j.seppur.2024.126673.



## Abbreviations

(NH <sub>4</sub> ) <sub>2</sub> SO <sub>4</sub>	ammonium sulfate
ACN	acetonitrile
ASOs	antisense oligonucleotides
CC	CaptoCore 400
DLS	dynamic light scattering
DMD	Duchenne muscular dystrophy
DNA	deoxyribonucleic acid
DSP	downstream processing
DTT	dithiothreitol
DV	diafiltration volumes
<i>E. coli</i>	<i>Escherichia coli</i>
HBcAg	hepatitis B core antigen
HBV	hepatitis B virus
HCP	host cell protein
HPLC	high-performance liquid chromatography
HPV	human papillomavirus
IEX	ion exchange chromatography
mRNA	messenger ribonucleic acid
NA	nucleic acid
NA <sub>hc</sub>	host cell-derived nucleic acid
NA <sub>ther</sub>	therapeutic nucleic acid
NAGE	native agarose gel electrophoresis
ON	oligonucleotide
PCR	polymerase chain reaction
PEG	polyethylene glycole
qPCR	quantitative PCR
RISC	RNA-induced silencing complex
RNA	ribonucleic acid
RNAi	RNA interference
RP	reversed-phase
RSD	relative standard deviation
SC	spin column
SDS-PAGE	sodium dodecyl sulfate-polyacrylamide gel electrophoresis
SEC	size-exclusion chromatography
siRNA	small interfering RNA
SMA	spinal muscular atrophy
TEM	transmission electron microscopy

## Abbreviations

---

UV/Vis	ultraviolet and visible
VLP	virus-like particle

## Appendix A: Supplementary Material for Chapter 3

### S3.1 Oligonucleotides for Plasmid Cloning

The plasmids coding for Cp154, Cp157, Cp164 and Cp167 were made by modification of the pET11c plasmid coding Cp149. Regions encoding for the Cp149 on the pET11-based vector were amplified using overlapping oligonucleotides to introduce site-directed mutagenesis using the polymerase chain reaction. The wild-type HBcAg Cp183 was obtained by amplifying the Cp167 plasmid in the same manner. The forward and reverse primers used for the PCR reaction for the production of the different constructs, respectively, can be found in the Table S3.1.

Table S3.1 Overlapping oligonucleotides used for site-directed mutagenesis amplification used for the production of the different constructs

Primers	Overlapping oligonucleotides 5'- → -3'
<b>Cp154 forward</b>	AGGCGAAGAGGTCGTTAGGATCCGGCTGCTAACAAAG CCCGAAA
<b>Cp154 reverse</b>	AGGGAAGAGGTCGTTAGAACAACCGTAGTCTCCGGAA GTGTC
<b>Cp157 forward</b>	AGGCGAAGAGGTCGTTGCCCCGGTAGGATCCGGCTGC TAACAAAGCCCGAAA
<b>Cp157 reverse</b>	AGGCGAAGAGGTCGTTGCCCCGGAACAACCGTAGTCT CCGGAAGTGTC
<b>Cp164 forward</b>	TCGCCCCGGAGACGCACGCCCTCGCCCCGTTAGGGATC CGGCTGCTAACAAAGCCCGAA
<b>Cp164 reverse</b>	AGGCGAAGAGGTCGTTGCCCCGGAGACGCACGCCCTC GCCCCGTTAGAACAACCGTAGTCTCCGGAAGTGTC
<b>Cp167 forward</b>	AGGCGAAGAGGTCGTTGCCCCGGAGACGCACGCCCTC GCCCCGTAGGCGAAGATAGGATCCGGCTGCTAACAAA GCCCGAA
<b>Cp167 reverse</b>	AGGCGAAGAGGTCGTTGCCCCGGAGACGCACGCCCTC GCCCCGTAGGCGAAGAAACAACCGTAGTCTCCGGAAGT GTC

<b>Cp183 forward</b>	CGCCGACGTTTCGCAGTCACGGGAGAGCCAATGCTAGGA TCCGGCTGCTAACAAAGCCC
<b>Cp183 reverse</b>	TGACTGCGAACGTCGGCGGCGAGGACTTTGTGATCTTC GCCTACGGGGCGAGGGCGTG

### S3.2 SEC analysis

Size-exclusion chromatography (SEC) coupled with a diode array detector was used to evaluate the phase behaviour of the VLPs by quantifying and specifying differently sized species (dimers, capsids, aggregates) and determine the loading of the VLPs with nucleic acids. A typical chromatogram is shown in Figure S3.1. For samples after the disassembly reaction three main peaks were detected. Peak 1 was defined as aggregates, Peak 2 as HBcAg capsids and Peak 3 as HBcAg dimers. For the calculation of the dimer yield additionally control runs at the high-performance liquid chromatography system without a prefilter and column were performed to determine the amount of bigger aggregates that cannot appear in the SEC chromatogram due to their size. For the analysis of the loading, Peak 2 at 280 nm and 260 nm was consulted to calculate the A260/A280 coefficient.

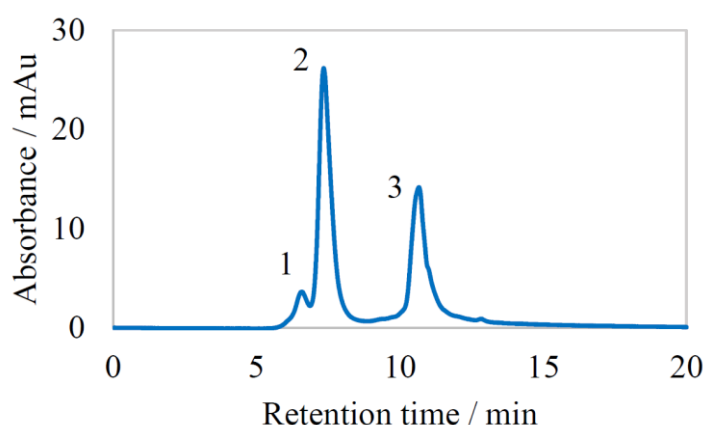


Figure S3.1 Size exclusion chromatography chromatogram VLP solution showing absorbance at 280 nm over retention time. Peak 1 represents VLP aggregates, peak 2 VLP capsids and peak 3 dimers; SEC, size-exclusion chromatography; VLP, virus-like particle

A detailed investigation of the re-dissolution behaviour similarly to the disassembly experiments was not found to be practicable, because a precise analysis of the individual components, especially the determination of the dimer content, were unfeasible due to impurities with the similar size giving overlapping chromatography peaks with the analytical setup used in this study.

### S3.3 Results of Western Blot Analysis

The expression of the constructs Cp149, Cp154, Cp157, Cp164, Cp167 and Cp183 was verified by Western Blot analysis. Results are displayed in Figure S3.2.

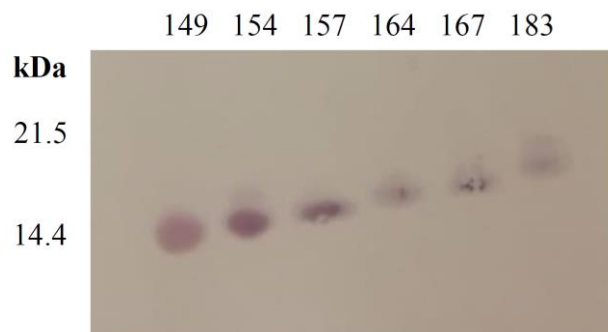
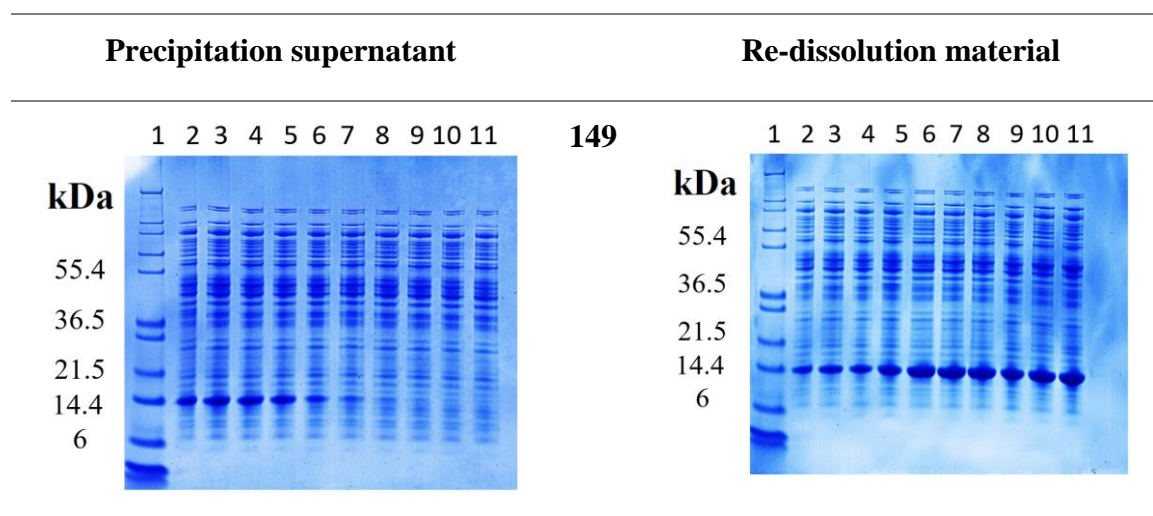


Figure S3.2 Scan of Western Blot analysis. Re-dissolved VLPs were analysed by SDS-PAGE and transferred onto a nitrocellulose membrane. As primary antibody an anti-HBcAg antibody was used, followed by an anti-mouse; HBcAg, Hepatitis B core Antigen

### S3.4 SDS-PAGE Scans for Precipitation and Re-dissolution experiments

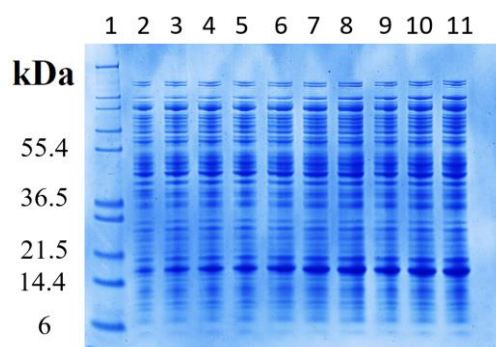
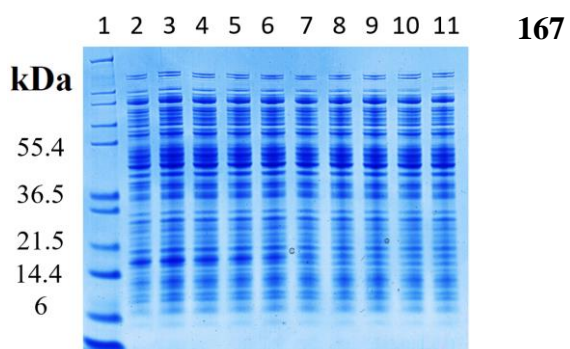
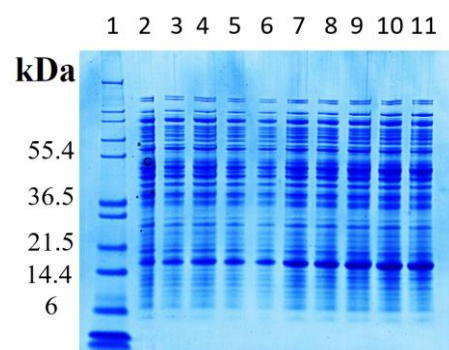
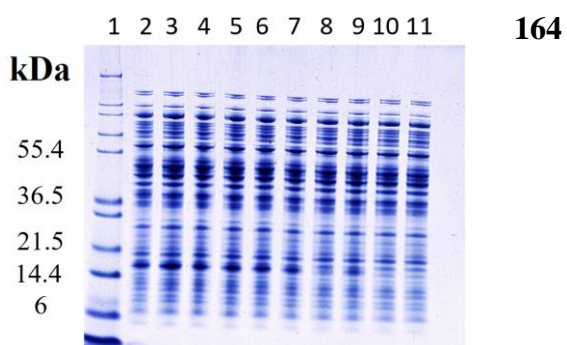
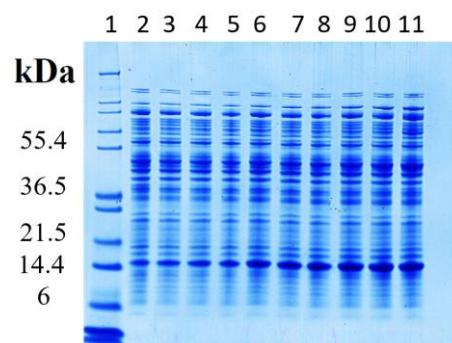
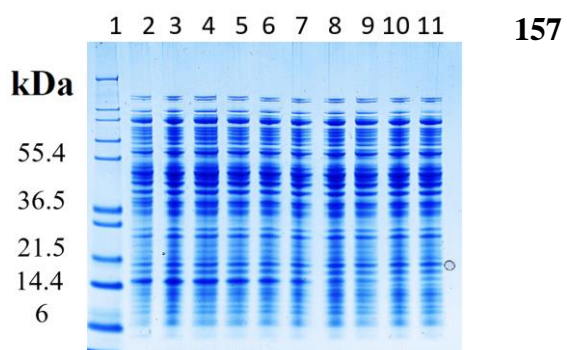
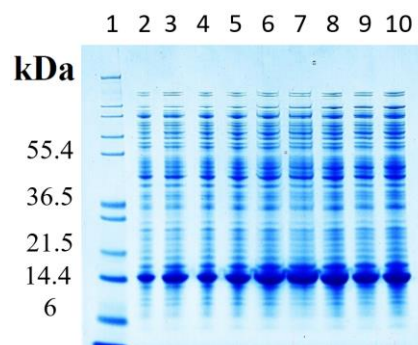
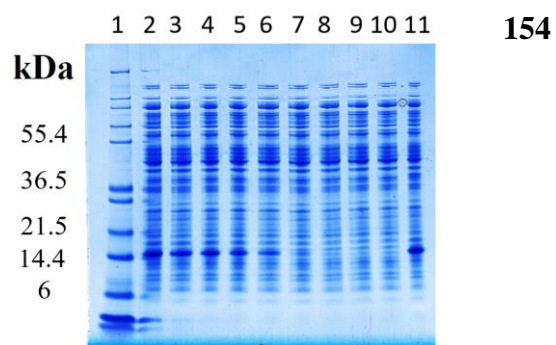
To investigate the precipitation behavior of the VLP constructs, ammonium sulfate concentrations from 0.75 M up to 1.15 M were examined. After the precipitation reaction, the supernatant was analysed for the remaining VLPs as well as the respective re-dissolution material for precipitated and re-dissolved VLPs by SDS-PAGE. The corresponding gel images can be found in the Table S3.2.

Table S3.2 SDS-PAGE scans of the supernatant after precipitation (left column) and the respective re-dissolution material (right column) for. Protein standard in lane 1, and samples for ammonium sulfate concentrations from 0.75 M up to 1.15 M in lanes 2 to 11, respectively. For re-dissolved Cp 154 lane 11 with 1.15 M is missing on the gel.

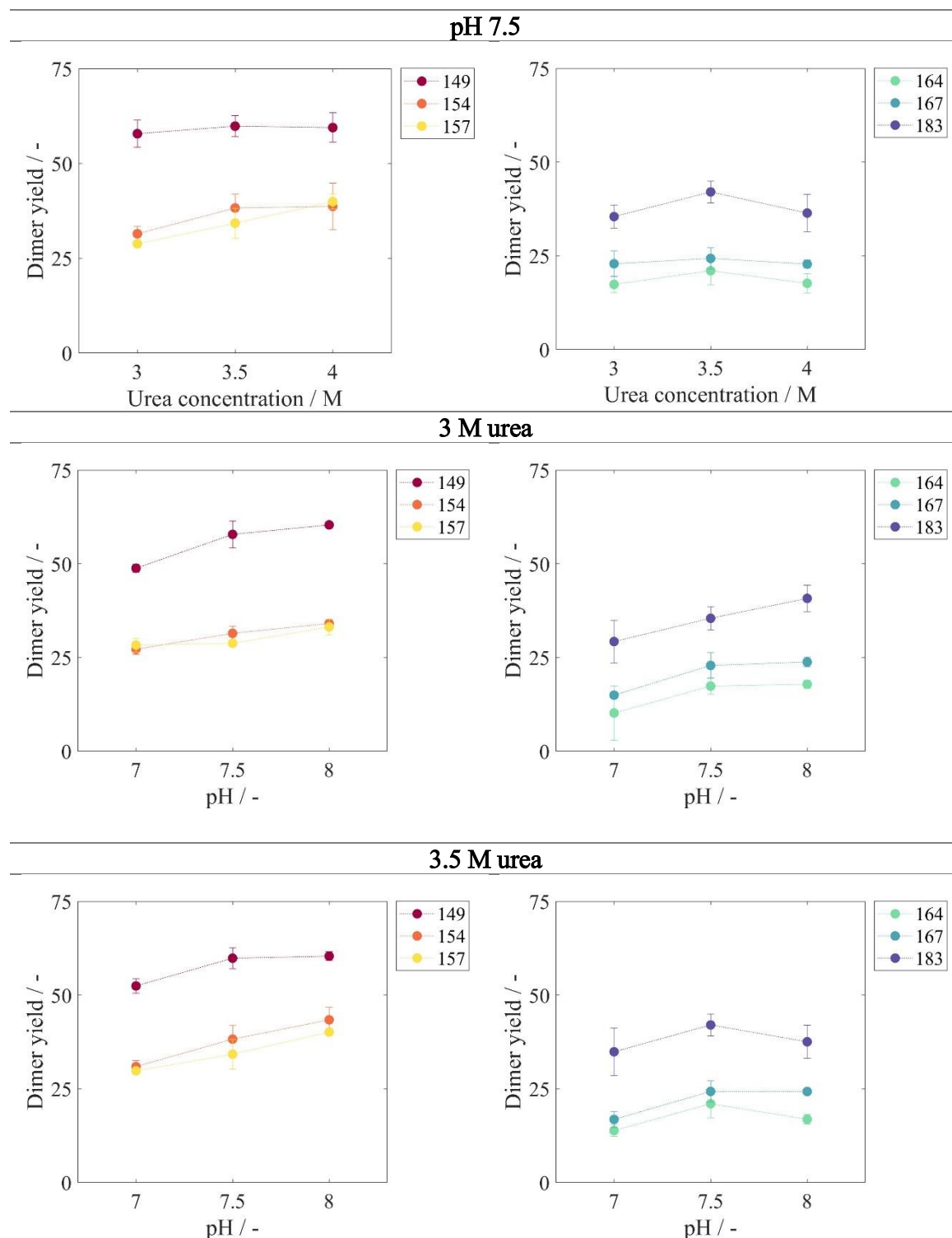


**Precipitation supernatant**

**Re-dissolution material**









## Appendix B: Supplementary Material for Chapter 4

### S4.1 Components of flow-through fraction of silica-SC based extraction of the EasyPure Kit on NAGE

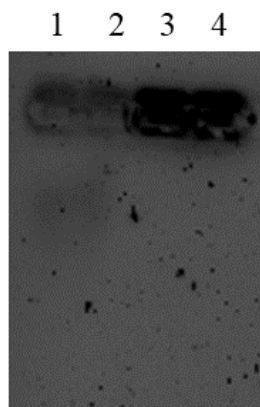


Figure S4.1 Components of flow-through fraction of silica-SC based extraction of the EasyPure Kit on NAGE. In lane 1 proteinase K, lane 2 binding buffer 5, lane 3 Tris buffer and lane 4 ethanol. NAGE: native agarose gel electrophoresis; SC: spin column

### S4.2 Remaining protein impurities in the extracts after silica-SC based extraction for de novo extractions of CC purified Cp164 VLP

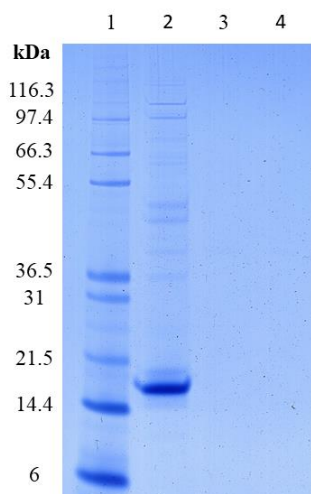


Figure S4.2 Remaining protein impurities in the extracts after silica-SC based extraction for de novo extractions of CC purified Cp164 VLP with the lysis time of 60 min (lane 3 and 4) on SDS-PAGE for diluted Cp164. Marker in lane 1 and initial Cp164 VLP sample before silica-based extraction in lane 2. CC: CaptoCore 400; SC: spin column; VLP: virus-like particle

### S4.3 Recoveries for preliminary experiments with varying silica-SC based extraction procedures

Table S4.1 Recoveries for preliminary experiments with varying silica-SC based extraction elution procedures, different loads, using Cp157, Cp164 HBcAg VLP constructs and dsDNA, and PicoGreen, RiboGreen assay and qPCR. HBcAg: Hepatitis B core Antigen; VLP: virus-like particle

Elution procedure	Construct / NA	Quantification by	Load [ $\mu$ g]	Recovery [%]
2 x 25 $\mu$ L	Cp164	RiboGreen	0.275	11.89
4 x 25 $\mu$ L	Cp164	RiboGreen	0.275	31.74
8 x 25 $\mu$ L	Cp164	RiboGreen	0.275	53.18
4 x 25 $\mu$ L	Cp157	PicoGreen	1.929	72.61
4 x 25 $\mu$ L	Cp157	PicoGreen	1.929	73.18
4 x 25 $\mu$ L	Cp157	PicoGreen	1.929	72.46
4 x 25 $\mu$ L	dsDNA	RiboGreen / qPCR	1.139 (RiboGreen) / 0.837 (qPCR)	61.67 / 60.28 (qPCR)
4 x 25 $\mu$ L	dsDNA	RiboGreen / qPCR	1.139 (RiboGreen) / 0.837 (qPCR)	67.61 / 55.22 (qPCR)
4 x 25 $\mu$ L	dsDNA	RiboGreen / qPCR	1.139 (RiboGreen) / 0.837 (qPCR)	67.17 / 70.36 (qPCR)
4 x 25 $\mu$ L	Cp157	RiboGreen	0.814	70.99
8 x 25 $\mu$ L	Cp157	RiboGreen	0.814	71.03
1 x 200 $\mu$ L	Cp157	RiboGreen	0.814	77.78

1 x 200 µL	Cp157	RiboGreen	4.67	92.69
1 x 200 µL	Cp157	RiboGreen	2.80	85.21
1 x 200 µL	Cp157	RiboGreen	1.40	81.04
1 x 200 µL	Cp157	RiboGreen	0.47	54.68
1 x 200 µL	dsDNA	qPCR	3.12	85.64
1 x 200 µL	dsDNA	qPCR	1.87	85.29
1 x 200 µL	dsDNA	qPCR	0.94	20.59
1 x 200 µL	dsDNA	qPCR	0.31	64.43

#### S4.4 Nucleic acid concentrations for Cp157 without and with preliminary silica-SC based extraction and respective standard and relative standard deviation

Table S4.2 Nucleic acid concentrations for Cp157 without and with preliminary silica-SC based extraction and respective standard and relative standard deviation for performed PicoGreen and RiboGreen assay.

Quantification sample details	PicoGreen / RiboGreen		
	Concentration in ng/µL	Mass in µg	relative standard deviation [-]
VLP without extraction	$2.18 \pm 0.93 / 5.52 \pm 2.55$	0.44 / 1.10	42.64 / 46.13
VLP with extraction	$1.38 \pm 0.13 / 9.65 \pm 0.24$	0.14 / 0.96	9.08 / 2.51
Recovery extraction #1	$1.54 \pm 0.22 / 14.01 \pm 2.73$	0.15 / 1.40	14.43 / 19.49
Recovery extraction #2	$1.63 \pm 0.14 / 14.12 \pm 0.26$	0.16 / 1.41	8.58 / 1.87
Recovery extraction #2	$1.45 \pm 0.24 / 13.98 \pm 0.98$	0.15 / 1.40	16.78 / 7.01

### S4.5 HPLC columns and mobile phase B screen in preliminary experiments for the RP based extraction and quantification

Table S4.3 HPLC columns and mobile phases B (A: water + TFA for every condition) of screened in preliminary experiments for the RP based extraction and quantification of HBcAg VLP proteins and bound nucleic acids. HPLC: high performance liquid chromatography; TFA: trifluoroacetic acid; VLP: virus-like particle

HPLC column	Mobile phase B (+ TFA)	% B in binding condition	Outcome
TSKgel Protein C4-300 (3 $\mu$ m, 4.6x150 mm) from Tosoh Bioscience	acetonitrile	5, 8, 10, 20, 40, 50	High resolution of proteins
	50% acetonitrile / 50% isopropanol	20	
	25% acetonitrile / 75% isopropanol	5, 10, 20, 40, 50	
	isopropanol	20	
BioSuite pPhenyl (10 $\mu$ m, 4.6x75 mm) from Waters	acetonitrile	5, 10, 20, 40, 50	Low recovery
TSKgel TMS-250 (10 $\mu$ m, 4.6x75 mm) from Tosoh Bioscience	acetonitrile	5	Low resolution, low recovery

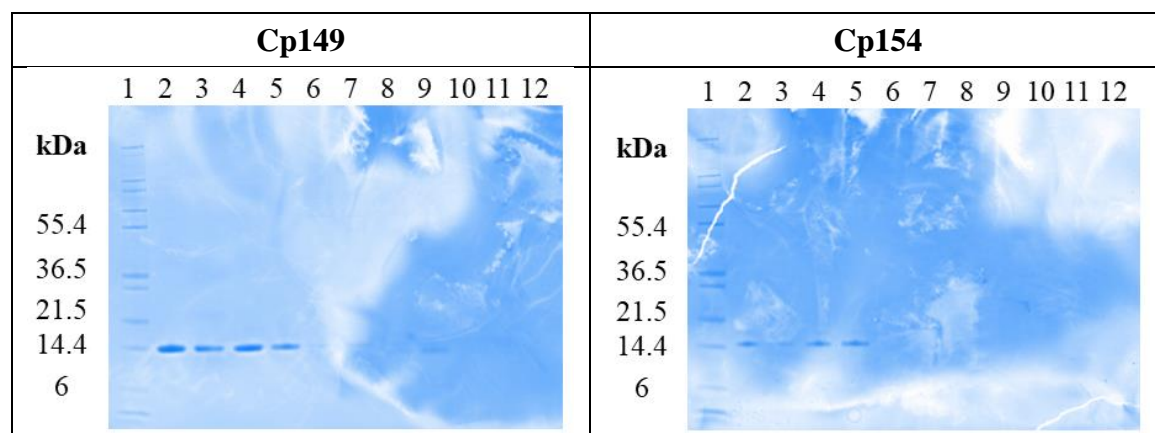
## Appendix C: Supplementary Material for Chapter 5

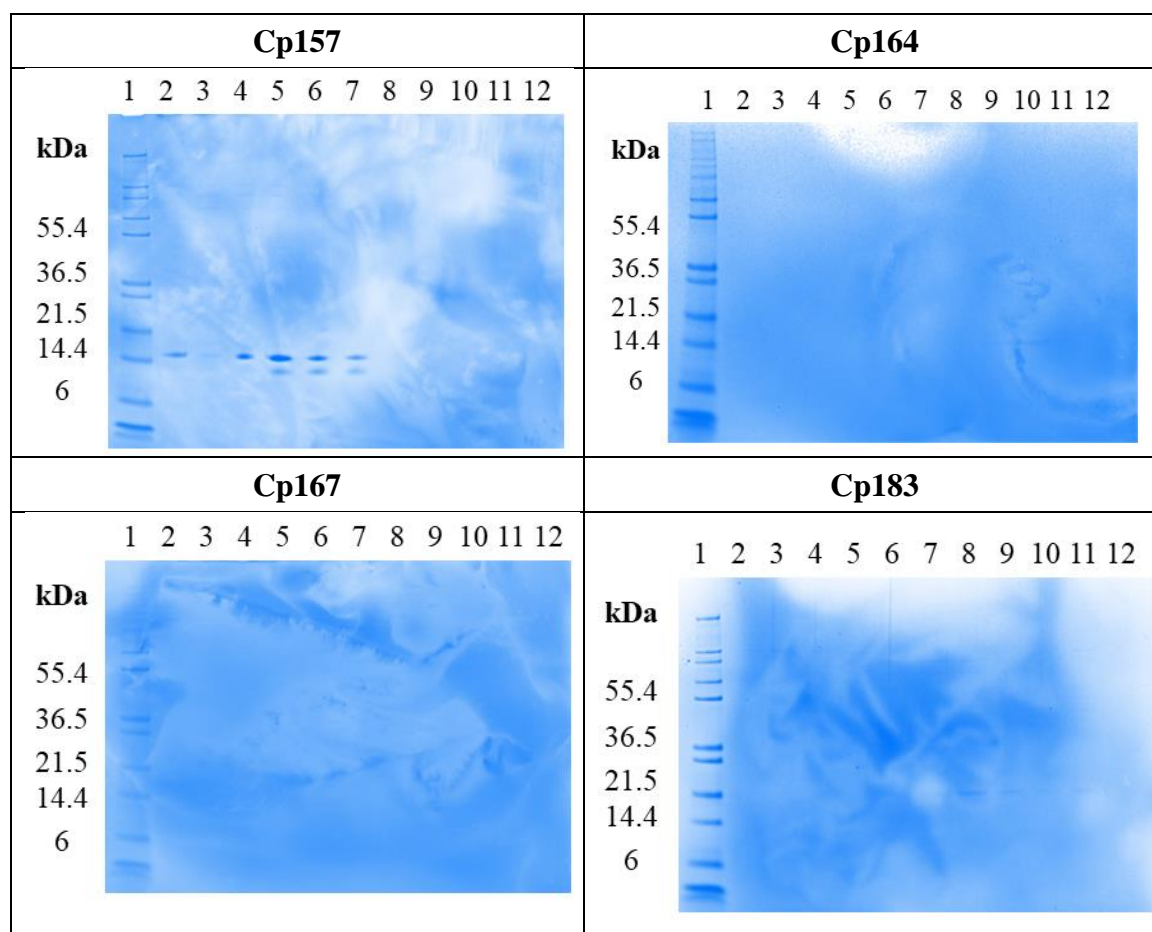
### S5.1 SDS-PAGE analysis of heparin chromatography for different HBcAg VLP constructs

Table S5.1 Overview samples investigated by SDS-PAGE for the different HBcAg VLP constructs during heparin chromatography. M: marker, I: initial sample, FT: flow-through, E: elution

Lane	1	2	3	4	5	6	7	8	9	10	11	12
Cp149	M	I	FT 1	FT 2	FT 3	E 1	E 2	E 3	E 4	-	-	-
Cp154	M	I	FT 1	FT 2	FT 3	E 1	E 2	E 3	E 4	-	-	-
Cp157	M	I	E 1	E 2	E 3	E 4	E 5	FT 1	FT 2	FT 3	FT 4	FT 5
Cp164	M	I	FT 1	FT 2	FT 3	FT 4	E 1	E 2	E 3	E 4	-	-
Cp167	M	I	FT 1	FT 2	FT 3	FT 4	E 1	-	E 2	-	E 3	E 4
Cp183	M	FT 1	FT 2	FT 3	FT 4	E 1	E 2	E 3	E 4	E 5	I	-

Table S5.2 Gel scans of SDS-PAGE analysis of flow-through and elution fractions of heparin chromatography of HBcAg VLP constructs Cp149, Cp154, Cp157, Cp164, Cp167, and Cp183.




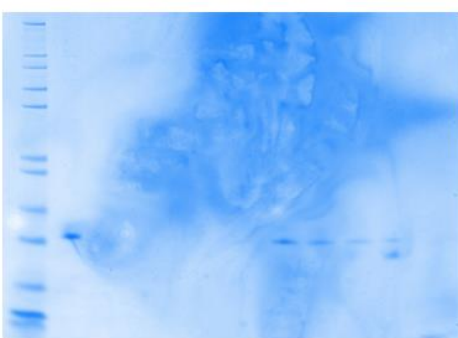
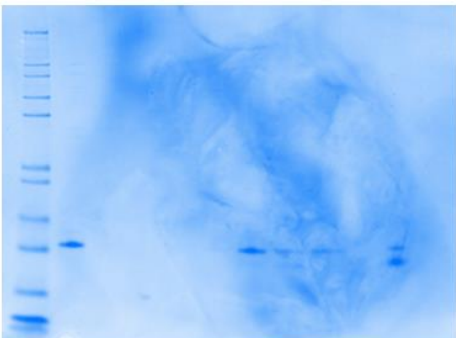
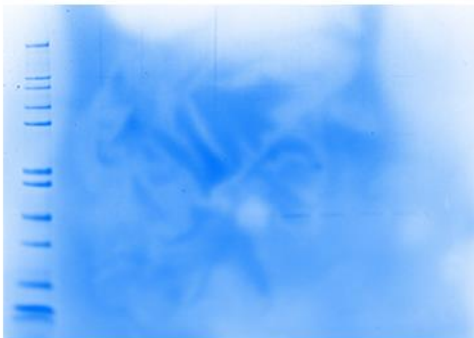
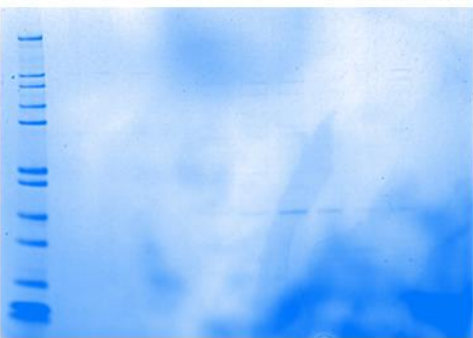



## S5.2 SDS-PAGE analysis of heparin and sulfate chromatography with and without prior nuclease treatment

Table S5.3 Overview of samples investigated by SDS-PAGE for HBcAg VLP constructs Cp157 and Cp183 and heparin and sulfate chromatography with and without prior nuclease treatment. M: marker, I: initial sample, FT: flow-through, E: elution, +: with nuclease treatment

Lane	1	2	3	4	5	6	7	8	9	10	11	12
Cp157 Heparin with nuclease	M	I	E 1	E 2	E 3	E 4	E5	FT 1	FT 2	FT 3	FT 4	FT 5
Cp157 Sulfate without nuclease	M	I	FT 1	FT 2	FT 3	FT 4	E 1	E 2	E 3	E 4	W	-
Cp157 Sulfate with nuclease	M	I	FT 1	FT 2	FT 3	E 1	E 2	E 3	E 4	-	W	-
Cp183 Heparin without nuclease	M	FT 1	FT 2	FT 3	FT 4	E 1	E 2	E 3	E 4	E 5	I	-
Cp183 Heparin with nuclease	M	FT 1	FT 2	FT 3	FT 4	E 1	E 2	E 3	E 4	E 5	I	-
Cp183 Sulfate with (+) / without nuclease	M	FT 1	FT 2	FT 3	E 1	E 2	E 3	FT 1 +	FT 2 +	FT 3 +	E 1 +	I

Table S5.4 Gel scans of SDS-PAGE analysis of flow-through and elution fractions of heparin and sulfate chromatography with and without prior nuclease treatment and HBcAg VLP constructs Cp157 and Cp183.

Cp157; heparin with nuclease													Cp157; sulfate without nuclease												
	1	2	3	4	5	6	7	8	9	10	11	12		1	2	3	4	5	6	7	8	9	10	11	12
kDa																									
Cp157; sulfate with nuclease													Cp183; Heparin without nuclease												
	1	2	3	4	5	6	7	8	9	10	11	12		1	2	3	4	5	6	7	8	9	10	11	12
kDa																									
Cp183; heparin with nuclease													Cp183; sulfate without/with (+) nuclease												
	1	2	3	4	5	6	7	8	9	10	11	12		1	2	3	4	5	6	7	8	9	10	11	12
kDa																									

### S5.3 SEC chromatograms and gel electrophoresis analysis of LiCl precipitation

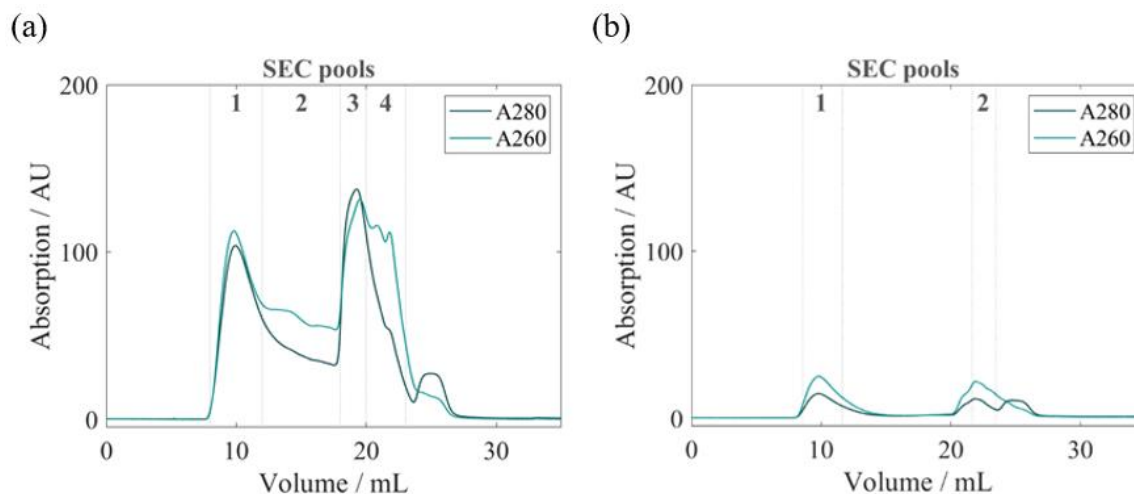


Figure S5.1 Chromatograms of the final SEC and fraction segmentation for analysis of host cell-derived nucleic acid removal by LiCl precipitation for (a) Cp157 and (b) Cp183.

Table S5.5 Overview of samples investigated by SDS-PAGE for HBcAg VLP constructs Cp157 and Cp183 during LiCl precipitation. M: marker, I: initial sample, C: after centrifugation, SEC: size-exclusion chromatography pools

Lane	1	2	3	4	5	6	7	8	9	10	11	12
Cp157	M	I	I	C	SEC 1	SEC 2	SEC 3	SEC 4	-	-	-	-
Cp183	M	I	I	C	SEC 1	SEC 2	-	-	-	-	-	-

Table S5.6 Gel scans of SDS-PAGE analysis of HBcAg VLP constructs Cp157 and Cp183 during LiCl precipitation.

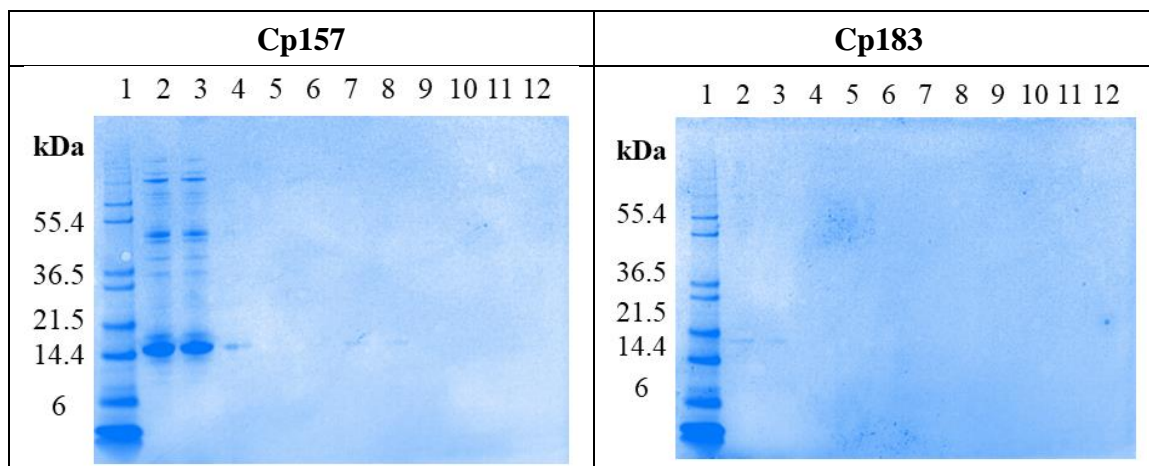




Table S5.7 Overview of samples investigated by NAGE for HBcAg VLP constructs Cp157 and Cp183 during LiCl precipitation. M: marker, I: initial sample, C: after centrifugation, SEC: size-exclusion chromatography pools

1	2	3	4	5	6	7	8	9	10	11	12	13
Cp157 I	Cp157 I	Cp157 C	Cp157 SEC 1	Cp157 SEC 2	Cp157 SEC 3	Cp157 SEC 4	-	Cp183 I	Cp183 I	Cp183 C	Cp183 SEC 1	Cp183 SEC 2

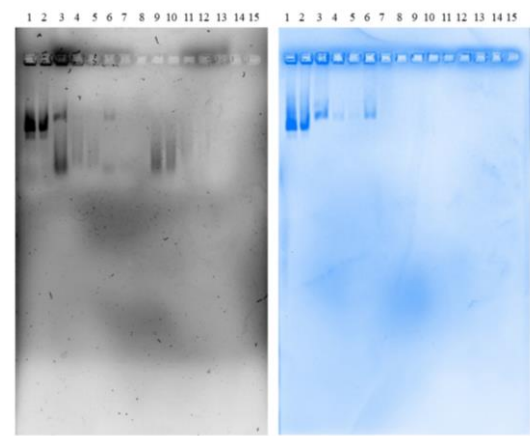


Figure S5.2 Gel scans of NAGE analysis of HBcAg VLP constructs Cp157 and Cp183 during LiCl precipitation by midori green (left) and Coomassie (right).

#### S5.4 SEC and gel electrophoresis analysis of alkaline treatment

Table S5.8 Overview of samples after dialysis in neutralization buffer investigated by SDS-PAGE for HBcAg VLP constructs Cp157 and Cp183 during alkaline treatment. M: marker, I: initial sample, w: with preliminary dialysis, w/o without preliminary dialysis

1	2	3	4	5	6	7	8	9
M	Cp157 I	Cp157 w treatment	Cp157 w/o treatment	-	Cp183 I	Cp183 w treatment	Cp183 w/o treatment	-

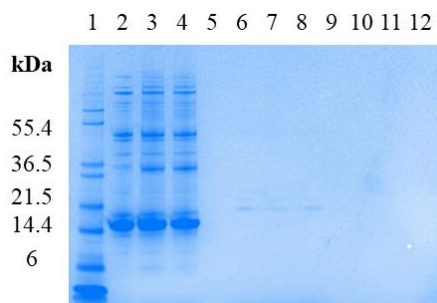


Figure S5.3 Gel scan of SDS-PAGE analysis of HBcAg VLP constructs Cp157 and Cp183 after dialysis in neutralization buffer during alkaline treatment.

Table S5.9 Overview of samples after dialysis in neutralization buffer investigated by NAGE for HBcAg VLP constructs Cp157 and Cp183 during alkaline treatment. M: marker, I: initial sample, w: with preliminary dialysis, w/o without preliminary dialysis

1	2	3	4	5	6	7	8
Cp157 I	Cp157 w treatment	Cp157 w/o treatment	-	Cp183 I	Cp183 w treatment	Cp183 w/o treatment	-

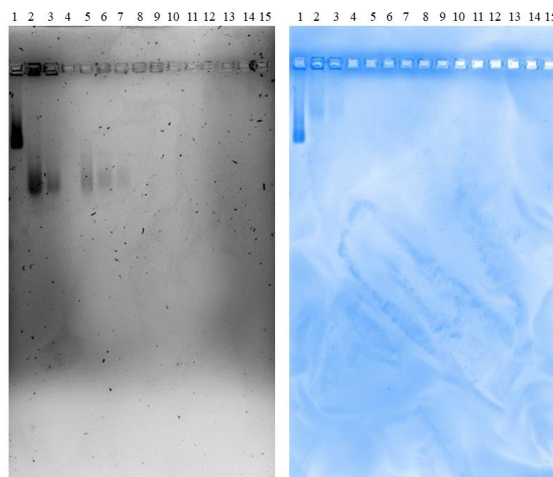


Figure S5.4 Gel scans of NAGE analysis of Cp157 and Cp183 samples after dialysis in neutralization buffer during alkaline treatment by midori green (left) and Coomassie (right).

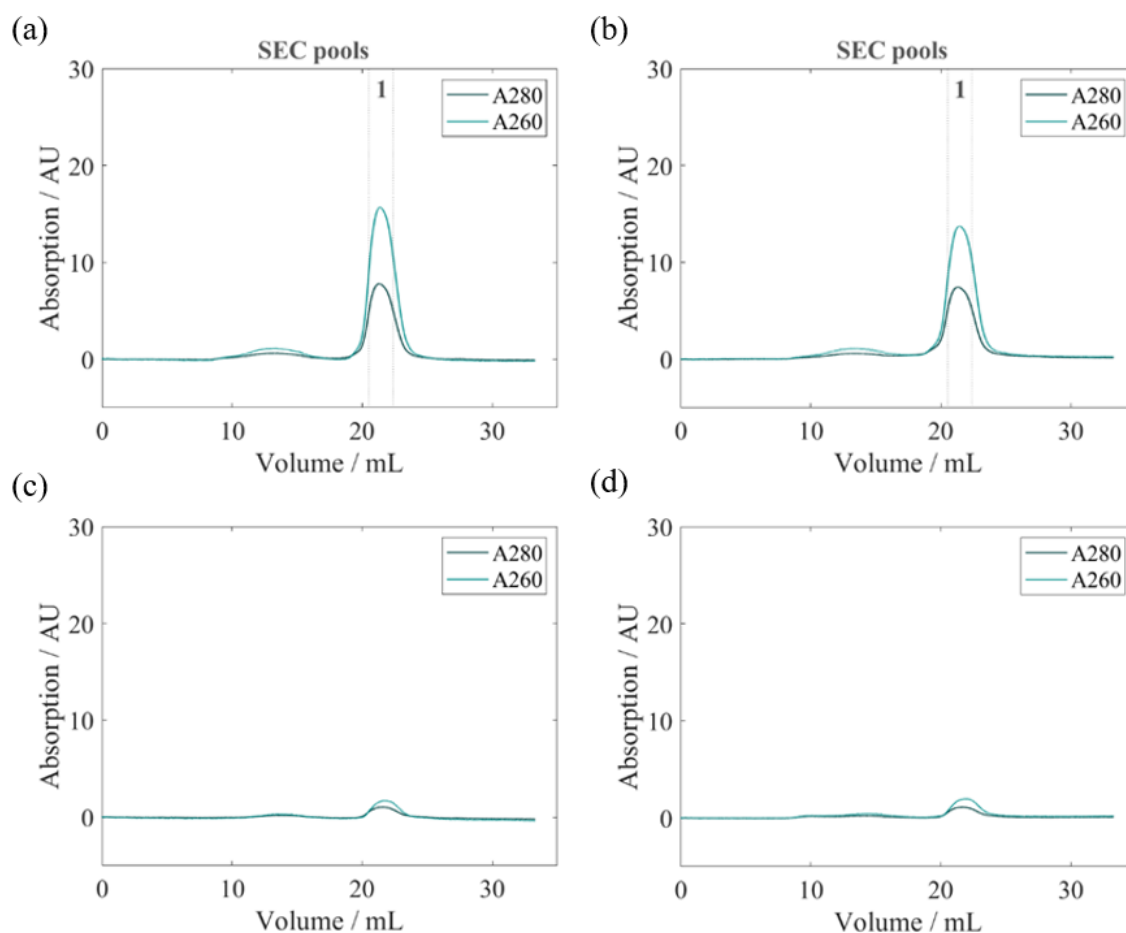


Figure S5.5 Chromatograms of the final SEC and fraction segmentation for analysis of host cell-derived nucleic acid removal by alkaline treatment for Cp157 with (a) and without (b), and Cp183 with (c) and without (d) preliminary dialysis.

Table S5.10 Overview of samples after re-dissolution and SEC fractions investigated by SDS-PAGE and NAGE for HBcAg VLP constructs Cp157 and Cp183 during alkaline treatment. M: marker, I: initial sample, w: with, w/o without, PT: preliminary treatment, RD: re-dissolution

1	2	3	4	5	6	7	8	9	10
Cp157 I	Cp157 w PT RD	Cp157 w/o PT RD	Cp157 w PT SEC 1	Cp157 w/o PT SEC 1	-	Cp183 I	Cp183 w PT RD	Cp183 w/o PT RD	-

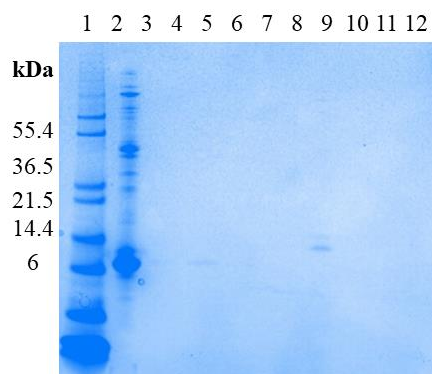


Figure S5.6 Gel scan of SDS-PAGE analysis of Cp157 and Cp183 samples after re-dissolution and SEC fractions during alkaline treatment.

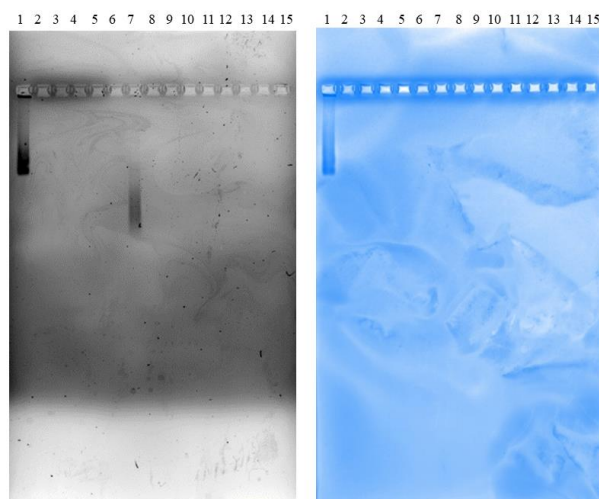


Figure S5.7 Gel scans of NAGE analysis Cp157 and Cp183 samples after re-dissolution and SEC fractions during alkaline treatment by midori green (left) and Coomassie (right).

## Appendix D: Supplementary Material for Chapter 6

### S6.1 Proportion of dimers, capsids and aggregates for HBcAg VLP constructs (a) Cp149 and (b) Cp157 during reassembly by centrifugal concentrators

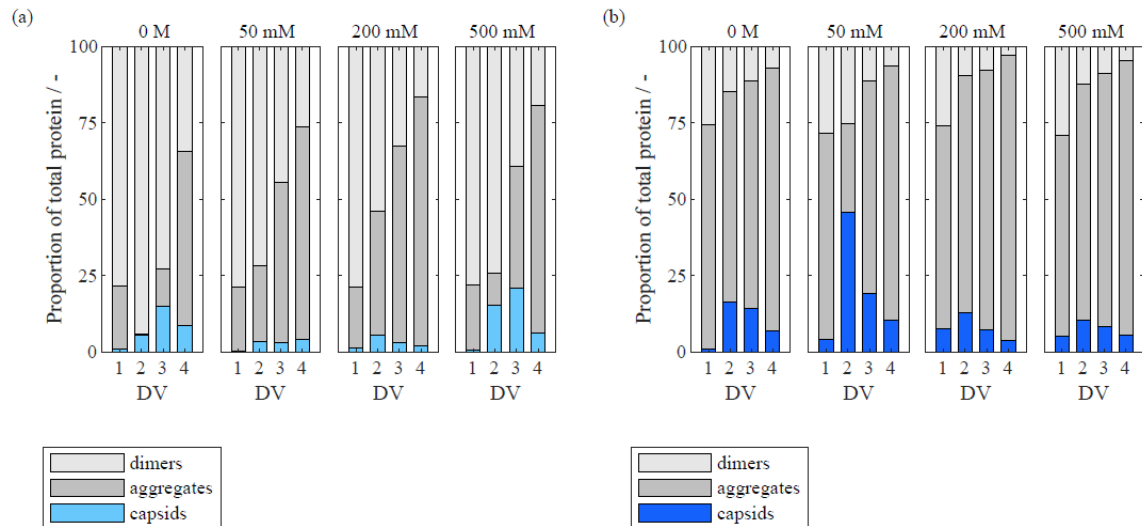


Figure S6.1 Proportion of dimers, capsids and aggregates for HBcAg VLP constructs (a) Cp149 and (b) Cp157 during reassembly by Vivaspin® centrifugal concentrators with 50 mM Tris, pH 7.2 buffer with different NaCl molarities in four diafiltrating steps. Constructs were mixed with DNA ON in a dimer/ON\_DNA ratio of 60. DV: diafiltration volume, HBcAg: hepatitis B core antigen, ON: oligonucleotide, VLP: virus-like particle

## S6.2 Overview of samples in lanes of NAGE analysis of HBcAg VLP constructs Cp149 and Cp157 during reassembly by centrifugal concentrators

Table S6.1 Overview of samples in lanes of NAGE analysis of HBcAg VLP constructs Cp149 (a, b, e, f, i, j) and Cp157 (c, d, g, h, k, l) during reassembly by Vivaspın® centrifugal concentrators with 50 mM Tris, pH 7.2 buffer with different NaCl molarities (0: 0 mM NaCl, 50: 50 mM NaCl, 200: 200 mM NaCl, 500: 500 mM NaCl) in four diafiltrating steps. Constructs were either mixed with dsDNA in a dimer/dsDNA ratio of 60 (a, b, d, e), mixed with ON\_DNA in a dimer/ON\_DNA ratio of 60 (e, f, g, h), or mixed with ON\_DNA in a dimer/ON\_DNA ratio of 2 (i, j, k, l). DV: diafiltration volume, I: initial VLP sample, M: marker, NA: nucleic acid, HBcAg: hepatitis B core antigen, ON: oligonucleotide, VLP: virus-like particle

Lane		1	2	3	4	5	6	7	8	9	10	11
<b>Cp149 + dsDNA (60)</b>	<b>a</b>	NA	I+ NA	-	0 DV 1	0 DV 2	0 DV 3	0 DV 4	50 DV 1	50 DV 2	50 DV 3	50 DV 4
	<b>b</b>	M	NA	I+ NA	200 DV 1	200 DV 2	200 DV 3	200 DV 4	500 DV 1	500 DV 2	500 DV 3	500 DV 4
<b>Cp157 + dsDNA (60)</b>	<b>c</b>	M	NA	I+ NA	0 DV 1	0 DV 2	0 DV 3	0 DV 4	50 DV 1	50 DV 2	50 DV 3	50 DV 4
	<b>d</b>	M	NA	I+ NA	200 DV 1	200 DV 2	200 DV 3	200 DV 4	500 DV 1	500 DV 2	500 DV 3	500 DV 4
<b>Cp149 + ON_DNA (60)</b>	<b>e</b>	I+ NA	0 DV 1	0 DV 2	0 DV 3	0 DV 4	50 DV 1	50 DV 2	50 DV 3	50 DV 4	-	-
	<b>f</b>	I+ NA	200 DV 1	200 DV 2	200 DV 3	200 DV 4	500 DV 1	500 DV 2	500 DV 3	500 DV 4	-	-
<b>Cp157 + ON_DNA (60)</b>	<b>g</b>	I+ NA	0 DV 1	0 DV 2	0 DV 3	0 DV 4	50 DV 1	50 DV 2	50 DV 3	50 DV 4	-	-
	<b>h</b>	I+ NA	200 DV 1	200 DV 2	200 DV 3	200 DV 4	500 DV 1	500 DV 2	500 DV 3	500 DV 4	-	-
<b>Cp149 + ON_DNA (2)</b>	<b>i</b>	I+ NA	I+ NA	0 DV 1	0 DV 2	0 DV 3	0 DV 4	50 DV 1	50 DV 2	50 DV 3	50 DV 4	-
	<b>j</b>	I+ NA	I+ NA	200 DV 1	200 DV 2	200 DV 3	200 DV 4	500 DV 1	500 DV 2	500 DV 3	500 DV 4	-
<b>Cp157 + ON_DNA (2)</b>	<b>k</b>	M	I+ NA	0 DV 1	0 DV 2	0 DV 3	0 DV 4	50 DV 1	50 DV 2	50 DV 3	50 DV 4	-
	<b>l</b>	M	I+ NA	200 DV 1	200 DV 2	200 DV 3	200 DV 4	500 DV 1	500 DV 2	500 DV 3	500 DV 4	-

### S6.3 Gel scans of NAGE analysis of HBcAg VLP constructs Cp149 and Cp157 during reassembly by centrifugal concentrators

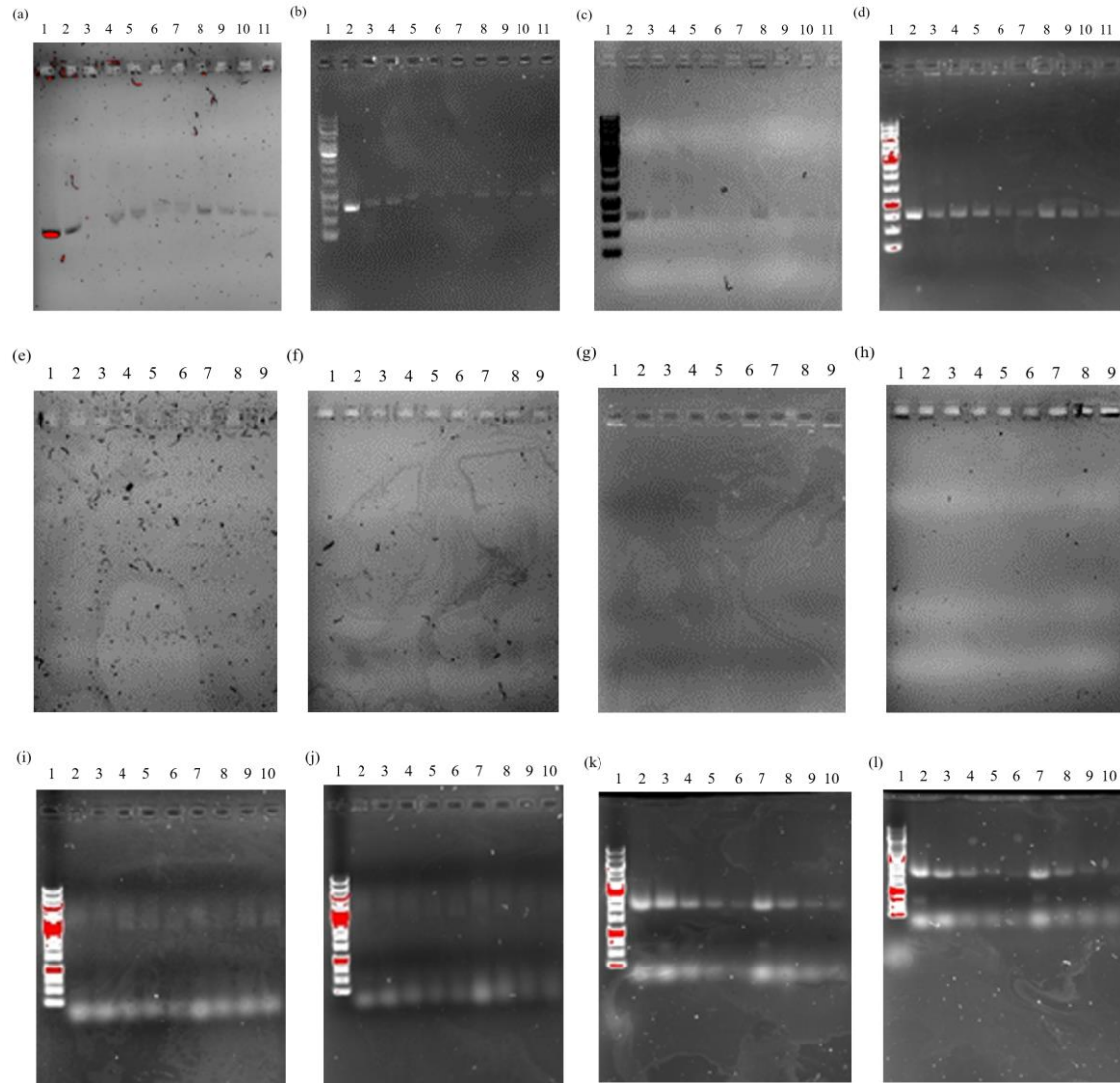


Figure S6.2 Gel scans of NAGE analysis of HBcAg VLP constructs Cp149 (a,b, e, f, i, j) and Cp157 (c, d, g, h, k, l) during reassembly by Vivaspin® centrifugal concentrators with 50 mM Tris, pH 7.2 buffer with different NaCl molarities in four diafiltration steps. Constructs were either mixed with dsDNA in a dimer/dsDNA ratio of 60 (a, b, d, e), mixed with ON\_DNA in a dimer/ON\_DNA ratio of 60 (e, f, g, h), or mixed with ON\_DNA in a dimer/ON\_DNA ratio of 2 (i, j, k, l). Allocation of samples in lanes can be found in Table S6.1. HBcAg: hepatitis B core antigen, ON: oligonucleotide, VLP: virus-like particle